REACTION PATHWAYS IN COPROCESSING

Leon M. Stock and Michael D. Ettinger
Chemistry Department
The University of Chicago, Chicago, IL 60637, U.S.A.

and

John G. Gatsis
Universal Oil Products Research Center
25 E. Algonquin Road, Des Plaines, IL 60017, U.S.A.

Keywords: Coprocessing, Catalysis, Hydrogen Utilization

INTRODUCTION

The coprocessing of coal and petroleum resid has been under active study as a method for the simultaneous utilization of two lower-valued fossil resources. Our research has focused on the coprocessing technology that was developed by Gatsis and coworkers[1,2] in which optimal reaction conditions (3000 psi total pressure, 420°C, 2:1 resid:coal, and 1 wt percent of a molybdenum-based Universal Oil Products catalyst) enabled the conversion of about 90% of the coal to toluene-soluble products and about 80% of the asphaltenes to heptane-soluble products. We have investigated the chemistry by carrying out the reaction in a dideuterium atmosphere at low and high severity[3] and by studying the reactions of representative aliphatic and aromatic hydrocarbons and phenols.[4]

EXPERIMENTAL

Materials. Illinois No. 6 coal was prepared by the Kentucky Center for Applied Energy Research and was used as received (Anal. % C, 68.60; % H, 4.51; % N, 1.39; % S, 3.04; % O, 9.65; % H_2O, 3.15; % ash, 9.65). Lloydminster petroleum resid (Anal. % C, 83.6; % H, 10.3; % S, 4.77; % N, 0.59; % O, 0.54) was obtained from the UOP Research Center. The catalyst was a molybdenum-based UOP proprietary material.

Procedure. Lloydminster petroleum resid (280 g) and Illinois No. 6 coal (165.4 g) and the catalyst (0.2 wt % Mo) were added to an 1800-mL rocking autoclave. The autoclave was sealed and pressurized first with hydrogen sulfide and then with dideuterium to give a 10 vol % hydrogen sulfide and 90 vol % dideuterium at the desired total pressure. The autoclave was heated to the desired temperature in about two hours and then cooled or retained at the temperature as appropriate. The work-up procedure, which has been described previously,[3] enabled the isolation of gases and insoluble products as well as the solvent separated oil, resin, and asphaltene.

Analysis. Elemental analyses of the starting coals, resids, and solvent separated products were carried out at Universal Oil Products. Gas analyses for deuterated methanes, ethanes, propanes, butanes, butenes, benzenes, and toluenes were carried out at the Institute of Gas Technology.

Deuterium NMR spectra were obtained on a Varian XL 400-MHz spectrometer, and proton NMR spectra were recorded at 500 MHz. The D/(H + D) ratio was evaluated for the aromatic and the alpha, beta, and gamma aliphatic positions. Detailed procedures that describe the magnetic resonance experiments have been published.[3,5]

RESULTS

The extent of conversion of the coal and resid into gases, oils, resins, asphaltenes, and solids is displayed in Figure 1. Typical results that illustrate the manner in which deuterium is incorporated into the reaction products are shown in Figure 2. The reaction chemistry of 1-pentyl-2-naphthol, which illustrates the complexity of the catalyzed transformations of even rather simple molecules, is summarized in Figure 3.

DISCUSSION

Molybdenum catalysts have been under study for many years. Indeed, more than 25 contributions were presented at a symposium of the Division of Petroleum Chemistry in Washington in August, 1994. While the detailed molecular mechanisms for these catalysts are not yet fully established, they are effective agents for the reduction of aromatic molecules, especially bi- and trinuclear substances, and for hydrodeoxygenation, hydrodesulfurization, and hydrodenitrogenation. Their hydrodeoxygenation activity is illustrated in Figure 3. In high severity coprocessing, the catalyst removes virtually all the oxygen, 74% of the sulfur, and 42% of the nitrogen from the products of Illinois No. 6 coal and Lloydminster resid. The catalyzed transformations of pure hydrocarbons and heterocycles have been studied by many research teams. For example, Curtis and her coworkers showed that the heteroatom removal and reduction reactions lead to monobenzenoid aromatic compounds, thus benzofuran yields ethylbenzene and 2-naphthol provides tetralin.[6]

The catalyst apparently also accelerates electrophilic reactions, and alkylation occurs during the process. Thus, when low concentrations of phenol are incorporated into the coprocessing reaction system, it undergoes alkylation before it is deoxygenated.[4] Aromatic deuterium exchange also apparently proceeds in an electrophilic order as suggested by the fact that phenols exchange much more rapidly than benzenes.

Hydrogen-deuterium exchange is facile. The selectivity for the incorporation and exchange of aromatic as well as alpha, beta, and gamma [Aromatic$CH_2(\alpha)CH_2(\beta)CH_2(\gamma)$] aliphatic hydrogen was measured for the series of coprocessing reactions. The results at high reaction severity indicate that the hydrogen and deuterium content has almost reached the equilibrium value dictated by the relative abundances than substances in the reaction system. At low severity, the deuterium is selectively incorporated at the aromatic and alpha aliphatic positions. Then, as the reaction proceeds, the amount of deuterium in the beta and gamma aliphatic positions increases, and the quantity of this isotope in the aromatic and alpha positions eventually decreases. Deuterium exchange in thermal reactions shows a much different order. The reactivity at activated benzylic (alpha) positions is clearly dominant under these conditions, with much less chemistry at the aromatic and unactivated aliphatic positions. The molybdenum catalyst and the reagents that were used in this study present a novel pattern of reactivity in which both free radical hydrogen transfer and ionic proton transfer occur rapidly. This dualism of parallel radical and electrophilic chemistry importantly contributes to the success of this coprocessing process.

The outcome is strongly influenced by the high initial hydrogen sulfide concentration, which is augmented by the formation of additional amounts of this acid from the resid and coal. Molybdenum sulfide catalysts contain thiol groups with H/Mo ratios from 0.12 to 0.37.[7,8] Furthermore, it is known that the exchange of H_2 and D_2 is very rapid.[9] Thus, the rapid equilibration of H_2S with the D_2 atmosphere in this reaction system is assured.

$$H_2S + D_2 \rightleftharpoons \text{Catalyst} \rightleftharpoons HDS + HD \rightleftharpoons \text{Catalyst} \rightleftharpoons D_2S + H_2$$

Hydrogen sulfide is certainly effective as a hydrogen atom transfer agent in thermal coal conversion chemistry.[10] Thus, the myriad of different radicals that are formed in the initial thermal decomposition of the coal macromolecules are rapidly converted to stable molecules by very fast hydrogen atom transfer reactions. The catalyst probably does not participate in these initial reactions, other than by insuring the exceedingly rapid conversion of ineffectual dideuterium into effective hydrogen deuterium sulfide. The thermal coal to asphaltene conversion is not the limiting reaction in coprocessing, Figure 1. One important factor in this successful conversion is the fact that the reaction between the initial coal fragment radicals and other coal constituents can be effectively suppressed by rapid hydrogen transfer. A second factor is that the smaller core molecules are efficiently converted by the catalyst into desirable hydrocarbons free of heteroatoms. These suggestions can be coupled with current ideas of coal structure and coal decomposition to provide a reasonably satisfying picture of coal conversion during coprocessing.

It is well known that the slow conversion reactions of the collections of molecules that constitute the asphaltenes limit the success of this coprocessing reaction.[1,2] Our new results show that this situation prevails in spite of the fact that the hydrogen atoms of the asphaltenes exchange quite readily, Figure 2. The parameters that govern the reactivity of these molecules have not yet been adequately elaborated.

Acknowledgment. We are indebted to the coal sample program at the Kentucky Center for Applied Energy Research for starting material. We also gratefully acknowledge the special efforts of the analytical group at Universal Oil Products and the Institute of Gas Technology. Irene Fox of the Analytical Chemistry Laboratory at Argonne National Laboratory provided insight concerning the interpretation of the H/D analyses that were obtained by LECO equipment. We are also indebted to the United States Department of Energy for the support of this research via AC22-88PC88811.

References

1. Gatsis, J.G.; Nelson, B.J.; Lea, C.L.; Nafsis, D.A.; Humbach, M.J.; Davis, S.P. *Continuous Bench-Scale Single Stage Catalyzed Coprocessing.* Contractor's Review Meeting, Pittsburgh, October 6-8, 1987.
2. Nafsis, D.A.; Humbach, M.J.; Gatsis, J.G. *Coal Liquefaction Coprocessing*, Final Report, DOE/PC/70002-T6, 1988.
3. Ettinger, M.D.; Stock, L.M.; Gatsis, J.G. *Energy Fuels* **8**, 960 (1994).
4. Ettinger, M.D.; Stock, L.M. *Energy Fuels* **8**, 808 (1994).
5. Ettinger, M.E. *Reaction Pathways in Coal/Petroleum Coprocessing*, University of Chicago Libraries (1993).
6. Kim, H.; Curtis, C.W. *Energy Fuels* **4**, 214 (1990) and previous articles in this series.
7. Sampson, C.; Thomas, J.M.; Vasadevan, S.; Wright, C.J. *Bull. Soc. Chem. Belg.* **90**, 1215 (1981).
8. Li, X.S.; Xin, Q.; Guo, X.X.; Granges, P.; Delmin, B. *J. Catal.* **137**, 385 (1992).
9. Blackburn, A.; Sermon, P.A. *J. Chem. Technol. Biotechnol* **33A**, 120 (1983).
10. Stock, L.M. "Hydrogen Transfer Reactions in Coal Conversion" in *The Chemistry of Coal Conversion*, Schlosberg, R., Ed., Plenum Publishing Co., Ch. 6, 1985.

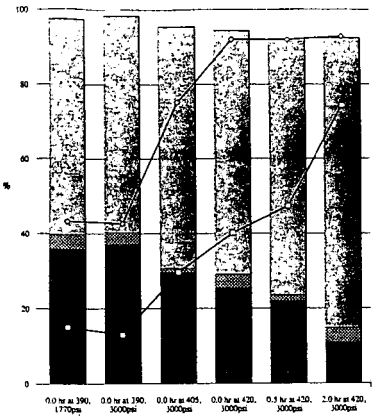

Figure 1. Coal (40 to 90%) and asphaltene (15 to 75%) conversion are portrayed by the lines. The yields of solids, asphaltenes, resins, oils, and gases are displayed from bottom to top in black, gray and white in the bar graph as a function of reaction conditions for the coprocessing reaction of Lloydminster resid and Illinois No. 6 coal.

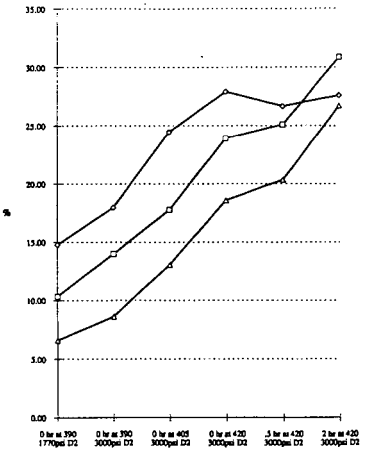

Figure 2. Aromatic % deuterium content, D / [H + D], in the oil (triangle), resin (square), and asphaltene (diamond) fractions as a function of reaction conditions for the coprocessing reaction of Lloydminster resid and Illinois No. 6 coal. Related information is available for alpha, beta, and gamma aliphatic positions.[5]

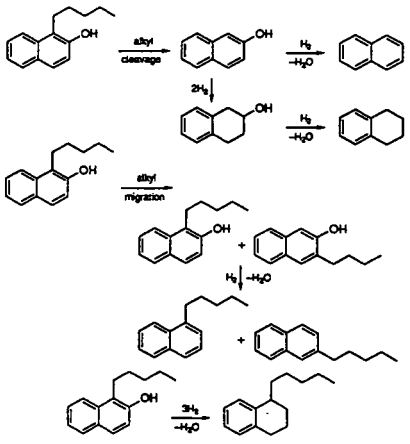

Figure 3. Reaction pathways for 1-pentyl-2-naphthol under the conditions of the catalyzed coprocessing reaction.[4]

DEPOLYMERIZATION-LIQUEFACTION OF PLASTICS AND RUBBERS. 1. POLYETHYLENE, POLYPROPYLENE AND POLYBUTADIENE.

Xin Xiao, Wlodzimierz Zmierczak and Joseph Shabtai
Department of Chemical and Fuels Engineering
University of Utah
Salt Lake City, Utah 84112

ABSTRACT

Processing conditions were developed for high-yield depolymerization-liquefaction of isotactic polypropylene (M.W., ~250,000) into a light, gasoline-like product. At 380-420 °C, an initial H_2 pressure of 1200 psig, with 1 wt% of finely dispersed Fe_2O_3/SO_4^{2-} or ZrO_2/SO_4^{2-} as solid superacid catalysts, the polypropylene is converted (yields, 72-83 wt%) into a liquid product consisting predominantly of C_5-C_{12} branched paraffins. The change in product composition as a function of reaction temperature, time, and catalyst concentration, was examined and optimal conditions for production of gasoline-range branched paraffins determined. Depolymerization-liquefaction of polyethylene with the same catalysts required higher processing temperature (420-450 °C) and longer reaction time. Liquid yields in the range of 78-85 wt% were obtained and the product consisted of a mixture of C_5-C_{30} (mostly C_5-C_{12}) normal paraffins, accompanied by some branched isomers. Polybutadiene (98 wt% cis) was depolymerized-liquefied at 400 °C and 1200 psig initial H_2 pressure in ~85 wt% liquid yield. The product consisted of a mixture of paraffins and cyclic compounds, including alkylcyclohexanes, alkylcyclopentanes, and alkylbenzenes with C_1-C_3 alkyl groups.

Keywords: depolymerization, liquefaction, plastics

INTRODUCTION

The effective disposal of waste industrial polymers is now recognized to be a major environmental problem in North America. Plastics and rubbers are troublesome components for landfilling, inasmuch as they are not presently biodegradable. Their destruction by incineration poses serious air pollution problems due to the release of airborne particles and carbon dioxide into the atmosphere. An alternative would be true recycling, i.e., conversion into monomers that can be reused. However, polyethylene and polypropylene do not depolymerize thermally to ethylene or propylene with sufficient selectivity. On the other hand, waste plastics and rubbers can be regarded as a potentially cheap and abundant source for fuels. Thermodegradation of polyolefins has been investigated extensively since World War II[1-5], but relatively few studies on the catalytic conversion of the polymers have been carried out, especially for production of liquid fuels. Recently there have been reports on the pyrolysis of polyolefins to aromatic hydrocarbons with activated carbon-supported metal catalysts[6,7]; cracking of polystyrene and polyethylene on silica-alumna[8]; and reforming of heavy oil from waste plastics using zeolite catalysts[9]. Most of these catalytic studies were conducted under nitrogen at ambient or low pressure. The present paper is concerned with an investigation of the catalytic depolymerization-liquefaction behavior of three representative commercial polymers, i.e., polypropylene, polyethylene and polybutadiene using superacid catalysts[10-16] under high H_2 pressure. The objective was to determine suitable conditions for conversion of such polymers into light liquid fuels, as well as to obtain data needed for predictive moldeling of waste polymers coprocessing with coal.

EXPERIMENTAL

Materials. High density polyethylene (d, 0.959 g/cm^3; M.W., 125,000) and isotactic polypropylene (d, 0.900 g/cm^3; M.W., 250,000) were obtained from Aldrich Chemical Company; and polybutadiene (98% cis; d, 0.910 g/cm^3; M.W., 197,000) from Scientific Polymers Products, Inc.

Catalysts. Three types of solid superacid catalysts, i.e., Fe_2O_3/SO_4^{2-}, ZrO_2/SO_4^{2-} and Al_2O_3/SO_4^{2-} were synthesized. The preparation of the first two was the same as recently described in detail elsewhere[16]. Al_2O_3/SO_4^{2-} was prepared by the following procedure: 12.4 g of $Al_2(SO_4)_3 \cdot (14\text{-}18)H_2O$ was dissolved in 44 ml of distilled water and subjected to hydrolysis at room temperature by slowly adding 28-30% NH_4OH with vigorous mixing, until pH = 8.5 was reached. The precipitate was filtered, washed with distilled water, and then dried at 110 °C for 2 h. The dry solid was pulverized and calcined at 550 °C for 2 h. The resultant Al_2O_3, 2.0 g, was treated with 50 ml of an aqueous solution with concentrations of 1.5M $(NH_4)_2SO_4$ and 1.0 M H_2SO_4 for 1 h with continuous stirring, then filtered, washed with ~100 ml of water, dried at 110 °C for 2 h, and calcined at 600 °C for 3 h.

Experimental Procedure. A mixture of the polymer, 10.0 g, and catalyst, 0.1 or 0.2 g (without any solvent), was introduced in a 50 ml Microclave reactor (Autoclave Engineers). The latter was closed, purged with nitrogen, and then pressurized with hydrogen to a selected initial pressure. The reactor was heated to the desired temperature in 12-15 min, and stirring (500 rpm) was started after reaching the melting or softening point of the polymer (130-189°C). Initial H_2 pressures from ambient to 2000 psig resulted in reaction pressures between 350-3600 psig in the reaction temperature range of 380-465 °C.

Analytical Methods. At the end of each experiment, the reactor was cooled down and the gas product was passed through a stainless steel trap kept at liquid nitrogen temperature. After weighing, the condensed gas was analyzed by GC. It consisted mostly of C_1-C_4 components, accompanied by some C_5, C_6, and traces of C_7, C_8 compounds. In runs with partial conversion, the liquid and solid products were removed from the reactor and weighed. The liquid was separated by decantation and filtration. The solid was rinsed with a little of n-hexane, dried, and weighed. The solid was then washed with n-hexadecane (~80 °C) and n-hexane (room temperature), dried and weighed in order to determine the weight of recovered catalyst. In this way, the product was separated and the weight of gas, liquid, solid and recovered catalyst was determined. The mass balance of the runs was 90-95% (relative to the weight of the feed). Gas and liquid products were identified mainly by GC, *GC/MS* and *FTIR*, and quantitatively analyzed by gas chromatography and simulated distillation (SIMD). Columns used for gas products: 4 m x 0.3 cm o.d. stainless steel packed with Chromosorb 102; for liquid products: 4 m x 0.3 cm o.d. stainless steel packed with 10% OV-17 on Chromosorb W-HP; for SIMD: 0.5 m x 0.3 cm o.d. stainless steel, Supelco PETROCOL™ B column.

RESULTS AND DISCUSSIONS

1. Polypropylene. At 390 - 420 °C and an initial H_2 pressure of 1500 psig, with 1.0 wt% of ZrO_2/SO_4^{2-} as catalyst, and a reaction time of 2.0 hours, the polypropylene was converted in very high yield (over 90 wt%) into a low-boiling liquid product. Branched C_5-C_{10} paraffins (and some olefins) were predominant components of the product. Results on the change in product composition as a function of reaction temperature are given in Figure 1. As seen, the gasoline range fraction (C_5-C_{12}) reached a maximum (~64.5 wt%) at 400-410 °C, then decreased slowly at higher temperature. The C_{13+} components decreased and the C_1-C_4 gas increased with increase in temperature. At 400 °C, about 64 wt% of gasoline range, 29 wt% of higher hydrocarbons and 7 wt% of gas are produced. The depolymerization-liquefaction of polypropylene was investigated also as a function of reaction time. The change in product composition showed the same trends as those indicated above for the temperature effect. This demonstrated the potential of a controllable stepwise depolymerization of polypropylene into light liquid hydrocarbons. The H_2 pressure effect was smaller compared with those of reaction temperature and time. Increase in H_2 pressure from 15 to 500-1500 psig suppressed gas formation, decreased the amount of C_{13+} products, and increased gasoline boiling range production. A comparative study of the three different types of solid superacid, i.e., Fe_2O_3/SO_4^{2-}, ZrO_2/SO_4^{2-} and Al_2O_3/SO_4^{2-} (see Experimental) was also performed, keeping other processing variables constant (reaction temperature, 410 °C, time 1.0 h, initial H_2 pressure 1500 psig, catalyst amount, 1.0 wt%). For comparison, a run without catalyst was also carried out. The extent of depolymerization of the feed into gasoline range hydrocarbons was significantly higher in the catalytic runs as compared with that in the thermal (non-catalytic) run. Among the catalysts examined, the order of depolymerization activity was $Al_2O_3/SO_4^{2-} > ZrO_2/SO_4^{2-} > Fe_2O_3/SO_4^{2-}$. Based on the change in product composition as a function of reaction temperature and reaction time, a plausible carbonium ion mechanism for depolymerization of polypropylene can be considered (see Figure 4).

2. Polyethylene. Liquid yields in the range of 76-87 wt% were found for polyethylene with ZrO_2/SO_4^{2-} as catalyst at reaction temperatures in the range of 420-450 °C. The product consisted of a mixture of C_5 -C_{30} (mostly C_5-C_{12}) normal paraffins and smaller amounts of branched isomers. Results on the change in product composition as a function of reaction temperature are given in Figure 2. The gasoline range fraction increased to a maximum of 63 wt% at 450 °C and then decreased at 465 °C. The C_{13+} components decreased while C_1-C_4 gas increased with increase in reaction temperature. The change in product composition as a function of reaction time (between 0.5-3.0 h) showed trends similar to those of the temperature effect. This was in good agreement with the above results for polypropylene and again demonstrated the controllable stepwise break-down of the polymer. The effect of H_2 pressure (500-2000 psig) on the product composition was relatively weak. As the H_2 pressure was increased from 500 to 1500 psig, the gasoline boiling range fraction increased while the C_{13+} fraction decreased. However, for H_2 pressures higher than 1500 psig , the concentrations of gasoline range and C_{13+} fractions remained relatively stable.

3. Polybutadiene. Polybutadiene was smoothly depolymerized-liquefied at 400 °C and 1200 psig initial H_2 pressure, with 1 wt% of Fe_2O_3/SO_4^{2-} as catalyst. The liquid yield was about 85 wt%. Figure 3 shows the GC/MS of the gasoline boiling range product. As seen, the product consists of a mixture of paraffins and cyclic compounds, including alkylcyclohexanes, alkylcyclopentanes, and alkylbenzenes with C_1-C_3 alkyl groups (C_1-C_3 indicating either single or two alkyl substituents). The formation of cyclic hydrocarbons from polybutadiene can be explained as follows. Butadiene obtained by depolymerization of polybutadiene, can undergo fast cyclodimerization to form 4-vinylcyclohexene, which undergoes a sequence of rearrangement and aromatization (or ring hydrogenation) reactions to yield a full range of alkylsubstituted naphthenes and benzenes[17].

CONCLUSIONS

It is found that representative polyolefins, e.g., polypropylene, polyethylene and polybutadiene, undergo high-yield depolymerization-liquefaction in the temperature range of 380-450 °C, under H_2 pressures of 1200-2000 psig, and in the presence of catalytic amounts of finely dispersed solid superacids, i.e., Al_2O_3/SO_4^{2-}, ZrO_2/SO_4^{2-} or Fe_2O_3/SO_4^{2-}. The depolymerization-liquefaction process is easily controllable for preferential formation of gasoline-range hydrocarbons. Production of the latter can be rationalized in terms of stepwise breakdown of the polymeric chains by a carbonium ion mechanism. The data obtained can be used for predictive modeling of coal coprocessing with waste polymers.

ACKNOWLEDGMENT

The authors wish to thank the U.S. Department of Energy for financial support through the Consortium for Fossil Fuel Liquefaction Science (DE-FC22-90PC90029). Thanks are also due to Professor H. L. C. Meuzelaar for helpful discussion of GC/MS data.

REFERENCES

(1) Jellinek, H. H. G. *J. Polym. Sci.* **1949**, 4, 13.
(2) Madorsky, L. *J. Polym. Sci.* **1952**, 9, 133.
(3) Inaba, A.; Inoue, H. *Kagaku Kogaku Ronbunshu* **1980**, 6, 95.
(4) Kuroki, T.; Honda, T.; Sekiguchi, Y.; Ogawa, T.; Sawaguchi, T.; Ikemura, T. *Nippon Kagaku Kaishi* **1977**, 894.
(5) Murata, K.; Sato, K. *Kagaku Kogaku Ronbunshu* **1981**, 7, 64.
(6) Uemichi, Y.; Makino, Y.; Kanazuka, T. *J. Anal. Appl. Pyrolysis* **1989**, 16, 229-238.
(7) Scott, D. S.; Czernik, S. R.; Piskorz, J.; Radlein, D. St. A. G. *Energy & Fuels* **1990**, 4, 407-411.
(8) Yamamoto, M.; Takamiya, N. *Bulletin of science and Engineering Research Laboratory Waseda University* **1985**, 111, 8-14.
(9) Songip, A. R.; Masuda, T.; Kuwahara, H.; Hashimoto, K. *Applied Catalysis B: Environmental* **1993**, 2, 153-164.
(10) Yamaguchi, T.; Jin, T.; Tanabe, K. *J. Phys. Chem.* **1986**, 90, 3148.
(11) Hino, M.; Arata, K. *Chemistry Lett.* **1979**, 477.
(12) Hino, M.; Arata, K. *Chemistry Lett.* **1979**, 1259.
(13) Wen, M. Y.; Wender, I.; Tierney, J. W. *Energy & Fuels* **1990**, 4, 372-379.
(14) Arata, K.; Hino, M. *Applied Catalysis* **1990**, 59, 197-204.
(15) Garin, F.; Andriamasinoro, D.; Abdulsamad, A.; Sommer, J. *J. Catalysis* **1991**, 131, 199-203.
(16) Zmierczak, W.; Xiao, X.; Shabtai, J. *Energy & Fuels* **1994**, 8, 113-116.
(17) Gil-Av, E.; Shabtai, J.; Steckel, F. *Ind. Eng. Chem.* **1960**, 52, 31.

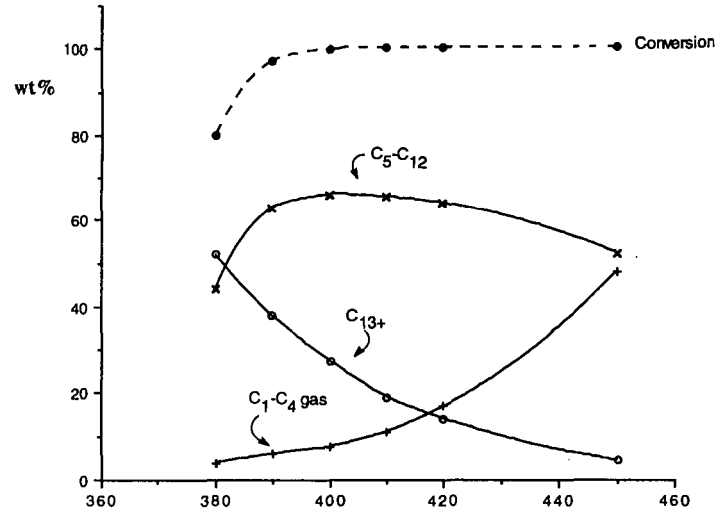

Fig. 1. Change in Product Composition from Depolymerization of Polypropylene as a Function of Reaction Temperature, °C.

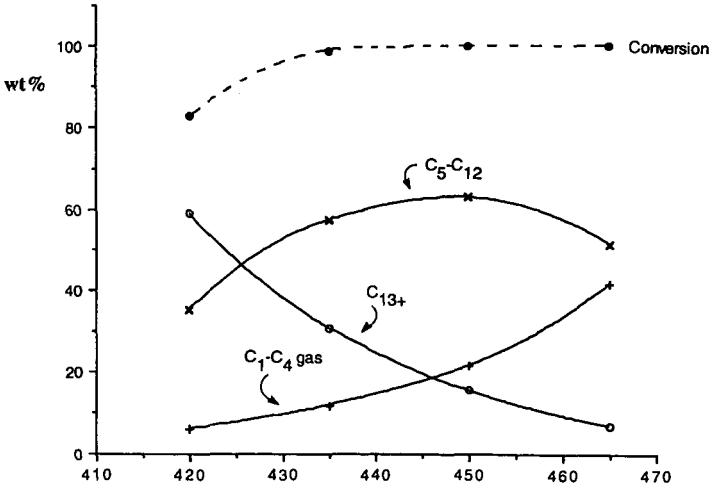

Fig. 2. Change in Product Composition from Depolymerization of Polyethylene as a Function of Reaction Temperature, °C.

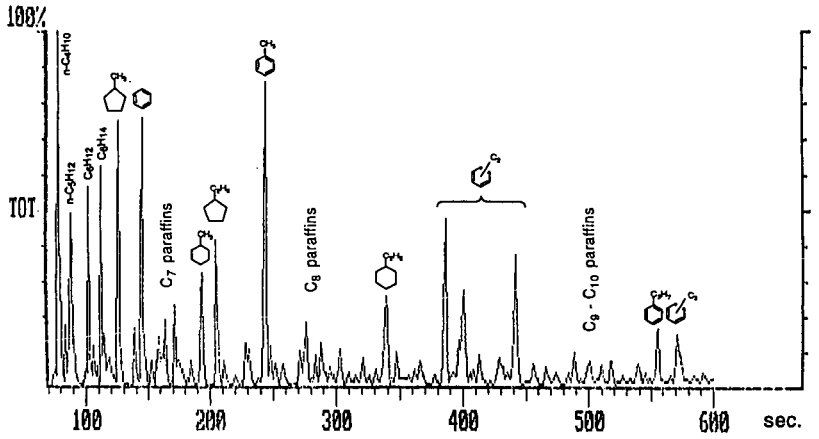

Fig. 3. GC/MS of Liquid Product (Gasoline-Range Fraction) from Depolymerization-Liquefaction of Polybutadiene, 98% cis.

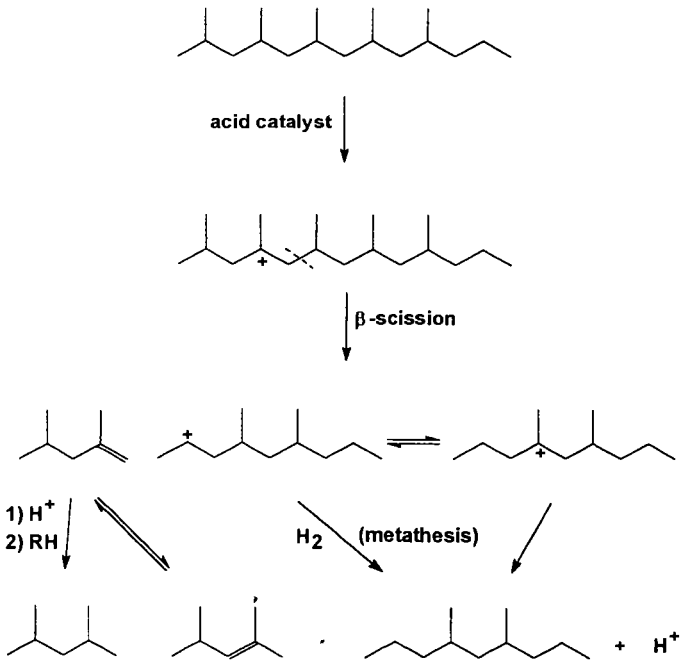

Fig. 4. Example of Proposed Mechanism for Polypropylene Depolymerization into Branched Paraffins and Olefins.

CATALYTIC REACTIONS IN WASTE PLASTICS AND COAL STUDIED BY HIGH PRESSURE THERMOGRAVIMETRY WITH ON-LINE GC/MS

Kui Liu, William H. McClennen and Henk L.C. Meuzelaar
Center for Micro Analysis & Reaction Chemistry, University of Utah
Salt Lake City, UT 84112

Keywords: on-line TG/GC/MS, waste plastic, coal, catalysis

INTRODUCTION

Waste plastics account for roughly 40% of landfill trash, of which only about 3% is recycled. The disposal of waste plastics is an important environmental problem. Clearly, the dominant components of waste plastics; mainly polyethylene, polystyrene, polypropylene are rich in carbon and hydrogen - the building blocks of petroleum, so that the possibility of converting waste plastic into liquid fuels is a productive alternative for plastic recycling. On the other hand, coal is hydrogen deficient, so co-processing of coal with waste plastics could be another way to recycle waste plastics into useful products.

Pyrolysis is a simple method to break the carbon-carbon bonds into relatively small molecular compounds by heating the polymers, but the major limitation of straight pyrolysis has been the poor selectivity for co-processing of coal and waste plastics. The use of various catalysts is a promising way of improving selectivity and yield. Catalytic liquefaction of coal has been widely studied[1,2,3], but little is known about catalytic conversion of waste plastics and co-processing of coal with waste plastics[4,5].

Development of efficient processes for converting solid waste materials and coal to useful products is often hindered by the lack of detailed fundamental data on real time thermal and catalytic reactions. A recently developed high pressure thermogravimetry (TG) system with on-line gas chromatography/mass spectrometry (GC/MS) modules provides detailed information on the pathways and mechanisms of the reactions which should benefit the screening of catalysts, help optimize reaction conditions, promote understanding of the function of the catalysts and provide a rapid and cost effective intermediate product analysis.

EXPERIMENTAL

Experiments with commingled waste plastic in the presence of various catalysts and co-processing runs of coal and commingled waste plastic were performed in a high pressure TG/GC/MS system at 900 psi hydrogen or helium pressure. Details of the high pressure TG/GC/MS system have been described previously[6]. The commingled waste plastic analyzed was obtained by washing the colored plastic bottles and containers to remove contaminants and labels before sizing and shaving. Final size reduction was done by grinding in a k-TEC kitchen mill. The coal was Blind Canyon DECS-6 high volatile bituminous coal (-100 mesh) from the Penn State Coal Sample Bank. The characteristics of the commingled waste plastic and coal have been listed elsewhere[5]. The preparation of the superacid catalysts Fe_2O_3/SO_4^{2-}, ZrO_2/SO_4^{2-} was described by Shabtai et al.[7]. The superacid catalysts Al_2O_3/SO_4^{2-}, Al_2O_3/SO_4^{2-} (promoted by 0.5% Pt) were also prepared by Shabtai and co-workers, as will be described in this meeting[8]. The 25% SiO_2-75%Al_2O_3 catalyst was supplied by Gulf Research and Development Company and sized to 100-140 mesh. The catalyst Ni-Mo/Al_2O_3, provided by Engelhard Corporation was mixed with $SiO_2Al_2O_3$ in a ratio of 4:1 (20-40 mesh size) and then sulfided.

RESULTS AND DISCUSSION

A characteristic example of the type of analytical results obtainable with the system is shown in Figure 1. Hydropyrolysis of Blind Canyon DECS-6 coal was conducted at 900 psig H2 pressure while heating at 10 C/min up to 700 C. During this process three distinct stages can be distinguished from both the TG weight loss curve (Figure 1a) and the total ion chromatogram (Figure 1b), namely bitumen desorption, hydropyrolysis and hydrogasification. Product distributions are shown in Figure 2 by expanding the chromatograms to a single sampling interval. The first process stage (Figure 2a) occurs over the temperature range of 250-350 C with products consisting mainly of substituted two-ring aromatics and long chain alkanes from bitumen desorption due to the evaporation of unattached molecules[9,10,11]. The second stage spans the temperature range of 370-550 C. The products, primarily thought to be due to hydropyrolysis of the coal, include short chain aliphatics, substituted phenols and also long chain n-alkenes and -alkanes (Figure 2b)[11,12]. The compounds produced in the final hydrogasification stage (at temperatures above 550 C) are mainly non-substituted aromatics including benzene, naphthalene, anthracene/phenanthrene and four-ring aromatics and hydroaromatics (Figure 2c). By selecting a particular ion chromatogram over the entire reaction temperature range, it can be illustrated how the corresponding product is evolved during the reaction. Figure 3 illustrates evolution profiles of propyl phenol, anthracene/phenanthrene, and C5-substituted naphthalene. By looking at the

selective ion chromatograms, it is shown that phenol evolves during the second stage of the process, whereas nonsubstituted aromatics evolve mainly during the third stage, and substituted aromatics evolve during both first and second stages.

Commingled Waste Plastics

Commingled waste plastic (about 35 mg) was subjected to three different temperature programs using a constant heating rate of 20 C/min up to 410 C, 420 C or 430 C separately, isothermal hold for 30 mins and then heating up to 700 C at 20 C/min to observe how decomposition reactions occur at a hydrogen pressure of 900 psig.

Figure 4 illustrates how temperature affects the decomposition reactions as measured by the weight loss as a function of temperature history and reaction time. At the end of the 30 min isothermal period at 410 C, weight loss of the waste plastic is approx. 17%, whereas at 430 C, approx. 84% of the weight is lost. These results illustrate that thermal decomposition reactions of waste plastic (in hydrogen) are strongly dependent on relatively small changes in reaction temperature. As indicated in our previous paper[13], isothermal runs at relatively low temperatures are found to be effective in bringing out differences between catalytic and thermal processes. By contrast at a linear heating rate of 10 K/min, thermal reactions overwhelm the catalytic effect. An isothermal plateau at 420 C, producing approx. 54% weight loss within 30 min without catalyst, was selected to investigate catalytic effects by comparing the relative decomposition reaction rates, residual char amounts and time-resolved product evolution profiles of thermal and catalytic runs, respectively.

Experiments on the decomposition of commingled waste plastic in two different reactor gas atmospheres (helium and hydrogen) and with several different catalysts were performed at 900 psig using the temperature program mentioned above. Catalysts studied include solid superacids such as Fe_2O_3/SO_4^{2-}, Al_2O_3/SO_4^{2-}, Al_2O_3/SO_4^{2-} promoted by 0.5% Pt, and ZrO_2/SO_4^{2-} added at 10% to the feed, as well as conventional cracking catalyst, SiO_2/Al_2O_3, hydrocracking catalyst, $NiMo/Al_2O_3$ mixed with $SiO_2Al_2O_3$ in a 4:1 ratio (added at 50%) and HZSM-5 zeolite (added at 10%). Different shapes of the TG profiles (weight loss vs. reaction time) in Figure 5 indicate catalytic effects on reaction rates and residue formation during waste plastic decomposition reactions.

At 420 C, all catalysts tested increase decomposition reaction rates to a varying degree, as indicated by the slopes of the curves in Figure 5. At these high catalyst addition levels, the SiO_2/Al_2O_3 and HZSM-5 catalysts show the highest conversion rates. For the SiO_2/Al_2O_3 catalyst, measurable decomposition reactions occur at temperatures lower than 420 C. For the solid superacid catalysts studied, the approximate order of cracking activity is $ZrO_2/SO_4^{2-} > Al_2O_3/SO_4^{2-} > Pt/Al_2O_3/SO_4^{2-} > Fe_2O_3/SO_4^{2-}$ > no catalyst. The weight loss after 30 min at 420°C is presented in Table 1 to illustrate how atmosphere and catalysts increase the yields of volatile products. In a hydrogen atmosphere the conversion yield is slightly increased compared to a helium atmosphere. Although $NiMo/Al_2O_3$, mixed with SiO_2/Al_2O_3 catalyst is not as effective as SiO_2/Al_2O_3 in cracking ability, it gives less residue formation due to the hydrogenation activity of the sulfided metal component. For catalysts such as SiO_2/Al_2O_3, $NiMo/Al_2O_3$ mixed with SiO_2/Al_2O_3 and HZSM-5, the decomposition reactions are completed at 420°C within 30 minutes. Therefore, no further reactions occur upon the increase of temperature.

The catalysts tested clearly improve the conversion rate of the commingled waste plastic, thereby lowering reaction temperature and/or shortening reaction time..

By examining the evolution profiles of volatile products by means of GC/MS changes in volatile product distributions as a function of reaction gas and catalysts can be measured. Several total ion chromatograms representing a single selected sampling period at different conditions are presented in Figure 6. The results show that thermal cracking, either in helium or hydrogen (only shown in hydrogen, Figure 6a) produced more evenly distributed long straight chain aliphatics including alkenes and alkanes (alkenes and alkanes are not separated by the 2 meter short GC column). With the catalysts, such as Al_2O_3/SO_4^{2-}, $Pt/Al_2O_3/SO_4^{2-}$, ZrO_2/SO_4^{2-}, $SiO_2Al_2O_3$, $Ni-Mo/Al_2O_3$, mixed with $SiO_2Al_2O_3$, more isomers of aliphatic products are produced (only shown with ZrO_2/SO_4^{2-}; Figure 6c). The stronger the cracking catalysts, the lighter the aliphatics (only shown for $SiO_2Al_2O_3$; Figure 6b). Strong cracking catalysts such as SiO_2/Al_2O_3 and HZSM-5 (zeolite) not only produce light aliphatics but also give high yields of substituted aromatics due to cyclization reactions promoted by acid catalysts as indicated in Figure 6d.

Co-Processing of Coal with Commingled Waste Plastic

Co-processing runs of Blind Canyon DECS-6 coal with commingled waste plastic (in a 1:1 ratio) involved adding several selected catalysts. Samples were subjected to the same temperature history at a hydrogen pressure of 900 psig. Figure 7 illustrates the TG weight loss curves of the coal, the waste plastic as well as the coal plastic mixture under non-catalytic conditions. The dotted line is the predicted weight loss curve of the mixture which is the linear sum of the individual component curves. The mixture of coal with waste plastic shows a slightly

lower reaction rate than the predicted value at 420 C. Subsequently, catalysts found effective in promoting the decomposition reactions of waste plastic including ZrO_2/SO_4^{2-}, SiO_2/Al_2O_3, $NiMo/Al_20_3$ mixed with SiO_2/Al_2O_3 and HZSM-5 Zeolite were applied to the mixture of coal with plastic. The TG weight loss curves presented in Figure 8 indicate that catalytic co-processing of coal with plastic is more difficult than catalytic processing of commingled waste plastic alone. The solid superacid catalyst ZrO_2/SO_4^{2-} and the cracking catalyst SiO_2/Al_2O_3 (added at the 10% level) have little influence upon the decomposition reactions of the mixture. A possible explanation could be that the presence of coal-derived nitrogen compounds poisons the active sites of the acid catalysts.. By adding relatively large amounts (50%) of the SiO_2/Al_2O_3 catalyst, the decomposition rate is increased, but to a lesser degree than for waste plastic alone. The HZSM-5 catalyst shows a very promising result for co-processing of coal and waste plastic by increasing both reaction rate and volatile product yield. This confirms earlier results by Huffman and co-workers[4]. Apparently, the active sites of the HZSM-5 catalyst are much less readily poisoned by the coal compared to other catalysts. On the other hand, a mixture of $NiMo/Al_2O_3$ with SiO_2/Al_2O_3 reveals better activity than the SiO_2/Al_2O_3 catalyst, whereas the opposite is true for plastic alone.

CONCLUSIONS

High pressure TG/GC/MS is demonstrated to be a viable and useful technique for screening candidate catalysts for processing waste plastic and for co-processing coal with waste plastic.

At the high catalyst levels used the results reveal catalytic waste plastic cracking activity in the following order: SiO_2/Al_2O_3 > HZSM-5 > $NiMo/Al_2O_3$ mixed with SiO_2/Al_2O_3 > solid superacids. Of the solid superacids studied, the ZrO_2/SO_4^{2-} catalyst possesses the highest cracking activity and the approximate order of cracking activity is ZrO_2/SO_4^{2-} > Al_2O_3/SO_4^{2-} > $Pt/Al_2O_3/SO_4^{2-}$ > Fe_2O_3/SO_4^{2-} > no catalysts.

The HZSM-5 zeolite catalyst shows most promising results for co-processing of coal with commingled waste plastic by increasing greatly the rate of the decomposition reactions albeit at the cost of lower MW products (high gas yields) and higher aromatic yields. Hydrocracking catalysts such as $NiMo/Al_2O_3$ mixed with SiO_2/Al_2O_3 show potential promise for co-processing of coal with commingled waste plastic due to their hydrogenation and cracking ability.

ACKNOWLEDGEMENTS

The authors gratefully acknowledge Professor J.S. Shabtai and Mr. X. Xin for preparing the superacid catalysts. This work was supported by the U.S. Department of Energy through the Consortium for Fossil Fuel Liquefaction Science (Grant No. UKRF-4-43576-90-10).

REFERENCES

1. Taghiei, M.M., Huggins, F.E., Mahajan, V., Huffman, G.P. *Energy & Fuels*, 8 (1994), 31.
2. Ibrahim, M. M., Seehra, M. S. *Energy & Fuels*, 8 (1994), 48.
3. Srivastava, R.D., Gollakota, S.V., Baird, M.J., Klunder, E.B., Lee, S.R., McGurl, G.V. *ACS Prep. Pap - Am. Chem. Soc. , Div. Fuel Chem.*, 37, 1, (1992), 124.
4. Taghler, M.M., Huggins, F.E., Huffman, G.P. *ACS Prep. Pap - Am. Chem. Soc. , Div. Fuel Chem.*, 38 (1993), 810.
5. Anderson, L.L., Tuntawiroon, W., *ACS Prep. Pap - Am. Chem. Soc. , Div. Fuel Chem.*, 38, (1993), 816.
6. Liu, K. Jakab, E., McClennen, W. H., Meuzelaar, H.L.C., *ACS Prep. Pap - Am. Chem. Soc. , Div. Fuel Chem.*, 38 (1993), 823.
7. Zmierczak, W. Xiao, X., Shabtai, J. *Energy & Fuels*, 8, (1994), 113.
8. Xiao, X., Zmierczak, W., Shabtai, J. *ACS Prep. Pap - Am. Chem. Soc. , Div. Fuel Chem.* (1995), Anaheim, CA.
9. Marzec, A. *Fuel*, 68 (1989), 1104.
10. Meuzelaar, H.L.C., Yun, Y., Simmleit, N., Schulten, H.R. *ACS Prep. Pap - Am. Chem. Soc. , Div. Fuel Chem.*, 34(3) (1989), 693.
11. Solomon, P.R., Serio, M.A., Carangelo, R.M., Bussilakis, R. *Energy & Fuels*, 4 (1990), 319.
12. Solomon, P.R., Hamblen, D.G., Carangelo, R.M., Serio, M.A., Deshpande, G.V. *Energy & Fuels*, 2 (1988), 405.
13. Liu, K., Jakab, E., Zmierczak, W., Shabtai, J., Meuzelaar, H.L.C. *ACS Prep. Pap - Am. Chem. Soc. , Div. Fuel Chem.*, 39(2) (1994), 576.

Table 1
Weight Loss Data from High Pressure TG

Items	Weight Loss, %
He	55%
H2	59%
Fe_2O_3/SO_4^{2-}, 10%	75%
$Pt/Al_2O_3/SO_4^{2-}$, 10%	79%
Al_2O_3/SO_4^{2-}, 10%	83%
ZrO_2/SO_4^{2-}, 10%	86%
$NiMo/Al_2O_3$, mixed with SiO_2/Al_2O_3, 50%	97%
SiO_2 Al_2O_3, 50%	94%
HZSM-5, 10%	97%

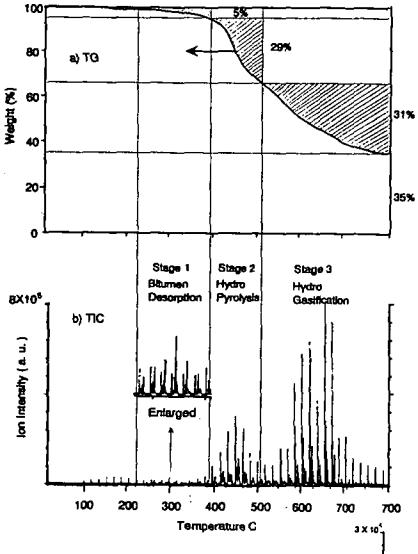

Figure 1. Hydropyrolysis of Blind Canyon DECS-6 coal. a) TG weight loss curve, b) total ion chromatogram.

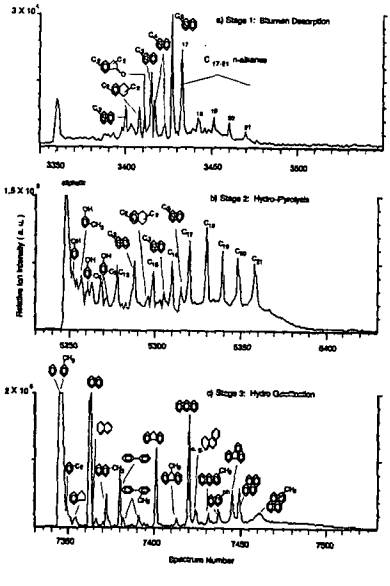

Figure 2. Product distribution obtained during hydropyrolysis of Blind Canyon DECS-6 coal. a) first stage-bitumen desorption; b) second stage - hydropyrolysis; and c) third stage - hydrogasification.

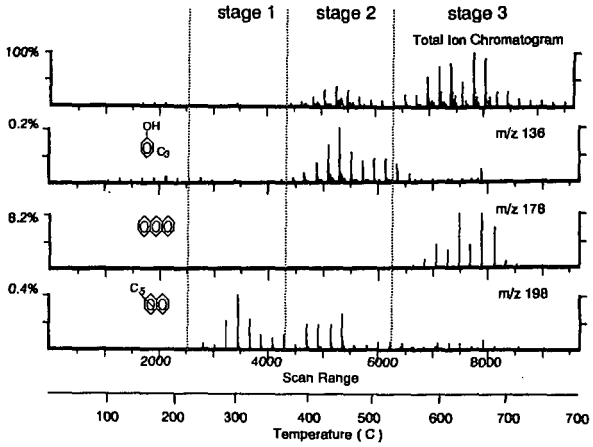

Figure 3. Evolution profiles of several products during hydropyrolysis of Blind Canyon DECS-6 coal by selective ion chromatograms.

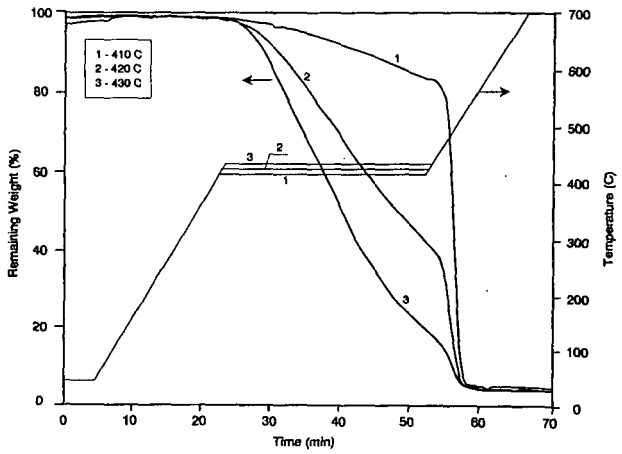

Figure 4. TG curves of the commingled waste plastic at 900 psig (H_2).

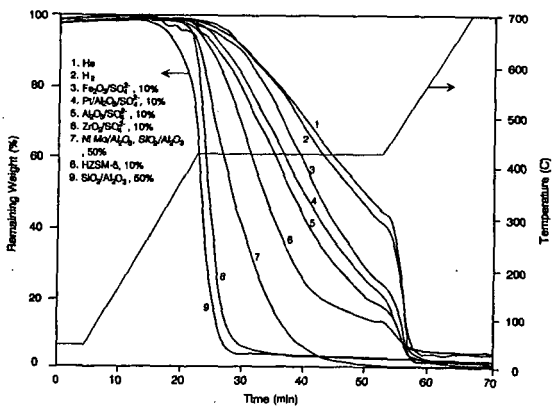

Figure 5. Effects of reactor gas atmospheres and catalysts on decomposition reactions of the commingled waste plastic at 900 psig.

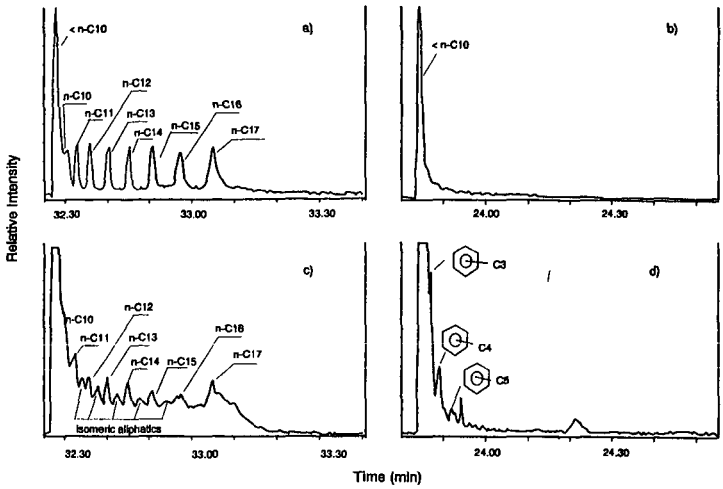

Figure 6. Total ion chromatograms of one sampling period of plastic decomposition products. a) in hydrogen; b) $SiO_2Al_2O_3$; c) ZrO_2/SO_4^{2-}; and d) HZSM-5.

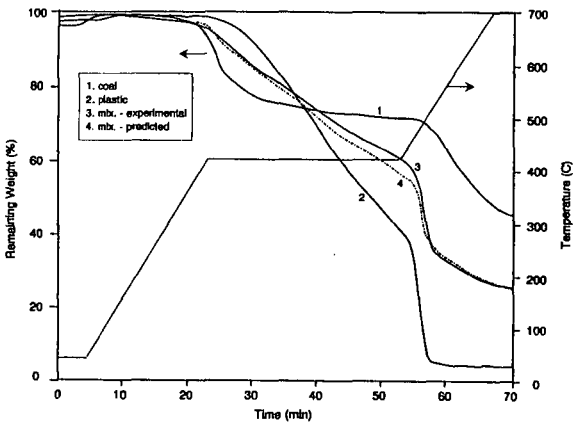

Figure 7. TG curves of co-processing of coal with plastic at 900 psig (H_2).

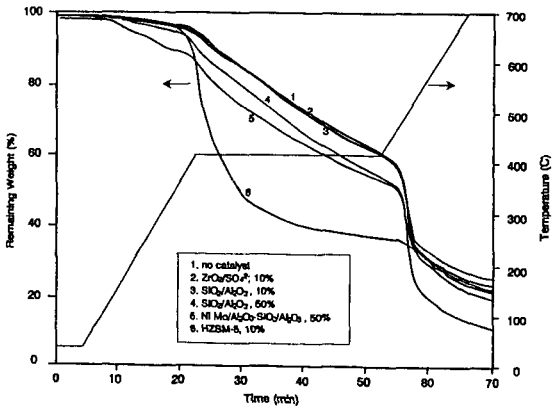

Figure 8. Effects of catalysts on co-processing of coal with plastic at 900 psig (H_2).

EFFECT OF MODIFYING HOST OIL ON COPROCESSING

Paul E. Hajdu, John W. Tierney, and Irving Wender
Department of Chemical & Petroleum Engineering
University of Pittsburgh, 1249 Benedum Hall
Pittsburgh, PA 15261

Keywords: coprocessing, pretreatment of host oil.

INTRODUCTION

The world's supply of petroleum crudes is becoming heavier in nature so that the amount of vacuum bottoms has been steadily increasing. Coprocessing of coal with these resids (1000°F+) is an attractive way of obtaining useful distillates from these readily available cheap materials. Petroleum resids and coals differ in several ways; coal is more aromatic with a lower H/C ratio, contains more inorganic material than found in heavy resids, is richer in oxygen, and has smaller clusters of organic material. Heavy oils are more aliphatic and less aromatic, have very little oxygen, somewhat smaller amounts of nitrogen, significantly more sulfur, and contain relatively small amounts of vanadium, nickel and iron, some of which are trapped in porphyrin structures.

The objective of this work is to pretreat the host oil in ways that would improve its performance in coprocessing with coal. The following are examples of some ways in which heavy oil could be made into a better host oil: converting aromatic structures to hydroaromatics capable of donating hydrogen to coal, cracking the heavy oil to lower molecular weight material that would be a better solvent, and removing metals, sulfur, and nitrogen.

Other investigators have found that coprocessing performance can be improved by pretreating the host oil. Takeshita and Mochida[1] showed positive results by using a petroleum pitch that had been hydrotreated at high pressure over a Ni/Mo/Al_2O_3 catalyst. A similar approach was taken by Sato and coworkers[2] who obtained high coal conversion and high distillable oil yields after a tar sand bitumen they were using was hydrotreated with a Ni-Mo catalyst. Curtis and coworkers[3,4,5] have shown the importance of hydrogen donor compounds in host oil for achieving high coal conversion. Hydroaromatic compounds (hydrogen on a naphthenic carbon at the alpha or beta position from the aromatic ring) are one class of hydrogen donor compounds that are important in coal liquefaction.

EXPERIMENTAL

The work reported here used a Venezuelan oil obtained from the Corpus Christi refinery of Citgo. Its properties are listed in Table I as are those of another heavy oil for comparison; the latter is a vacuum resid from a wide mixture of crudes, obtained from AMOCO. Two coals, Illinois No.6 and Wyodak subbituminous, were coprocessed with host oils; both coals were Argonne premium coal samples. Properties of the coal samples have been previously published[6].

Four pretreatments of the resid were conducted in a well-stirred 300 ml stainless-steel autoclave batch reactor. Table II lists conditions and yields for the runs. One pretreatment, subsequently referred to as Pretreatment-A, involved cracking the resid at 440°C under H_2, 1000 psig (cold), for 2 hrs; molybdenum naphthenate (MN), supplied by ICN Biomedical Inc, and elemental sulfur, were added at a level of 1000 ppm Mo to suppress coke production to below 3 wt% (in runs made without MN at these conditions, coke production reached levels above 11%). The other three pretreatments involved hydrogenating the resid at milder conditions where cracking is suppressed. In Pretreatment-B the resid was reacted at 375°C under H_2, 1000 psig (cold), for 5 hrs using 1000 ppm of MN. In Pretreatment-C the resid was treated using a finely dispersed Mo/Fe_2O_3/SO_4 catalyst[7,8] (2 wt%) at the same conditions used in Pretreatment-B. In Pretreatment-D the resid was dissolved in toluene and hydrogenated using a homogeneous catalyst, dicobalt octacarbonyl ($Co_2(CO)_8$), at 130°C for 2 hrs under 2600 psig of 1:1 synthesis gas. Friedman and coworkers[9] found this system to be effective for selectively hydrogenating polynuclear aromatic compounds to their hydroaromatic derivatives; e.g., anthracene to 9,10-dihydroanthracene and pyrene to 4,5-dihydropyrene.

Pretreated products were removed from the 300 ml autoclave and separated into three fractions. The workup procedure ensured maximum recovery of products while minimizing losses of lighter material. Light oils (bp < 195°C) produced during pretreatments at 440°C were removed by distillation at atmospheric pressure. Pretreatments made at 375°C and below, generally produced no light oils. In these runs, distillation was not necessary. Products not removed by distillation were recovered by washing the contents of the reactor with THF. After filtration the THF was removed by distillation. Because the boiling point of THF is well below that of the pretreated heavy oils, good separation was possible. For runs made with $Co_2(CO)_8$, the THF-

washed products were refluxed for three hours to destroy the carbonyl. To further facilitate removal of the cobalt, silica-alumina powder was added to the liquid mixture prior to filtering. All THF-insoluble solids were vacuum dried overnight prior to weighing.

Coprocessing experiments were conducted in a horizontal, stainless-steel microreactor at 425°C for 30 min under 1000 psig (cold) H_2. Three weight ratios of host oil to coal were used; 9:1, 2:1 and 1:1. Most coprocessing runs were made with no added catalyst, but a few were made with either MN (2000 ppm Mo) or 2 wt% $Mo/Fe_2O_3/SO_4$, plus elemental sulfur. Products from the microreactor were recovered and separated into three fractions; pentane-soluble oils, asphaltenes and THF-insoluble solids. Pentane was removed from the filtered oil by rotovapor under atmospheric pressure to prevent losses of light products. Under these mild separation conditions a small amount of pentane remained with the oil. This was later measured by simulated distillation.

Gases were analyzed using an HP 5880A GC. Pentane-soluble oils (free of ash and asphaltenes) were analyzed using an HP 5890 series II GC/HP 5970 mass selective detector. A boiling curve for pentane-soluble oil samples was determined by simulated distillation[10] using an HP 5890 series II GC. Original and pretreated oil samples were analyzed by ^1H NMR spectroscopy using a Bruker 300 MSL spectrometer; samples were prepared in deuterated chloroform with tetramethylsilane for internal reference.

Catalytic dehydrogenation was used to measure the "available" hydrogen of resids and pretreated oils. Available hydrogen was defined as the amount of hydrogen gas evolved when an oil sample dissolved in phenanthridine was catalytically dehydrogenated for 285 min over a reduced $Pd/CaCO_3$ catalyst at atmospheric pressure.

Metal contents (Ni, Fe and V) of selected samples were determined by The Pittsburgh Applied Research Corp. using the ICP technique. Elemental analyses were conducted by Galbraith Laboratories Inc. and CONSOL Inc.

RESULTS AND DISCUSSION

Table III lists properties of the pretreated Citgo host oils. The Pretreatment-A oil was lighter, based on wt% of distillate, than the untreated resid as well as the other pretreated host oils. This is a result of the higher pretreatment temperature used. The available hydrogen content of the pretreated oils was higher than that of the untreated resid, which had a value of 9.8 H atoms/100 C atoms. This infers that the pretreated oils contain more donatable hydrogen. The increase in available hydrogen for the oils from Pretreatments B, C and D was slightly below the amount of hydrogen consumed during these runs, indicating significant hydrogen utilization. All pretreated host oils, with exception of the Pretreatment-D oil, had higher H/C atomic ratios than that of the untreated resid; although the increases were not large. The pretreated host oils had lower sulfur concentrations than the untreated resid; nitrogen concentrations remained unchanged.

Figure 1 shows the effect of coal slurry concentration on Illinois No.6 coal conversion to THF-solubles in thermal (no added catalyst) coprocessing runs made with the different host oils. Coal conversion was calculated from the amount of unconverted (THF-insoluble) material recovered from the products after correcting for ash, added catalyst and petroleum-derived coke (this was less than 3 wt% based on repeat runs made without coal). The Figure shows that coal conversions in the oils from Pretreatments B-D were higher than levels achieved in the untreated Citgo resid or the oil from Pretreatment-A. Coal conversions in the Citgo resid and in the oil from Pretreatment-A decreased as the concentration of coal in the feed was increased. This trend has been observed by other investigators[11,12] demonstrating the limited ability of these host oils to bring about coal dissolution. On the other hand, coal conversions in the oils from Pretreatments B-D appeared to be independent of coal slurry concentration up to 50 wt%. Illinois No.6 coal conversion in these pretreated host oils were slightly higher than conversions obtained when the coal was catalytically coprocessed in the Citgo resid using either MN (2000 ppm) or $Mo/Fe_2O_3/SO_4$ (2 wt%). These results clearly demonstrate that the host oils from Pretreatments B, C and D are good coprocessing solvents. When these host oils were coprocessed with coal in the absence of hydrogen gas, conversions were significantly less than levels achieved under hydrogen gas.

Figures 2 and 3 show how distillable product yields varied with coal slurry concentrations when Illinois No.6 coal was coprocessed with the untreated resid and the oil from Pretreatment-C, respectively. Distillable product yields are defined as the wt% of ash-free feed converted to gases and pentane-soluble oil that had a simulated distillation boiling point below 565°C. The lower line in the Figures represents the contribution from the host oil assuming no interaction

between coal and host oil. This line was drawn by assuming the distillate yield from the host oil obtained at zero coal concentration did not change. The shaded area above the lower line represents the contribution of distillable product from coal. This value was based on the yield from a thermal coal liquefaction run made with Illinois No.6 and the solvent diphenylmethane. During the run, 84.5% of Illinois No.6 coal was converted to THF-soluble products, of which an estimated 50% was distillable. Rahimi and coworkers[12] also concluded that up to 40-50 wt% of converted coal ends up in the distillate (bp < 525°C).

At coal slurry concentrations below 50 wt%, distillable product yields were generally above the level calculated assuming no interaction between coal and host oil, with exception of runs made with the oil from Pretreatment-A (not shown), which yielded distillate below this level. These results show a possible synergism between coal and host oil, a behavior that has been reported[11,12,13] by others.

CONCLUSIONS

We have found that mild pretreatment of a Citgo resid (1000°F) using either Mo naphthenate or $Mo/Fe_2O_3/SO_4$, as well as a pretreatment using the homogenous catalyst $Co_2(CO)_8$ under synthesis gas can increase the available (donatable) hydrogen content of the resid. When these pretreated oils were thermally (no added catalyst) coprocessed with an Illinois No.6 coal, about 90 wt% of the coal (maf) was converted to soluble products. This high coal conversion was realized even at a high coal loading of 50 wt%. Pretreatments at 440°C, that crack the resid without adding much available hydrogen, showed little promise for improving coal conversion above levels achieved with untreated resid. The products from coprocessing coal and oil were equally split between high boiling material, mostly asphaltenes, and distillate. Distillate yields appeared to be affected by the concentration of coal in the feed, with maximum yields at coal loadings below 50 wt%.

ACKNOWLEDGEMENTS

This work was supported by a grant from the U.S. Department of Energy (DE-AC22-91PC91054). We are grateful to Genea Lee for her assistance in dehydrogenation experiments. We would like to thank Citgo as well as AMOCO for providing the resid samples. We would also like to thank the EXXON Educational Foundation for their generous support.

REFERENCES

1. Takeshita, K. and Mochida, I., Jap. Pat. 80-45703 (1980)

2. Sato, Y., Yamamoto, Y., Kamo, T., Inaba, A., Miki, K., and Saito, I., Energy & Fuels, **5** (1991) 90-102

3. Curtis, C.W., Tsai, K.-J. and Guin, J.A., Fuel Processing Technology, **16** (1987) 71-87

4. Bedell, M.W., Curtis, C.W. and Hool, J.L., Fuel Processing Technology, **37** (1994) 1-18

5. Owens, R.M. and Curtis, C.W., Energy & Fuels, **8** (1994) 823-829

6. Bedell, M.W., et al., Fuel Processing Technol, **37** (1994) 1-18

7. Pradhan, V.R., Hu, J., Tierney, J.W., and Wender, I, Energy & Fuels, 7 (1993) 446

8. Pradhan, V.R., Herrick, D.E., Tierney, J.W., and Wender, I., Energy & Fuels, **5** (1991) 712-720

9. Friedman, S., Metlin, S., Svedi, A., and Wender, I., J. Org. Chem., **24** (1959) 1287

10. ASTM Designation: D 2887-89, Annual Book of ASTM Standards

11. Cugini, A.V., Lett, R.G. and Wender, I., Energy & Fuels, **3** (1989) 120-126

12. Rahimi, P.M., Fouda, S.A., Kelly, J.F., Malhotra, R., and McMillen, D.F., Fuel, **68** (1989) 422-429

13. McMillen, D.F., Malhotra, R. and Tse, D.S., Energy & Fuels, **5** (1991) 179-187

14. Brown, J.K. and Ladner, W.R., Fuel, **39** (1960) 87

Table I. Properties of Petroleum Resids (1000°F+)

	Citgo Resid	Amoco Resid
C, wt%	85.4	84.3
H, wt%	10.1	10.2
S, wt%	3.4	4.6
N, wt%	0.8	0.5
O, wt%	0.3	0.4
Atomic H/C	1.42	1.45
V, ppm	555	251
Ni, ppm	110	57
Fe, ppm	12	13
Pentane Insolubles, wt%	27.3	20.1
Aromatic Carbons[a], fraction	0.33	0.32

a:Based on ^{1}H NMR by Brown and Ladner's method[14]

Table II. Reaction Conditions and Product Yields for Pretreatments of Citgo Resid

	Oil-A	Oil-B	Oil-C	Oil-D
Catalyst, concentration	MN, 1000 ppm	MN, 1000 ppm	$Mo/Fe_2O_3/SO_4$,2 wt%	$Co_2(CO)_8$, 6.2 wt%
Atmosphere	H_2	H_2	H_2	CO/H_2 (1:1)
Temperature, °C	440	375	375	135
Pressure (cold), psig	1,000	1,000	1,000	2,000
Time, hrs	2	5	5	2
Gas yield, wt%	10-25	1-12	3	0
Oil yield, wt%	72-87	86-97	95	100
Coke yield, wt%	3	2	2	0

Table III. Properties of Citgo Pretreated Host Oils

	Oil-A	Oil-B	Oil-C	Oil-D
b.p. < 565°C[a], wt%	62.6	29.7	33.3	17.9
b.p. > 565°C, wt%	37.4	70.3	66.7	82.1
C, wt%	85.1	85.9	85.6	83.7
H, wt%	10.6	10.4	10.8	9.7
S, wt%	2.2	2.7	2.9	2.8
N, wt%	0.9	0.9	0.8	0.8
O, wt%	1.2	0.1	0.0	3.0
Atomic H/C	1.49	1.45	1.51	1.39
V, ppm	392	----	477	----
Available[b] Hydrogen per 100 C atoms	12.4	16.8	14.0	17.5

a: b.p. < 565°C consists of pentane-soluble oil having a simulated distillation b.p. < 565°C (1050°F). b.p. > 565°C consists of pentane-insoluble asphaltenes, and pentane-soluble oil having simulated distillation b.p. > 565°C.
b: Value based on catalytic dehydrogenation, experiment described in text.

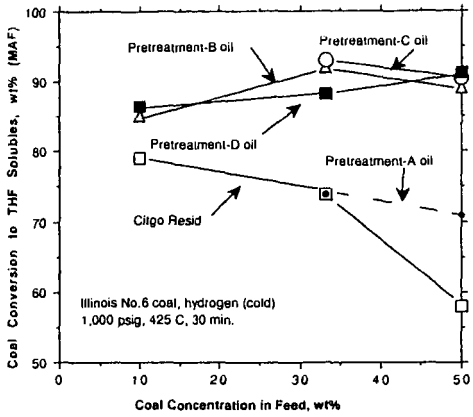

Figure 1. Effect of coal concentration on Illinois No.6 coal conversion to THF solubles in thermal coprocessing with Citgo resid and pretreated host oils (Pretreatment-A: 1000 ppm MN, 440°C, 1000 psig (cold) H_2, 2 hr reaction time; Pretreatment-B: 1000 ppm MN, 375°C, 1000 psig (cold) H_2, 5 hr reaction time; Pretreatment-C: 2% $Mo/Fe_2O_3/SO_4$, 375°C, 1000 psig (cold) H_2, 5 hr reaction time; Pretreatment-D: 6.2% $Co_2(CO)_8$, 135°C, 2650 psig CO/H_2 (1:1), 2 hr reaction time).

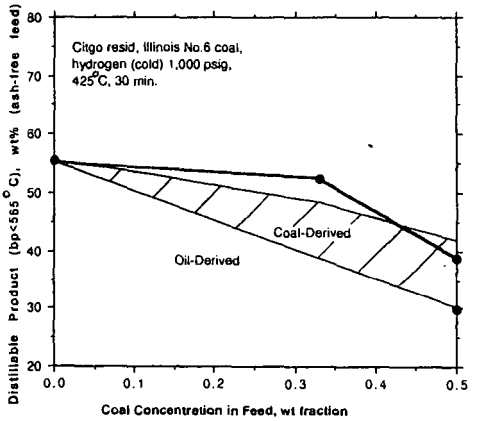

Figure 2. Effect of coal concentration on distillable product yields in coprocessing Illinois No.6 coal with Citgo resid.

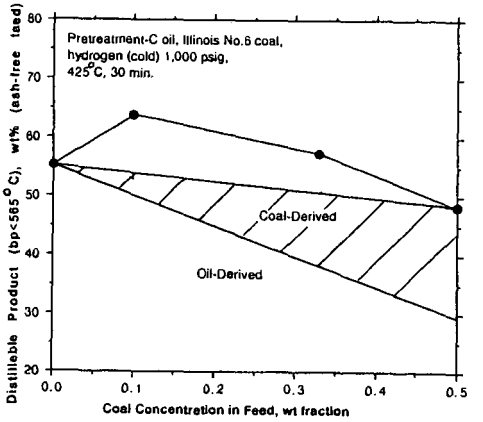

Figure 3. Effect of coal concentration on distillable product yields in coprocessing Illinois No.6 coal with pretreatment-C (2% $Mo/Fe_2O_3/SO_4$, 375°C, 1000 psig (cold) H_2, 5 hr reaction time) oil.

A TECHNO-ECONOMIC ASSESSMENT OF INTEGRATING A WASTE/COAL COPROCESSING FACILITY WITH AN EXISTING REFINERY

David Gray and Glen Tomlinson
The MITRE Corporation
McLean VA 22102

Keywords: waste/coal coprocessing, plastics, rubber, liquefaction.

INTRODUCTION

About 97 million tons of waste plastics, paper, oils, and tires are generated annually in the United States. The vast majority of this waste is paper, accounting for more than 73 million tons, and the second most abundant waste is plastic, accounting for more than 16 million tons. The number of waste passenger tire equivalents generated in the United States is about 300 million; considerably more than the population. On a rubber basis, this is approximately equal to 1.6 million tons: For waste oils, the average rate of annual generation is about 4.8 million tons, equivalent to about 32 million barrels[1]. This rate of waste generation constitutes a major waste management problem with respect to land availability for landfills and public health and pollution concerns. Mandatory recycling of waste paper and plastics is in effect in several states, but the rate of generation of these wastes exceeds existing demand.

Solutions to the problem of excess waste are being put into effect nationwide. Paper can be recycled to a certain extent. Waste oils can be cleaned and re-refined. Plastics that are not recycled can be combusted for thermal value, and tires can either be burned whole in cement kilns, or shredded and used as a supplementary fuel for utility boilers, the so called tire derived fuel or TDF[2]. Another potential solution to the waste problem is coprocessing of the wastes either with heavy oils or with coal to produce hydrocarbon liquids that can be refined like petroleum to give transportation fuels. This paper addresses the technical and economic feasibility of this coprocessing approach by examining the potential for co-siting a waste/coal coprocessing facility adjacent to an existing oil refinery.

METHODOLOGY

The conceptual waste/coal coprocessing facility is assumed to be sited at a refinery close to the greater Philadelphia metropolitan area. In this area it has been estimated that approximately 3100 tons per day of waste plastics is generated, 250 tons of tire rubber, and about 9000 barrels per day of used oil[1]. It is assumed in this analysis that about 25 percent of the waste plastics can be transported and utilized at the site , 15 of the waste oil, and 50 percent of the tires. Four cases were analyzed and these are shown in table 1. In case 1, only plastic and coal is fed to the plant on an equal weight basis. In Case 2, plastics, coal and waste oil are fed to the plant, Case 3 uses plastics, oil, tires and coal. Case 4 is a coal-only case, and is analyzed to provide a comparison by which to measure any potential economic advantages of co-feeding the wastes. In all cases, petroleum coke from the refinery is used as a gasification feed to provide hydrogen both for the refinery and for the coprocessing facility. Figure 1 is a schematic showing the coprocessing facility and how it integrates with the adjacent refinery. These integrations include: letting the refinery process purge gases from the coprocessing plant, sharing of waste water treatment facilities, refining of the raw liquids from the coprocessing plant in the refinery, selling hydrogen and fuel gas to the refinery, and utilizing the petroleum coke from the refinery in the coprocessing facility for hydrogen production.

When this techno-economic analysis was performed there was little data available from continuous units operating in a coprocessing mode with coal and plastics, rubber, and oils. Since then, Hydrocarbon Research Inc. (HRI) has demonstrated the technical feasibility of coprocessing coal with plastic and rubber in their proof-of-concept (POC) facility in New Jersey under the sponsorship of the United States Department of Energy (DOE). For this analysis, it was necessary to make various assumptions as to the performance of coal/ waste coprocessing in the HRI Catalytic Two-Stage Liquefaction (CTSL) process. These assumptions can be summarized as follows: the presence of the coprocessed waste materials do not effect the coal conversion, plastics (excluding PVC) convert to 98 percent to oils and gases, plastics produce four times the gas as coal, waste oil converts to 98 percent oil and gas, tires contain 33 percent carbon black inerts and 98 percent of the remainder converts to oil and gas. It is further assumed that coal is $25 per ton, and the acquisition costs for the waste materials at the plant gate is zero. The petroleum coke is also free at the plant gate. However, the waste feed stocks must be prepared for coprocessing. It is assumed that it costs $25 per ton to shred tires, $20 per ton to shred plastics, and $5 per ton to prepare the waste oil. The coprocessing plant

can sell hydrogen to the refinery for $2/Mscf, and fuel gas for $1/MMBtu. Sulfur and ammonia by-product credit to the coprocessing facility is priced at $80 and $150 per ton respectively. For processing the fuel gases the refinery charges the coprocessing facility $6 million per annum, $5 million for waste water treatment, and $3 million to recover sulfur.

To conduct this analysis, conceptual, commercial waste/coal coprocessing plants were developed using the MITRE coal liquefaction cost model methodology based on performance data from the CTSL process. MITRE has developed commercial liquefaction simulation models and these can be used to analyze the impact of process variables on performance and the resulting required selling price of products for any desired set of economic parameters. For this analysis, the performance of the coprocessing plants was based on the known performance of the coal-based process together with the estimated performance of the waste materials from the assumptions noted above. The four cases were analyzed based on the capacity of one liquefaction train of the CTSL process. The size of the overall facility was based on the availability of the waste feedstock and this train size for CTSL is not the optimum size from an economic viewpoint. A larger CTSL train size could be utilized by feeding more coal to the facility but the impact of this was not considered in this analysis.

RESULTS OF THE ANALYSIS

Table 2 summarizes the results of this economic analysis for the three coprocessing facilities and the coal-only plant. The components that make up the capital costs of the coprocessing facility consist of the CTSL train, gasification to produce hydrogen including air separation, and the ROSE-SR deashing process (CSD). In Case 3, the Texaco Tire dissolution process[3] is included to dissolve the tires. Total capital for these plants ranges between $330 and $350 million ($1993). Operating costs include feedstock preparation costs for the wastes, coal costs, power, and operating and maintenance costs. Netbacks is the difference between the price paid to the coprocessing facility for hydrogen, fuel gas, sulfur, and ammonia, and the service costs that the coprocessing facility pays to the refinery for sulfur recovery, waste water treatment, and acid gas processing. The required selling price (RSP) of the raw liquid products is calculated from the capital and net operating costs from a DCF analysis based on a fixed set of economic parameters. The liquid product outputs from the four cases are tabulated in Table 1.

This preliminary economic analysis indicates that waste/coal coprocessing has the potential to reduce the RSP of raw liquid products from coal liquefaction by about 30 percent if the assumptions made in this study can be verified experimentally. This conclusion is based on the comparison between the coal-only case (Case 4) where the RSP is $40 per barrel and Case 2 where coal, plastics, and waste oil are coprocessed together to yield an RSP of only $28 per barrel. The primary reasons for this significant decrease in the RSP of products from coprocessing lies in the high liquid yields obtained from the plastics and oils, and the lower hydrogen requirement compared to coal liquefaction by itself. Plastics and oils have hydrogen contents of about 14 weight percent compared to coal at only about 5 percent, therefore considerably less hydrogen is required to make liquid hydrocarbons from coprocessing a mixture of plastics and coal. Obviously, the larger the quantity of plastics in the mix the less hydrogen is required and hence the better the resulting economics. The other conclusion from this study is that siting such a coprocessing facility adjacent to an oil refinery offers opportunities for integration and hence can reduce costs. However, since this study is based on little actual continuous performance operations in a coprocessing mode, a comprehensive bench and continuous scale research and development program is needed to verify the assumptions made in this paper and to optimize coprocessing performance.

These above cases were all based on the assumption that the acquisition costs of wastes were zero at the plant gate. This implies that the costs of transporting the wastes to the plant are balanced by the savings in tipping fees. A sensitivity to this assumption has been investigated in this study, and the economic impact on the RSP of products by varying the acquisition costs has been estimated. If tipping fees are increased in the future so that the plant gate acquisition cost is negative $20 per ton, then the RSP of liquids drops to about $23 per barrel. If, on the other hand, acquisition costs are greater than zero, for example +$20 per ton, then the RSP of liquids would rise to about $32 per barrel.

The overall economic potential for this concept of coprocessing coals and waste materials to make transportation fuels does offer considerable promise. The roles that coal may play in this concept can be summarized as follows: coal allows process flexibility by acting as a feedstock flywheel to stabilize the system during periods of waste feedstock variability; the plant output can be doubled by using up to 60 percent coal and hence benefits of scale can be obtained;

there may be potential chemical synergy with coal by scavenging heavy metals in the coal ash; there may be a catalytic effect of the carbon black in tires; the hydrogen donor recycle solvent from the coal may assist the kinetics of plastics and rubber dissolution; there may be an ability to neutralize chlorine from PVC by coprocessing with low rank coals having alkaline mineral matter; coal allows several different wastes to be utilized simultaneously.

REFERENCES

1) Personal communication, Burns and Roe Services Corporation.
2) Denhof, D., *Bridging the Experience Gap: Burning Tires in a Utility Boiler.* "Solid Waste and Power", Mar-Apr 1993.
3) Volk, William P, *Texaco Tire Liquefaction for Gasification and Other Uses.* Texaco Inc. Nov 1993.

ACKNOWLEDGMENT

This work was supported at the MITRE Corporation by Sandia National Laboratories which is funded by the United States Department of Energy under contract number DE-AC04-76DP00789.

Table 1. Cases Analyzed

Feed (TPD)	Case 1	Case 2	Case 3	Case 4
Plastics	866	866	866	—
Coal (dry)	872	872	872	1,728
Petroleum Coke	1,248	1,248	1,225	1,095
Waste Oil	—	210	210	—
Tires	—	—	135	—
Total C_3^+ Products (BPSD)	8,830	10,170	10,455	7,360

Table 2. Economic Summary ($MM)

	Case 1	Case 2	Case 3	Case 4
Capital				
CTSL	110	110	110	110
Hydrogen	97	97	98	97
CSD	10	10	10	11
Other	28	28	28	28
	245	245	246	246
Tire Dissolution	0	0	15	0
Total Capital	332	332	350	338
Operating Costs				
Feedstock	7	7	7	14
Waste Prep	6	6	7	0
Power	17	17	17	17
Other	23	24	26	25
Gross O&M	53	54	57	56
Netbacks	-17	-17	-17	-8
Net Operating	36	37	40	48
RSP $/Bbl	32	28	29	40

Figure 1. Waste/Coal Coprocessing—Refinery Integration

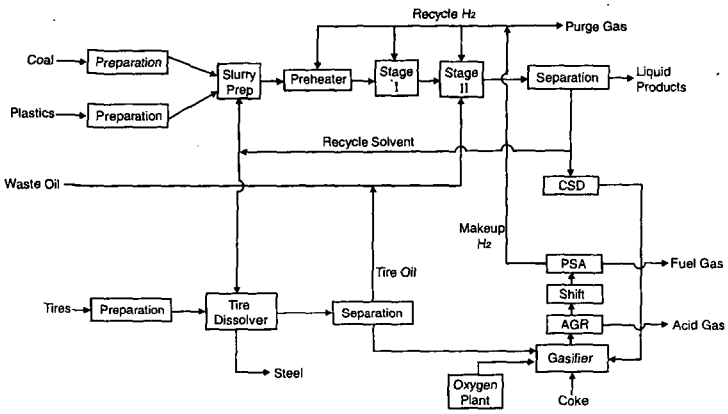

VIABILITY OF CO-LIQUEFYING COAL AND PLASTIC WASTES

Anthony Warren and Mahmoud El-Halwagi
Chemical Engineering Department
Auburn University

ABSTRACT

Efforts have been undertaken to assess the technical and economic feasibility of a new process for co-liquefying coal and plastic wastes. This assessment is based on incorporating recent experimental data on plastic/coal liquefaction within a conceptual process framework. A preliminary design was developed to co-liquefy 30,000 kg/hr of plastic waste with an equivalent amount of coal on a weight basis. The plant products include hydrocarbon gases, naphtha, jet fuel and diesel fuel. Material and energy balances along with plant-wide simulation were conducted for the process. Furthermore, the data on plastic-waste availability, disposal, and economics have been compiled. The results from the economic analysis identify profitability criteria for gross profit and return on investment based on variable conversion, yield, and tipping fee for plastic waste processed.

INTRODUCTION

Finding cost-effective energy sources has been a rising concern of our nation for the past twenty years. Coal liquefaction research is at the forefront of potentially feasible options for two reasons. One reason is that coal is the most abundant natural resource readily available in the United States. Furthermore, when coal is liquefied a liquid fraction is produced which can be upgraded to yield transportation fuels (e.g., jet fuel, gasoline, diesel fuel, etc.). At present, the liquefaction of coal alone is not economically feasible. One way of rendering the liquefaction process feasible is to include additional raw materials (e.g. municipal solid waste) that can significantly alter the process economics.

In addition to the energy problem, environmental issues have also been the focus of public attention. The solid-waste problem has escalated to a staggering magnitude. Efficient ways of disposing of/converting solid wastes must be determined. Thus, more focus has been placed on co-processing of coal with waste materials (e.g., tires, plastics, cellulosic material, waste oil, etc.). This alternative is attractive mainly because the waste materials, when co-processed with coal, provide a raw material that increases production capacity and can improve the process economics. This directly offers hope for potential commercialization.

Recent research efforts (Taghiei et al., 1993; Anderson and Tuntawiroon, 1993) have shown that the conversion of coal and plastic waste into liquid fuel is possible on a lab scale. This conversion is achieved by processing coal and waste plastics at a relatively high temperature (400 - 450 ^{o}C) and moderate to high hydrogen pressure (800 - 2000 psi). Conversion as high as 100% is achievable for reactions involving plastic waste alone with yields to the oils fraction ranging between 86 - 92% (Taghiei et al., 1993). However, coal/plastic mixtures attain somewhat lower conversions and yields ranging from 53 - 93% and 26 - 83%, respectively. The oil fraction is the portion of the product that can be refined to yield naphtha, light, middle, and heavy distillates. Therefore, it is important to achieve good conversion and to attain high yields to oils.

The objective of this paper is to provide a technical and economic assessment of co-liquefying coal and plastic waste. First, the availability and current technologies for utilizing plastic waste is reviewed. Then, the problem to be addressed in this work is formally stated. A process flowsheet is conceptualized. Then, the material and energy balances for the process along with a plant-wide simulation using the software ASPEN PLUS will be undertaken. Finally, the economic aspects of the process will be analyzed and some profitability criteria will be assessed.

PLASTIC WASTE AVAILABILITY AND CONVERSION

Each year, our nation produces an estimated 58 billion pounds of plastic resin 90% of which are used in the United States (Hegberg et al, 1992). Lat year, approximately 32 billion pounds of plastics have entered into the municipal solid waste [MSW] stream as post-consumer plastic waste. The MSW generated annually totals 200 million tons and is composed of yard wastes (17.6%), paper (40%), metals (8.5%), glass (7.0%), plastics (8.0%), food wastes (7.4%), and other material (11.6%). Although plastics make-up only 8% of the MSW by weight, of the estimated 400 million cubic meters of annual MSW, plastic wastes are responsible for 20%. This fact creates a major concern for the dwindling legal landfills that already have limited room. Landfilling as an option of disposal is becoming an expensive, undesirable alternative. The average cost for landfilling today is $20/ton and can be as expensive as $150/ton depending on location. Landfills are also becoming unacceptable because of social and public-health reasons (e.g. they provide breeding grounds for mosquitoes). Despite the problems associated with landfilling, the low recycling rates for plastics (<1.5%) suggest that plastics end up in landfills or are perhaps illegally dumped.

PROCESS CONCEPTUALIZATION AND SIMULATION

The first step in designing the process for co-liquefying coal and plastic wastes is to develop a conceptual flow sheet. The conceptualized process flow diagram is schemtically illustrated in Figure 1. The waste plastics are sent to a shredder which chips the plastics into processible pieces. Coal is first crushed then distributed to the slurry mixer and to hydrogen generation. The waste plastics and crushed coal are mixed with a recycled solvent to form a slurry. This slurry mixture is fed to a preheater. The preheated slurry is then forwarded to an adiabatically operated reactor which yields vapor, liquid and solid products. The vapor, leaving the reactor at 800 °F and 2200 psi, is first relinquished of hydrogen which is recycled back to the reactor after being mixed with the fresh hydrogen feed. The remainder of the stream is then separated into vapor and liquid products by utilizing a flash column. The gas leaving this flash column is sent to an acid-gas removal system. The remaining gas consists of light petroleum fuel gases. The removed hydrogen sulfide is processed in a Claus unit to yield elemental sulfur. The slurry leaving the reactor is first flashed in the gas oil column. The column yields a vapor product which contains most of the valuable hydrocarbon fractions. The bottom product leaving the column includes heavy hydrocarbons along with the unreacted coal and ash. The vapor stream leaving the gas-oil flash column is hydrotreated and distilled to yield light, middle and heavy distillates. A hydroclone is employed to process the bottoms from the gas oil flash column. The product leaving the top of the hydroclone contains the heavy boiling point fraction (>650 °F). This fraction is recycled to the slurry mixer as a hydrogen-donor solvent. Additional liquid from the fraction is removed using the Wilsonville evolved Residuum Oil Supercritical Extraction-Solid Rejection [ROSE-SR] unit. The recovered liquid is combined with the recycled solvent and this mixture is returned to the slurry mixer. The solid effluent from the ROSE-SR unit, along with some fresh coal, are then used to generate hydrogen needed for processing. A useful fuel gas is also produced in the hydrogen generation process.

Having developed a conceptual flow sheet for the process, one is now in a position to simulate the plant and conduct the necessary calculations for material and energy balances as well as other technical aspects. Material and energy balances for the plant have been conducted. In addition, a plant-wide simulation has also been undertaken using the software ASPEN Plus. Optimization of some units/systems has been carried out to minimize capital and operating costs. In order to yield an environmentally benign plant, the removal and recovery of the sulfur by-product has been achieved via a desulfurization system. Heat integration has also been done for all process streams.

ECONOMIC ANALYSIS

In this section, the economic aspects of this co-processing plant are discussed. Fixed capital investment, total capital investment, total production cost, and annual revenue is evaluated initially. Next, a profitability analysis is accomplished by analyzing the effects of varying conversion, yield and tipping fee on process economics.

Fixed Cost Estimation

Estimation of fixed cost is done by identifying the total purchased equipment cost by relating equipment capacity to cost utilizing available data in literature (e.g., Peters and Timmerhaus, 1991). In particular, the cost of several pieces of equipment was determined by scaling-down based on a recent Bechtel/Amoco study (US DOE-PETC, 1993). This DOE-funded study provides an extensive economic evaluation of direct coal-liquefaction in which Illinois #6 coal is liquefied to yield naphtha, light, middle, an heavy distillates. Design aspects throughout the plant were taken from several pre-existing liquefaction projects (Breckinridge, Wilsonville, HRI, etc.). Based on the capacities of the pieces of equipment needed in this co-liquefaction study, the cost may be calculated using the suggested Bechtel/Amoco scaling exponent of 0.71. For example, at 70% conversion and 90% yield, the total purchased equipment cost is about $77 million. The liquefaction system (reactor, ebullating pumps, etc.), accounting for $42 million (approximately 55% of the total purchased equipment cost. This high cost is due to the very specialized design of the ebullated-bed liquefaction system needed for this type of conversion. From this purchased equipment cost, the fixed and total capital investments were estimated to be $373 million and $439 million, respectively.

Total Production Cost

The total production cost has two components; operational and depreciation costs. The main contributors to operational cost are the cost of shredding plastic waste and the cost of raw material and catalyst needed for liquefaction and hydrogen production. The plant utilizes 30,000 kg/hr of waste plastics that must be shredded before being processed. The cost of shredding is about 5 million/yr based on plant operation of 8760 hours per annum and unit cost for shredding of $0.02/kg. The cost of raw material is an important element in calculation of operational cost. This plant also utilizes and additional 20,000 kg/hr of coal for the production of hydrogen which costs about $10 million/yr (based unit cost for coal of $20.5/ton). The amount of catalyst needed for liquefaction and hydrogen generation can be calculated by scaling down based on capacities and cost available in literature (US DOE-PETC, 1993) and assuming that the catalyst cost-capacity functionality behaves linearly. The estimated cost of catalyst for this facility is about $7 million per annum. Also, waste plastics may have a positive raw material cost if incoming plastics to be processed is paid for, or a negative raw material cost (i.e., generate revenue) if a tipping fee is charged for all incoming plastics to be processed. This issue will be discussed later. The total annual operating cost, excluding depreciation, is approximately 22 million/yr. By using a 10-year straight-line depreciation scheme, one obtains an annual total production cost of $59million/yr for conversion and yield of 70% and 90%, respectively. Similarly, the total production cost can be evaluated at various conversions and yields.

Annual Sales

Annual revenue which is obtained in this facility is partially attributed to the sale of the liquid and gaseous fuels produced in process. At 90% yield and 70% conversion, $60,000 kg/hr of oil and gaseous products is produced. The average value of oil was assumed to be $0.68/gal, which translates into $79 million per annum. Revenue can also gained via tipping fees charged for all plastic waste processed at this facility. Annually, 263 million kilograms of plastic waste are processed in this facility. Processed plastic wastes can potentially generate revenue. For example, this facility can function as a non-conventional waste-management facility at which plastic waste material is disposed. In this case, a tipping fee is charged for all waste materials disposed/processed. The tipping fees will increase the

annual revenue generated. In general, plastic wastes can be a source of revenue (via tipping fees) or an expenditure (through vendor charges). For this case study, the tipping fee was varied from free disposal (-$0.06 to 0.02/kg). The $ 0.02/kg corresponds to the plant collecting two cents on each kg of plastic waste as tipping fees. On the other hand, -$0.06/kg corresponds to a post-consumer plastic material which is purchased from a vendor for six cents per kilogram. At a tipping fee of $0.02/kg, as shown in Figure 2, the annual revenue generated from processing waste material is about $5 million. This leads to a total annual revenue of $84 million for the entire plant. At a tipping fee of -$0.06/kg (the least profitable scenario), 70% conversion, and 90% yield, the annual cost of processing plastic waste material is approximately $16 million. The total annual revenue for this scenario is about $63 million.

Profitability

Two important indicators, commonly used in economic assessment, are gross profit and return on investment [ROI]. Gross profit is defined as the difference between the total annual revenue and the total production cost. ROI is determined by dividing this gross profit by the total capital invested. Gross profit and ROI were calculated for several scenarios which include a range of 70 to 90% for yield, 15 to 90% for conversion, and -$0.06 to 0.02/kg for tipping fee. As conversion increases, profitability also increases. For example, at 70% conversion, 90% yield, and a tipping fee of $0.02/kg, the gross profit is $25 million, as shown in Figure 2. By recalling that the total capital investment for degree of conversion and yield is 439 million dollars, the ROI is approximately 5.7%, as shown is Figure 3. The most profitable scenario assessed in this case-study exists at 90% conversion, 90% yield, and a $0.02/kg tipping fee. For this case, the annual gross profit and ROI have been determined to be approximately 30 million and 7.8%, respectively.

CONCLUSIONS

We have conducted a survey of the current status and availability of plastic wastes. Technical assessment of the proposed conceptual plant, process simulation, and economic analysis have be undertaken. Preliminary screening reveals that it is readily feasible to break-even at reasonable conversion, yield, and tipping fee. In this case, a co-liquefaction facility may be viewed as a waste-management facility for the disposal of plastic waste material and generation of fuel. However, if high ROI and annual gross profit are required, higher tipping fees must be charged for processing waste plastic material or further research must be conducted to identify ways of attaining higher conversion and yield.

BIBLIOGRAPHY

Anderson, L. L. and W. Tuntawiroon, "Co-Liquefaction Coal and Polymers to Liquid Fuels", Preprints of ACS Meeting, Chicago, pp. 816-822, August 1993.

Taghiei , M. M., F. E. Huggins and G. P. Huffman, "Co-Liquefaction of Waste Plastics with Coal", Preprints of ACS Meeting, Chicago, pp. 810-815, August 1993.

Hegberg, B., G. Brenniman, W. Hallenbek, 1992, "Mixed Plastics Recycling Technology", Noyes Data Corporation, Park Ridge, NJ.

Peters, M. and K. Timmerhaus, 1991, "Plant Design and Economics for Chemical Engineers", 4th ed., Chemical Engineering Series.

U.S. DOE Pittsburgh Energy Technology Center [PETC], 1993, "Direct Liquefaction Baseline Design and System Analysis", Final Report on Baseline and Improved Baseline, vol. IIa, March.

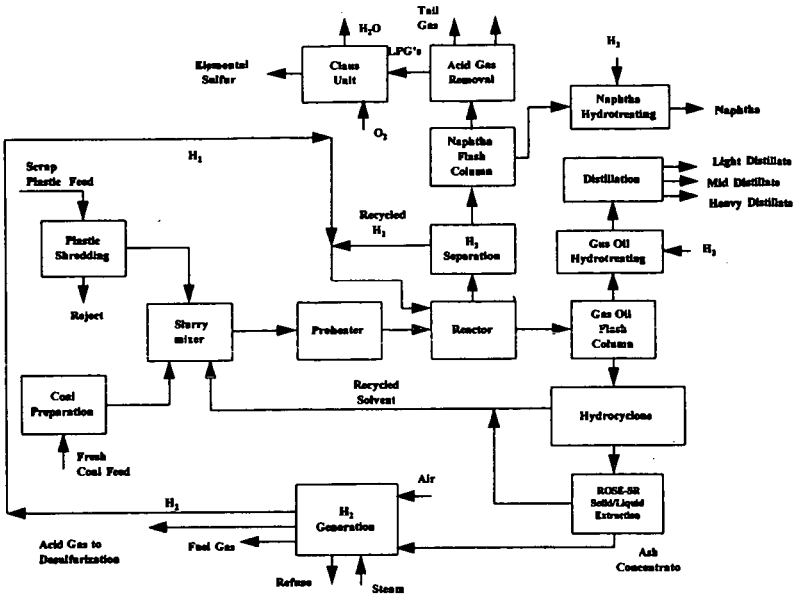

Figure 1: Conceptual Process Flow Diagram for the Co-Liquefaction Plant

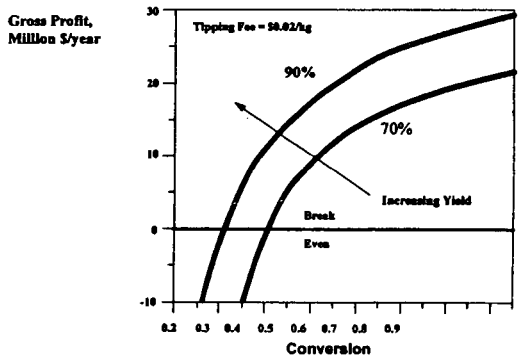

Figure 2: Gross Profit

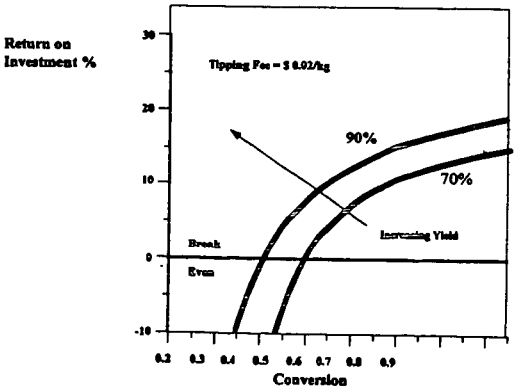

Figure 3: Return on Investment

CO-CONVERSION OF COAL/WASTE PLASTIC MIXTURES UNDER VARIOUS PYROLYSIS AND LIQUEFACTION CONDITIONS

S.R. Palmer, E.J. Hippo, D. Tandon and M. Blankenship
Department of Mechanical Engineering and Energy Processes,
Southern Illinois University at Carbondale,
Carbondale, Illinois 62901-6603, USA.

Keywords: Copyrolysis, coliquefaction, coal/waste plastic

INTRODUCTION

For strategic and economic reasons the conversion of coal to liquid fuels has been a constant goal of the coal science community (1). Although the economics of coal liquefaction are primarily governed by the price of crude oil, other factors such as the need for large quantities of hydrogen gas, play an important role. If methods could be found that reduce the amount of hydrogen gas required for liquefaction, considerable benefits would be realized. To explore this possibility the use of waste plastics as materials capable of upgrading coal into liquid fuel products has been investigated.

The use of waste plastics for this purpose could become possible because over 30 million tons of synthetic polymer material is produced in the United States every year (2). Some projections estimate that this production will double by the year 2000 (3). The vast majority of this material ends up in the waste stream and is simply landfilled. It is estimated that of the 160 millions tons of municipal solid waste that needs disposal every year in the United States, waste plastics contribute 7-9% by weight and over 20% by volume (4,5). 70% of the discarded plastic is derived from packaging materials of which polyethylene (PE) represents 63%, polypropylene (PP) 9%, polystyrene (PS) 11%, polyvinyl chloride (PVC) 5% and poly(ethylene terephthalate) (PET) 7%.

The concept of using waste plastic to aid the liquefaction of coal is based on the premise that the hydrogen present in many waste plastics can be used to hydrogenate coal. It is believed that this would be possible because waste plastics usually have very high hydrogen contents (14.3 % for PE and PP) compared to most raw coals (5-6%). It is anticipated that coal/waste plastic co-pyrolysis procedures could allow for hydrogen migration from the plastic to the coal via radical abstraction and radical combination reactions. This would increase the hydrogen content of the coal so that either, liquid fuels could be formed directly, or less hydrogen gas would be required during subsequent liquefaction and upgrading.

This concept has been investigated by several research groups. Most studies have involved co-pyrolysis in a hydrogen atmosphere with added catalysts (6-11). It has been found that higher conversions to oil are obtained using a hydrogen versus an inert atmosphere (7) and that molybdenum based catalysts can also improve liquid yields. In many instances it has been determined that although conversions for individual materials are high, when they are mixed together liquid yields are somewhat diminished (8). Rubber tires have been found to enhance coal liquefaction, presumably via hydrogen donation, while PS and PE are reported to enhance the hydrocracking of coal (9).

In this study co-conversion experiments were performed on single plastics, an Illinois No.6 coal and coal/plastic blends. After initial screening studies using a thermogravimetric analyzer (TGA), several pyrolysis/liquefaction environments were examined using stainless steel microreactors. Pyrolysis was conducted in nitrogen, steam and hydrogen environments, while liquefaction reactions used tetralin/H_2 conditions. Various reaction times and temperatures were investigated. No added catalysts were used in these experiments.

EXPERIMENTAL

Materials

Samples of PE, PS and PP were obtained from Aldrich Chemical Company. The coal sample (Illinois No. 6) was obtained from the Coal Research Center at Southern Illinois University at Carbondale. The coal was physically cleaned to remove mineral matter

via a combination of micronization and centrifugation in a solution of cesium chloride of 1.6 specific gravity. Ultimate analysis of the cleaned coal sample gave: 76.2% C, 5.02% H, 1.07% N, 2.79%S, 3.89% ash and 7.32% moisture. (All reported on a dry basis except moisture.)

Thermogravimetric Analysis
Initial screening experiments were performed on a Perkin-Elmer TGA7 using a sample weight of about 10mg. An inert gas flow of nitrogen was maintained throughout the heating period which was ramped from room temperature to 1000°C at 15°C per minute. Weight loss was measured continuously at a frequency of 0.2Hz. Pyrolysis profiles were presented as a function of weight loss versus temperature and also as a first derivative of weight loss versus temperature.

Microreactor Experiments
The microreactor apparatus used consisted of a 15 mL stainless steel tube type reactor sealed at one end but open to a three-way valve at the other. The other connections to the three-way valve incorporated a gas sampling device to acquire gas samples, a 2000 psi safety valve, a pressure transducer, and a quick-connect/disconnect assembly for easy gas charging. Typical co-conversion experiments used a 2g charge of coal, plastic or coal/plastic mixture. After the sample was loaded, air was eliminated from the system by repeatedly pressurizing then depressurizing with the desired gas (nitrogen or hydrogen). The microreactor was then immersed in a fluidized sand bath maintained at the desired reaction temperature. After completion of the reaction period the microreactor was cooled in a cold fluidized sand bath. (A cold water bath was found to cause the development of leaks in the microreactor set-up.) The microreactor was continuously shaken throughout the reaction period. When steam and tetralin were used, 2 mL of distilled water or tetralin were added to the microreactor respectively. A cold pressure of 500psig of hydrogen was used for the hydropyrolysis and liquefaction experiments. Conversions were measured via extraction of the products with tetrahydrofuran (THF) using soxhlet apparatus. The percentage conversion is given by the difference in weight between the original charge and the THF insoluble material, divided by the original charge weight.

RESULTS

Thermogravimetric Analysis of Co-pyrolysis
Initial examination of the behavior of a co-pyrolyzing system using the TGA suggested that there was significant interaction between the components of the system. This data has been examined in some detail and has been submitted for publication and therefore will receive only brief mention here. Generally it was found that characteristic pyrolysis parameters such as the temperature of weight loss onset, the temperature of maximum rate of weight loss, the temperature of final char formation and the temperature range of volatilization are all dramatically altered by the presence of another component in the system. For example, the presence of coal appears to retard the volatilization of both PP and PE such that the observed weight loss onset temperatures for the coal/plastic mixtures are higher than either the coal or the plastic. Also, the addition of PP and PE to coal appears to aid the conversion of the coal. Lower normalized chars yields are obtained when these plastics are co-pyrolyzed with the coal. In addition, these increased coal conversion are obtained at much lower temperatures than when the plastic is absent. These results point to an interaction between the coal and plastic as they both pyrolyze. Such interactions are necessary if our goal of liquefying coal using waste plastics is to be realized.

Microreactor studies
i) Conversion in Nitrogen:- Table 1 reports the conversions of single materials and their 1:1 blends obtained at various temperatures during a one hour standard reaction time. In general, conversions increase up to a temperature of 425°C where they remain constant until about 475°C after which they tend to decline. This can be attributed to the initial decomposition of the plastics into soluble materials at the lower temperatures, but then to the formation of char at higher temperatures. In general, the conversion data for the 1:1 blends in a nitrogen pyrolysis atmosphere is very close to that predicted by simply averaging the conversions of the individual components. This is an indication that the apparent synergisms observed in the TGA experiments do not transfer to confined microreactor tests.

In another two series of experiments the pyrolysis temperature was held constant at 425° C and 475° C respectively, but the reaction time varied from 5 minutes to 2 hours. It was found that in most cases maximum conversions were obtained after only 15 minutes. In general, longer reactions times did not improve the conversions and in some cases actually led to diminished conversions. This indicates a tendency towards char formation at longer reaction times. Small synergistic conversions for some coal/plastic blends were observed at the shorter reaction times. At longer reaction times this apparent synergism was lost.

ii) Conversion in Steam:- Table 2 reports conversions obtained at various temperatures in a steam atmosphere. Both 5 minute and one hour reaction times were investigated. In general, coal conversion of 25 to 30% was obtained which is similar to that obtained in nitrogen. The plastic conversions in a steam environment were somewhat lower than they were under nitrogen. Thus, the steam appears to retard plastic depolymerization. Some apparent synergistic conversion of the coal/plastic blends is observed especially for the coal/PP mixture. However, most of this synergism appears to result from the retardation of the plastic decomposition under steam. In general, the conversion values obtained for the blends in the steam atmosphere are similar to those obtained in nitrogen.

iii) Conversion in Hydrogen:- The conversions obtained using various temperatures with a 5 minutes and one hour reaction time in 500 psig (cold pressure) hydrogen are reported in Table 3. Somewhat surprisingly the conversions obtained for both the individual materials and the blends were similar to those obtained in nitrogen. Thus, the presence of hydrogen does not appear to enhance the conversion of these materials to soluble products.

iv) Conversion in Hydrogen/Tetralin:- Table 4 reports conversions obtained using 500 psig hydrogen and a 1:1 tetralin to charge ratio. Not surprisingly coal conversions are significantly higher in the liquefaction environment. However, the conversion of the individual plastics appears to be dramatically inhibited by these liquefaction conditions. Indeed, PP conversions as low as 14% were observed after 15 minutes at 425° C in the presence of tetralin and hydrogen gas. Under similar conditions in a nitrogen environment a PP conversion around 95-100% is observed. In some case the total conversions of the coal/plastic blends do not show that much improvement over those obtained in the other pyrolysis environments. However, other coal/plastic mixtures, especially those involving PP, do show higher conversions in the liquefaction environment compared to the other pyrolysis environments. Due to the low conversions of the individual plastics, the conversions of the coal/plastic blends often indicate significant synergistic conversion. Either short time high temperature or long time low temperature conditions appear to give the best results.

v) Product analysis:- Ultimate analysis was performed on some of the insoluble residues obtained from the microreactor experiments. Although the data is preliminary at this time it is clear that many of the insoluble residues from the co-pyrolysis and co-liquefaction experiments have very high volatile matter contents. For instance, a coal/PE blend reacted at 400° C in the liquefaction environment gave a conversion of 60% based on THF solubility. However, the residue was found to contain a 90% volatile yield when heated in the TGA. If we assume all the material soluble in THF is volatile, then distillation of this product would give a distillate yield of 95%. Comparison of elemental compositions showed that the residues derived from coal/plastic blends were depleted in sulfur but enhanced in hydrogen compared to the residues derived from the coal alone. This suggests that hydrogen was transferred from the plastic to the coal and helps to explain the high volatile matter contents of many of the insoluble residues.

SUMMARY AND CONCLUSIONS

Initial investigation of the co-pyrolysis behavior of coal with plastics using a TGA indicated that there were significant interactions between the coal and plastic as both degraded simultaneously. These interaction led to increased coals conversion at lower temperatures. Attempts to repeat these results using microreactors were only partially successful with much of the synergism that was observed during the TGA experiments apparently being lost when the larger scale and higher pressure microreactors were used. This discrepancy between the TGA and microreactor conversion data should not be that surprising since the TGA conversions are based on distillate yield whereas

microreactor conversions are based on solubility in THF. Indeed, many of the THF insoluble residues from the microreactors contain significant volatile matter contents which would have been reported as converted material in a TGA analysis.

In general, it was found that the conversion of pure plastics to liquid or gaseous products was almost complete during pyrolysis experiments but was significantly retarded in a liquefaction environment. On the other hand the highest conversions of coal and coal/plastic blends, especially coal/PP blends, were achieved under these liquefaction conditions. The majority of the conversion values obtained in a reactive pyrolysis environment such as steam or hydrogen, were very similar to those obtained in an inert nitrogen atmosphere. In some instances the presence of the steam or hydrogen gas appeared to hinder the formation of THF soluble material. Throughout the series of co-conversion systems examined in this study there was a general trend towards lower conversions with increasing process temperature and increased reaction time. This is attributed to char formation under these conditions. Although the results gathered so far are preliminary in nature, it can be appreciated that the use of waste plastics in coal liquefaction processes has great potential.

ACKNOWLEDGEMENTS

We would like to thank the following for support of this research: Illinois Clean Coal Institute (project No. 93-1/1.1B-2M), United States Department of Energy (grant No. DE-FC22-92PC92521), Office of Solid Waste Research at the University of Illinois, and the Materials Technology Center at SIUC.

REFERENCES

1. Farcasiu, M. PETC Review, 1991, p4-15.
2. Ainsworth, S.J. Chemical and Engineering News, August 31 1992, p34-55.
3. Reisch, M.S. Chemical and Engineering News, May 4 1992, p29-42.
4. Erwin, L. and L.H. Jr. Healy. Packaging and Solid Waste. Management Strategies. 1990, American Management Association, New York.
5. Hegberg, B.A., G.R. Brenniman, and W.H. Hallenbeck. Technologies for recycling post-consumer mixed plastics. 1991, University of Illinois.
6. Taghiei, M. M., Huggins, F.E. and Huffman, G.P. Am. Chem. Soc. Div. Fuel Chem. Prepr., 1993, 38(3), pp 810-815.
7. Liu, K., Jakab, E., McClennen, W.H. and Meuzelaar, H.L.C. Am. Chem. Soc. Div. Fuel Chem. Prepr., 1993, 38(3), pp 823-830.
8. Anderson, L.L and Tuntawiroon, W. Am. Chem . Soc. Div. Fuel Chem. Prepr., 1993, 38(3), pp 816-822.
9. Ibrahim, M.M. and Seehra, M.S. Am. Chem. Soc. Div. Fuel Chem. Prepr., 1993, 38(3), pp 841-847.
10. Orr, E.C., Tuntawiroon, W., Anderson, L.L. and Eyring, E.M. Am. Chem. Soc. Div. Fuel Chem. Prepr., 1994, 39(4), pp 1065-1072.
11. Hodek, W. Proc. Int'l. Conf. Coal Sci., 1991, Newcastle-Upon-Tyne, pp782-785.

TABLE 1.

Conversions obtained after 1 hour in a nitrogen atmosphere.

Temperature	Coal	PE	PP	PS	Coal/PE	Coal/PP	Coal/PS
350	21		35	97	62	13	
400	26	55	97	98	63	57	50
425	27	100	98	99	64	60	60
450	26	99	99	99	64	59	55
475	23	99	94	100	63	60	57
500	27	89	91		54	56	
525	31	85	85	83	55	60	57
550	23	82	79	84	56	54	52

Table 2.

Conversions obtained in a steam pyrolysis atmosphere

	5 minutes			60 minutes	
	425°C	475°C	525°C	425°C	475°C
Coal	24	30	25	26	18
PE	32	35	98	95	60
PP	70	82	79		70
PS				94	93
Coal/PE	35	50	57	64	60
Coal/PP	54	50	57	51	
Coal/PS				64	62

Table 3.

Conversions obtained in a hydrogen pyrolysis atmosphere

	5 minutes			60 minutes		
	425°C	475°C	525°C	425°C	475°C	525°C
Coal	27	25	20	20	25	24
PE	23	95		97	96	93
PP	26	99	95	96	87	87
Coal/PE	32	55	63	50	58	58
Coal/PP	66	58	60	63	57	58

Table 4.

Conversions obtained in a liquefaction environment.

	15 minutes			60 minutes		
	400°C	425°C	450°C	400°C	425°C	450°C
Coal	55	51	54	52	62	52
PE	45	47	79	42	48	70
PP	10	14	82	39	53	96
Coal/PE	60	40	60	44	62	
Coal/PP	61	62	84	79	71	73

DIRECT LIQUEFACTION OF PLASTICS AND COLIQUEFACTION OF COAL-PLASTIC MIXTURES

G.P. Huffman*, Zhen Feng*, Vikram Mahajan*, P. Sivakumar+, H. Jung+, J.W. Tierney+, and Irving Wender+; *CFFLS, 341 Bowman Hall, University of Kentucky, Lexington, KY 40506-0059; +Department of Chemical & Petroleum Engineering, University of Pittsburgh, Pittsburgh, PA 15261

Introduction

In previous work,[1] we have investigated the direct liquefaction of medium and high density polyethylene(PE), polypropylene(PPE), poly(ethylene terephthalate)(PET), and a mixed plastic waste, and the coliquefaction of these plastics with coals of three different ranks. The results established that a solid acid catalyst(HZSM-5 zeolite) was highly active for the liquefaction of the plastics alone, typically giving oil yields of 80-95% and total conversions of 90-100% at temperatures of 430-450 °C. In the coliquefaction experiments, 50:50 mixtures of plastic and coal were used with a tetralin solvent(tetralin:solid = 3:2). Using ~1% of the HZSM-5 catalyst and a nanoscale iron catalyst, oil yields of 50-70% and total conversions of 80-90% were typical. Our earlier work on the coliquefaction of paper(newsprint) with coal[2] also established that high total conversions were obtained; however, the gas yields were high, while the oil yields were moderate.

In the current work, we have conducted further investigations of the liquefaction reactions of PE and the coliquefaction reactions of PE, PPE and Black Thunder subbituminous coal. We have also investigated the coliquefaction reactions of PE, PPE, and newsprint. Several different catalysts have been used in these studies. Initial work has been completed on the direct liquefaction of a commingled waste plastic obtained from the American Plastics Council.

Experimental Procedure

The feedstock materials used in the work reported in this paper included medium density polyethylene (PE), polypropylene (PPE), a commingled waste plastic obtained from the American Plastics Council(APC), and a subbituminous coal (Black Thunder). Proximate and ultimate analyses for the coal and APC waste plastic are shown in Table 1. The experiments used 3 types of catalysts: a commercial HZSM-5 zeolite catalyst[2], an ultrafine ferrihydrite treated with citric acid(FHYD/CA), and a ternary Al/Si/ferrihydrite with Al:Si:Fe=1:1:18 ($FHYD_{0.90}/Al_{0.05}Si_{0.05}$). The ultrafine ferrihydrite catalysts are synthesized in our laboratory. For all runs, 1 wt.% of catalyst was added. Dimethyl disulfide (DMDS) was sometimes added to convert the ultrafine ferrihydrite to pyrrhotite during the reaction. The preparation, structure, and liquefaction activity of the ferrihydrite catalysts has been discussed in detail elsewhere[3,4].

The liquefaction experiments were conducted in tubing bomb reactors with a volume of 50ml which were shaken at 400 rpm in a fluidized sand bath at the desired temperature. The reaction times were 20-60 min. and the atmosphere in the bomb was either hydrogen or nitrogen (cold pressure 100-800 psi). Usually 5 g of plastic or plastic + coal with 7.5 g of solvent(tetralin and/or waste oil) were charged in the tubing bombs. The reactor was cooled in a second sand bath, and gas products were collected and analyzed by gas chromatography[5]. The other products were removed from the reactor with tetrahydrofuran (THF) and extracted in a Soxhlet apparatus. The THF solubles were subsequently separated into pentane soluble (oils) and pentane insoluble (PA + AS) fractions. Total THF conversion was determined from the amount of insoluble material that remained (residue). Any added catalyst was subtracted from the residue sample weight.

Table 1. Proximate and ultimate analyses of Black Thunder coal and APC commingled waste plastic used in this research.

Proximate[a]	Black Thunder Coal	APC Waste Plastic
% Ash	6.33	0.45
% Volatile	45.40	98.8
% Fixed Carbon	48.27	0.74
Ultimate[b]		
% Carbon	71.59	84.65
% Hydrogen	4.83	13.71
% Nitrogen	1.51	0.65
% Sulfur	0.49	0.01
% Oxygen	15.24	0.98

a = Dry basis, b = Dry ash free basis.

Results and Discussion

Previously, we have shown that a solid acid catalyst(HZSM-5 zeolite) is highly active for the liquefaction of PE, PPE, and mixed waste plastic. Some interesting new results for PE are shown in Figure 1, where it is shown that oil yields are not strongly dependent on hydrogen pressure. Moreover, the oil yield as determined by pentane solubility is as high under nitrogen as it is under hydrogen. The total conversion(THF soluble) was nearly 100% in all cases. Figure 1 also shows the time dependence of the reaction for PE in the presence of HZSM-5.

Figure 1. Liquefaction results for PE as a function of time and pressure. T=430 C, t=60 min., tetralin:PE=3:2, 1 wt.% HZSM-5

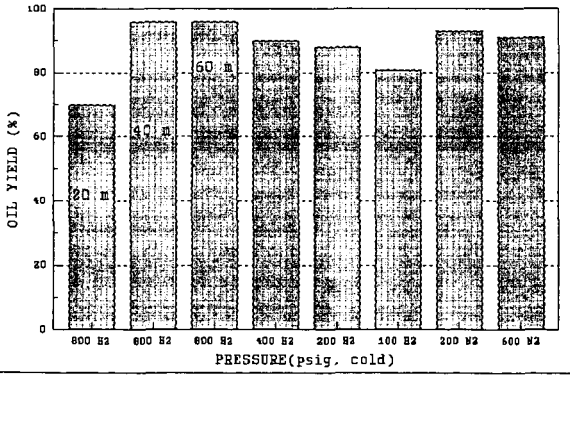

Our previous paper[1] examined the coliquefaction of a mixed waste plastic with both a bituminous and a subbituminous coal. Oil yields of 60-70% and total conversions of over 90% were observed in the presence of both the HZSM-5 catalyst and an iron catalyst(430 °C, 800 psi H_2-cold, 60 min., tetralin solvent). We are currently studying the response of individual plastic resins to various catalysts and conditions in more detail.

Some typical results are shown in Table 2. PE and PPE both respond strongly to the HZSM-5 catalyst. PPE also responds very well to the citric acid-treated ferrihyrite although PE does not. It is also seen that the mixtures of PE and coal do not liquefy as well as PPE-coal mixtures or as well as we observed previously for a mixed plastic[1]. Neither the HZSM-5 or the FHYD/CA catalyst has a strong effect on the liquefaction of PE-coal mixtures.

Table 2. Liquefaction results(yields in wt.%) for medium density polyethylene(PE), polypropylene(PPE), and 50:50 mixtures of PE and PPE with Black Thunder coal.

FEED	CATALYST	T (°C)	OIL	GAS	PA+A	TOT.
PE	NONE	430	26	1	39	65
PE	FHYD/CA	430	33	1	34	68
PE	HZSM-5	430	96	1	2	99
PE/COAL	NONE	430	41	3	26	69
PE/COAL	FHYD/CA	430	42	4	22	68
PE/COAL	HZSM-5	430	41	4	28	72
PPE	NONE	420	83	<1	4	88
PPE	FHYD/CA	425	98	2	0	100
PPE	HZSM-5	425	100	<1	0	100
PPE/COAL	HZSM-5	430	71	4	18	93

Some interesting results for a commingled waste plastic provided by the American Plastics Council are shown in Table 3. Here, we have examined the effect of varying both the catalyst and the solvent. It is seen that at 445 °C the nature of the solvent has a larger effect on the oil yield and total conversion than the catalyst. Both catalysts are moderately effective at this temperature; however, the solvent has a much larger effect, with the oil yields increasing from 30-40% to ~90% as tetralin is replaced with a waste motor oil.

Paper and other lignocellulosic wastes constitute a major fraction of the organic portion of municipal wastes. Previous work has focused on the coliquefaction of coal with lignocellulosic materials by two approaches: Route A used H_2, a molybdenum catalyst and tetralin, while Route B used CO and water in the presence of alkali.[2] Both approaches gave good results, although an improvement in product quality was achieved via Route B.

Table 3. *Liquefaction results(yields in wt.%) for APC waste plastic with different solvents and catalysts. Experiments conducted at 445 °C, 800 psig H_2(cold) in a tubing bomb, with 7.5 g of solvent and 5 g of plastic.*

FEED	CAT.	SOLV.	OIL+ GAS	OIL	GAS	PA+AS	TOTAL
W.PL	HZSM-5	OIL-7.5	89.3			5.1	94.4
W.PL	HZSM-5	TET.-2.5 OIL-5.0	88.4			5.7	94.1
W.PL	HZSM-5	TET.-5.0 OIL-2.5	66.8	63.7	3.1	17.8	84.6
W.PL	HZSM-5	TET.-7.5	42.9			12.3	55.2
W.PL	NONE	OIL-7.5	87.1			7.9	95.0
W.PL	NONE	TET.-2.5 OIL-5.0	48.6			27.1	75.7
W.PL	NONE	TET.-5.0 OIL-2.5	51.0	48.3	2.7	15.2	66.2
W.PL	NONE	TET.-7.5	35.8			23.2	58.9
W.PL	FHYD AlSi	OIL-7.5	90.9			4.8	95.7
W.PL	FHYD AlSi	TET.-2.5 OIL-5.0	61.8	58.4	3.4	21.2	83.0
W.PL	PHYD AlSi	TET.-5.0 OIL-2.5	51.2	48.6	2.6	22.2	73.4
W.PL	FHYD AlSI	TET.-7.5	30.2			16.5	46.7

In more recent work, a high conversion of plastics such as polypropylene, polystyrene and polyethylene terephthalate was achieved at 400 °C using Route B. With Route A, however, the conversion of polypropylene did not exceed 20% at 400 °C. Coliquefaction of coal and polypropylene in Route B showed an increase in the overall oil product and a decrease in the asphaltene fraction from coal. A similar effect was observed in the liquefaction of polypropylene and newsprint using Route B. Oxygen contents of liquid fuels from biomass are usually high, especially using the Route A process. However, the oxygen content of the oil product from Route B was less than 9% because of decarboxylation. The oxygen content of the oil from the coprocessing of polypropylene and newsprint was 3.5%.

Summary

New results for plastics liquefaction and coal-plastic coliquefaction suggest that the nature of the plastic, the solvent, and the reaction atmosphere can all have a significant on product yields. A thorough experimental matrix is needed to explore this parameter space. Further catalyst development aimed at producing cheaper, more robust catalysts for coal-waste plastic coliquefaction is required.

References:

1. M.M. Taghiei, Z. Feng, F.E. Huggins, and G.P. Huffman, Energy & Fuels, **1994**, *8*, 1228-1332.
2. H. Jung, J.W. Tierney, and I. Wender, ACS Div. Fuel Chem. Preprints, **1993**, *38(3)*, 880-885.
3. United Catalysts Inc., P.O. Box 32370, Louisville, KY 40232.
4. J. Zhao, Z. Feng, F.E. Huggins, and G.P. Huffman, Energy & Fuels, **1994**, *8*, 38-43.
5. J. Zhao, Z. Feng, F.E. Huggins, and G.P. Huffman, Energy & Fuels, **1994**, *8*, 1152-1153.
6. H.G. Sanjay, A.R. Tarrer, and Chad Marks, Energy & Fuels, **1994**, *8*, 99-104.
7. C.J. Lafferty, C. Eloi, R.K. Anderson, and J.D. Robertson, ACS Div. Fuel Chem. Preprints, **1994**, *39(1)*, 812.

INVESTIGATION OF FIRST STAGE LIQUEFACTION OF COAL WITH MODEL PLASTIC WASTE MIXTURES

Kurt S. Rothenberger, Anthony V. Cugini, Michael V. Ciocco,
Richard R. Anderson, and Garret A. Veloski
U. S. Dept. of Energy - Pittsburgh Energy Technology Center,
P.O. Box 10940, Pittsburgh, PA 15236

KEYWORDS: coal-waste coprocessing, liquefaction, plastics

INTRODUCTION

As part of the U.S. Department of Energy (USDOE) Fossil Energy program, the Pittsburgh Energy Technology Center (PETC) recently initiated research in coal-waste coprocessing. Coal-waste coprocessing is conversion to liquid feedstocks of a combination of any or all of the following: coal, rubber, plastics, heavy oil, and waste oil. The current effort is on the combined processing of coal, waste oil, and plastics. One reason commonly cited for coprocessing of coal and plastic materials is the higher hydrogen-to-carbon ratio in most plastics as compared to coal, which is hydrogen deficient relative to the petroleum-like liquids desired as products. Furthermore, the free radicals which are present in coal and believed to be produced in the early stages of coal dissolution could aid in the breakdown of plastic polymers.

In this study, screening tests have been conducted in microautoclave reactors, 1-L semi-batch stirred autoclave reactors, and a small-scale continuous unit. All tests employed Black Thunder subbituminous coal with plastic waste streams containing polyethylene (PE), polystyrene (PS), and poly(ethylene terephthalate) (PET) in various combinations and proportions. The materials and conditions were chosen to be compatible with those being investigated by other participants in the USDOE Fossil Energy program [1,2], including the proof-of-concept (POC) scale plant at Hydrocarbon Research, Inc. (HRI) in Princeton, NJ [3]. Due to the rapidly evolving nature of the coal-waste coprocessing initiative, many of the experiments reported here were designed to identify potential problem areas for scheduled runs on larger units rather than to systematically map out the chemistry involved with coliquefaction of coal and plastic materials. However, insights into both chemistry and operability of coal-waste coprocessing can be gained from the data.

EXPERIMENTAL SECTION

Materials. Liquefaction experiments were conducted with -200 mesh Black Thunder mine coal (Wyodak-Anderson seam, Campbell County, WY). High-density polyethylene (PE), melting point 135°C, density 0.96 g/mL, was manufactured by Solvay Polymers. Polystyrene (PS), melting point 95°C, was manufactured by BASF. Poly(ethylene terephthalate) (PET), melting point 215°C, density 1.4 g/mL, was manufactured by Hoescht Celanese as IMPET EKX-105. All plastics were supplied to PETC by HRI as 3.2-mm (1/8-in) extrudates. A mildly hydrogenated (9% hydrogen) fluid catalytic cracking (FCC) decant oil, obtained as the 340-510°C (650-950°F) fraction from run POC-1 on the proof-of-concept coal liquefaction unit at HRI, was used as a vehicle in the coal-waste coprocessing tests. Aged Akzo AO-60 Ni-Mo/Al_2O_3 catalyst was obtained from run POC-1 at HRI. Ni-Mo Hydrous Titanium Oxide (HTO) catalyst on Shell 324 blank was obtained from Sandia National Laboratory [4]. A dispersed sulfated iron catalyst (Fe-S) was prepared at PETC by precipitation of ferric ammonium sulfate in basic solution resulting in Fe_2O_3 doped with 3-4 wt% of SO_4 according to the method of Pradhan [5].

Reactions. Microautoclave reactions were conducted in 43-mL cylindrical, stainless-steel batch reactors constructed at PETC [6]. The base conditions of the tests were 2:1 hydrogenated FCC decant oil vehicle : coal-plastics mixture, one hour at 430°C, 7 MPa (1000 psi) cold hydrogen gas pressure, and 3.3 g aged Akzo AO-60 catalyst, although variations in time, temperature, and catalyst composition were also made. A detailed description of the reaction conditions for each run is listed in Table I. During workup, the reactor contents were sonicated in tetrahydrofuran (THF) for 30 minutes and subsequently filtered through a 0.45-micron filter under 40 psi nitrogen gas pressure. The THF soluble material was stripped of solvent on a rotary evaporator and re-extracted with heptane to produce a heptane soluble fraction. Conversion was calculated from the measured mass of insolubles adjusted for catalyst and coal mineral matter, based on the mass of plastic and MAF coal. The mass of the catalyst was also adjusted for the presence of entrained oil in the material as determined in a separate extraction step. The PE and PET plastics showed no significant solubility in either THF or heptane under the workup conditions used. PS did show appreciable solubility in THF, rendering those conversion calculations meaningless.

Four semi-batch (batch slurry, flow-through gas) tests were performed in a 1-L stirred-tank reactor system [7]. The feed charge consisted of 350 g of slurry that typically consisted of a 2:1 ratio of vehicle:feed with 30 g aged AO-60 catalyst. The feed compositions are listed in Table II. All tests were done at 430°C under 17.5 MPa (2500 psi) hydrogen gas pressure flowing at a rate of 1.9 L/min (4 SCF/h). The products were characterized in terms of gas yield and composition,

solubility in heptane and THF, and 450°C conversion [conversion of all material distilling above 450°C (850°F), including MAF coal, plastics, and 450°C+ oil, to material distilling below 450°C].

A continuous mode catalytic liquefaction experiment was conducted in a computer controlled 1-L bench-scale unit [7]. The unit is a once-through system without recycle. A typical charge consisted of a feed:vehicle mixture of 70:30 at an overall slurry feed rate of 146 g/h. The catalyst, 35 g of aged AO-60, was contained in an annular basket surrounding the stirrer to simulate the action in an ebullated bed. The coprocessing tests were done at a reactor temperature of 430°C under 17.5 MPa (2500 psi) of a 97% H_2 / 3% H_2S gas mixture flowing at a rate of 2.4 L/min (5 SCF/h). The system was run at the conditions listed in Table III. The products were characterized by distillation into three fractions - those boiling below 340°C (650°F), between 340°C-450°C (650°F-850°F), and above 450°C (850°F).

Gas and Pressure Analyses. Microautoclave reactor gas samples were collected at the completion of each run. Product gases were analyzed at PETC by a previously published method [8], and corrected for molar compressibility. Hydrogen consumption was calculated, based on the difference between initial and final (cold) gas pressure as adjusted for product gas composition [9]. Semi-batch unit gas samples were collected once slowly during the run (tail gas), and at its completion (flash gas). Hydrogen consumption was calculated, based on the assumption that the tail gas sample was representative of the gas make throughout the run.

Viscosity Measurements. Viscosity measurements were made to obtain data on feed mixtures in support of a continuous unit run. These measurements were conducted on a CANNON Model MV 8000 rotational viscometer equipped with an optional heating jacket and spindle capable of measuring viscosities as high as 500,000 cP at temperatures up to 260°C. The sample holder was loaded with 10.5 mL of material and tests were conducted over the temperature range corresponding to actual operating conditions. Viscosities were also measured over a series of sheer rates, again corresponding to unit operating conditions. Regressions indicated that the oil-coal-plastics mixtures are well represented as power law fluids.

RESULTS AND DISCUSSION

Microautoclave Tests. The THF conversion, heptane conversion, and hydrogen consumption results for the microautoclave reactions are found in Table I. The Black Thunder coal yields 83% THF solubles and 51% heptane solubles with the hydrogenated FCC decant oil vehicle at 430°C for 60 minutes with AO-60 catalyst. Under these conditions, PE does not convert. Whether the THF insoluble plastic product has undergone any degradation or molecular weight reduction as a result of processing cannot be determined from the data available. The negative conversion given in Table I is attributed to the fact that the PE probably melted over the catalyst surface, trapping some of the entrained oil in the catalyst, thus inflating the mass of the insoluble extraction residue. In these and the semi-batch experiments, sheetlike deposits of plastic were observed in the residual material, indicating unconverted PE was present and had re-solidified upon cooling. At a temperature of 465°C for 30 minutes, the PE does convert, yielding a light, grease-like mixture of wax and oil vehicle in the heptane solubles. However, about half of the PE ends up in the form of C, to C_4 gases with production of approximately 10 - 15 mmol each of methane, ethane, propane, and butanes. PE is expected to show random degradation along the polymer chain, as all the carbon-carbon bonds are equal [10]. Under the base conditions, PS converts quantitatively to heptane solubles. PS is expected to depolymerize to styrene monomer [10], which would subsequently hydrogenate to ethylbenzene (EtBz) in the reducing environment. EtBz has been observed in GC/MS and LVHRMS analysis of products from other PS-containing feeds, such as the HRI POC-2 run. In fact, PS converts to heptane solubles in the absence of catalyst. Under the base conditions, PET shows nearly quantitative conversion to heptane solubles. PET is expected to undergo scission at the C-O linkages, because they have a lower bond strength than the C-C bond [10]. Under hydrogenation conditions, this would yield two moles of carbon dioxide, one mole of ethane, and one mole of benzene, all requiring two moles of H_2 per mole of monomer. Substantial quantities of both carbon dioxide and ethane were observed, providing qualitative support to the postulated breakdown.

Several binary and multicomponent systems were studied. In Table I, the THF and heptane conversions are compared with those predicted from the assumption of a noninteracting system. A predicted conversion is calculated based on the assumptions that coal conversion is as given by run I; PE conversion to both THF and heptane solubles is zero; and PS and PET conversion to both THF and heptane solubles is 100. This simple assumption is able to predict the THF conversions of the five two-component and multicomponent runs of similar time, temperature, and catalyst composition (VIII, XI, XII, XVI, and XVII) surprisingly well, with average absolute deviations of about two percent. The heptane conversions are not predicted nearly as well by this method, with average absolute deviations of about five percent. It is noteworthy that all the heptane conversion numbers are better than would be predicted from the assumption of a noninteracting system, with the greatest deviations occurring in the three runs which contained coal (VIII, XVI, and XVII). These preliminary results indicate that there may be some beneficial effect on the coconversion of coal with plastics, an effect also reported by other workers [1]. The coal plus plastics system also seems to be quite sensitive to the reaction conditions of time,

temperature, and catalyst composition, although varying the vehicle-to-feed ratio between 2:1 and 1:1 does not appear to have a significant effect on the results. In the remaining five runs where time, temperature, or catalyst differed from the base conditions (IX, X, XIII, XIV, XV), the THF and heptane conversions varied widely, particularly in runs XIV and XV, made at both longer time (120 min) and higher temperatures (445°C). A more systematic approach will be required to determine the influence of reaction conditions on conversion.

Semi-Batch Tests. The tests at semi-batch scale were performed very early in the program. As evidenced by the results in Table II, the conversion and hydrogen consumption results were highly inconsistent, and no conclusions could be made from these data. The semi-batch unit has provided consistent results in the past with coal-only systems, and the erratic behavior was unexpected. This unpredictability is likely due to issues in reactor configuration, which may be appropriate for coal-only slurries, but not for mixtures containing plastics. More needs to be learned about the influence of reactor design when processing coal-plastics mixtures.

Viscosity Measurements. Successful operation of a continuous unit introduces another important requirement, that of pumping the feed slurry. To determine the feasibility of pumping these composite feedstocks, viscosity measurements as a function of temperature were made on several oil-coal-plastics mixtures. Figure 1 shows viscosity as a function of temperature for three mixtures of 70% vehicle and 30% plastic. The plastics content varies from all PS, to all PE, with an intermediate commingled mixture of PE, PS, and PET in the ratio 50:35:15. Although the viscosity of all mixtures is quite high, the PE appears to be most responsible for the increase in viscosity with plastics content.

Figure 2 shows viscosity measurements as a function of temperature for four model feed mixtures. All of the mixtures contained 70% vehicle and 30% coal-plastics material, with commingled plastics in the ratio 50:35:15 / PE:PS:PET. The coal:plastics ratios ranged from 75:25 to 50:50. The data show an increase in viscosity with increasing plastics content (decreasing coal content) at all temperatures. All samples also show a decrease in viscosity with increasing temperature, although the decrease was greatest for those samples with the highest plastics content. The 75:25 and 50:50 mixtures were subsequently fed to a continuous liquefaction unit.

Continuous Unit Test. The continuous unit was operated for 116 hours without plugging or stoppage, including over 80 hours of coprocessing coal with plastics. The run conditions and distillation results are given in Table III. Successful operation of the continuous unit required control of the feed slurry viscosity by means of the temperature. When viscosity was too high, the mixture could not be pumped. When viscosity was too low, the coal would settle out, causing plugging. In the continuous tests, the 75:25 coal:plastics mixture could be pumped at a temperature of 120°C. However, the 50:50 coal:plastics mixture became extremely viscious at 150°C, the upper limit for the heated lines on the continuous unit. Because of the high pressure drop associated with pumping such a viscious mixture, it was decided to terminate the run after eight hours at this condition. As a result of these observations, it has been decided to modify the lines on the continuous unit to allow for pumping at higher temperatures.

SUMMARY AND CONCLUSIONS

Individually, plastics degrade as reported in the literature, and products rapidly hydrogenate to saturation. PE generally requires more severe conditions for conversion to solubles than either PS or PET. The traditional solvent extraction methods for evaluating coal conversion are not particularly appropriate for plastics. For PS and PET, degradation is rather straightforward, but better characterization of PE products, especially of the "insoluble" fraction, is needed.

To realize an advantage from the higher hydrogen content of plastics, degradation rates must be carefully controlled. Under traditional liquefaction conditions, each C-C bond scission still consumes one molecule of H_2, because any olefinic products formed as a result of depolymerization rapidly hydrogenate to saturates. This is particularly true with PE, which tends to degrade randomly along the polymer chain. If gas production can be minimized, less hydrogen will be required to produce saturated products from plastics, since the average waste plastic stream is less aromatic than coal.

In the two-component and multicomponent microautoclave tests, THF solubles could be reasonably well predicted from the behavior of the individual components under similar conditions. However, the heptane solubles were greater than that predicted by the assumption of individual behavior. This may be indicative of some type of synergistic behavior in coliquefaction of coal with plastics. Further work in this area is warranted.

The results on two-component and multicomponent mixtures were highly sensitive to reaction conditions, especially those of time and temperature. This is of special concern for PE-containing mixtures, where degradation to gases would be undesirable. Information concerning the rate of thermal degradation vs. gas formation in coal-plastics mixtures would be valuable. The optimum conditions for coal-waste coprocessing may not be the same as for liquefaction of coal alone.

The erratic results from the semi-batch unit indicate that more needs to be learned about the effects of reactor design.

The viscosity of coal-plastics mixtures increases significantly as the plastics concentration increases. PE seems to have the greatest influence on viscosity. Higher temperatures were required to pump the mixture when the composition was raised from 25% to 50% plastics. Control of viscosity by control of temperature was the key to successful operation of continuous mode coprocessing.

DISCLAIMER

Reference in this report to any specific commercial product, process, or service is to facilitate understanding and does not necessarily imply its endorsement or favoring by the United States Department of Energy.

REFERENCES

1. Taghiei, M. M.; Feng, Z.; Huggins, F. E.; Huffman, G. P. Energy and Fuels, **1994**, 8, 1228-1232.

2. Anderson, L. L.; Tuntawiroon, W. Am. Chem. Soc., Fuel Chem. Div., Prepr. Pap. **1993**, 38(3), 816-822.

3. Comolli, A. G. Proc., Coal-Waste Coprocessing Workshop, September 9, 1994, Pittsburgh, PA. To be published.

4. Lott, S.; Dosch, R. Proc., 10th Ann. Int'l Pittsburgh Coal Conf., Chiang, S. H., Ed., p. 229-234, September 20-24, 1993.

5. Pradhan, V. R. Ph.D. Thesis, University of Pittsburgh, 1993.

6. Rothenberger, K. S., Cugini, A. V.; Schroeder, K. T.; Veloski, G. A.; Ciocco, M. V. Am. Chem. Soc., Fuel Chem. Div., Prepr. Pap. **1994**, 39(3), 688-694.

7. Cugini, A. V.; Krastman, D.; Lett R. G.; Balsone, V. D. Catalysis Today, **1994**, 19(3) 395-408.

8. Hackett, J.P.; Gibbon, G.A. In Automated Stream Analysis for Process Control, Manka, D.P., Ed., Academic Press, 1982; pp 95-117.

9. M. V. Ciocco, A. V. Cugini, K. S. Rothenberger G. A. Veloski, and K. T. Schroeder. Proc., 11th Ann. Int'l Pittsburgh Coal Conf., 1, 500-505, September 12-16, 1994.

10. Madorsky, S. L. Thermal Degradation of Organic Polymers; John Wiley and Sons: New York, 1964.

TABLE I: SUMMARY OF MICROAUTOCLAVE REACTION CONDITIONS AND RESULTS

Run	Feed Mixture (%) Coal	PE	PS	PET	Vh:F[1]	Catal	Time min.	Temp. (°C)	Conv, % THF	Hept	H_2 cons (mmol)	Pred.Conv.,%[2] THF	Hept
Single-Component Reactions													
I	100	0	0	0	2:1	AO-60	60	430	83	51	50		
II	0	100	0	0	1:1	AO-60	60	430	-19	-20	28		
III	0	100	0	0	2:1	AO-60	30	465	79	76	75		
IV	0	0	100	0	2:1	none	60	430	94	77	N/A		
V	0	0	100	0	2:1	AO-60	60	430	98	98	N/A		
VI	0	0	100	0	2:1	AO-60	60	430	97	96	54		
VII	0	0	0	100	2:1	AO-60	60	430	93	86	N/A		
Two-Component Reactions													
VIII	33	67	0	0	1:1	AO-60	60	430	28	26	38	28	17
IX	50	50	0	0	6.5:1	HTO	60	430	36	27	41		
X	50	50	0	0	6.5:1	HTO	60	430	34	24	39		
XI	0	67	33	0	1:1	AO-60	60	430	36	36	N/A	33	33
XII	0	67	0	33	1:1	AO-60	60	430	35	35	46	33	33
Multicomponent Reactions													
XIII	70	15	10	5	2:1	AO-60	60	445	71	37	73		
XIV	70	15	10	5	2:1	AO-60	120	445	48	13	N/A		
XV	70	15	10	5	2:1	Fe-S	120	445	67	26	N/A		
XVI	50	25	16	9	2:1	AO-60	60	430	65	57	54	67	51
XVII	50	25	16	9	2:1	AO-60	60	430	63	56	49	67	51

TABLE II: SUMMARY OF SEMI-BATCH CONDITIONS AND RESULTS

Run	Feed Mixture (%) Coal	PE	PS	PET	Vh:F[1]	Catal	Time min.	Temp. (°C)	Conversion, % THF	Hept	450°C	H_2 cons. (mmol) Tot	/g MAF feed
I	50	25	17	8	70:30	AO-60	60	430	47	49	36	760	10
II	50	25	17	8	70:30	AO-60	60	430	58	56	47	1100	13
III	50	25	17	8	70:30	AO-60	60	430	32	28	-12	660	8
IV	50	25	17	8	70:30	AO-60[3]	60	430	57	56	51	311	4

TABLE III: SUMMARY OF CONTINUOUS UNIT TEST CONDITIONS AND RESULTS

Cond	Feed Mixture (%) Coal	PE	PS	PET	Vh:F[1]	Catal	Duration (hr)	Temp. (°C)	Average Conv, % (°C) 0-340	340-450	450+
I	100	0	0	0	70:30	AO-60	36	430	66±10[4]	25±6[4]	10±5[4]
II	75	12	9	4	70:30	AO-60	72	430	47±6[5]	34±4[5]	19±3[5]
III	50	25	17	8	70:30	AO-60	8	430	N/A	N/A	N/A

[1] 2:1 Vehicle:Feed (Vh:F) represents 6.6g vehicle : 3.3g feed; 1:1 Vh:F = 3.3g vehicle : 3.3g feed; 6.5:1 Vh:F = 6.6g vehicle : 1g feed
[2] Prediction conversion calculated assuming Coal(THF)=83%, Coal(Hept)=51%, PE(THF)=PE(Hept)=0%, PS(THF)=PS(Hept)=PET(THF)=PET(Hept)=100%
[3] Silica, 2 g, was added to semi-batch run IV.
[4] Average of 5 determinations
[5] Average of 25 determinations

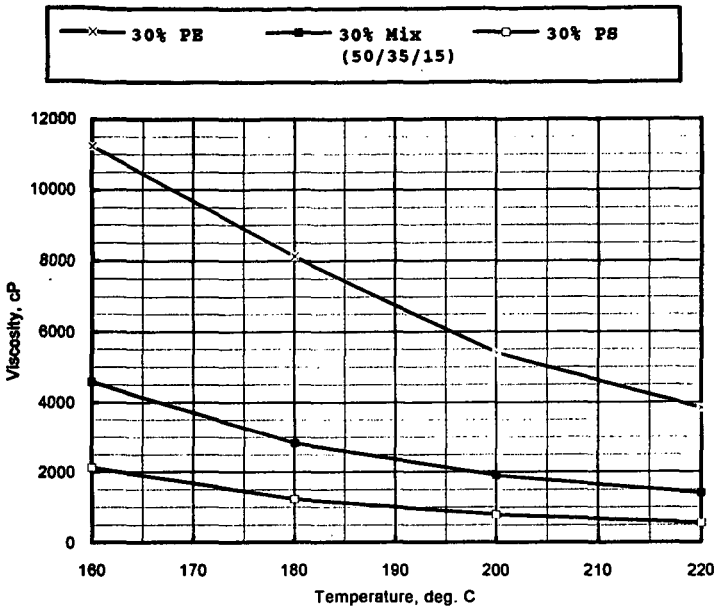

Figure 1. Effect of Plastics Composition on Viscosity

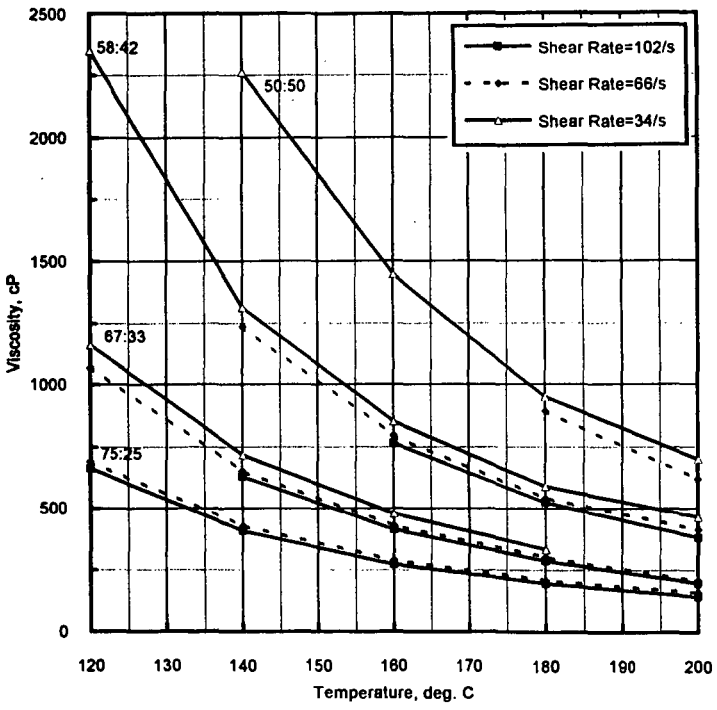

Figure 2. Viscosities of Coal:Plastics Mixtures

THERMAL AND CATALYTIC COPROCESSING OF COAL AND WASTE MATERIALS

E. C. Orr, W. Tuntawiroon, W. B. Ding, E. Bolat, S. Rumpel, E. M. Eyring, and L. L. Anderson, University of Utah, Salt Lake City, Utah 84112

KEYWORDS: Coal liquefaction, Waste Rubber Tires, Waste Plastics

Introduction

Coprocessing of coal with waste materials to produce liquid fuels with emphasis on finding reasonable reaction pathways and catalysts for such processing is presently the subject of intensive investigation. Polymer wastes such as polyethylene, polystyrene, polypropylene and used rubber tires are not naturally degraded over time. More than 22 million tons of plastic waste are annually discarded in landfills and over 75 percent of used rubber tires are similarly treated.[1] In order to obtain distillate liquids or petroleum compatible refined products from coal, addition of hydrogen is necessary. A possible method for hydrogen addition is coprocessing of coal with polymeric waste materials since these latter materials contain hydrogen at levels much higher than are found in coal. The breakdown of waste rubber tires is interesting because the liquids derived may prove to be important as a coal dissolution and/or hydrogen donor solvent.[2] Recently, Badger and coworkers[3] reported that hydrogenated tire oils (hydrogenated in the presence of CoMo catalyst) were effective for the dissolution of coal. Studies on the coprocessing of coal and waste materials have only recently been done intensively. Limited data are available on reaction conditions and catalytic effects for processing coal mixed with post-consumer wastes. The purpose of the present study was to determine the effects of reaction temperature, pressure, catalysts, and mixture ratio on the coprocessing of coal and waste materials.

Experimental

Blind Canyon (Utah) coal (DECS-6, -60 mesh) was obtained from the Penn State Coal Sample Bank and stored under nitrogen. Ground waste rubber tire material (-20 mesh, 0.4 % moisture, 68.7 % volatile carbon, 7.6 % ash, and 23.3 % fixed carbon) was obtained from the University of Utah Center for Microanalysis. Ground waste rubber tire was stored under air at ambient conditions. The commingled plastic mixture (mostly high density polyethylene) used in this experiment was obtained in two batches. The first batch was obtained from a recycling center in Utah (Recycling Corporation of America) in the form of detergent or soft-drink bottles. Samples were washed to remove the labels and contaminants before size reduction by cutting and shaving. Final size reduction was done by grinding in a kitchen flour mill (stainless steel) to -8 +25 mesh before analyses and use in coprocessing experiments.

The second waste plastic was obtained through the American Plastic Council (APC) from a recycling center in Oregon. Polyethylene and polystyrene were purchased from Aldrich Chemical Co. Melting and softening temperatures of some plastic polymers are given below:

Plastic	*Temperature*
Low Density Polyethylene	T.M. : 115° C
Mid Density Polyethylene	T. M. : 120° C
High Density Polyethylene	T.M. : 130 °C
Polypropylene	T.M. : 189 °C
Polystyrene	T.S. : 60-93° C

T.M. = Melting Temperature, T.S. = Softening Temperature

Reaction feed samples were composed of various amounts of waste plastic and rubber tire combined with Blind Canyon DECS-6 coal. When catalysts were used they were added to the mixture and their content given as a weight per cent of the solid feed material. Before reaction the feed solids were vacuum dried for two hours at 100°C. Samples were placed in glass tubes stoppered with glass wool. The glass tubes were placed in 27 cm^3 tubing bomb reactors, purged with nitrogen, and pressurized to 1000 psig H_2 (cold). Reactors were heated by a fluidized sandbath held at various reaction temperatures. The tubing reactors were shaken vertically at 160 rpm for various lengths of time, removed, and allowed to cool overnight under pressure.

Rubber tire/coal reaction products were removed and extracted with tetrahydrofuran (THF). The THF solubles were filtered to remove carbon black. The THF was removed with a rotary evaporator, and the THF soluble portion was dried under vacuum for two hours. The

sample was then extracted with cyclohexane. The cyclohexane was removed using a rotary evaporator leaving rubber tire/coal oil. The cyclohexane insoluble residue will be referred to as preasphaltenes and asphaltenes. The THF-insoluble portion is referred to as char. All product yields are calculated on a dry, ash-free, and carbon black-free basis.

Plastic/coal reaction products were removed and extracted with cyclohexane. The cyclohexane was removed with a rotary evaporator and the residue (preasphaltenes and asphaltenes) was dried under vacuum for two hours. Cyclohexane-insolubles were subsequently extracted with THF. The THF-insoluble portion is referred to as char. This char also contains any inorganic material present in the coal or waste polymer feed. Products soluble in THF were obtained using a rotary evaporator, and dried for two hours under vacuum at 100°C. All product yields are calculated on a dry, ash-free basis.

Results

Waste Rubber Tire Material

Figure 1 shows the breakdown of products including the total conversion, oil + gas yields, and preasphaltene/asphaltene yields for various mixtures of tire rubber and Blind Canyon DECS-6 coal coprocessed under hydrogen for one hour at 350°C with a molybdenum catalyst (ammonium tetrathiomolybdate). Total conversion values reported here are reproducible within $\pm$ 2%. Figure 1 suggests that as the rubber tire content of the mixture increased, so also did the oil and gas yields. Accordingly, as the tire rubber percentage decreases and coal becomes the dominant reactant, the yield of asphaltenes increases, and oil + gas yields decrease. Since tire rubber breaks down into THF soluble components quite readily, the increase of the gas and oil products and the decrease in preasphaltenes/asphaltenes with increasing tire rubber content is not surprising. The straight diagonal line is drawn on Fig. 1 to indicate the conversion expected for a tire and coal sample mixture calculated from samples consisting only of tire/catalyst and only of coal/catalyst assuming no interaction of the two reactants takes place that would inhibit or enhance total conversion. The total conversion points above the solid line show that there is some synergism for sample compositions between 10% tire rubber and 30% tire rubber by weight. It appears from the preasphaltene/asphaltene curve in Fig. 1 that this may be related to an increase in production of preasphaltenes/asphaltenes. Figure 2 presents results of further work with various mixes of tire rubber and coal with the same molybdenum catalyst but at 430°C. Again the solid line indicates a theoretical value for the total conversion based on samples consisting of only coal/catalyst liquefied at 430°C and only tire/catalyst at 430°C. It is interesting to note that the synergism which takes place at 350°C does not seem to occur at the same tire/coal composition at which synergism is observed for samples processed at 430°C. Instead, at 430°C the synergism is noted for almost all samples coprocessed. The observed synergism at 430°C also is due to an increase in yields of preasphaltenes/asphaltenes.

Coprocessing for one hour periods at 430°C is found to be more beneficial than at 350°C for enhancement of product yields (Figure 3). Table 1 shows the amount of zinc found in the oil products from coal/tire coprocessing. Samples obtained by reaction at 430°C were found to contain less zinc than samples obtained at 350°C. Higher temperatures may enhance zinc deposition in the ash or zinc scavenged by the coal, thus diminishing the amount of zinc found in the products. Such scavenging could be beneficial in eliminating the need for a secondary process to remove zinc from the coprocessing-derived oils. While processing samples at different temperatures, we have noted a difference in the amount of carbon black found in the product oils. The carbon black is thought to be unsuited to hydrotreatment. During the extraction procedure using THF, some carbon black passes through the cellulose filters into the extraction mixture. The carbon black tends to stick to the solvent extraction apparatus. We have further noted that samples coprocessed at 430°C tend to dirty the glassware less. In order to calculate conversion to products accurately the carbon black is filtered out. We then observed for some of these samples coprocessed at higher temperatures and made up of more than 50% tire rubber that less carbon black was being filtered out. Figure 4 compares the amount of carbon black that was filtered out for samples coprocessed at 350°C and 430°C. The percentage of carbon black filtered out of the THF solubles is plotted versus the composition of the tire/coal mixture. At the lower temperatures and at higher tire rubber percentages larger amounts of the carbon black passed through the cellulose filter. This result may only be related to conditions of coprocessing with a tubing reactor and the manner in which we extracted our samples, but the result may be of some use in decreasing the amount of carbon black that becomes mixed into the oil products in a commercial operation.

Plastic Wastes

We have studied extensively the liquefaction of Blind Canyon coal, which has a low pyrite content. Hydroliquefaction of this and other coals of similar rank gives high yields of liquid products at temperatures around 350-430°C. As shown in Fig. 5, liquefaction of coal at higher temperatures results in decreased liquid yields and higher quantities of gases being produced. Maximum oil production was obtained at 430°C.

Commingled plastic wastes used in these experiments contained some polystyrene, and other plastics, but the most abundant polymer in this waste was high density polyethylene (HDPE). HDPE has the highest decomposition temperature of the plastic materials we tested (400-430°C) which made the optimum reaction temperature for processing commingled plastic higher than for coal.

From Fig. 6 (processing of commingled plastic for one hour), the maximum total conversion was reached (96%) at 430°C and higher temperatures. Oil production increased as the reaction temperature increased. Maximum oil production occured at 430°C. Once the temperature was above 430°C the oil yield dramatically decreased as the gas production increased. Coprocessing plastic and coal together showed optimum conditions for total conversion and oil production at 430°C and a reaction time of one hour (Fig. 7).

As shown in Fig. 8, mixing plastic with coal did not result in any improvement of total conversion. Synergism was observed only for oil production for coal/plastic coprocessing. The observed synergism appears to be due to a decrease in the yield of asphaltenes.

Summary

Coprocessing at 430°C was found to give the highest total conversion yields for coal/ rubber tire material coprocessing for one hour under a hydrogen atmosphere with a molybdenum catalyst. The zinc and carbon black contamination in the derived liquids was diminished when samples were coprocessed at 430°C. Coprocessing of coal with commingled plastic showed a synergistic effect on oil production but not on the total conversion

References

1. Franklin Associates, Ltd.; Characterization of Plastic Products in Municipal Solid Waste; Final Report February 1990; prepared for the Council for Solid Waste Solution.
2. Farcasiu, M.; Smith, C., Prepr. Pap. Am. Chem. Soc., Div. Fuel Chem., 1992, 37 (1), 472.
3. Badger, M. W.; Harrison, G., Ross, A. B., 1994, Prepr. Pap. Am.Chem. Soc., Div. of Petroleum Chem., 39 (3), 438.

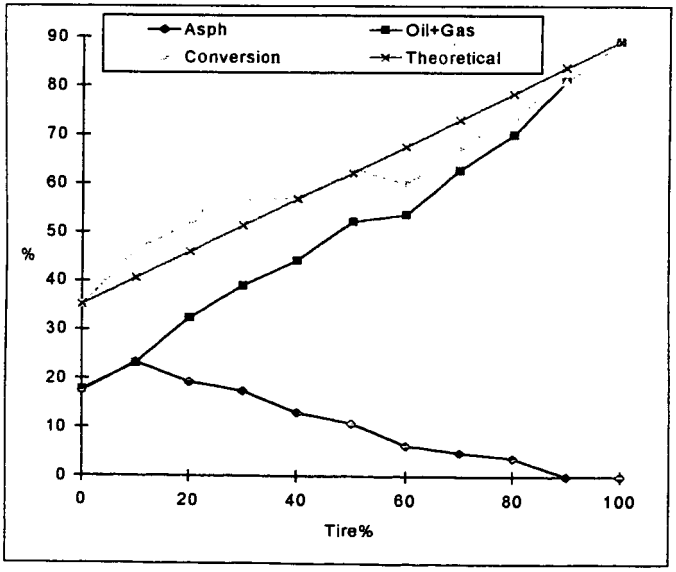

Fig. 1. Tire/coal products from coprocessing at 350 Celsius for 1 hour in tubing bomb reactors under 1000 psig (cold) hydrogen with a molybdenum catalyst.

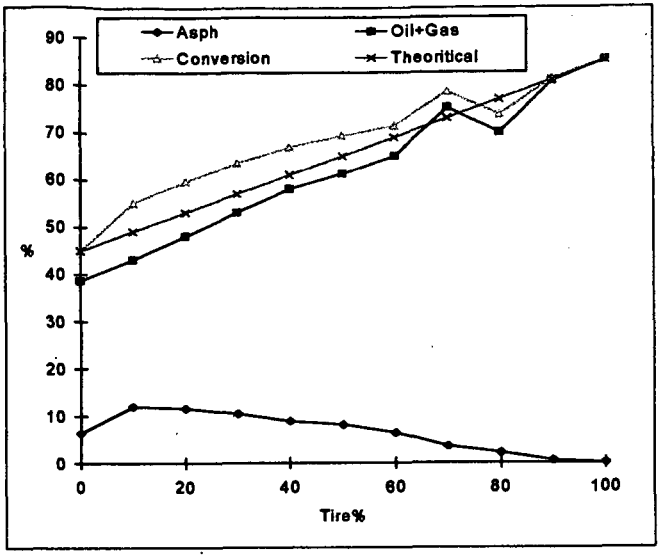

Fig. 2. Tire/coal products from coprocessing at 430 Celsius for 1 hour in tubing bomb reactors under 1000 psig (cold) hydrogen with a molybdenum catalyst.

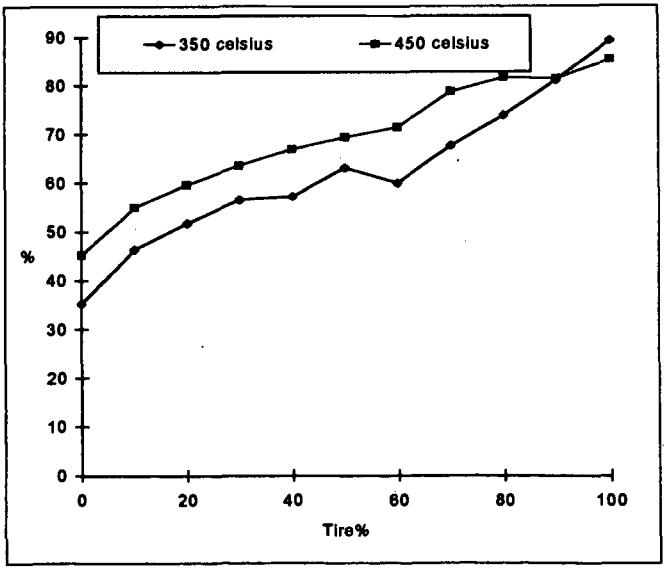

Fig. 3. Tire/coal total conversion comparison for samples coprocessed at 430 Celsius and 350 Celsius for 1 hour in tubing bomb reactors under 1000 psig (cold) hydrogen with a molybdenum catalyst.

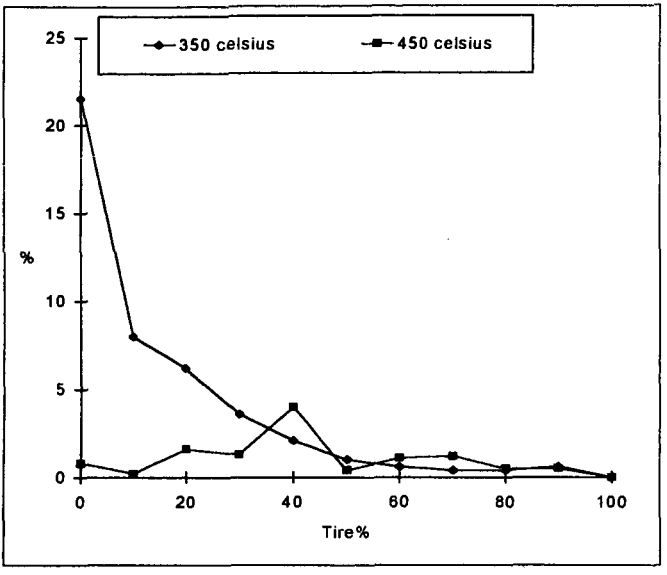

Fig. 4. Percentage of carbon black filtered out of THF soluble liquids for coal/tires samples coprocessed at 350 Celsius and 430 Celsius for 1 hour in tubing bomb reactors under 1000 psig (cold) hydrogen with a molybdenum catalyst

Table 1. Percentage of zinc (by weight) in cyclohexane soluble oils obtained from coal/tire rubber samples coprocessed in tubing bomb reactors with reaction times of 1 hour under at 1000 psig (cold) hydrogen with a molybdenum catalyst.

Coal %	Tire %	350° Celsius	430° Celsius
0	100	0.017 %	0.007 %
30	70	0.016 %	0.008 %

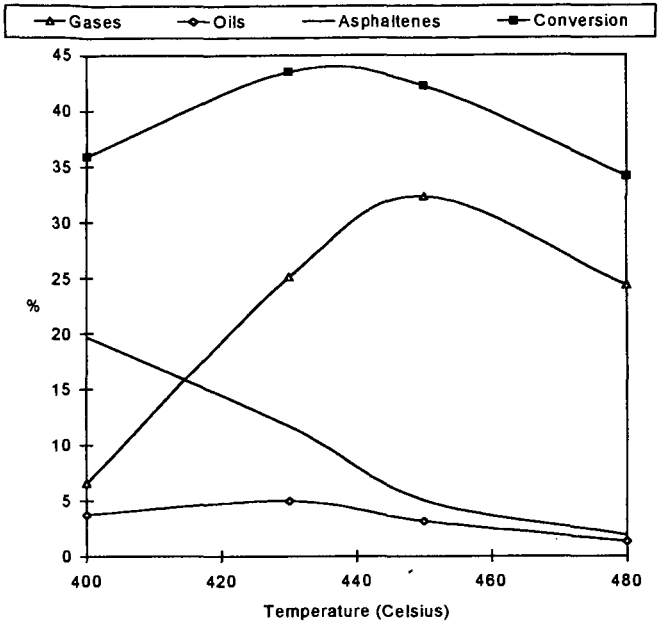

Fig. 5. Liquefaction results for DECS-6 coal hydrotreated for 1 hour in tubing bomb reactors under 1000 psig (cold) hydrogen

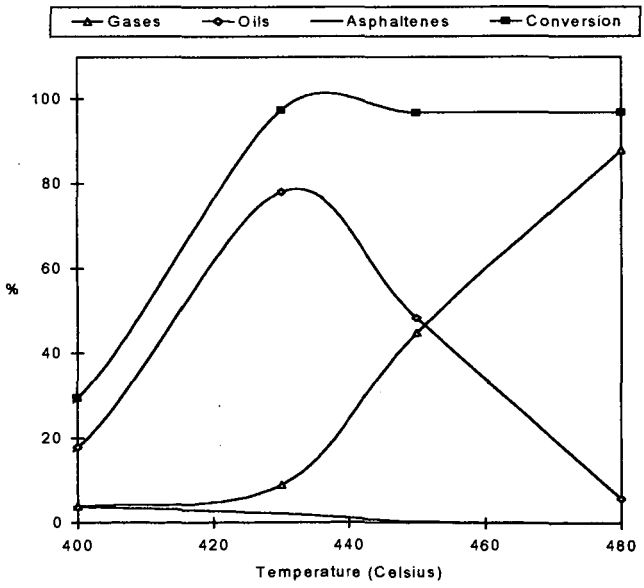

Fig. 6. Liquefaction results for commingled plastic #2 [APC] hydrotreated for 1 hour in tubing bomb reactors under 1000 psig (cold) hydrogen.

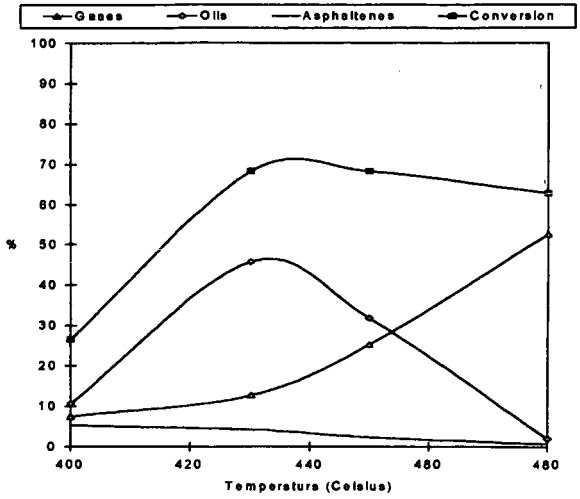

Fig. 7. Results for coprocessing of commingled plastic #2 [APC] and DECS-6 coal for 1 hour in tubing bomb reactors under 1000 psig (cold) hydrogen.

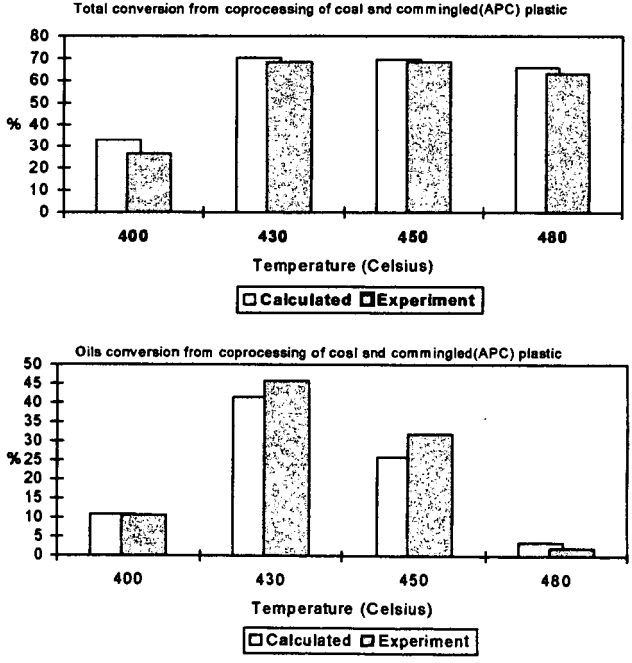

Fig. 8. Experimental and calculated results for coprocessing of commingled plastic #2 [APC] and DECS-6 coal for 1 hour in tubing bomb reactors under 1000 psig (cold) hydrogen.

COPROCESSING OF WASTE HYDROCARBON FEEDSTOCKS USING COUNTERFLOW REACTOR TECHNOLOGY

Richard J. Parker and Dennis W. Carson
Alberta Research Council
1 Oil Patch Drive, P.O. Bag #1310, Devon, Alberta TOC 1EO

Keywords: Co-Liquefaction, waste plastics, rubber tires

INTRODUCTION

Like many jurisdictions in North America, the Province of Alberta is in the early stages of introducing measures to collect and recycle hydrocarbon wastes. In 1992 a levy of $4 was added to the purchase price of each automotive tire. This levy was accumulated in a fund to promote the use and recycle of waste rubber tires.[1] The fund has supported several diverse uses of the waste tires, including incineration in cement kilns and rubber crumb generation for marketable products. To date these projects have only utilized 1.8 million of the 2.5 million tires which are discarded annually and have not started to reduce the backlog of over 4 million tires which was accumulated prior to 1992.

Recently several European plastics manufacturers have joined together to invest in a pilot project to convert waste plastic containers into oil.[2] In this process the produced naphtha will be converted into hydrocarbon monomers which can then be fed to polymerization units for complete recycle to fresh plastics. Similar efforts are underway in North America to recycle hydrocarbon wastes to oil or gaseous products. Much of this work is directed at co-liquefaction of polymers and coal, and has been reviewed by Huffman.[3] Indications are that waste plastics and rubber tires can be converted into liquids using technologies which have been developed for the liquefaction of coal. Both Taghiei[4] and Anderson[5] have reported that there is a synergistic effect when coal and plastics are co-liquefied. Similarly enhanced coal liquefaction performance has been observed when co-liquefying waste tires and coal.[6,7]

Alberta Research Council together with Canadian Energy Developments have developed technologies for the direct liquefaction of coal[8] and coprocessing of coal and heavy oil/bitumen.[9] It was a small step to envision the application of these technologies to the processing of other hydrocarbons such as waste plastics and rubber tires. This paper reports on a preliminary experimental program that was conducted to investigate the coprocessing of waste hydrocarbons with coal and heavy oil.

CO-LIQUEFACTION CONCEPT

The generic waste processing scheme is depicted in Figure 1. Initially there is a simple preparation step in which the waste hydrocarbon (and catalyst) is blended into a slurry with a recycle solvent or a refinery derived stream. Depending upon the feed characteristics the preparation step may be a digester to partially melt or solubilize the feed. The feed slurry is then introduced close to the top of the counterflow reactor (CFR) which is the heart of the process. This unit, operating at or near coal liquefaction temperatures and pressures, converts the hydrocarbon waste into liquid or gaseous products. The lighter boiling components are swept from the top of the reactors by the carrier gas. The carrier gas is most likely hydrogen but could be carbon monoxide or natural gas depending on the nature of the waste or solvent.

Light products are separated by conventional refinery processes. Liquid components from the bottoms slurry could be separated by a variety of procedures geared to the particular feed, including centrifugation, filtration or flashing. With plastic wastes the bottoms stream would be small and solids virtually absent. The withdrawal rate would then be dependant on the need for the slurry solvent. Tires produce a solid residue which if treated successfully could give regenerated carbon black and other byproducts.

EXPERIMENTAL

Alberta Research Council has traditionally employed 1 litre batch autoclaves as a screening tool to test new concepts or process operating conditions for the CFR. The procedures have been described elsewhere[8]. Feedstock properties are listed in Table 1. The solvent LO-6282 (boiling range 250-550°C) was obtained from the HRI facility

in Princeton, New Jersey. It was generated from a liquefaction run using Illinois #6 coal. Cold Lake heavy oil was taken from the Alberta Research Council Sample bank.

In a typical test, 75g of feed (polyethylene, coal, rubber crumbs or mixtures of each), was slurried with 150g of the solvent or heavy oil, and if required catalyst was added. The autoclave was charged to 1250 psi (cold) with hydrogen. This gave an operating pressure of 2000-2500psi depending on the process temperature or feed/solvent composition.

At the completion of the run the gas was discharged and the autoclave was flushed with hydrogen. The combined gas sample was analyzed by gas chromatography. The liquid slurry was recovered from the autoclave and a portion was subjected to extraction, either with tetrahydrofuran (THF) or sequentially with toluene, then THF.

Hydrocarbon conversion is reported as:

$$\frac{\text{Feedstock(DAF)}_{In} - \text{THF Insolubles}_{Out}}{\text{Feedstock(DAF)}_{In}} \times 100 \quad \text{weight\%}$$

where feedstock is polyethylene or rubber crumb or mixtures of either with coal.

In a limited number of runs a liquid sample was prepared by filtration to allow more detailed characterization.

RESULTS AND DISCUSSION

Co-Liquefaction of Polyethylene

The influence of temperature, catalyst and coal concentration, as well as a soak step were investigated for the co-liquefaction of polyethylene. By itself polyethylene proved intractable. At 425°C for 60 minutes, where coal conversion exceeded 90%, polyethylene conversion was barely 20% (Table 2). After correction for solvent decomposition, less than 1% of hydrocarbon gas was produced. Introduction of coal into the system improved feedstock converion with Fe_2O_3 catalyst. Assuming that coal conversion at this temperature was 90% then the predicted feedstock conversion was calculated to be 28.3% with a coal to polyethylene ratio of 1:9, and 41.3% at a ratio of 1:1. Thus the experimental results suggest that there was a synergestic effect in this system. Product quality was visually poor; the almost clear polyethyelene pellets had been transformed into a greyish rubbery solid. The hydrogen: carbon ratio of the solid residue from Run W-1 was 1.93, less than in the polyethylene 2.0. Further tests are in progress to determine if the polymer degradation products had incorporated chemically bonded solvent.

Increasing the process severity to 440°C for 30 minutes, and replacing the catalyst with the potentially more active molybdenum naphthenate (~600 ppm Mo on feed), improved feedstock conversion, but not to those levels which might be acceptable in a commercial process (nominally set at >90%). Polyethylene itself gave 65% conversion and almost the entire conversion product slate was a liquid (THF soluble). Coal addition did little to enhance the polyethylene conversion. Using an assumed value of 90% for coal conversion, the predicted values for feedstock conversion for Runs W-5 and W-6 matched the experimental.

The maximum potential for conversion and liquid yields had not been reached at 440°C/60minutes (Run W-7). Feedstock conversion had risen to 83% with the majority of the additional product being oils. Again assuming 90% coal conversion only 78% of the polyethylene had been solubilized or converted to gases. Therefore there was an opportunity to produce more liquid products from this feedstock combination by maximizing the process severity. This scenario was dependant on the stability of the solvent which at 440°C/60 minutes generated 2.3g of gas/100g solvent.

Finally the benefit of a soaking period prior to the hydroprocessing step was investigated (W-8). Polyethylene melts at ~125°C and a soaking or digestion step might help liquefy or solubilize the material and in a continuous operation improve flow and transfer characteristics of the feedstock slurry or solution. Dimethyl disulphide was also added to the charge as a sulphiding agent for the molybdenum. A small increase in feedstock conversion was recorded but it was

within the reproducibility of ±2% found in 1L batch autoclave tests. Hydrocarbon gas yield rose by about the amount attributable to the methane produced by the decomposition of the dimethyl disulphide.

Co-Liquefaction of Rubber Crumb

Following the preliminary program with polyethylene the conditions selected initially for rubber crumb were the relatively high severity 440°C/60 minutes using the molybdenum naphthenate catalyst. At these process conditions, Run W-9, the residual solids (THF insoluble), 34.7g/100g feed, corresponded almost exactly to the sum of the fixed carbon plus ash in the rubber crumb, 34.6g/100g (Table 3). Gas production was moderate at 3.9g/100g feed much of which can be attributed to decomposition of the solvent, i.e. 2.3g/100g solvent at similar process operating conditions. Product recovery and mass balances both for this Run and W-10, were well below the norm of 98-98%, which suggested that large quantities light hydrocarbons were produced and lost during the workup procedure. Characterization of the liquid product by simulated distillation indicated that the bulk of this material was within the naphtha boiling point range (<183°C).

Introduction of coal into the feed, Run W-10, resulted in essentially complete conversion of both coal and rubber crumb. Using the previous value for rubber crumb conversion (Run W-9), the coal conversion was estimated to be greater than 95%. Gas production increased but was largely due to carbon oxides derived from the coal.

The above conditions were selected in most part to ensure coal liquefaction. Since the rubber crumb was at its maximum conversion, less severe condition might be effective. Lower temperature (375°C), in the absence of catalyst or hydrogen were taken as the opposite end of the spectrum of processing severity (Run W-13). Even so the liquefaction of the rubber crumb was then close to its maximum, 62.5% versus 65% for the high severity run. Gas production was minimal and product recovery was 99% indicating that fewer light hydrocarbon had been produced from the rubber or solvent. A simulated distillation of the filtered liquid product showed that the rubber crumb derived components were heavier than for the high severity run and were largely concentrated in the middle distillate fraction (183-343°C).

Performance, in terms of rubber crumb conversion and production distribution, was unchanged when using the catalyst and hydrogen atmosphere at 375°C. Liquid product quantities increased due to the large uptake of hydrogen during the run (W-14). This contrasted with the nitrogen run where hydrogen was actually produced. Characterization of the liquid products by gas chromatography with a mass spectroscopy detector displayed a concentration of monocyclic hydrocarbons with isopropyl and methyl group attached to the ring. In the presence of hydrogen the cyclics were mostly cyclohexane or cyclohexene with lesser quantities of the corresponding aromatic analogues. In the nitrogen atmosphere the situation was reversed with the aromatics dominating. Still the presence of partially and fully hydrogenated rings pointed to the transfer of hydrogen from the solvent. This leads to the question of what type of solvent is the preferred medium. In coal liquefaction hydrogen donor and transfer properties are valued. With rubber crumb hydrogen donation may prove disadvantageous since the products formed by hydrogen addition may not be the best choice either for gasoline blending or as a petrochemical feedstock.

The proposed waste processing scheme would have to accept a variety of feedstocks and solvents. Alberta heavy oilsand bitumens are proven solvents for subbituminous coals.[9] The effectiveness of Cold Lake heavy oil for solubilizing both coal and rubber crumb was demonstrated in Run W-12. Feedstock conversion was comparable with the LO-6282 solvent. The high severity led to low product recovery and very high hydrogen consumption. This was deceptive since consumption was reported on g/100g feedstock basis (coal + rubber crumb) but much of the hydrogen would have been used during the upgrading of the bitumen. The same reasoning applies to gas yield which incorporates bitumen derived gases including hydrogen sulphide which had not been observed from the coal or rubber crumb.

CONCLUSIONS

Batch autoclave tests indicated that counterflow reactor technology was a promising procedure for co-liquefaction of waste plastics and rubber tires. The versatility of the process has been demonstrated by coprocessing coal, wastes and reactive solvent (heavy oil). It was successful at producing an all liquid slate of products from all the potentially convertable hydrocarbon in the rubber crumb.

REFERENCES

1. Tire Recycling Management Board, Information Kit, P.O. Box 189, Edmonton, Alberta, Canada, T5J 2J1
2. Oil Patch Magazine, Vol. 13, #6, pg. 13, June/July 1994.
3. Huffman, G.P., 1994 ACS Div. Env. Chem. Preprints, 36, 478-481.
4. Taghiei, M.M.; Huggins, F.E. and Huffman G.P., 1993, ACS Div. Fuel Chem. Preprints 38 (4), 810-815.
5. Anderson, L.L. and Tuntawiroon, W.,1993, ACS Div. Fuel Chem. Preprints 38 (4), 810-815.
6. Farcasiu, M.; Smith, C.M.; 1992, Prepr. Div. Fuel Chem. 37(1), 472-479.
7. Liu, Z.; Zondlo, J.W. and Dadyburjor, D.B.; 1993, Energy and Fuels 8, 607-612.
8. Berger, D.J.; Simpson, P.L. and Parker, R.J., Proceedings Coal Liquefaction Review Meeting, 397-416, Pittsburgh, Sept. 1993.
9. Berger, D.J.; Wuerfel, H. and Anderson, N.E., ACS Div. Fuel Chem. Preprints 35(4), 998-1005.

Figure 1 GENERIC WASTE PROCESSING SCHEME USING COUNTERFLOW REACTOR TECHNOLOGY

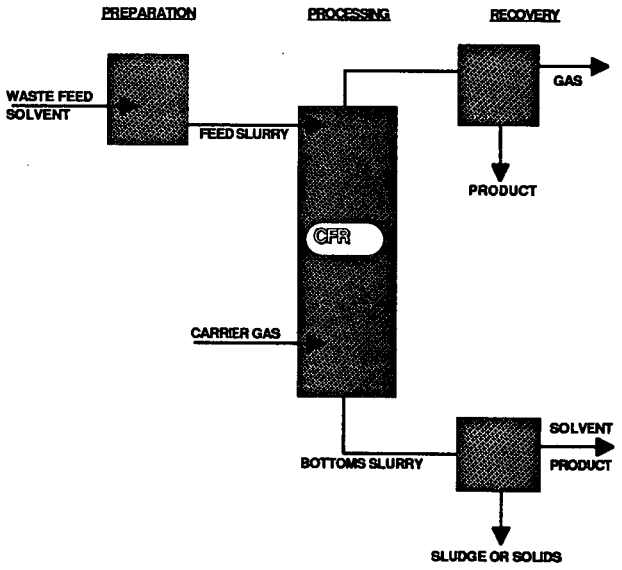

Table 1 Feedstock and Solvent Properties

	Rubber Crumb	Coal	Solvent LO-6282	Heavy Oil
Source	Alberta Environmental Rubber Products	Black Thunder	HRI	Cold Lake
Nature	1 to 5mm	*sub-bituminous*	250-525°C	Full range
				47% +525 resid
Characterization,Weight %				
Carbon	83.1	71.0	88.5	82.8
Hydrogen	7.4	5.2	10.5	10.4
Sulphur	2.4	0.97	0.07	4.6
Ash	5.8	6.2		
Fixed Carbon	29.1	51.4	1.9*	12.6*

* Conradson Carbon Number

Table 2 Co-Liquefaction of Polyethylene

Run #	W-1	W-2	W-3	W-4	W-5	W-6	W-7	W-8
Feedstock								
PolyE	100	90	50	100	50	90	50	50
Coal		10	50		50	10	50	50
Catalyst		Fe2O3/DMDS			Mo naph		Mo naph	
Solvent		LO-6282			LO-6282		LO-6282	
Process Conditions								
Temperature,°C		425			440		440	
Pressure,psi(cold)		1250			1250		1250	
Time, min		60			30		60	
Process Performance								
Recovery, %	99	99	98	99	97	99	100	96
Conversion, weight %	19	35	61	64	72	62	82	84
Predicted@90%		28	43		75	66		
Yields, g/100gMAF feed								
Gas	3.2	4.1	7.3	2.0	6.8	2.9	8.8	9.4
Oils	16.8	33.0	56.2	63.2	66.2	59.6	74.1	77.1
Solids	81.1	64.6	38.9	35.7	27.9	38.2	18.4	15.7
Hydrogen consumption	1.21	1.67	2.39	0.89	0.98	0.66	2.32	2.14

Table 3 Co-Liquefaction of Rubber Crumb

Run #	W-9	W-10	W-13	W-14	W-12
Feedstock					
Rubber Crumb	100	50	100	100	50
Coal		50			50
Catalyst		Mo naph	None		Mo naph
Solvent		LO-6282			Cold Lake
Process Conditions					
Temperature,°C		440	375	375	440
Pressure,psi(cold)		1250	0(H2)	1250	1250
Time, min		60	60	60	60
Process Performance					
Recovery, %	94	94	99	98	89
Conversion, weight %	65	80	62	64	78
Predicted@90%cc		77			77
Yields, g/100gMAF feed					
Gas	3.9	8.4	0.4	0.7	13.4
Oils	53.7	74.3	61.5	67.0	69.0
Solids	34.7	20.0	37.5	36.2	22.3
Hydrogen consumption	2.38	2.71	-0.49	3.85	8.71

COAL-TIRE CO-LIQUEFACTION

Ramesh K. Sharma, Dady B. Dadyburjor, John W. Zondlo,
Zhenyu Liu and Alfred H. Stiller
Department of Chemical Engineering
West Virginia University
P.O. Box 6102, Morgantown WV 26506-6102

Keywords: Tire liquefaction, coal liquefaction, iron catalyst.

ABSTRACT
Co-liquefaction of ground coal and tire rubber was studied at 400°C both with and without catalyst. Two different tire samples were used. In the non-catalytic runs, the conversion of coal increased with the addition of tire and the increase was dependent on tire/coal ratio and hydrogen pressure. Using a ferric sulfide-based catalyst, the coal conversion increased with an increase in the catalyst loading. However, the increase was more pronounced at loadings of around 0.5 wt%. The addition of tire to coal in the catalytic runs was not particularly beneficial, especially, when the tire/coal ratio was above 1.

INTRODUCTION

Disposal of used tires is a major environmental problem. Recently, the liquefaction of such tires in conjunction with coal was suggested as an alternative for their disposal [1,2]. Liu et al. [1] studied the co-liquefaction of tire and DECS-6 coal. The tire sample was prepared from an used Goodyear Invicta tire. When the tire and coal were co-liquified at 400°C it was observed that the conversion of coal increased in the same way as with the addition of tetralin (a good hydrogen donor solvent) to coal. Similar results were obtained by Farcasiu and Smith [2] for the liquefaction of tire and Illinois No. 6 coal at 425°C. In both these studies a complete conversion of tire was obtained.

In this work, the effect of H_2 pressure and tire/coal ratio on the co-liquefaction of tire and coal was studied at 400°C. Two different tire samples were used. Runs were made with tire and coal separately as well as using tire-coal mixtures with tire/coal ratios of 0-4. The hydrogen pressure was varied between 0-1500 psi (cold). Experiments were also done using a ferric sulfide-based catalyst at loadings of up to 1.67 wt% based on coal.

EXPERIMENTAL

The coal used was DECS-6 which is a high-volatile- A bituminous coal from the Blind Canyon seam in Utah. Two different tire samples were used. The first sample was prepared from a Goodyear Invicta tire, recycled in-house at WVU (Tire-1). The other sample was obtained from the University of Utah Tire Bank and represented mixed recycled tires ground to -30 mesh. The proximate and ultimate analyses showed that the Tire-1 contained 67 wt% volatile matter (on a dry, ash-free basis) and 33 wt% fixed carbon while Tire-2 contained 71 wt% volatile matter and 29 wt% fixed carbon. The fixed carbon essentially represents the content of carbon black in the tires. The amounts of volatile matter and fixed carbon in coal were 49 wt% and 51 wt%, respectively.

The experimental equipment, run procedures and analytical techniques have been described earlier [1] and are given briefly. A stainless steel tubing bomb reactor with a volume of 27 ml was used for the liquefaction. The reactor was loaded with the feed and, purged and pressurized with H_2 or helium to the desired pressure. The feed consisted of tire or coal or a mixture of the two in different ratios. In the catalytic runs, the catalyst was impregnated in-situ on the coal. The gaseous products were collected and analyzed by gas chromatography. The solid and liquid products in the reactor were washed and extracted with tetrahydrofuran (THF) for 24h. The THF-insoluble material (TI) was separated by filtration. The conversion is calculated from the amount of THF-insoluble material.

After the removal of THF by rotary evaporation, the THF-solubles were extracted with hexane for 2h. The extract was separated into hexane-insoluble (HI) and hexane-soluble (HS) fractions by filtration. The HS fraction was used to recover the 'oil fraction'. The THF-soluble/ hexane-insoluble fraction, i.e. the HI fraction, represents asphaltenes. The conversion (X) and the yield of asphaltenes (A) were calculated as follows:

$$X = (F_m - TI)/F_{daf} \quad (1)$$

$$A = HI/F_{daf} \quad (2)$$

where F_m and F_{daf} represent the amount of feed on moisture-free and dry, ash-free (daf) basis, respectively. The gas yield (G) was determined independently from the gas analysis. The oil yield (O) was obtained by difference:

$$O = X - A - G \quad (3)$$

In many cases, the combined oil + gas yield was calculated by difference. Most runs were made in duplicate and the experimental error was ±2.5%.

In the co-liquefaction runs, the overall conversion and the yields of asphaltenes and oil + gas fractions were calculated as above. However, in order to get a better insight, the results were also analyzed in terms of incremental conversion and yields, based on coal, which were calculated as follows;

$$X_{cm} = (X_{ov} - w_t x_t)/w_c \quad (4)$$

where X_{ov} is the total conversion and w_t and w_c are the weight fractions of tire and coal in the feed, respectively. In equation (4), x_{cm} is the estimated conversion of coal in the mixture and x_t is the conversion of tire which was assumed to be the same as in tire-alone runs. The yield of oil + gas from coal was estimated similarly. The asphaltenic yield from coal was calculated by difference. It should be recognised that the conversion of tire in the co-liquefaction runs may be different from that in tire-alone runs. However, the above assumptions were made simply to 'lump' the entire incremental effect into a single component, i.e., coal.

RESULTS AND DISCUSSION

Effect of Hydrogen Pressure

The effect of hydrogen pressure on the product slate from coal-alone and tire-alone (Tire-2) was studied at 400°C. The runs at zero hydrogen pressure were made using 1000 psi (cold) helium. The effect of hydrogen pressure on the tire conversion was found to be minimal. Also, the hydrogen pressure affected the coal results only slightly. The conversion of coal increased with increase in hydrogen pressure, resulting in an increase in the yields of both asphaltenes and oil+gas fractions. At all the pressures, the yield of asphaltenes was lower than that of oil plus gas. Thus it appears that the gaseous hydrogen is necessary to stabilize the coal radicals. This is consistent with the observations of Malhotra and McMillen [3] and Whitehurst et al. [4] that the retrogressive reactions in coal liquefaction become more pronounced under hydrogen-deficient conditions. The results indicated that the relative contribution of hydrogen to the stabilization of asphaltenic radicals is somewhat greater than to the radicals in the oil range.

Figures 1 and 2 show the effect of hydrogen pressure in the co-liquefaction runs using Tire-1 and Tire-2, respectively. The tire/coal ratio was unity. The conversion and oil + gas yield from tire were assumed to be the same as those for the liquefaction of tire alone and the results are reported on coal-alone basis. It is seen that, with Tire-1 (Figure 1), both the conversion and oil+gas from coal increase with an increase of H_2 pressure, up to around 500 psi (cold). At higher H_2 pressures, the results are relatively insensitive to the pressure. However, when Tire-2 was used, the conversion of coal increased monotonically with the H_2 pressure (Figure 2). This led to increase in the yields of both asphaltenes and oil+gas. When these results were compared to those for the coal alone, it was found that the effect of hydrogen pressure on the product slate is greater in the co-liquefaction runs than in the coal-alone runs. The synergistic effect of Tire-2 also appears to depend on H_2 pressure, i.e. there is an increased synergism at high hydrogen pressures. The yields of asphaltenes in the co-liquefaction runs (Figure 2) are almost double those which were observed in the coal-alone runs. On the other hand, the yields of oil+gas are lower compared to those in coal-alone runs, especially at low hydrogen pressures. This indicates that both the gaseous hydrogen and the tire radicals are used in the stabilization of coal radicals that are in the asphaltenic range. Further, the contribution of tire to the radical stabilization and bond scission is considerably higher compared to that of hydrogen. In contrast, the coal radicals in oil range are probably stabilized mainly by the hydrogen and the addition of tire seems to have little effect especially at low hydrogen pressures.

Effect of Tire/Coal Ratio

The effect of tire/coal ratio on conversion and product yields using Tire-1 is shown in Figure 3. As before, the results are based on coal, i.e. the contribution of tire has been subtracted out. The conversion of coal increases from around 35 wt% in the absence of tire to over 65 wt% when the tire/coal ratio was 4. The yield of oil+gas appears to be independent of tire/coal ratio. Similar results were obtained with Tire-2 where the effect of tire addition was found to be more significant at low tire/coal ratios (Figure 4). The conversion of coal increases from 38 wt% (coal-alone runs) to 49 wt% at tire/coal ratio of 1. At higher ratios, the addition of tire has only a small effect on coal conversion. There seems to be a slight maximum in the conversion at tire/coal ratio of 3 where the conversion was 54 wt%. The oil yield for the co-liquefaction may be maximum at a tire/coal ratio of 2.

Effect of Using Ferric Sulfide-based Catalyst

The catalytic runs were made using catalyst based on iron sulfide, Fe_2S_3. The catalyst was impregnated *in-situ* on the coal. The coal was first mixed with a dilute aqueous solution of Na_2S and agitated vigorously before adding $FeCl_3$ solution. The suspension containing coal and catalyst was filtered, washed and dried in N_2 under vacuum.

Figure 5 shows the effect of catalyst loading on the conversion and product yield. In these runs, Tire-1 was used and the tire/coal ratio was 1. Again, the results are based on coal. The conversion of coal increases from around 45 wt% in the absence of catalyst to over 80 wt% when the catalyst loading was 1.67 wt%. The yield of oil+gas increased from 10 wt% to 20 wt%. This indicates that the increased loading is beneficial to the activity and selectivity of the catalyst. However, the incremental effect of catalyst loading is more pronounced at loadings of around 0.5 wt%.

The effect of tire/coal ratio on the conversion and product yields in the catalytic runs is presented in Figure 6. These runs were made with Tire-2 and the catalyst loading was 1.67 wt%. The addition of tire appears to have only a small effect on the conversion and product yields below a tire/coal ratio of 1. At higher ratios, both the conversion and yields decrease indicating that the addition of excess tire is deterimental to the activity of the catalyst. This may be due to the poisoning of the catalyst by the polymeric compounds present in the tire rubber.

CONCLUSIONS

1. The co-liquefaction of tire rubbers with coal has a considerable synergistic effect on the conversion and product yields from coal.
2. The synergism due to the addition of tire increases with an increase in hydrogen pressure and tire/coal ratio.
3. The conversion and product yields from coal increase using ferric sulfide-based catalyst. However, the synergistic effect of tire in the catalytic runs is small, especially, at high tire/coal ratios where the conversion and yields actually decrease.

ACKNOWLEDGEMENT. This work was conducted under U.S. Department of Energy Contract No. DE-FC22-90PC90029 under the cooperative Agreement to the Consortium for Fossil Fuel Liquefaction Science.

REFERENCES

1. Liu, Z., Zondlo, J.W. and Dadyburjor, D.B. *Energy & Fuels* 1994, 8(3), 607.
2. Farcasiu, M. and Smith, C.M. *Prepr. Pap.- Am. Chem. Soc., Div. Fuel Chem.* 1992, 37(1), 472.
3. Malhotra, R. and McMillen, D.F. *Energy & Fuels* 1993, 7, 227.
4. Whitehurst, D.D., Mitchell, T.D. and Farcasiu, M. *Coal Liquefaction*, Academic Press: New York, 1980.

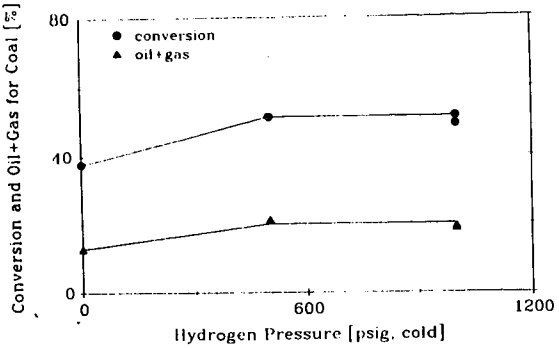

Figure 1. Effect of H_2 pressure on conversion and yields of coal in a coal/tire mixture. Conditions: 400°C, 30 min, tire/coal =1. Tire-1 and DECS-6 coal were used.

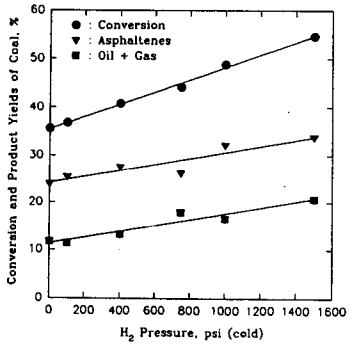

Figure 2. Effect of H_2 pressure on conversion and yields of coal in a coal/tire mixture. Conditions: same as in Figure 1. Tire-2 and DECS-6 coal were used.

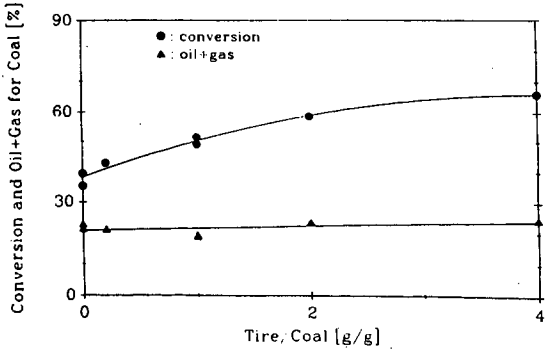

Figure 3. Effect of tire/coal ratio on conversion and yield of coal in a coal/tire mixture. Conditions: 400°C, 30 min, H_2 pressure = 1000 psi (cold). Tire-1 and DECS-6 coal were used.

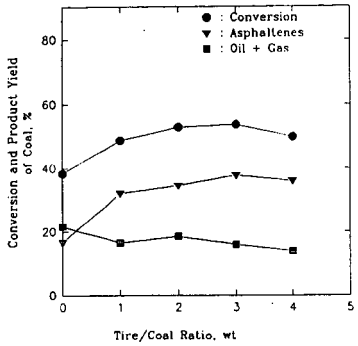

Figure 4. Effect of tire/coal ratio on conversion and yield of coal in a coal/tire mixture. Conditions: Same as Figure 3. Tire-2 and DECS-6 coal were used.

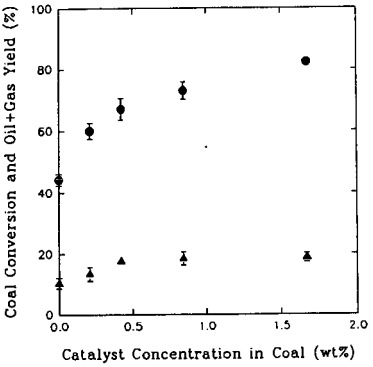

Figure 5. Effect of catalyst loading on conversion and yield of coal in a tire/coal mixture. Conditions: same as in Figure 3. Tire-1 and DECS-6 coal were used.

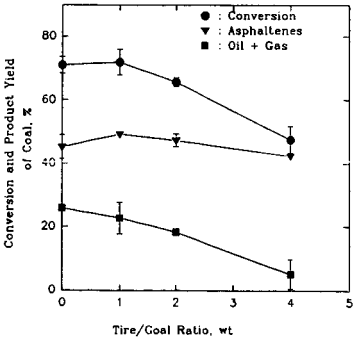

Figure 6. Effect of tire/coal ratio on conversion and product yields of coal. Conditions: 400°C, 30 min, 1000 psi (cold), 1.67% catalyst loading. Tire-2 and DECS-6 coal were used.

WOOD COFIRING EXPERIENCE IN CYCLONE BOILERS

David A. Tillman
Robert W. Stahl

Foster Wheeler Environmental Corporation
2525 Natomas Park Drive, Suite 250
Sacramento, CA 95833

Key Words: wood waste, cyclone boilers, cofiring

ABSTRACT

Wood waste has been cofired with coal in cyclone boilers at the Allen Fossil Plant of TVA, the King Station of Northern States Power Co., and other generating stations. This practice is sufficiently interesting that TVA plans long term testing of cofiring wood at Allen. This practice can be separate from, or combined with, cofiring tire-derived fuel (TDF) in cyclone boilers. Cofiring has been practiced with the wood waste being fed to the boilers simultaneously with the coal, and with the wood waste being introduced into the secondary air system of cyclone boilers, for separate feeding. The practice of cofiring wood waste with coal in cyclone boilers has been shown to reduce emissions of SO_2 and NO_x, while also reducing the cost of fuel in selected locations. Foster Wheeler Environmental Corporation has evaluated this practice both with engineering design studies and with field testing for the Electric Power Research Institute and the Tennessee Valley Authority. This paper summarizes testing and experience in several locations, focusing upon the following issues: 1) the impact of cofiring on boiler performance and consequent airborne emissions, 2) the alternative designs to accomplish cofiring, and 3) the economics of cofiring under various conditions.

INTRODUCTION

Cofiring of biofuels with coal provides utilities with the opportunity to accomplish the following objectives: 1) reduce fuel costs by utilizing residuals from the forest products industry; 2) reduce formation of SO_2 by using a fuel which contains virtually no sulfur; 2) reduce formation of NO_x by using the biofuels that are low in nitrogen and that burn at lower temperatures than most coals (e.g. wood wastes; some agricultural materials can be high in nitrogen and therefore do not satisfy this objective); 3) reduce the formation of CO_2 from fossil fuels, thereby addressing issues associated with the global climate challenge; and 4) support economic development in the utility's service area, thereby enhancing baseload customer growth and plant utilization. All of these objectives are mandated by law and regulation, results of voluntary utility actions (e.g. fossil CO_2 reductions), or are conventional utility practice for managing costs and loads.

From a materials handling and fuel preparation perspective, the biofuels are fundamentally different from coal. They can not be ground by traditional pulverizing methods, but must be shredded or chopped. Biofuels are fibrous. Consequently, fuel preparation methods can be fundamentally different. Biofuels respond to hammermills and derivative systems, but not to ball mills, bowl mills, and other coal pulverizing technologies. The additional material handling property of consequence is bulk density. Coal is typically on the order of 40 - 50 lb/ft^3 while wet wood is on the order of 18 - 20 lb/ft^3, dry wood is about 10 - 12 lb/ft^3 and most agricultural wastes are on the order of 8 - 12 lb/ft^3 as well. These bulk densities require careful management practices such that the fuel storage system is not compromised when cofiring is considered.

Chemically, biofuels, particularly wood waste, are fundamentally different from coal as is shown in Table 1. As mentioned previously, biofuels are low in sulfur content. Further the wood wastes are typically very low in nitrogen content, although some agricultural wastes including rice hulls and alfalfa stems may have nitrogen contents that are at moderate to high levels (e.g. 0.5 - 2.0%, dry basis). These fuels are somewhat oxygenated, typically moist, and have modest heat contents. Of more consequence, these fuels can have low to moderate ash percentages (e.g. 3 - 6%). The ash, however, is fundamentally different from coal with high concentrations of alkali metals: potassium, calcium, and sodium.

Base/acid ratios are in the range of 2.0 - 6.0, with some B/A values exceeding 10.

The behavior of biofuel/coal blends in combustion systems can be readily predicted from weighted arithmetic averaging of the properties of the individual fuels, with particular attention to proximate and ultimate analysis, higher heating value, and formation of combustion products. The one exception is ash fusion temperature, where blending shifts the base/acid ratio towards 1.0, and consequently impacts ash fusion temperatures according to the following equations:

$$AFT_i = 1268.7W^2 - 980W + 2336 \quad [1]$$

$$AFT_h = 1025.9W^2 - 494W + 2069 \quad [2]$$

Where AFT_i is the initial deformation temperature, W is the weight percentage of wood (dry basis) in the blend, and AFT_h is the hemispherical temperature (reducing environment).

The high concentration of alkali metals in the ash further complicates the analysis based upon the potential for slagging and fouling. The potassium oxide is of particular concern due to the low temperatures at which it vaporizes, leading to the potential for condensation in backpasses of the boiler.

The consequence of these characteristics is that biofuel cofiring, particularly wood cofiring, is more readily achieved with cyclone boilers than with pulverized coal (PC) boilers; this ease of accomplishment is particularly apparent at moderate cofiring percentages which are on the order of 10 - 15% by heat input or 20 - 30% by mass.

BACKGROUND

Within the past few years, several utilities have initiated cofiring experiments or practices. Northern States Power (NSP) has initiated cofiring at its cyclone-based King Station, and consumes wood waste from the Andersen Windows manufacturing plant on a regular basis. This practice has gone on for the past several years, and NSP has been very successful. Cofiring occurs in 3 of the 12 cyclone barrels at the plant, and firing levels of 15% wood (heat input basis) have been achieved. The wood, which is dry and pulverized, is introduced through the secondary air system. Wood fuel storage and preparation is separated from coal storage and preparation. The Big Stone Plant of Otter Tail Power also has cofired wood waste in the form of railroad ties. This plant, also a cyclone boiler, was designed for lignite. It has provisions for fuel drying. It also has a very large primary furnace in order to ensure burnout of char particles.

TVA and EPRI initiated cofiring investigations in 1992. The investigations included both PC boilers and cyclone boilers, with the latter focusing upon cofiring at the Allen Fossil Plant (ALF) in Memphis, TN. The concept developed had broader application than the design used at the King Station of NSP: in this concept, wood waste is mixed with coal in the fuel yard and simultaneously transported to the fuel bunkers and then to the cyclone burners. TVA also contemplated using green wood (40 - 50% moisture) as opposed to the dry wood (8 - 12% moisture) being fired at the King Station of NSP (See Fig 1).

EPRI/TVA INVESTIGATIONS

The EPRI/TVA investigations, through Foster Wheeler Environmental Corporation (then Ebasco Environmental Corporation) were initiated by development of conceptual process designs and associated calculations. These were followed by mechanical systems designs, cost estimates, evaluations of environmental impacts, and economic assessments.

The studies generally demonstrated that cofiring at 10% by heat input, or 20% by mass, would have the following impacts: 1) not affect the ability of the plant to achieve capacity based upon fan capacities and related factors, 2) reduce boiler efficiency by about 1.5%, depending upon the specific condition of the wood, 3) reduce the SO_2 emissions as a function of fuel substitution, and 4) reduce NO_x emissions disproportionately based upon fuel effects

(reduced nitrogen content in the fuel) and temperature effects in the cyclone barrel.

The initial designs, calculations, and evaluations led to the conclusion that cofiring would be economically feasible at the ALF location. The economics were favorable as a consequence of the following factors: 1) a low capital cost ($130 - $200/kW supported by wood waste), a fuel price differential of $0.40/$10^6$ Btu between wood and Western Kentucky bituminous coal delivered to the site, 3) modest incremental operating and maintenance costs utilizing one additional person and capitalizing upon existing maintenance infrastructure at the plant, and 4) modest credits for SO_2 removal ($136/ton SO_2 based upon recent market prices). No credits were taken for NO_x or fossil CO_2, although they are the source of significant economic analysis.

The initial investigations led to a week of parametric testing at the facility. The testing involved evaluations of the ability to achieve capacity at ALF when cofiring wood with coal, boiler efficiency when firing wood and coal at various levels, and reductions in airborne emissions. The testing program involved cofiring at percentages ranging from 1.6 to 20%, mass basis. The wood was obtained from local sources, and the coal was a Western Kentucky coal (see Table 1).

The testing confirmed the results from the calculations: capacities were largely not impacted by cofiring, boiler efficiencies were reduced by less than 2% when cofiring even at significant wood percentages, SO_2 emissions declined in proportion to the Btu substitution of wood for coal, and NO_x emissions declined in response to fuel substitution and temperature effects.

Additional testing performed under this program involved storage and flow characteristics of wood/coal blends; and this work was performed largely by Reaction Engineering International in support of the Foster Wheeler Environmental program. This testing demonstrated that wood waste improved the flow of fuel through the bunkers, and virtually eliminated dusting on the coal belts. Additional testing performed by Foster Wheeler Environmental also documented that the wood did not compromise storage from the perspective of inducing spontaneous combustion.

The parametric tests and supporting investigations were initial indications of the potential for wood cofiring. They have resulted in the decision to pursue additional tests during the first half of 1995, pursuant to commercializing cofiring using the system shown in Fig. 1. These tests will be conducted firing wood with Utah bituminous coal, and with combinations of coal, wood, and tire-derived fuel (TDF).

CONCLUSIONS

The cofiring program conducted at the Allen Fossil Plant of TVA is advancing to extended testing, more detailed materials handling engineering, and additional economic analyses. This program integrates the EPRI/TVA approach to cofiring into the range of options being pursued by other utilities. Such utilities are testing cofiring wood waste at low percentages in PC boilers, transporting <5% wood (mass basis) through the pulverizers with the coal. Such testing is also considering cofiring wood in PC boilers at higher percentages, using separate biofuel preparation. These systems fire the biofuels through dedicated burners into the boiler. Utilities pursuing such options include TVA as well as Georgia Power, Savannah Electric, New York State Electric and Gas, and others. The cofiring program at the Allen Facility has not yet completely proven the commercial viability of cofiring in cyclone boilers using the design configuration shown in Fig. 1; however the program is sufficiently advanced that such commercial demonstration is anticipated as a consequence of the next sequence of tests plus some planned long term test activities.

ACKNOWLEDGEMENTS

This is to acknowledge support for the program from the Electric Power Research Institute and the Tennessee Valley Authority.

Table 1. Typical Fuel Compositions for Eastern Bituminous Coal, Wood, and Alfalfa Stems

	Bituminous Coal	Wood Fuel	Alfalfa Stems
Proximate Analysis (wt %, dry basis)			
Volatile Matter	37.22	84.58	76.03
Fixed Carbon	52.97	14.26	17.45
Ash/Inerts	9.81	1.16	6.52
Ultimate Analysis (wt %, dry basis)			
Carbon	74.77	49.23	45.35
Hydrogen	5.08	5.93	5.75
Oxygen	6.32	43.27	40.24
Nitrogen	1.44	0.38	2.04
Sulfur	2.31	0.02	0.10
Chlorine	0.27	0.01	0.15
Ash/Inerts	9.81	1.16	6.52
Heating Value (Btu/lb)			
As-Received	11,748	5,431	7,108
Dry Basis	13,040	8,338	7,940
Moisture/Ash Free	14,457	8,437	8,494
Typical Moisture Content			
Weight Percent	10	40	10
Ash Analysis (wt %)			
SiO_2	44.16	23.70	1.44
Al_2O_3	22.89	4.10	0.60
TiO_2	1.00	0.36	0.05
Fe_2O_3	22.86	1.65	0.25
CaO	2.16	39.95	12.90
MgO	0.47	4.84	4.24
Na_2O	0.25	2.25	0.61
K_2O	1.97	9.81	40.53
P_2O_5	0.50	2.06	7.67
SO_3	1.93	1.86	1.60
Undetermined	1.81	9.43	17.44
Ash Fusibility			
Base/Acid Ratio	0.41	2.08	28.01
T_{250} Temperature (°F)	2,397	2,440	---
Ash Fusion Temperatures (°F)			
Oxidizing Atmosphere			
Initial	2,406	2,546	> 2,700
Softening	2,545	2,563	> 2,700
Hemispherical	2,552	2,566	> 2,700
Fluid	2,565	2,577	> 2,700
Reducing Atmosphere			
Initial	2,082	2,274	> 2,700
Softening	2,273	2,577	> 2,700
Hemispherical	2,325	2,583	> 2,700
Fluid	2,429	2,594	> 2,700

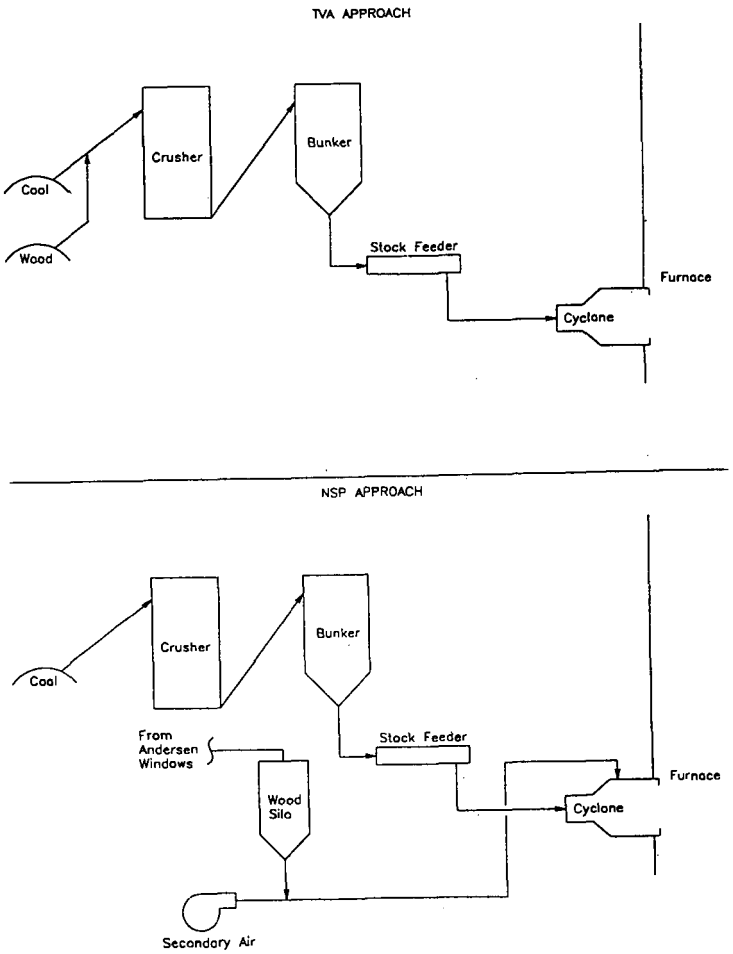

Fig. 1. Alternative Approaches to Cyclone Cofiring

COFIRING WASTE BIOFUELS AND COAL FOR EMISSIONS REDUCTION

J. Brouwer, W.D. Owens, N.S. Harding, and M.P. Heap
Reaction Engineering International

D.W. Pershing
University of Utah

Keywords: waste biofuels, coal, reburning, NO emissions

ABSTRACT

Combustion tests have been performed in two pilot-scale combustion facilities to evaluate the emissions reduction possible while firing coal blended with several different biofuels. Two different boiler simulations, pulverized coal fired boilers and stoker coal fired boilers, were simulated. The pc-fired studies investigated the use of waste hardwood, softwood and sludge as potential reburning fuels and compared the results with coal and natural gas. The use of these wood wastes is attractive because: wood contains little nitrogen and virtually no sulfur; wood is a regenerable biofuel; wood utilization results in a net reduction in CO_2 emissions; and, since reburning accounts for 10-20% of the total heat input, large quantities of wood are not necessary. The results of this program showed that a reduction of 50-60% NO was obtained with approximately 10% wood heat input. Reburn stoichiometry was the most important variable. The reduction was strongly dependent upon initial NO and only slightly dependent upon temperature.

The stoker program investigated barriers for the successful blending of coal with waste railroad ties. Parameters evaluated included blending firing rate, chip size, optimum feed location, overfire/underfire air ratio, and natural gas addition. The results of this study demonstrated that NO emissions can be reduced by more than 50% without any significant increase in CO or THC emissions by the proper use of zoned reburning.

Both programs demonstrated several benefits of biofuel blends, including: 1) lower operating costs due to reduced fuel prices; 2) reduced waste disposal; 3) reduced maintenance costs; 4) reduced environmental costs; and 5) extension of the useful life of existing equipment.

INTRODUCTION

Reburning is a combustion modification technology which removes NO_x from combustion products by using fuel as the reducing agent. The concept was originally introduced by John Zink Company[1] and Wendt et al.[2], based on the principle of Myerson et al.[3] that CH fragments can react with NO. Reburning is accomplished by secondary fuel injection downstream of the fuel-lean primary combustion zone. The second stage or reburning zone is usually operated at overall fuel-rich conditions, allowing a significant fraction of the primary NO to be reduced to N_2 and other nitrogenous species. In the third zone, additional air is introduced to establish overall fuel-lean conditions and allow for the burnout of remaining fuel fragments.

Reduction of NO occurs primarily in the reburn zone by reaction of NO with hydrocarbon fragments (CH, CH_2). These reactions typically produce hydrogen cyanide which decays in the reburning zone along the chemical pathway

$$NO + CH_i \Rightarrow HCN \Rightarrow NCO \Rightarrow NH \Rightarrow N \Rightarrow N_2$$

This reburning concept is utilized in both experimental projects presented herein.

The waste biofuels that were tested include: pulverized hardwood and softwood waste from wood manufacturing, a wood-derived sludge, and chipped railroad ties. Discarded railroad ties represent a significant alternate energy resource and are available throughout the U.S. The wood manufacturing waste and wood-derived sludge materials are transportable but generally only available near the manufacturing locations. These and other similar products can be removed from the waste stream and can be significant alternative fuel sources. For example, approximately 16 million railroad ties are discarded or abandoned per year in the U.S., with a potential energy availability from RTDF of 2×10^{13} Btu/yr; equivalent to fueling a 350 MW power station.

Generally, the cost of these waste fuels is approximately 50 percent of coal on an energy basis. The wood-derived sludge is even less expensive, although its use may involve drying costs due to high moisture content (~65%). Although the cost incentive is apparent, the process parameters controlling the replacement of coal with biofuel wastes in boilers have not been defined. The purpose of these projects was to develop an understanding of the combustion of biofuels in conjunction with coal on stoker grates and in pc-fired boilers in order to define retrofit hardware that will allow replacement of coal and concurrent pollutant emissions reduction.

APPROACH

Experiments were carried out in two facilities which are described below. Gaseous and solid samples were withdrawn from both furnaces at various locations. Gas samples were withdrawn through a water cooled, stainless steel probe, then filtered and dried. The gas sample was analyzed for NO (chemiluminescence), O_2 (paramagnetic), CO (NDIR) and N_2O/NH_3 (FTIR). Temperatures are measured throughout each furnace with bare-wire, type-B thermocouples and a moveable suction pyrometer probe.

Pilot Scale Spreader-Stoker

The pilot-scale spreader stoker facility, shown in Figure 1, is 3.2 m high and the stoker has a 0.09 m^2 grate. The furnace was designed to fire at rates from 126,000 to 252,000 kcal/hr. The base of the furnace provides support and houses the ash drawer. Air is injected under the grate and at various heights above the grate. Ports vertically located along the furnace allow for the addition of fuel and air for secondary burning. Coal was fed from the hopper via a metering auger to a rotating multi-vane spreader. Railroad ties were weighed into discrete predetermined quantities and fed into the stoker via the coal chute. The spreader is located 0.8 m above the bed and distributes the solid fuels uniformly across the bed. All of the furnace sections contain multiple ports for sample extraction, observations, and overfire air or natural gas injection. Three different stoker configurations were used: industrial, 2-U, and 2-N. In the 2-U configuration, overfire air was through the main gas burner ports and 2.2 m above the bed; reburning natural gas was injected 1.8 m above the bed. In the 2-N configuration, overfire air was added 1.8 and 3.2 m above the bed; natural gas was injected 2.2 m above the bed.

Pilot Scale Pulverized Coal Furnace

Figure 2 shows the 38 kW, pulverized coal fired combustion research facility at the University of Utah. The main burner is located at the top left section and is down-fired. Access ports are available along the entire length of the furnace. The combustion chamber is 16 cm diameter and 7.3 m long and is constructed of composite refractory walls to minimize heat loss. The furnace is divided into three sections. The first section is the primary section where the main fuel burns at overall fuel-lean conditions. The second section is called the reburning section which begins at the point of injection of the reburn fuel (typically in the horizontal section of furnace as shown in Figure 2). The third section is the burnout section into which air is added to achieve overall fuel-lean conditions for burnout of the remaining fuel fragments.

Solid fuels were transported to the furnace by a transport fluid (usually air) which was laden with the solid fuel that was metered by a twin screw feeder. The feeder is a volumetric feeder with a variable speed motor that was calibrated for mass flow rates of each of the fuels tested.

Objectives

The objectives of this paper are to report on experimental results which: 1) determine the feasibility of cofiring coal with waste biofuels, 2) compare the effectiveness of these fuels to natural gas in reburning, and 3) establish performance goals for the co-firing of coal and waste biofuels for emissions and waste reduction in both spreader-stoker and pc-fired boiler environments.

RESULTS

Stoker Experiments:

Initially, coal alone, and coal blended with hogged railroad ties were evaluated under typical industrial conditions where the overfire air was divided into two approximately equal segments above and below the spreader. Hogged railroad ties were fired with coal in an 80/20 coal/railroad ties ratio. Figure 3 presents the NO_x and CO emis-

sions measured for these tests.

Under clean operating conditions (greater than 50 percent excess air and CO emissions less than 20 ppm), the NO_x emissions were lowered by about 30% with coal/railroad tie co-firing. This is likely due in part to the fact that the railroad ties contained essentially no nitrogen (0.22 percent).

The CO data (Figure 3) suggests that at low excess air levels the RTDF mix burns more completely. This is likely due to the presence of increased fines and the partially oxygenated nature of the wood fuel. The corresponding total hydrocarbon data for these fuels, tested at the commercial practice conditions, indicated there was little difference in the total hydrocarbon emissions for the co-firing case compared to the coal only case (the total hydrocarbon emissions were less than 20 ppm).

Application of Low NO_x Concepts - Reburning

To evaluate the applicability of the low-NO_x concepts described earlier, a series of co-firing experiments was conducted with 20 percent railroad ties in conjunction with natural gas addition. Figure 4 shows the NO_x and CO emissions for the RTDF/coal blend at an overall stoichiometric ratio of 1.28 and varying amounts of natural gas injection in the upper furnace. With 15 percent natural gas co-firing, the NO_x emissions were reduced to about 0.25 lbs NO_x/MBtu in this configuration and the CO was approximately 50 ppm. The baseline NO_x emissions were approximately 0.45 lbs/MBtu with a CO level of about 50 ppm for the coal only case. Also, CO concentrations decrease significantly with increased gas utilization.

The experience in this study suggests that a properly designed system could likely accommodate railroad tie feed rates higher than 20%. No problems with either bed slagging or other pollutant emissions were observed at the rates tested in this study. In a future test program, it would be desirable to investigate waste fuel firing rates up to 50 percent in this small scale unit to determine whether there are important scientific or practical reasons to limit the waste-fuel firing.

PC-fired Experiments:

Experiments conducted in the pc-fired facility (Figure 2) were preformed without blending of the primary fuel with the waste biofuel. The biofuels were fired separately (and individually) in the reburning zone in each case.

Reburn Stoichiometry

The parameter that most dramatically influences the effectiveness of wood reburning is the stoichiometry in the reburn zone. The stoichiometric ratio (SR) in the reburn zone is determined by calculating the amount of oxidant required to convert all of the elements of the wood, the wood carrier, and the baseline products from the primary zone to carbon dioxide and water. Stoichiometric ratios less than 1 indicate fuel-rich conditions, while SR > 1.0 indicates excess air conditions. Figure 5 presents the effect of reburn stoichiometry for reburning with hardwood at various temperatures. The variation in temperature was accomplished through movement of the position of the reburning zone in the furnace, with higher temperatures corresponding to reburn zones that are closer to the primary zone. In each of the cases the residence time in the reburn zone is held constant at about 400 ms. Notice that wood reburning is more effective at lower stoichiometries corresponding to increased wood reburning rate. The NO reduction achieved by hardwood reburning improves with increasing temperature as shown in Figure 5.

Reburn Fuel Comparisons

Figure 6 presents a comparison of hardwood, softwood, and wood sludge at the lower reburn temperature of 1398 K. The NO reduction achieved by the two wood types is very comparable except at stoichiometries less than 0.95 where the softwood performs slightly better than the hardwood. Each of the woods performs better than the wood sludge except at low stoichiometric ratios (0.85). A comparison of softwood, hardwood, wood sludge, coal and natural gas is presented in Figure 7 for the higher temperature reburning condition of 1721 K. At these high temperature conditions all of the fuels perform quite well leading to a reduction in NO of around 60% for SR $\leq$ 0.9.

Figure 7 presents the very surprising result, that wood seems to reduce NO just as well as coal and natural gas at the high temperature reburn fuel injection condition of 1721 K. The wood sludge performs slightly worse except at low stoichiometries. This is surprising since wood is not expected to produce the same number of CH-radicals that

are required to begin the process of NO reduction to N_2. The similar performance of these fuels may be due to different factors, including possible enhanced mixing, and a delayed release of hydrocarbon species for the solid fuels compared to the natural gas. Although the fuels all seem to perform well as reburning fuels for the standard conditions investigated, they do not perform equally as well when NO levels into the reburning zone are lowered from 500 to 200 ppm, as indicated in Figure 8. For the case of only 200 ppm NO entering the reburn zone, wood and natural gas are significantly better reburning fuels than coal. This is most likely due to the increased nitrogen content of the coal (compared to the wood and gas).

SUMMARY

These experimental studies have demonstrated that:

1) NO_x emissions can be reduced by more than 50 percent without any significant increase in CO or total hydrocarbon emissions by the proper use of natural gas in conjunction with appropriate tailoring of the stoichiometry distribution throughout the combustion zone in a pilot-scale stoker.
2) Railroad ties can be used as a co-firing fuel up to at least the 20 percent level without any detrimental effect on the pollutant emissions. Further, no combustion related operating problems were observed during the experimental studies.
3) To minimize overall NO_x emissions, one must control both the bed stoichiometry and the stoichiometry in the suspension phase combustion zone of a stoker.
4) Wood wastes (including a wood-derived sludge) can be used effectively as reburning fuels in a pc-fired furnace.
5) Reburn stoichiometry is the single most important parameter which determines the effectiveness of reburning with the waste biofuels, with optimal stoichiometric ratios around 0.85.
6) These biofuel waste streams can be utilized in a manner that reduces operating costs, and reduces environmental costs (including reductions in NO and CO emissions, and a net reduction in CO_2 emissions) which makes them excellent candidates for practical application.

REFERENCES

1 Reed, R.D., Process for the Disposal of Nitrogen Oxide. John Zink Company, U.S. Patent 1,274,637, 1969.
2 Wendt, J.O.L., Sternling, C.V. and Matovich, M.A., *Fourteenth Symposium (International) on Combustion*, The Combustion Institute, p. 897, 1973.
3 Myerson, A.L., Taylor, F.R. and Faunce, B.G., *Sixth Symposium (International) on Combustion*, The Combustion Institute, p 154, 1957.

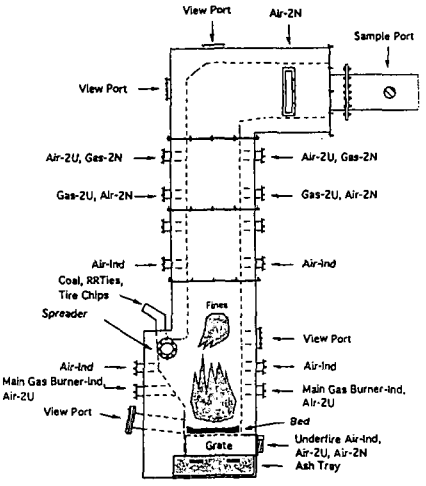

Figure 1. Pilot Scale Spreader-Stoker Facility.

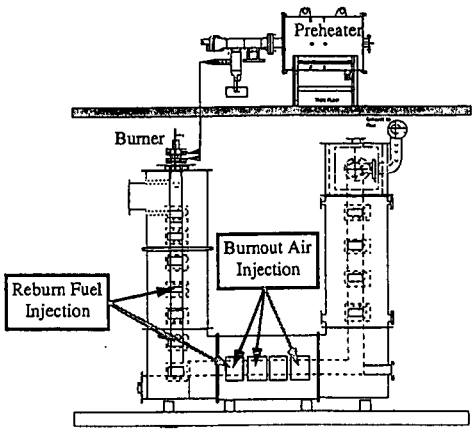

Figure 2. Pilot Scale Pulverized-Coal Fired Facility.

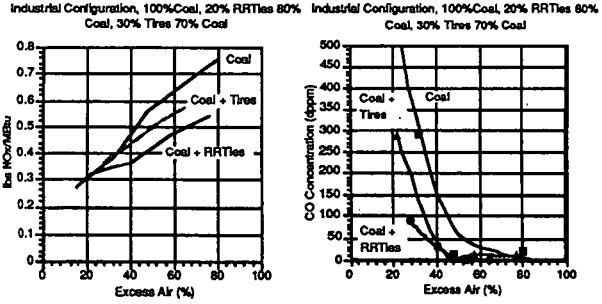

Figure 3. NO_x and CO emissions for coal and coal/RTDF blend.

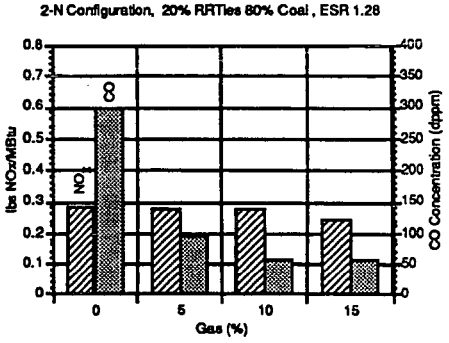

Figure 4. NO_x and CO emissions for coal/RTDF blend with reburning.

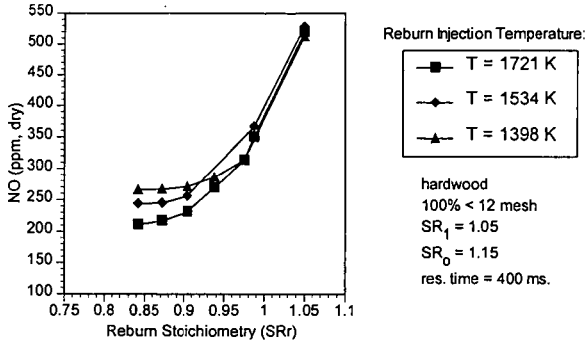

Figure 5. Effect of reburn zone stoichiometry on NO emission for hardwood at three reburn fuel injection temperatures.

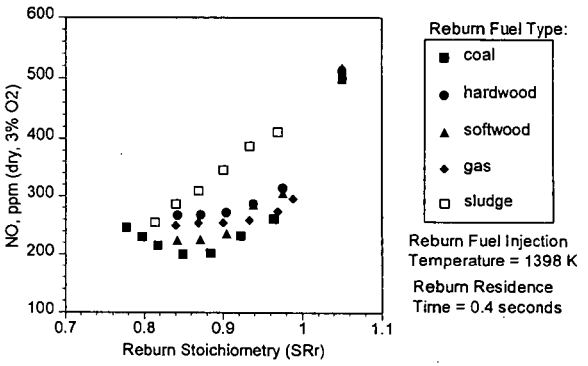

Figure 6. Reburn fuel comparisons at a reburn fuel injection temperature of 1398 K.

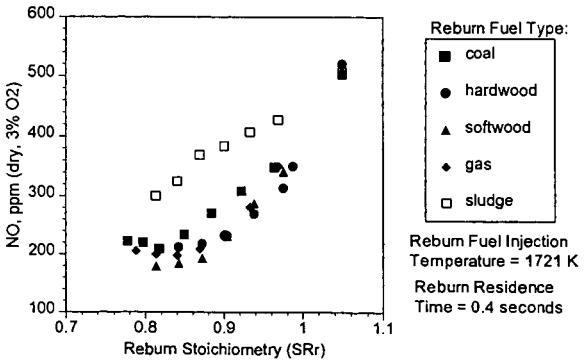

Figure 7. Reburn fuel comparisons at a reburn fuel injection temperature of 1721 K.

CHARACTERIZATION OF COAL AND BIOMASS FUEL BLENDS

David E. Prinzing
Kermit P. Hellem
W. John McVey

Foster Wheeler Environmental Corporation
2525 Natomas Park Drive, Suite 250
Sacramento, CA 95833-2900

Keywords: Fuel Characterization, Fuel Blending, Energy Generation

ABSTRACT

The cofiring of biofuels with coal in existing boilers presents significant potential benefits to electric power generators. The practice has been shown to reduce SO_2 and NO_x emissions, reduce fuel costs at some locations, and provide support to industrial customers from the forest products industry. One of the technical uncertainties associated with cofiring involves the characterization of the biomass and the coal, both separately and as fuel blends. Foster Wheeler Environmental Corporation has evaluated the practice of cofiring biomass with coal for the Electric Power Research Institute and the Tennessee Valley Authority. This paper reviews the characterization requirements and presents the analytical results for a number of coals and biomass wastes, focusing largely on the impact of fuel blending on ash fusibility and viscosity. Also, the consequences of these characteristics on the performance of pulverized coal and cyclone boilers is reviewed.

INTRODUCTION

Foster Wheeler Environmental Corporation has been evaluating the practice of cofiring waste wood residues with coal at existing Tennessee Valley Authority (TVA) power plants for the Electric Power Research Institute (EPRI) and TVA. This work has been directed toward specific TVA power plants at cofiring levels up to 15 percent on a heat input basis. The following benefits can be expected from such a cofiring program:

(1) A cost-effective program for reducing emissions of sulfur dioxide (SO_2) and oxides of nitrogen (NO_x);

(2) A cost-effective strategy for reducing fossil fuel based carbon dioxide (CO_2) emissions in concert with the global climate challenge of reducing the generation of greenhouse gases;

(3) Potentially reduced cost of fuel to coal-fired power plants, improving their economics and consequent capacity utilization;

(4) Increased support for the forest products industry in solving waste disposal problems.

The information presented here is focused specifically on cofiring waste wood residues with coal at the Allen Fossil Plant in Memphis, Tennessee and the Kingston Fossil Plant near Knoxville, Tennessee. The Allen Fossil Plant is equipped with three 265 MW cyclone boilers and has undergone parametric cofiring tests at low and moderate percentages of wood waste. The Kingston Fossil Plant is equipped with nine tangentially-fired pulverized coal boilers, four single furnace units rated at 136 MW_e each, and five twin furnace units rated at 200 MW_e each. The Kingston Fossil Plant has completed parametric testing of cofiring sawmill residues at low levels.

One of the technical uncertainties associated with wood cofiring lies in understanding the locally available fuels, with emphasis both on physical characteristics (particle size, specific gravity, and moisture content) and on fuel chemistry (proximate and ultimate analyses, higher heating value, and ash chemistry).

CHARACTERISTICS OF LOCALLY AVAILABLE FUELS AND FUEL BLENDS

To characterize the locally available waste wood residues, over 25 potential wood fuel suppliers (including both sawmills and manufacturing facilities) in each of the Memphis and Knoxville areas were selected and sampled in the fall of 1993. Repeat sampling of ten of the sources from each area was completed in the spring of 1994. The sources of wood were characterized, including process flow diagrams for the processes that generated the wood waste. Wood samples were prepared and sent to a fuels laboratory for determination of the proximate analysis, ultimate analysis, calorific value, ash elemental analysis, and ash fusibility characteristics. Also, samples of coal from the Allen and Kingston Fossil Plants were sent to the laboratory for the same analyses. For the Allen Fossil Plant, blends of coal and wood were prepared on a dry weight basis at four levels (5, 10, 20, and 30 weight percent wood; these correspond to heat inputs of about 2.5, 5, 10, and 15 percent respectively). These samples also were sent to the laboratory for analysis. Particle size distributions for each wood fuel source were determined using a sieve analysis.

The direct result of this work is the detailed characterization of the various fuels and fuel blends. For both the Allen and Kingston Fossil Plants, these include the baseline coals, the locally available waste wood fuels, and blends of the coal and wood at various levels. The baseline coal and average wood fuel characteristics fell within expected ranges for these kinds of fuels. With regard to the variability in fuel characteristics for the wood fuels sampled, it was found that the statistical confidence intervals were relatively small. Consequently, it is expected that the average values presented are representative of the waste wood fuels available from these sources, and that relatively little variation from these values is expected. Such a stable, well-defined fuel characterization helps reduce the uncertainties associated with cofiring wood in coal-fired boilers. Tables 1 and 2 provide summary data concerning these analytical results.

The characteristics of coal and wood fuel blends can be seen largely as arithmetic averages of the characteristics of the two fuels. The more interesting exception to this generalization lies in the fusibility characteristics of the ash resulting from the fuel blends. A significant eutectic was present in the ash from the blends, reducing the ash fusion temperatures to levels below that of either fuel by itself. These results are depicted graphically as polynomial regressions of measured data in Figure 1.

CONSEQUENCES FOR PULVERIZED COAL AND CYCLONE BOILERS

The issues of fuel characterization impact fuel handling, combustion, and ash management. From the perspective of fuel handling, the fine particle sizes obtained in the samples demonstrated that the fossil stations could avoid elaborate wood particle size reduction systems. Significant percentages of wood at <1/4", <1/8", and 1/16" document the fact that the materials handling system can consist of screens and magnets for pulverizer and boiler protection. Also, the materials handling system could include a wood fuel dryer, if desired. Extensive investments in hammer mills and related equipment can be avoided by procurement practices. Further, the wood moisture contents will likely be on the order of 40 to 50 percent, based upon the experience of the sampling teams in the field.

The characterizations of the fuel lead to assessments of their impact on boiler performance at cofiring levels of 10-15 percent (heat input basis). Such characterizations lead to the conclusion that, at operating conditions currently associated with the Allen and Kingston facilities, there would be no significant deleterious impact on boiler efficiency or net station heat rate. Similarly, there is no significant impact on flame temperatures.

Of more consequence is the impact on ash chemistry and the behavior of non-combustibles, particularly as it relates to the cyclones.

The reduction in the ash fusion temperatures associated with fuel blends is consistent with the fact that the base/acid ratio is increased relative to that of the coal used at the Allen Fossil Plant, and decreased relative to that of the wood available in the Memphis area. The resulting base/acid ratio associated with the blends approaches 1.0 from both "pure fuel" directions.

This analysis does not, and can not address the impact of fuel blending on the final ash consideration: the salability of flyash as a pozzolanic material, or the sale of slag for such products as roofing granules. Those questions can only be addressed by significant additional testing of the cofiring process.

In conclusion, the fuel characterization studies demonstrated the significant potential associated with cofiring. The wood fuels available to Allen and Kingston Fossil Plants are not unusual, and contain no significant problems.

ACKNOWLEDGMENTS

This is to acknowledge support for the program from the Electric Power Research Institute and the Tennessee Valley Authority.

Figure 1: Ash Fusion Temperatures for Coal/Wood Fuel Blends

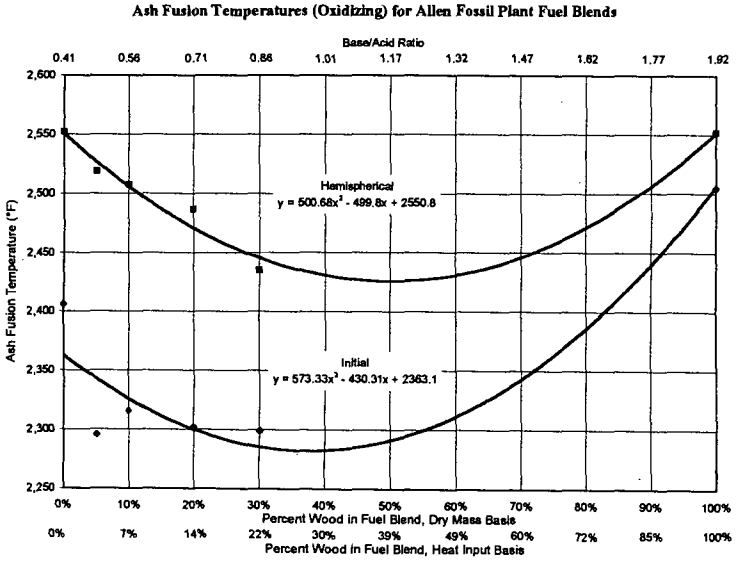

Table 1: Summary of Coal Characterizations

Parameter	Allen Coal	Kingston Coal
Proximate Analysis (wt %, as rec'd)		
Moisture	9.91	7.17
Volatile Matter	33.53	33.78
Fixed Carbon	47.73	49.06
Ash/Inerts	8.83	9.99
Ultimate Analysis (wt %, dry basis)		
Carbon	74.77	74.35
Hydrogen	5.08	5.02
Oxygen	6.32	7.19
Nitrogen	1.44	1.52
Sulfur	2.31	1.14
Chlorine	0.27	0.02
Ash/Inerts	9.81	10.76
Heating Value (Btu/lb)		
As Received	11,748	12,378
Dry Basis	13,040	13,334
Moisture/Ash Free	14,457	14,814
Ash Elemental Analysis (wt %)		
SiO_2	44.16	47.66
Al_2O_3	22.89	23.05
TiO_2	1.00	0.75
Fe_2O_3	22.86	19.08
CaO	2.16	2.37
MgO	0.47	0.93
Na_2O	0.25	0.56
K_2O	1.97	2.43
P_2O_5	0.50	0.43
SO_3	1.93	2.13
Undetermined	1.81	0.61
Alkali Metals (lb/MMBtu)		
CaO	0.15	0.18
MgO	0.03	0.07
Na_2O	0.02	0.04
K_2O	0.13	0.18
Ash Fusion Temperature (°F)		
Oxidizing Atmosphere		
Initial	2,406	2,481
Softening	2,545	2,528
Hemispherical	2,552	2,535
Fluid	2,565	2,553
Reducing Atmosphere		
Initial	2,082	2,081
Softening	2,273	2,300
Hemispherical	2,325	2,418
Fluid	2,429	2,444
T_{250} Temperature (°F)	2,397	2,463
Base/Acid Ratio	0.41	0.36
Slagging Index	0.94	0.40
Fouling Index	0.10	0.2

Table 2: Summary of Wood Fuel Characterizations

Parameter	Allen Wood Average	Allen Wood 95% Conf. Interval	Kingston Wood Average	Kingston Wood 95% Conf. Interval
Proximate Analysis (wt %, dry)				
Volatile Matter	84.32	0.70	84.85	0.65
Fixed Carbon	14.47	0.55	14.45	0.59
Ash/Inerts	1.21	0.47	0.70	0.16
Ultimate Analysis (wt %, dry)				
Carbon	49.24	0.21	49.81	0.31
Hydrogen	5.90	0.05	5.96	0.08
Oxygen	43.24	0.42	43.18	0.35
Nitrogen	0.39	0.27	0.32	0.21
Sulfur	0.02	0.00	0.02	0.00
Chlorine	0.01	0.01	0.01	0.01
Ash/Inerts	1.21	0.47	0.70	0.16
Heating Value (Btu/lb)				
Dry Basis	8,335	38	8,391	46
Moisture/Ash Free	8,437	34	8,450	45
Ash Elemental Analysis (wt %)				
SiO_2	22.90	5.29	17.93	4.05
Al_2O_3	4.43	1.11	4.55	1.16
TiO_2	0.46	0.48	0.78	1.04
Fe_2O_3	1.79	0.45	1.96	0.39
CaO	40.16	3.77	39.89	3.71
MgO	5.37	1.22	8.12	2.07
Na_2O	2.93	1.45	2.74	2.04
K_2O	9.48	1.78	10.33	1.81
P_2O_5	2.25	0.38	3.42	1.55
SO_3^-	2.07	0.91	2.08	0.58
Undetermined	8.16	---	8.20	---
Alkali Metals (lb/MMBtu)				
CaO	0.58	---	0.33	---
MgO	0.08	---	0.07	---
Na_2O	0.04	---	0.02	---
K_2O	0.14	---	0.09	---
Ash Fusion Temperature (°F)				
Oxidizing Atmosphere				
Initial	2,517	90	2,472	47
Softening	2,538	87	2,526	27
Hemispherical	2,541	88	2,530	22
Fluid	2,553	94	2,534	19
Reducing Atmosphere				
Initial	2,541	128	2,537	182
Softening	2,552	134	2,546	193
Hemispherical	2,558	128	2,549	191
Fluid	2,568	117	2,557	181
T_{250} Temperature (°F)	2,424	75	2,384	105
Base/Acid Ratio	2.15	---	2.71	---
Slagging Index	0.04	---	0.05	---
Fouling Index	6.30	---	7.43	---

CO-PROCESSING OF AGRICULTURAL AND BIOMASS WASTE WITH COAL

Alfred H. Stiller, Dady B. Dadyburjor, Ji-Perng Wann,
Dacheng Tian, and John W. Zondlo
Department of Chemical Engineering
West Virginia University, PO Box 6102
Morgantown, WV 26506-6102

Keywords: Co-liquefaction, Sawdust, Manure, Coal

INTRODUCTION

A major thrust of our research program is the use of waste materials as co-liquefaction agents for the first-stage conversion of coal to liquid fuels. By fulfilling one or more of the roles of an expensive solvent in the direct coal liquefaction (DCL) process, the waste material is disposed off ex-landfill, and may improve the overall economics of DCL. Work in our group has concentrated on co-liquefaction with waste rubber tires, some results from which are presented elsewhere in these Preprints. In this paper, we report on preliminary results with agricultural and biomass-type waste as co-liquefaction agents.

The ideal co-liquefaction agent has, at a minimum, three characteristics: it should be available in an unlimited supply; it should be expensive to dispose of, whether in a landfill or by other means; and it should contain components which can function as hydrogen-transfer agents and/or termination agents for free radicals. The first two of these allow for a significant economic impact on the DCL process, and the last ensures good processing properties. While no single agent fulfills all these requirements, the two categories used in the present work are viable candidates. In the category of biomass-type waste, we have used sawdust. In the category of agricultural waste, we have used horse manure, cow manure, and a more-prosaic (but perhaps more-reproducible) commercially available manure ("Supermanure").

All of these agents contain varying amounts of the following components: extractables (oils), cellulose, hemi-cellulose, lignin and ash. Typically, extractables can be removed by a simple water extraction. The insolubles, when extracted with concentrated HCl, yield a soluble cellulose/hemicellulose portion. The HCl-insoluble when subjected to NaOH extraction, yield lignin as the soluble phase while ash is classified as NaOH- (and HCl-) insoluble. Cellulose and hemi-cellulose have a more-or-less well defined structure, with six-membered rings of - $C_5H_5O(OH)_2CH_2OH$ - linked with -O-. The structure of lignin is much less defined, but is known to contain building blocks of phenylpropane with α-alkyl ether linkages and/or β-4' ether linkages. Breakage of these linkages may well involve DCL-solvent-like properties.

EXPERIMENTAL

Standard tubing-bomb reactors were used. They were filled with either coal alone or equal weights of coal and one of the co-liquefaction agents described above. The coal used throughout these runs was a high-volatile-A bituminous coal from the Blind Canyon seam, Utah, coded as DECS-6 by the Pennsylvania State University Coal Bank. The coal was ground to -60 mesh under nitrogen. For consistency with previous work, a small amount of sulfiding agent (0.1 ml CS_2) was added to all run batches. Reactions were carried out both in the absence of any additional solvent and with 5 ml of tetralin. Standard reaction conditions were used: 1000 psi (cold) hydrogen, 350°C, vertical agitation at 500 cpm, 1 h. After the reaction, the total conversion (of all solids) and the yields of asphaltene and preasphatene and oil+gas were obtained by solution of the remaining solids in tetrahydrofuran and *n*-hexane. Additional details can be found in e.g. [1]. Runs were repeated at least once. The reproducibility is typically 2%.

RESULTS AND DISCUSSION

Results for the co-liquefaction of DECS-6 coal and sawdust are summarized in Table I. Liquefaction results of the sawdust alone are significantly greater than those of the coal alone. The addition of tetralin improves the coal-alone results considerably, especially the yield of asphaltene+preasphaltene. The "DIFFERENCE" entries refer to the improvement (if positive) in the results of coal plus sawdust runs, relative to the average of the individual coal and sawdust runs. In the absence of tetralin, there is an improvement in the oil+gas yield at the expense of the asphaltene+preasphaltene yield, while the improvement in the total conversion is within experimental limits. These results indicate that sawdust may catalyze the formation of asphaltenes to oils or may cap low-molecular-weight radicals or other species to prevent retrograde formation of asphaltenic products by combination of oil-range products. The former appears to be unlikely in the light of the results with tetralin: in conversion and yields, there is negligible difference between the individual coal and sawdust runs and the coal-plus-sawdust run. Clearly, the sawdust under liquefaction conditions acts more as a solvent than a catalyst; when tetralin, a powerful solvent, is present, its effect overwhelms that of sawdust. Finally, it is interesting to note that the oil+gas yield after the run with sawdust plus coal is undistinguishable from that when tetralin is also added. Hence, the effects of 5 ml tetralin can be suitably substituted for by 3 g of sawdust. This is obviously of great economic importance.

Results with "Supermanure" are shown in Table II. As in Table I, the co-liquefaction agent alone shows greater conversion and oil+gas yield than coal alone, and the addition of the tetralin has a much smaller effect on the co-liquefaction agent alone than on the coal alone. In the absence of tetralin, the addition of "Supermanure" to the coal increases the oil+gas yield but decreases the overall conversion. Both changes are slight, but significant. In the presence of tetralin, the addition of "Supermanure" to coal appears to decrease the oil+gas yield fairly substantially and also decreases the total conversion slightly. This is a different effect than that observed in Table I. Clearly the constituents of sawdust and "Supermanure" are different, and this is manifested in the behavior when tetralin is present.

Table III summarizes the behavior of cow manure as a co-liquefaction agent. Acting alone, this agent is not liquefied as readily as "Supermanure" and does not yield as much oil+gas fraction. However, in the presence of coal, with or without tetralin present, there is a significant difference (improvement) in oil+gas yield, and this is achieved at the expense of the asphaltenic fraction.

Finally, we indicate in Table IV the effect of horse manure as a co-liquefaction agent. In the absence of tetralin, the presence of horse manure significantly improves the total conversion, and that difference is manifested almost entirely in the oil+gas yield. In the presence of tetralin, the difference in total conversion after adding horse manure is even larger, but that difference is manifested to a large extent in improving the asphaltenic yield. The total conversion and the yield of asphaltenic+preasphaltenic fractions are significantly increased when tetralin is added; the oil+gas yield is also increased but to a lesser extent. Clearly the effect of horse manure is not just to act as a substitute for a more-expensive solvent; there may well be some catalytic effects involved.

The temptation to ascribe the differences in behavior of manure from the horse and cow to differences in the diet of these two species is strong. However, we have not yet carried out analyses of these two co-liquefaction agents to test our hypothesis.

CONCLUSIONS

In the absence of tetralin, the total conversion of equal parts of

coal and a co-liquefaction agent is approximately equal for sawdust, "Supermanure" and horse manure; the value for cow manure is somewhat smaller. However, the greatest improvement (over the conversion of individual reactants) occurs for horse manure; the conversion for "Supermanure" is significantly smaller than the sum of the individual values. The absolute values of the oil+gas yields follow the same trends as those observed for the total conversions; and the improvement of this yield (over yields of individual reactants) also follows the same trends as the improvement of the total conversions.

In the presence of tetralin, both the absolute value of the total conversion and the improvement over conversions of individual species are observed for horse manure as the co-liquefaction agent. The total conversion is almost doubled when tetralin is present, relative to the value in the absence of tetralin, the absolute values of the oil+gas yield are somewhat greater for horse manure and for sawdust than for the other two. Interestingly, the greatest difference, i.e., improvement over individual oil+gas yields, is observed for the case of cow manure as the co-liquefaction agent. In fact, all other improvements in oil+gas yields are either negligible or negative.

Hence the use of biomass-type and agricultural waste was agents of co-liquefaction of coal is in general worthy of consideration.

REFERENCES

1. Dadyburjor, D.B., Stewart, W.E., Stiller, A.H., Stinespring, C.D., Wann, J.-P. and Zondlo, J.W., Energy and Fuels *8*, 19 (1994).

ACKNOWLEDGMENTS

This work was conducted under US Department of Energy contract DE-FC22--93PC93053 under the cooperative agreement with the Consortium for Fossil Fuel Liquefaction Science.

TABLE I
Results for Sawdust/Coal Co-liquefaction

Sawdust	Coal	Tetralin	Total Conversion (%)	Asphaltene+Preasphaltene Yield (%)	Oil+Gas Yield(%)
No	Yes	No	22.4	17.3	5.1
Yes	No	No	70.4	7.7	62.7
Yes	Yes	No	47.6	8.7	38.9
(DIFFERENCE)		No	+1.2	-3.8	+5.0
No	Yes	Yes	57.0	50.0	7.0
Yes	No	Yes	93.1	28.5	64.5
Yes	Yes	Yes	74.7	38.2	36.5
(DIFFERENCE)		Yes	-0.3	-0.8	+0.5

TABLE II
Results for "Supermanure"/Coal Co-liquefaction

Supermanure	Coal	Tetralin	Total Conversion (%)	Asphaltene+Preasphaltene Yield (%)	Oil+Gas Yield(%)
No	Yes	No	22.4	17.3	5.1
Yes	No	No	80.0	18.0	62.0
Yes	Yes	No	48.2	11.9	36.3
(DIFFERENCE)		No	-3.0	-5.8	+2.7
No	Yes	Yes	57.0	50.0	7.0
Yes	No	Yes	87.4	23.5	63.9
Yes	Yes	Yes	69.6	38.4	31.2
(DIFFERENCE)		Yes	-2.6	+1.6	-4.3

TABLE III
Results for Cow-Manure/Coal Co-liquefaction

Cow Manure	Coal	Tetralin	Total Conversion (%)	Asphaltene+Preasphaltene Yield (%)	Oil+Gas Yield(%)
No	Yes	No	22.4	17.3	5.1
Yes	No	No	57.4	17.8	39.6
Yes	Yes	No	39.8	12.2	27.6
(DIFFERENCE)		No	-0.1	-5.4	+5.2
No	Yes	Yes	57.0	50.0	7.0
Yes	No	Yes	66.9	17.7	49.2
Yes	Yes	Yes	62.1	29.2	32.9
(DIFFERENCE)		Yes	-0.1	-4.7	+4.8

TABLE IV
Results for Horse-Manure/Coal Co-liquefaction

Horse Manure	Coal	Tetralin	Total Conversion (%)	Asphaltene+Preasphaltene Yield (%)	Oil+Gas Yield(%)
No	Yes	No	22.4	17.3	5.1
Yes	No	No	66.2	13.4	52.8
Yes	Yes	No	48.2	14.4	33.8
(DIFFERENCE)		No	+3.9	-1.0	+4.8
No	Yes	Yes	57.0	50.0	7.0
Yes	No	Yes	88.2	22.1	66.1
Yes	Yes	Yes	81.5	43.4	38.1
(DIFFERENCE)		Yes	+8.9	+7.3	+1.5

STUDIES IN COAL/WASTE COPROCESSING AT HYDROCARBON RESEARCH, INC.

V.R. Pradhan - A.G. Comolli - L.K. (Theo) Lee - R.H. Stalzer
Hydrocarbon Research, Inc.
100 Overlook Center, Suite 400
Princeton, NJ 08540

Keywords: Waste Recycling, Catalytic Coprocessing, Co-Liquefaction

ABSTRACT: - The co-liquefaction of waste plastics with coal and waste tire rubber with coal was successfully demonstrated at a combined processing rate of 3 TPD at the Proof-of-Concept facility of Hydrocarbon Research, Inc. in Lawrenceville, N.J. The POC Program is jointly funded by the U.S. DOE, Hydrocarbon Research, Inc., and Kerr McGee Corporation. A total of 12 tons of plastics & coal and 5 tons of waste rubber tire & coal were processed to produce clean light distillates (IBP-343°C) with less than 40 ppm of nitrogen and 20 ppm of sulfur. Coal conversion was well maintained (92 W% maf) and nearly complete conversion of the organic waste to oils was achieved (65 W%+ maf distillate yields). Both the plastics and rubber contributed hydrogen to the liquefaction thereby reducing the hydrogen consumption by as much as 2 W% of the maf feed. This has a direct impact on reducing the cost of premium fuels from coal. Co-liquefaction of waste organic materials with coals provides for the recovery and recycle of waste materials back into the economy as premium fuels and feedstocks for petrochemicals. A concerted effort is underway to optimize the process to produce more value-added products with improved energy efficiency.

INTRODUCTION: - Increasing problems associated with waste disposal, combined with the recognition that some raw materials may exist in limited supply, dramatically increase interest in recycling. Recycling of paperboard, glass, and metal are well understood and these materials are now recycled in many areas around the world. Recycling of plastics presents greater technical challenges[1], primarily due to the differences in the chemical compositions/properties of various types of plastics. Used automobile tires, the main source of waste rubber, pose another environmental challenge. Most of the 200 million used tires that are discarded in the United States every year, end up in stockpiles or landfills, although recently some use of scrap tires is also reported as fuel for power generation. Other reported methods of recycling the scrap tires are based on pyrolysis which results in low thermal efficiency and also poor selectivity to liquid fuels.

RATIONALE : - Coal is an abundantly available fossil fuel source with low hydrogen contents. The cost of hydrogen is a significant portion of the total cost of converting coal to refined transportation fuels such as gasoline, kerosene, and diesel via the state-of-the-art conversion technology. These municipal solid waste components such as plastics or hydrocarbon oil in used tires are relatively richer in hydrogen contents than coal. Thus, using these as a part of the feed in coal liquefaction would significantly reduce the cost of hydrogen production. There also seems to be a distinct advantage in processing plastics/rubber waste in a liquid phase or slurry mode under conditions much milder than those used in pyrolytic methods of conversion. Coal as a component of the feed mixture can thus provide not only a way to liquefy these waste stream, but can also act as a "mitigator" in maintaining the overall composition/properties of the combined feedstocks more uniform. This mediator role of coal is very crucial for any waste-stream conversion/recycling process because the waste streams, depending on location, are going to be inherently different in their compositions. Thus, it appears to be practical to co-process the most abundantly available fossil fuel, coal, with hydrogen-rich, though inhomogeneous in composition/properties, waste streams. Feed mixtures consisting of between 20-40 W% wastes (esp. plastics) are considered realistic and are being studied for catalytic slurry processing at Hydrocarbon Research, Inc. For used rubber tires, co-processing with coal can provide a better way for disposal while the carbon black component of the tires is reported to provide catalytic action during coal conversion reactions[2].

LABORATORY-SCALE WORK: - Initial work carried out at Hydrocarbon Research, Inc., to a large extent, was a follow up of the research reported by the Consortium of Fossil Fuel Liquefaction Science[3]. It mainly constituted some microautoclave testing for the screening of the plastics feedstocks reactivity, process severity required, and the catalyst additive for plastics depolymerization. The lab-scale work focused primarily on the pure plastics, i.e., HDPE, Polystyrene, and PET, in the extrudate form. No lab-scale work was carried out in support of the coprocessing of used tire rubber with coal as HRI had a past experience in handling crumb rubber slurries from its H-Rubber process-related work. Our dissolution experiments with mixed plastics indicated that plastics (in coal/petroleum derived oil), especially HDPE, needed about 30-45 minutes at temperatures in excess of 220°C for complete dissolution. Adding coal to this plastics/oil mixture appeared to influence the fluidity of the total slurry in a positive way. The pre-mixed coal; plastics, and oil slurries at 33 and 50 W% of mixed plastics in solid feed exhibited a good pumpability behavior and when tested for reactivity in the 20 CC microautoclave at 440°C and 60 minutes reaction time, about 92 W% conversion to THF soluble products was obtained. Of the three plastics we tested individually at the lab-scale, HDPE was found hardest to convert while both the polystyrene and the PET converted almost completely under coal liquefaction condition.

PDU-SCALE EXPLORATORY WORK: - As a part of the US DOE sponsored Proof-of-Concept (POC) direct coal liquefaction program, the technical and operational feasibility of co-liquefaction of coal and plastics/rubber tire wastes was evaluated at a 3.0 TPD scale. A schematic of the HRI's PDU facility is shown in Figure 1. An eight day long extension of the PDU run POC-02 was carried out using Wyoming subbituminous coal from Black Thunder mine and pure forms of high density polyethylene, polystyrene, polyethylene terphthalate, and -20 mesh crumb tire rubber in a two-stage catalytic mode of operation, with an in-line hydrotreater. During the first six days, a total of 12 tons of mixed plastics were processed with coal (@30% plastics), while 5 tons of fiber-free -20 mesh crumb rubber tire (@26% of solid feed) was processed with coal during the last two days of continuous operation. The coal/waste feed was prepared in two steps: rubber/plastic waste was first slurried with recycle solvent and transferred to the slurry mix tank to which coal and more recycle solvent were added. It was found that a recycle solvent-to-solid feed ratio of about 2.25 was satisfactory for smooth pumping operations with plastics/rubber wastes. Some foaming problems were encountered at the slurry mix tank because of its high temperature and high moisture content of the feed coal. Table 1 contains detailed operating conditions. Because of the fact that the co-liquefaction operation/extension of the PDU run POC-02 was of short duration, the time allowed for process equilibration was not sufficient. As a result of this, the results obtained and presented in Table 2 should be considered with caution; also it should be viewed as directional data rather than an absolute performance during co-liquefaction. Table 2 compares the performance of the "coal--only" feed Period 36 with two coal-plastics cases (Periods 42 & 43) and one coal-rubber case (Period 45). The mixed plastic feed contained 50% HDPE, 35% PS, and 15% PET, simulating the compositions in a typical municipal solid waste. It can be seen from Table 2 that co-liquefaction resulted in a reduced hydrogen consumption, while maintaining total coal and resid conversions. The distillate liquid yields were also higher. The quality of the distillates obtained during the co-liquefaction periods was also premium with very low nitrogen and sulfur contents (Figure 2). Due to the overall process severity and short duration for the entire operation, a steady-state with respect to the recycle solvent was not achieved, i.e, significant portions of an external make-up oil had to be used to obtain a solvent/coal ratio of 2.25 (Figure 3). As a result, light fractions of the make-up oil were excessively hydrocracked increasing the yield of light gases. Some degration of heavy co-liquefaction products was also noticed across the solids-separation Vacuum Tower/ROSE-SR systems.

BENCH-SCALE WORK: As a follow-up of the exploratory PDU scale test of co-liquefaction, a bench test is being conducted to delineate the effects of process severity, catalysis, feed composition during coal/plastics co-processing, when process is at steady-state and is under complete solvent-balance. The same mixture of co-mingled plastics, used earlier at the PDU scale, and Illinois No.6 Crown II mine coal is being evaluated in a 20 Kg/Day two-stage bench-scale unit. Preliminary results confirm our earlier findings at the PDU level. The process is being operated in a catalytic/thermal mode with sulfated iron-molybdenum dispersed catalyst only in stage II. For the first 14 days of this operation so far, solvent-balance conditions have been achieved. Preliminary results are about 6-8% gas yields, 71-73% distillate liquid yields, and 6-7% hydrogen

consumption (all on maf basis) result from co-liquefaction at the overall process severities lower than that at the PDU scale. The final results of this work will be conferred at the meeting.

SUMMARY: - Overall co-liquefaction operations at the PDU scale were successful and established both the technical and operational feasibility of the process. In general, high total (coal+plastics/rubber) conversions were obtained with high resid conversions; the yield of light distillates was high and distillates were of high quality (high H/C, very low N & S contents). We were also successful at establishing a procedure for preparation and pumping under high pressure of the feed materials that contain as much as 26 W% co-mingled plastics and/or crumb rubber. It is well understood that since insufficient time was allowed for the equilibration of the process, recycle solvent-balance was never achieved any time during the operations. The problem of solvent-balance maintenance during continuous operations is being currently addressed at bench-scale. Our ongoing work addresses all the above issues such as optimum process severity, catalysis, solvent balance, and process equilibration. The final results of our latest work in this area will be discussed during the final paper.

REFERENCES

(1) "Recycling-Information pamphlet" from Dept. of Govt. Relations & Science Policy, Am. Chem. Soc., Washington, D.C.
(2) Farcasiu, M., "Another use for old tires", ChemTech, Jan. 1993, pp. 22-24.
(3) Proceedings of the Eighth Annual Meeting of the CFFLS, Snowbird, Utah, July 1994.

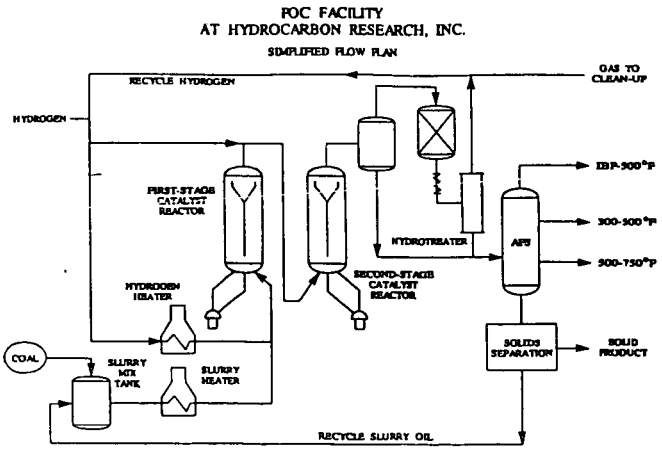

Figure 1

Inspection of Naphtha Stabilizer Bottom
SULFUR & NITROGEN REMOVAL

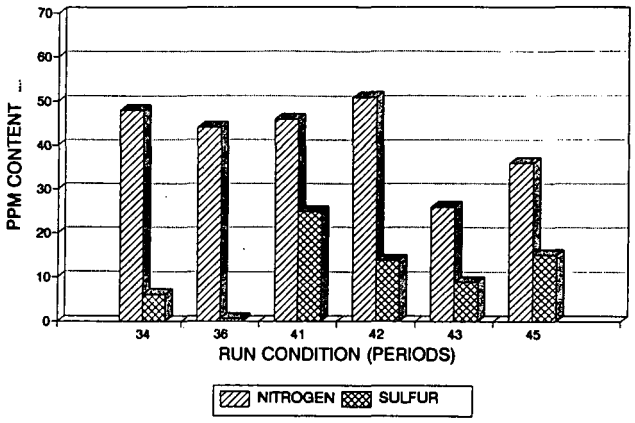

Figure 2

POC-02 PDU RUN 260-005
RECYCLE STREAM COMPOSITION

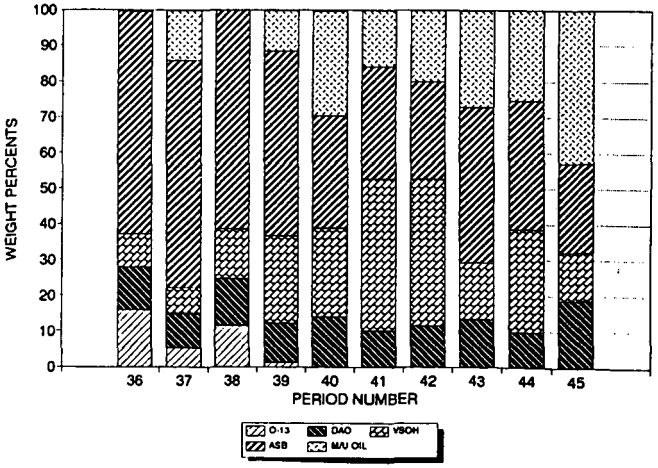

Figure 3

Table 1. Operating Summary During Co-Liquefaction

Process Conditions		5	6	6	7
		Rose-SR	Rose-SR	Rose-SR	Rose-SR
Period/s		35-36	42	43	45
Recycle Type		Ashy	Solids-free	Solids-free	Solids-free
Feed*, W%:	Coal	100.00	68.00	70.00	74
	Plastics (42,43) & Rubber (45)	0.00	32.00	30.00	26
	HDPE	n/a	19	15	n/a
	PS	n/a	13	10	n/a
	PET	n/a	0	5	n/a
	Ground Rubber	n/a	n/a	n/a	26
Space Velocity, Kg/hr/m3		614.50	379.00	433.60	398.40
K-1:					
	Temperature, Deg. C	432.20	428.30	431.10	430.00
	Cat Replac. Rate, Kg/Kg Ton MF Coal	0.75	0.45	0.45	0.00
	Catalyst Age, Kg MF Coal/Kg Cat	1026.00	1044.00	1056.00	1072.00
K-2:					
	Temperature, Deg. C	443.50	442.60	443.80	442.60
	Cat Replac. Rate, Kg/Kg Ton MF Coal	1.25	0.90	0.90	0.00
	Catalyst Age, Kg MF Coal/Kg Cat	626.00	632.00	641.00	660.00
Flow Rates					
Coal Feed, Kg/hr		138.40	80.00	88.80	86.40
	Plastics/Rubber	0.00	28.24	29.50	23.30
Oil Streams to SMT					
	O-43 Recycle to SMT, Kg/hr	67.85	103.50	64.68	71.56
	Make up Oil, Kg/hr	0.00	40.00	58.53	93.52
	ASB (thru' COT) to SMT, Kg/hr	108.85	55.67	96.20	54.49
Solvent/Coal Ratio, Kg/Kg		1.30	2.26	2.24	2.45

Table 2. Process Performance During Co-Liquefaction

Material & Ash Balances				
Liquefaction Section Recovery, W%	100.10	97.10	97.70	99.70
Overall Material Recovery, W%	99.35	97.80	100.30	98.80
Normalization Factor	1.00	1.03	1.02	1.00
Ash Balance, W%	103.70	118.99	108.90	116.44
NORMALIZED YIELDS, W% MAF FEED*				
[Based on Liquefaction Section: O-13 Bottoms]				
H2S	0.56	1.61	1.25	2.25
NH3	1.03	0.88	0.63	0.88
H2O	19.26	14.72	18.56	16.30
COx	1.16	0.49	0.99	0.85
C1-C3	10.11	14.39	10.28	11.04
C4-C6	4.50	7.77	4.17	6.61
IBP-177 C	16.28	27.61	22.04	22.05
177-288 C	24.91	36.31	31.08	40.16
288-343 C	1.32	15.39	15.94	24.27
343-524 C	8.42	-22.62	-3.73	-26.92
524 C+	12.01	-0.42	0.10	3.79
Unconverted Coal	8.51	7.20	7.20	5.32
PROCESS PERFORMANCE (Combined Feed Basis)				
Chemical H2-Consumption, W% MAF	8.05	8.34	8.50	7.47
Total Feed Conversion, W% MAF	93.50	92.80	92.80	94.68
524 C+ Conversion, W% MAF	81.50	93.20	92.70	90.90
Denitrogenation, W%	88.25	77.40	78.00	74.60
C4-343 C Net Distillates, W% MAF	49.00	90.30	73.20	93.10
C4-524 C Distillates, W% MAF	57.50	67.70	69.50	66.20
C1-C3 Selectivity, Kg/Kg of C4-524 C (X 100)	17.60	21.30	14.80	18.00
H2 Efficiency, Kg C4-524 C/Kg H2	7.16	10.70	10.70	8.90
Deasher Coal Conversion, W% MAF	90.9	79.00	85.50	85.50

*"Fresh Feed" is a combination of coal and plastics or coal and crumb rubber for Periods 42,43, & 45;

THERMAL PROCESSING OF UNUSED WASTE PRODUCTS; THE SASOL PERSPECTIVE

J H Slaghuis*, A M Ooms*, H B Erasmus**

*Sastech R&D Division
P.O. Box 1
Sasolburg 9570

**Sastech Technology Transfer Division
P.O.Box 5486
Johannesburg 2000

REPUBLIC OF SOUTH AFRICA

Keywords: Co-processing, waste, gasification

1. INTRODUCTION

The Sasol group of companies gasify approximately 28 x 10^6 metric tons of coal in their 97 Lurgi fixed bed gasifiers per annum. The syngas produced is used mainly in their Fischer-Tropsch plants for the production of transport fuels as well as a slate of other chemicals.

In a complex operation such as Sasol, various sources of unutilized products or waste exist. Tars produced during gasification contain a substantial amount of solid material, essentially fine char and ash. Through various steps of sedimentation and filtration most of the tar is recovered as a clear liquid ready for further work-up. However an amount of "dusty tar", high in solids (MIQ) is produced. In the operation of the Synthol (Fischer Tropsch) reactors, fine catalyst is carried over in the liquid product. This is also concentrated to form a waste product high in finely divided catalyst. Like any other large petrochemical facility from time to time waste from a number of sources is produced down-stream. Where re-working is not feasible, the material has to be disposed of.

In the 40 years of operation of Sasol One (now called Sasol Chemical Industries or SCN) as well as the approximately 15 years of operation of the Sasol Two and Sasol Three facilities (now collectively called Sasol Synthetic Fuels or SFF) substantial amounts of these unused products or wastes have been dumped in ponds. In the early days of the SCN operation, dumping was done rather ad-hoc in waste ponds which were not lined. In later years, properly lined disposal ponds were constructed. The SFF facilities were equipped with properly lined ponds from start-up.

In line with world trends, Sasol has adopted a stringent environmental policy and dumping of such materials is no longer acceptable. Furthermore, Sasol is signatory to the Responsible Care Program. It is now the official policy of the company, not only to eliminate dumping but also to clean up existing waste in an environmentally acceptable way. Thermal co-processing with coal has been identified as a means by which such waste can be upgraded to liquid and gaseous product with no additional toxic effluent.

2. THERMAL CO-PROCESSING WITH COAL: DEFINITION AND OPTIONS IN THE SASOL CONTEXT

Co-processing of waste with coal has to be compatible with the Sasol operations and business scenario. The often heterogeneous feed may not affect the integrity of Sasol operations. Furthermore, it is desirable that products, whether gaseous, liquid or solid are such that they can be upgraded in existing refining facilities and be compatible with products which are currently being marketed. No new toxic waste products are acceptable. Within the limitations of these requirements, Sasol has two options in terms of thermal co-processing of waste with coal: The use of existing fixed bed gasifiers or a dedicated reactor (Figure 1).

3 GASIFICATION

The 97 Lurgi gasifiers currently in operation offer an opportunity for co-processing waste with the existing coal feed. It makes economic sense in that it would significantly reduce the capital outlay needed otherwise. There is the further advantage that gas, liquid and solid products will be "automatically" worked away in the existing infrastructure, again saving on capital investment. Gases produced would end up in the gas loop of the factory. Liquids produced would be worked away in the current tar work-up systems. Both products would thus contribute to the net product yield of the factories and a money value could be attached to it. Exploratory tests on a single gasifier, replacing up to 3% of the coal with waste, had no apparent effect on the operability/stability of the unit. Unfortunately the gasifier had only limited monitoring possibilities and a large scale test involving 13 gasifiers is planned. A number of important but as yet unknown effects are to be investigated and monitored in this test:

3.1 Co-feeding of coal and waste

The gasifiers are fed by lump coal using conveyor belts. For technical reasons, it is desirable to feed the waste with the coal. This poses a problem as a large percentage of this material is liquid to semi-liquid. It has been found that mixing such materials with absorbents/binders such as fly-ash, cement or clay results in a product with a dry, crumbly appearance. Laboratory work has shown that, upon pyrolysis, a coarse char is formed which should move with the coal through the gasifier. The possible long-term effect of this material on the integrity of the conveyer belts is currently being investigated. Furthermore it is important that no "sticky" material is deposited in e.g. the coal bunkers and coal-locks of the gasifiers.

3.2 Effect on gasifier performance

Once inside the gasifier it may be expected that, in the hot upper part of the gasifier (450 - 550°C), volatile material will be flashed off together with the tar of pyrolysis of the feed coal. The effect that the solid carbonaceous residue containing the inorganic binder may have on the operation of the gasifier will have to be considered. Part of the solids may break up and be swept out of the gasifier. The rest will move down with the coal through the various stages of fixed bed gasification and end up as part of the ash. It is known that an increase in ash content of the coal increases the oxygen and steam requirements per unit gas. As up to 50%

inorganic binder is used with the waste, the average ash content in the gasifier increases by 1 - 1½%. Furthermore, it needs to be established whether the added inorganic binder breaks up further down in the gasifying vessel as this may lead to gas flow constrictions.

3.3 Down-stream effects - Primary tar separation

Condensables, tar and gas liquor, are scrubbed down-stream from the gas phase. Coal used in the Sasol operation produces approximately 1½ - 2% of Fischer-tar. The addition of 3% of a 50/50 mixture of "foreign" organic matter and inert binder may as much as double the net hydrocarbon yield. It is not expected that capacity should be a problem in the current primary tar separator system. However separator performance will have to be carefully monitored. It is especially the possibility of emulsion formation which is of concern as this would severely reduce the efficiency of the separators.

3.4 Down-stream effects - Quantity and compatibility of products

If the co-processed waste is of a coal tar origin, no problems, except for capacity down-stream, would be expected. However, if "non-coal" waste was to be present in the feed mixture, serious consideration should be given to the effect of interaction of species in the reactive vapour phase. The net product slate (including the raw gas composition) may change substantially which would affect down-stream processing as well as marketability of the final products. Homogeneity/miscibility of liquid materials will also have to be carefully investigated.

3.5 Down-stream effects - Gas liquor treatment

Gas liquor is treated in a Phenosolvan unit. The possibility of a change in gas liquor quality cannot be overlooked as this may have detrimental affects on plant performance as well as on the quality of the products. Finely dispersed solid material finds its way via the gas liquor system to the Phenosolvan plant where filters are used to clear the feed. Performance of these filters will have to be monitored to ascertain whether additional fine solid material originating from the waste mixture, find its way down-stream.

3.6 Down-stream effects - Tar work-up plant

Tar filtration is a critical pre-preparation step in the tar work-up plant. An increase in fine solid material in the tar feed, due to carry-over in the gasifier, may slow down filtration rate which in turn could limit the capacity of the work-up plant.

The possibility of a change in the composition of the tar feed (Par. 3.4) may also reduce existing plant capacity as well as product quality.

4. DEDICATED REACTOR

A number of proprietary thermal processes have been developed with the purpose of recovering hydrocarbons from solid materials. These distillation/pyrolysis processes (pyrolysis units) are typically designed to remediate contaminated soils or for the recovery of oil from tar sands and

oil shales. An in-depth study into the suitability of such processes for application in the Sasol scenario has been made. Following in-house research up to process development unit (PDU) scale, it was concluded that the only feasible processes were those where direct heating is applied. These processes include inter-alia the Lurgi-Ruhrgas process, the AOSTRA-Taciuk process and the TOSCO process.

Pilot plant testwork has shown that up to 80% of the quinoline soluble material could be recovered as a liquid with a minor amount of gas make. The residual char was shown to exhibit a high-enough heating value to fuel the processes making them energy self-sufficient. Following primary Pilot plant work a number of important criteria had to be assessed:

4.1 Co-processing with coal

This not only has to be technically feasible but should make economic sense as well. Of the processes mentioned, use is often made of a solid heat carrier. Testwork has shown that properly graded coal could serve this purpose. Sasol's gasification coal produces a relatively small amount of Fischer-tar (Par. 3.3) which would contribute little to the net liquid yield during co-processing. However some small coal deposits, yielding up to 12% of Fischer-tar, are present in the Secunda (SFF) coal field. These coal types have been shown to be suitable for co-processing with some of the waste material increasing the net yield of liquids.

4.2 Product compatibility with existing business

A dedicated pyrolysis unit has the distinct advantage that it does not interfere with the core Sasol operations. Products are collected independently and can be marketed on their own. In the Sasol operation it could be economically advantageous to co-process the products of pyrolysis in the existing tar work-up facilities. However the aspects of plant capacity and more important, product compatibility as described in Par. 3.4 will have to be carefully considered. Although pyrolysis units operate on a continuous basis, feed preparation can be done batch-wise. This creates the opportunity of diverting incompatible feedstocks away from the existing tar work-up facilities. Such products could be sold as fuel oils. The option of co-processing with coal could be considered on such a "batch system" as well.

5. SOIL REMEDIATION

Many pyrolysis units have shown to be eminently suitable for remediating contaminated soils. This is a distinct advantage. Treating such soils in the Lurgi gasifiers is technically feasible if a low feed rate is maintained. This becomes impractical if the amount of soil needing thermal remediation is high.

6. CONCLUSION

R&D work at Sasol has shown that thermal co-processing of coal and coal products will have a distinct role to play as part of a waste recovery project. Using the existing Lurgi gasifiers will result in a substantial saving in capital provided that due care is taken to preseve the integrity of current plant operation. The installation of a dedicated pyrolysis unit will be capital intensive. However, these costs could be off-set by, inter alia, avoiding the risk of production losses in current business. Pyrolysis units have the

added advantage that they are eminently suitable for the remediation of contaminated soils.

ACKNOWLEDGEMENT

The authors wish to thank mr Johan van Zyl for his input and Sastech for permission to publish this paper.

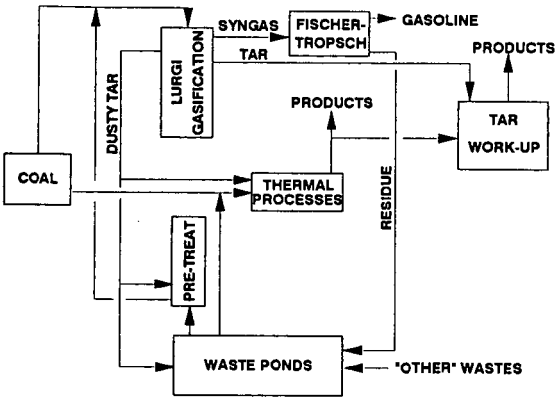

FIGURE 1 THERMAL CO-PROCESSING OF COAL AND WASTE THE SASOL OPTIONS

CHARACTERIZATION OF COAL/WASTE COPROCESSING SAMPLES FROM HRI RUN POC-2

Gary A. Robbins, Richard A. Winschel, and Francis P. Burke
CONSOL Inc., Research and Development
4000 Brownsville Road, Library, PA 15129-9566

KEYWORDS: coal liquefaction, coal/waste coprocessing, analysis

ABSTRACT
Coal and waste materials (plastics and rubber) were co-liquefied during Run POC-2 in HRI's 3 T/D direct liquefaction process development unit under the DOE-sponsored Proof-of-Concept program. Analytical characterizations were conducted of well-defined samples from representative periods of the run to provide information on the chemical transformation of these feedstocks and their distribution in product and recycle streams. The characteristics of the products and process streams were dependent on both feedstock changes and operating conditions. Several unusual process oil characteristics were observed when wastes were coprocessed with coal, especially during the coal/plastic operation. Implications of these results for future coal/waste liquefaction development and analytical characterization of the materials are discussed.

INTRODUCTION
Based on background work performed by the Consortium for Fossil Fuel Liquefaction Science[1] and the Pittsburgh Energy Technology Center, in July 1994 HRI completed nine days of coal/waste coprocessing during the DOE Proof-of-Concept direct liquefaction Run POC-2.[2-4] Several key accomplishments of the run were: subbituminous coal was processed without deposition problems such as were encountered at the Wilsonville pilot plant; an in-line hydrotreater was operated to produce high-quality distillate low in heteroatoms; an overall material balance of 99.6% was achieved; and the plant successfully converted fifteen tons of plastic and waste tires into premium fuels with high conversion and a lower hydrogen requirement than during coal-only operation. A diagram of the plant[5] as configured for HRI Run POC-2 is shown in Figure 1. CONSOL analyzed 65 samples collected throughout the run; sample points are shown in Figure 1. Run conditions for coal and coal/ waste operating periods are compared in Table 1. The main variables were feedstocks, reactor temperatures, space velocity, recycle type (ashy or solids-free), and solvent/feed ratio. The periods were relatively constant in severity, according to HRI's index.

ANALYTICAL APPROACH AND OBJECTIVES
Analysis of liquefaction process stream samples should always take place within a well-defined process framework. Sample origins and interrelationships should be understood in context to the process configuration and run conditions, and samples should cover representative periods of the entire run, not only the coprocessing periods. The analytical methods used here have been proven useful for liquefaction process stream characterization. Non-routine analyses were warranted in some cases for the coprocessing period samples. One objective was to determine the fates of the various waste feedstocks processed. Information is desired on the relative convertability of the feedstocks, the product streams to which the feedstocks are converted (bottoms vs. distillate), interactions of feedstocks, and their effects on product quality. In order to address these objectives, one must distinguish property characteristics reflecting feedstock differences from those caused by changes in other process conditions. In this case, process changes include: 1) ashy vs. ash-free recycle, 2) high make-up oil use in waste coprocessing periods, 3) high solvent/feed ratios in waste coprocessing periods, 4) ROSE-SR operations, and other factors, such as space velocity and catalyst age. Other performance issues of interest in HRI Run POC-2 include achievement of steady state unit performance (such as the ROSE deasher), retrograde reactions, and product stability issues.

EXPERIMENTAL AND SAMPLE DESCRIPTION
Information about the samples analyzed and methods used is given in Table 2. Sample points, SP-xx, given in the table correspond to those shown in Figure 1. In the following discussion, the abbreviations shown in Table 2 will be used, e.g., NSB for naphtha stabilizer bottoms, DAO for deashed oil. Experimental details about most of the analytical methods used have been provided elsewhere.[6,7] GC/MS analyses were done with a DB-5 column, 30 m x 0.25 mm, 0.25 μm film thickness. GC conditions were: 5 min at 10 °C; 2 °C/min to 100 °C, 4 °C/min to 320 °C, up to 20 min at 320 °C. The injection port was held at 300 °C. Carrier gas: He at 20 psig. One percent solution of make-up oil sample in tetrahydrofuran, or neat NSB samples were injected in the splitless mode. The mass spectrometer was scanned from 33 to 300 amu. Peak identifications were based on searches of the Wiley/NBS mass spectral library and retention times.

DISCUSSION
In this paper, we will highlight a few results that are of particular interest to coal/waste coprocessing. Most of the discussion will be concentrated on the

products (naphtha stabilizer bottoms (NSB) and ROSE-SR bottoms), the flashed second-stage oil (RLFVB), and ROSE-SR feed (VSB).

Plastics and Rubber Product Oils

Gas chromatography/mass spectrometry (GC/MS) total ion chromatograms are shown in Figure 2 for NSB product oils and the make-up oil. The make-up oil is used to supplement recycle when there is insufficient process-derived solvent. The NSBs contain paraffins with carbon numbers ranging up to about 24 (tetracosane, boiling point 736 °F); this generally is consistent with the expected boiling point of these products. The product from the coal/plastics and coal/rubber periods had more material boiling in the range 600-750 °F, in agreement with HRI's distillation data.[2] The make-up oil has a higher boiling point distribution than the NSBs, although the boiling points of the two overlap. The make-up oil may contribute to some of the higher boiling components seen in the NSBs from the coal/plastics and coal/rubber periods. Distillation, hydrogenation, and hydrocracking are all routes by which this higher-boiling make-up material may find its way into the NSB boiling range. Make-up oil comprised 27 wt % of the period 43 recycle stream composition and 43 wt % of the period 45 recycle stream composition, compared with none during the coal period 36. The contribution of make-up oil was exacerbated by the higher solvent/feed ratio of ≈2.4 in the waste/coal periods vs. 1.2 in the coal period. Thus, the higher-boiling material seen in the coprocessing period NSBs seems attributable to plant operating conditions, and not specifically to the feedstocks used. Since the plant was not in solvent balance during the coal/waste periods, sample and yield data may not represent plant operation at steady-state conditions.

Unusual Materials from Plastics Period

Significant amounts of ethylbenzene (EB) and methyl ethylbenzene (MEB) components were found in the NSB only from the plastics period, as determined by GC/MS (Figure 1, see marked peaks at retention times 16.77 and 21.85 minutes). Proton NMR confirms this, since distinctive peaks from ethylbenzene or diethylbenzene are present only in the spectrum (not shown) of the plastics period NSB product. These components are believed to be products from the liquefaction of the polystyrene. Thus, the presence of these components is attributable to the feedstock.

The DAO from the plastics period was extracted with THF and found to contain insolubles. This insoluble material is gray in color, waxy in appearance, and melts below 100 °C. Diffuse reflectance FTIR showed the material to contain methylene and methyl aliphatic groups, with essentially no aromatics or heteroatomics. Except for a more intense methyl C-H stretch peak in the DAO insolubles spectrum, it is very similar to that of a polyethylene film sample. The sharp doublets around 1470 and 720 cm^{-1} are excellent matches with polyethylene. The peak at ≈720 cm^{-1} is indicative of long-chain paraffins. The elemental composition of the DAO insolubles is similar to that of the polyethylene feed, and they are almost identical in H/C ratio (not shown). Since this is apparently non-distillable wax, much heavier than previously observed,[8] we suspect that this material results from polyethylene liquefaction. In fact, the evidence strongly suggests that this material is unreacted or partially reacted polyethylene.

Variations in IOM across the vacuum still and ROSE unit were observed in CONSOL data. The coal conversion determined by CONSOL (Table 3) was 57.5% based the RLFVB sample, 96.8% based on the VSB sample, and 77.3% based on the ROSE bottoms sample (sequential points through the process). In addition to the increased IOM in the ROSE bottoms, a significant amount of the waxy IOM is recycled in the DAO. A relatively high preasphaltene concentration in the period 43 DAO coincides with the presence of IOM in this stream (Table 3). These results may reflect unusual solubility characteristics of liquefied plastics, especially polyethylene. The results suggest that for studying plastics liquefaction, one may need to develop a practical method to distinguish "dissolved" plastic (unchanged in molecular weight) from "converted" plastic (decreased in molecular weight).

The NSB from the plastic/coal period contained about 14 ppm (mg/kg) of sediment not present in other samples from this run, or in product oil samples from prior Wilsonville pilot plant runs or from HRI bench-scale runs. A portion of the sediment is slightly soluble in THF or pyridine. A sample of sediment was obtained for characterization by filtration of the NSB through a silver membrane filter, followed by a hexane wash and vacuum drying. The filter deposit was characterized in-situ by diffuse reflectance FTIR and SEM/EDX. FTIR indicated a primarily aliphatic material with a hydrogen-containing functional group (such as O-H); some aromatic and some carbonyl seem also to be present. SEM/EDX showed the deposit to consist primarily of sulfur, with smaller amounts of carbon and oxygen also evident. The collective evidence suggests that the bulk of the sample is elemental sulfur, which has little infrared activity and limited solubility in common solvents.

CONCLUSIONS

Analyses were conducted on process oil samples from representative periods of HRI Run POC-2 in which coal, coal/plastic and coal/rubber were the feedstocks. Differences are apparent, some related to feedstock changes, others to operating condition changes. The high rate of make-up oil use in coal/plastics and coal/rubber periods may result in some of the higher boiling paraffinic components seen in NSBs from these periods. Significant amounts of ethylbenzene and methyl ethylbenzene components are present in the NSB product from coal/plastics operation; these appear to be products from the liquefaction of the polystyrene. There are unusual IOM characteristics in the coal/plastics period 43, perhaps as a result of unusual solubility characteristics of liquefied plastics, especially polyethylene. Heavy wax found as IOM in the DAO seems to be unreacted or partially reacted polyethylene. There is an apparent increase in conversion, followed by a decrease in conversion through a portion of the process. The conversion to THF solubles increased from 57% based on the second-stage product sample (RLFVB) to 97% based on the ROSE feed sample (VSB), and then decreased to 77% based on the ROSE bottoms sample. These results suggest a need to develop a method to distinguish "dissolved" plastic (unchanged in molecular weight) from "converted" plastic (decreased in molecular weight). The NSB sample from coal/plastics operation also contained a sediment not found in other samples.

Many products from liquefaction of plastics and rubber may not be chemically distinct from coal liquefaction products. It appears to be necessary to rely on "marker" compounds or materials (such as ethylbenzene from polystyrene) to demonstrate a non-coal origin of some product components. Proper interpretation of results is facilitated by analysis of liquefaction process stream samples within a well-defined process framework. Characteristics of products from HRI's Run POC-2 operation with coal/waste do not solely reflect feedstock differences from coal-only operation. Other conditions changed, as well, and the plant was not operating at steady-state when those materials were generated.

Run POC-2 operating experience should make it easier to avoid high make-up oil use in future runs with these feedstocks, since high make-up oil use lowers the quality of the analytical and yield information. There was no evidence that polystyrene did not convert completely, but there seem to be problems associated with polyethylene liquefaction (waxy DAO insolubles). The high oxygen content (32 %) of polyethylene terephthalate makes it less desirable as a feedstock, though it manifested no problems. It appears that polystyrene would be the preferred feedstock, based on this test. Liquefaction of the plastic feedstocks separately from each other would help resolve some issues. Coal/plastics product oil stability should be explored further.

ACKNOWLEDGMENT

This work was supported by the U.S. Department of Energy under Contract No. DE-AC22-94PC93054.

REFERENCES

1. Huffman, G. P. "Summary of Consortium Research in Waste/Coal Coprocessing", Presentation at the DOE Direct Liquefaction and Gas Conversion Contractors' Conference, September 7-8, 1994, Pittsburgh, PA.
2. Personal correspondence of authors with A. G. Comolli of HRI.
3. Comolli, A. G. "The Direct Liquefaction Proof of Concept Program", Presentation at the DOE Direct Liquefaction and Gas Conversion Contractors' Conference, September 7-8, 1994, Pittsburgh, PA.
4. Comolli, A. G. "Results of Recent POC Run at HRI on Waste/Coal Coprocessing", Proceedings of the DOE Workshop on Waste/Coal Coprocessing, September 9, 1994, Pittsburgh, PA.
5. Personal correspondence of authors with A. G. Comolli and L. K. Lee of HRI.
6. Burke, F. P.; Winschel, R. A.; Robbins, G. A. "Recycle Slurry Oil Characterization, Final Report, October 1980 through March 1985", DOE/PC 30027-61, March 1985.
7. Winschel, R. A.; Robbins, G. A., Burke, F. P. "Coal Liquefaction Process Solvent Characterization and Evaluation, Technical Progress Report, July 1985 through September 1985", DOE/PC 70018-13, December 1985.
8. Winschel, R. A.; Robbins, G. A.; Burke, F. P. "Improvement in Coal Liquefaction Solvent Quality by Dewaxing". Fuel 1987, 66, 654.

TABLE 1. CONDITIONS FOR COMPARISON PERIODS OF COAL AND COAL/WASTE LIQUEFACTION

Process Condition	Period			
	21	36	43	45
Feed	100% Coal	100% Coal	30% Plastics, 70% Coal	25% Rubber, 75% Coal
Reactor Temp.,°F				
K-1 (Ebullated-Bed)	775	810	810	810
K-2 (Ebullated-Bed)	830	835	830	830
K-3 (Fixed-Bed)	705	720	720	720
Severity, HRI Index	5.16	5.25	5.16	5.16
SV, lb MF coal/h/ft^3 reactor, per stage	30	40	30	30
Recycle/feed ratio	1.2	1.2	2.0	2.0
Recycle type	Ashy	Ashy	Solids-Free	Solids-Free
Other Information: run operated from June 1 through July 28, 1994; Black Thunder Mine subbituminous coal; ROSE-SR used for solids separation; 700°F$^+$ extinction recycle operation; catalyst addition rate in lb/T MF coal was 1.0-2.0 in K-1 and 2.0-2.5 in K-2; plastics were new in ratio 50/35/15 high-density polyethylene/polystyrene/polyethylene terephthalate; rubber was from scrap tires; Ni/Mo supported catalysts were Akzo AO-60 in K-1 and K-2 and Criterion 411 in K-3 (the on-line hydrotreater).				

TABLE 2. CONSOL ANALYSES OF SAMPLES FROM HRI WASTE/COAL COPROCESSING RUN POC-2

Sample Description (Name); Vessel; Sample Point	Periods	Technique & Information Sought (Refer to Key)
Atmospheric Still Bottoms (ASB); N-2 BTMS; SP-4	5, 15, 21, 36, 43, 45	A,B
Vacuum Still Bottoms (VSB); N-3 BTMS; SP-6	21, 36, 43, 45	E; THF Extract - A,B,F
Naphtha Stabilizer Bottoms (NSB); N-5 BTMS; SP-3	15, 21, 36, 43, 45	A,B,C,D
Recycle Oil; O-43 Oil; SP-11	5, 15, 34, 36, 43, 45	A,G,H; Dist. - A,B,G; Resid - E; Resid THF Extract - A,B,F
Reactor Liquid Flash Vessel Bottoms (RLFVB); O-46 Material; SP-9	5, 15, 21, 34, 36, 43, 45	A,G,H; Dist. - A,B,G; Resid - E; Resid THF Extract - A,B,F
ROSE Btms; O-63; SP-27A/B	15, 21, 34, 36, 43, 45	E; THF Extract -A,B,F
Deashed Oil (DAO); O-65 DAO; SP-25	15, 21, 34, 36, 43, 45	A,B,F; E(Some Periods); D
Make-Up Oil (M/U); Tank 4 Oil; SP-28	1	A,B,C,G

KEY TO TECHNIQUES AND INFORMATION SOUGHT:

A = ^{1}H-NMR for hydrogen distribution (7 classes), aromaticity (degree of hydrogenation), paraffinicity, hydrogen donors; **B** = FTIR in THF solution for phenolic -OH content; **C** = GC-MS for composition, carbon numbers of paraffins; **D** = special analyses as described in Discussion section (Period 43); **E** = THF extraction and ash for resid, ash and IOM content, for coal and resid conversion; **F** = solvent fractionation (oils, asphaltenes, preasphaltenes) for resid composition; **G** = microautoclave test with standard coal for donor solvent quality; **H** = 850°F distillation for distillate content.

TABLE 3. DATA INDICATING UNUSUAL IOM CHARACTERISTICS IN COAL/PLASTICS PERIOD

Period	Sample	Coal Conversion, wt % (a)	Phenolic -OH in Soluble Resid, meq/g	Component of Soluble Resid, wt %	
				Asph.	Preas.
15 Coal	Recycle Oil	87.3	0.18	7.3	6.5
	RLFVB	89.3	0.24	12.4	7.7
	VSB	—	0.20	13.1	3.2
	ROSE Btms	86.1	0.29	28.8	14.7
	DAO	—	0.14	5.5	0.7
21 Coal	RLFVB	92.5	0.27	18.4	6.1
	VSB	91.9	0.22	18.6	2.8
	ROSE Btms	91.8	0.28	18.8	8.3
	DAO	—	0.14	7.0	1.4
36 Coal	Recycle Oil	91.3 (91.0*)	0.35 (0.30*)	13.4 (12.2*)	7.7 (5.4*)
	RLFVB	—	0.45	21.8 (20.0*)	3.7 (3.9*)
	VSB	91.2	0.36	20.7	2.7
	ROSE Btms	91.9 (90.1*)	0.55 (0.44*)	25.9 (23.5*)	8.5 (12.7*)
	DAO	—	0.24 (0.29*)	5.8 (8.6*)	0.1 (0.3*)
43 Coal/Plastics	Recycle Oil	—	0.12	21.0	2.6
	RLFVB	57.5	0.28	19.8	9.8
	VSB	96.8	0.16	13.2	1.0
	ROSE Btms	77.3	0.23	22.0	8.7
	DAO	—	0.13	5.0	11.1

* From Per. 34, at same conditions, but without Mo additive used in Per. 36.
(a) MAF % Conversion = [(100 - ash% in dry feed) - (sample % IOM)*(ash% in dry feed)/(sample % ash)]*100/(100 - ash% in dry feed); plastics ash content was assumed to be 0%.

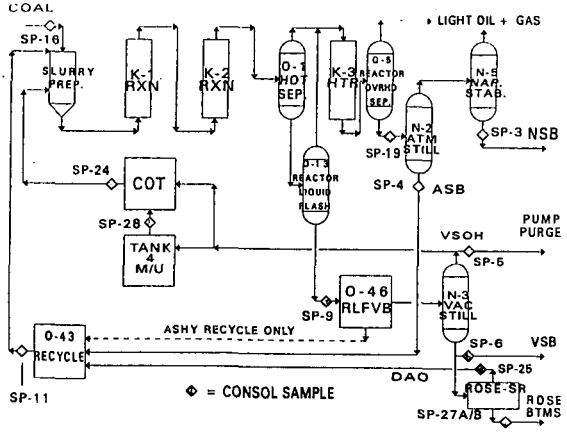

Figure 1. Diagram of the HRI Proof-of-Concept Plant Showing Sample Points, as Configured for Run POC-2.

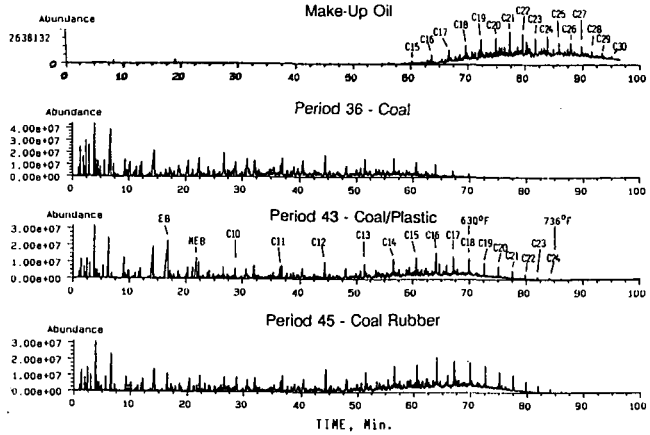

Figure 2. GC-MS Total Ion Chromatograms of Make-Up Oil and Product Oils From HRI Run POC-2.

OPPORTUNITIES FOR TECHNOLOGICAL ADVANCES IN THE CONVERSION OF NATURAL GAS TO LIQUID FUELS AND CHEMICALS.

Imre Puskas
Research Services
939 Brighton Drive
Wheaton, IL. 60187

KEYWORDS: Natural gas, synthesis gas, methanol, syncrude.

INTRODUCTION.

Natural gas is a premium fuel because of its high heating value (210.8 kcal/g-mole methane) and clean burning characteristics. However, transportation costs from source to market may prevent its fuel use. Alternative uses of natural gas are conversions to chemicals and liquid fuels. Natural gas is the favored starting material for ammonia and methanol. Natural gas can also be converted to easily transportable liquid fuels. However, conversions to alternative fuels with lower heating values (~156-167 kcal/carbon atom for hydrocarbons; 170.9 kcal/g-mole for methanol) can be rational and economical only under special circumstances.

Excellent reviews are available by Rostrup-Nielsen (1), Fox (2), Mills (3), Fierro (4), Lunsford (5), Kuo et al. (6), and by many others on the research and development status of the natural gas conversion technologies. By comparing salient chemical, technological, historical and economic features of the major conversion technologies, this study is an attempt to define the best opportunities for further technological advances.

SYNTHESIS GAS FROM NATURAL GAS.

Synthesis gas is a common intermediate in the syntheses of ammonia, methanol and synthetic crude. Natural gas can be converted to synthesis gas by three different reactions: 1./ Steam reforming. 2./ Reforming by carbon dioxide. 3./ Partial oxidations.

Steam reforming. The overall reaction is shown by Equation 1 (E1). This reaction takes place in two steps. First methane is decomposed to carbon and hydrogen (E2), which is followed by a carbon-steam reaction (E3). All three reactions are endothermic equilibrium reactions and require high temperatures for favorable equilibria. During steam reforming, the water gas shift reaction (E4) is an inevitable side reaction. This latter is exothermic; its equilibrium is shifted to its reversal (i.e. to the left) by increasing temperature. Steam reforming requires a catalyst. Nickel on alumina is used most widely. The temperature of most of the reformers is in the 730-860 °C range. Steam is used in large excess (2-5 fold) for faster rates and to prevent carbon build-up on the catalyst.

E1 $CH_4 + H_2O \rightleftharpoons CO + 3H_2$ ΔH=+49.3 kcal/mole (@25°C)

E2 $CH_4 \rightleftharpoons C + 2H_2$ ΔH=+17.9 kcal/mole (@25°C)

E3 $C + H_2O \rightleftharpoons CO + H_2$ ΔH=+31.4 kcal/mole (@25°C)

E4 $CO + H_2O \rightleftharpoons CO_2 + H_2$ ΔH=-9.7 kcal/mole (@25°C)

Review articles (7-10) provide details on the chemistry and technology of methane steam reforming. Some aspects are highlighted here. Kinetic evidence suggests that the reaction rate is controlled by diffusion. Steam reforming is carried out in furnaces which contain parallel catalyst tubes made of HK-40 alloy (25% Cr, 20% Ni, 0.35-0.45% C). The tubes are designed for a minimum life of 10 years. Inside the tubes is the catalyst. The tubes are heated from the outside by burners. Reforming pressure on the tube side can be as high as 500 psi. Since natural gas is usually available under high pressure, reforming under pressure can result in substantial savings in downstream compression costs if compressed synthesis gas is needed. Due to improved heat recovery and efficient energy management, current steam reformers operate with good thermal efficiency (11-12).

Carbon dioxide reforming. This reaction has much resemblance to steam reforming. The overall reaction is illustrated by E5. It is

E5 $CH_4 + CO_2 \rightleftharpoons 2CO + 2H_2$ ΔH=+59 kcal/mole (@25°C)

E6 $C + CO_2 \rightleftharpoons 2CO$ ΔH=+41.2 kcal/mole (@25°C)

highly endothermic. It occurs in two separate steps, the first step being methane decomposition (E2). In a subsequent step, the carbon is gasified by carbon dioxide (E6). The reverse reaction of E6 is the Boudouard reaction, which can be a source of carbon deposition. Carbon dioxide reforming, as indicated by E5, cannot be practiced commercially because the carbon gasification by E6 is not fast enough to prevent carbon accumulation. Steam addition to the feed is required for successful operations. Commercial interest in carbon dioxide reforming originates from the need for synthesis gas compositions with low H_2 to CO ratios. Haldor-Topsoe (13,14) and Calorific GmbH (15) reported on process developments. The Midrex-Process for the reduction of iron ores generates syngas essentially by carbon dioxide reforming with low steam usage (16).

Partial oxidation. Controlled reaction of methane with oxygen can give good yield of synthesis gas. The desired reaction is shown by E7. However, early studies (17) have already revealed, that even if a 2:1 molar mixture of methane and oxygen is reacted, the initial reaction is complete burning (E8) and incomplete burning (E9 and E10). These are very fast reactions, requiring only milliseconds. Following the initial fast reactions, the unreacted methane reacts with steam and carbon dioxide generated by the reactions E8-E10. However, these reforming reactions are slower

E7 $CH_4 + 0.5O_2 \rightleftharpoons CO + 2H_2$ ΔH=-8.5 kcal/mole (@25°C)

E8 $CH_4 + 2O_2 \rightleftharpoons CO_2 + 2H_2O$ ΔH=-192 kcal/mole (@25°C)

E9 $CH_4 + 1.5O_2 \rightleftharpoons CO + 2H_2O$ ΔH=-124 kcal/mole (@25°C)

E10 $CH_4 + O_2 \rightleftharpoons CO_2 + 2H_2$ ΔH=-78 kcal/mole (@25°C)

by more than an order of magnitude. The reaction temperature depends on the preheat temperature of the reagents. Mixing occurs in a burner. A flame is spontaneously produced with adequate preheat, even though at room temperature the composition would be non-flammable. Outside the flame, the temperature quickly falls due to the endothermic reforming reactions. The reactor is a refractory-lined vessel. The first commercial installation of a non-catalytic partial oxidation unit using 95% pure oxygen was in the Brownsville synthetic fuel plant in 1950, operating at 425 psi (18). The new synfuel plant in Malaysia designed by Shell International Gas Ltd. uses a similar process (19).

Partial oxidation can be conducted catalytically. The catalyst maintains the reaction without a flame, and accelerates the slower reforming reactions to establish thermodynamic equilibria. However, truly catalytic partial oxidations have been restricted mostly to laboratory studies (20). Most of the commercial "catalytic partial oxidation" processes consist of a sequence of non-catalytic partial oxidation and catalytic reforming. Synthesis gas generation for copper smelters may involve truly catalytic partial oxidation (21).

The oxidant in the partial oxidation processes can be air or pure oxygen. In case of air use, the nitrogen appears in the synthesis gas as a diluent.

Combined reforming. Steam reforming, carbon dioxide reforming and partial oxidation supply synthesis gas with greatly differing composition. The H_2/CO ratios from the three processes are >3, <1 and <2, respectively. Combination of the various processes can lead to the desired synthesis gas compositions. Furthermore, combination of steam reforming and partial oxidation also led to the development of more energy-efficient reactors and processes. These advances came from BASF (22), Haldor-Topsoe (23), Lurgi (24), ICI (25) and Uhde GmbH (26), etc. A recent review by Orphanides (27) gives more detail on the progress. Some of the advances will be illustrated by specific examples:

For ammonia synthesis, hydrogen is required rather than synthesis gas. The CO content of the synthesis gas is converted to hydrogen and carbon dioxide by the water gas shift reaction (E4). In newer ammonia plants, the steam reforming furnaces have been replaced by two reactors (Figure 1). The first reactor is the "Gas Heated Reformer" (GHR) where about 75% of the methane is reformed to synthesis gas around 700 °C and up to 600 psia. The heat for the reforming is supplied by the effluent gases of the second reactor. This latter one is an "autothermal reformer" which converts the residual methane of the first reactor effluent by partial catalytic air oxidation. This combination has the following benefits: 1./ It introduces the nitrogen required in the ammonia synthesis step. 2./ It generates heat in the second reactor which is very efficiently utilized in the first reactor and eliminates the need for the bulky steam reformer furnaces. Heat transfer in the GHR is much better than in the old furnaces because both sides of the exchanger tubes are under pressure. In some of the newer ammonia plants, a single reformer replaces the two reactors of Figure 1 (as in Figure 2).

Figure 1. Combined Reforming.

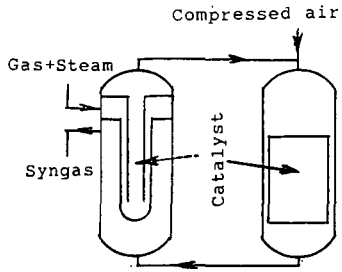

Figure 2. Schematic Showing of a Combined Autothermal Reformer.

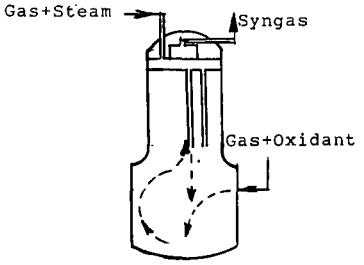

The synthesis gas generated by the conventional steam reforming furnaces is acceptable for methanol synthesis even though the hydrogen content is too high. The combined reforming concept shown in Figure 1 is also applicable to methanol synthesis if pure oxygen is the oxidant in the second reformer. According to Lurgi (24), the process economics are more favorable for the combined reforming option because of improved methane to methanol conversion efficiency. The Combined Autothermal Reformer (CAR) (Figure 2) currently under development by Uhde GmbH (26) appears attractive for the next generation methanol plants.

If inexpensive carbon dioxide is available at the site of the methanol plant, a combination of steam reforming (E1) and carbon dioxide reforming (E5) results in more favorable synthesis gas composition and also in higher methane-based conversion efficiency to methanol. For these reasons, natural gas sources with 10-30% carbon dioxide content might be particularly favored for methanol synthesis. Indeed, good methanol yield was reported from the CO_2-containing gas fields of New Zealand (28-29).

AMMONIA SYNTHESIS.

Ammonia production from hydrogen and nitrogen was pioneered by Haber and Bosch in 1913. This led to the development of the giant ammonia industry which provides fertilizer to agriculture to feed the growing world population. Ammonia is one of the largest volume chemicals. World production is estimated at 110 MM tons per annum. About 84% of the production goes to fertilizers. Ammonia prices during the last fifteen years ranged from less than $100/ton to $350/ton due to variations in supply and demand.

Scheme 1. Ammonia Synthesis from Natural Gas and Air.

Natural gas purification	Combined reforming	Shift reaction	CO_2 removal	Gas purifications	Compression	NH_3 loop

Scheme 1 illustrates the process steps involved in ammonia synthesis starting with natural gas (7). The ammonia synthesis step is shown by E11. The reaction is exothermic and leads to equilibrium. The synthesis is conducted at 2000-5000 psi and

E11 $3H_2 + N_2 \rightleftharpoons 2NH_3$ ΔH=-26 kcal/2moles of NH_3

475-500°C over an alkalized, promoted magnetite catalyst. About 13-16% conversion is obtained in commercial recycle operations, with 100% selectivity to ammonia. The ammonia is recovered by condensation after refrigerating the gas stream. A small purge stream is taken from the synthesis loop to prevent inert buildup. Two kinds of converter designs are in commercial use: tubular and multiple bed. Recent developments in the synthesis loop include more efficient converter designs (30) and the introduction of magnetite-ruthenium catalyst combination for higher conversion (31). The largest ammonia plants have 1800 t/d capacity.

During the last two decades, the economics of ammonia production have substantially improved due extensive modernization programs. The progress is reflected by reduction of the energy requirements (i.e. the heating value of the feed including fuel use) per ton of ammonia from about 36 GJ to about 28 GJ. The overall process efficiency based on E12 is about 82%.

E12 $CH_4 + 1.3974\ H_2O + 0.3013\ O_2 + 1.132\ N_2 \rightarrow CO_2 + 2.264\ NH_3$

METHANOL SYNTHESIS.

Synthetic methanol has become available in 1923. Currently worldwide production is approaching 30 MM ton per annum. Nearly half goes for formaldehyde synthesis, which represents a declining market. Other uses include acetic acid synthesis, synthesis of methyl esters, solvent use and recently methyl t-butyl ether (MTBE) synthesis. This latter use is rapidly growing because MTBE is the most preferred octane booster for reformulated gasoline. In recent years, possible "clean fuel" use of methanol was also widely studied (32). The energy crises of the seventies motivated broad range of scientific research in methanol-related subjects as indicated by review articles (33-37). In the last two decades, large capacity plants were constructed near to inexpensive gas sources, exerting a downward trend on methanol prices. During the last decade prices ranged between $0.35-0.75/gal until a recent escalation to above $1/gal.

E13 $2H_2 + CO \rightleftharpoons CH_3OH$ ΔH=-21.7 kcal/mole (@25°C)

The synthesis gas from the reformer requires water removal and compression before methanol synthesis. The synthesis (E13) is an exothermic equilibrium reaction. The original catalyst was zinc-chromium oxide which required high temperatures and pressures. Since the late sixties, copper-zinc oxide catalysts have been adopted which function well at much lower temperature and pressure (230-270°C; 700-2000 psi). The reactors in commercial service are either of the "quench type" or exchanger type; slurry reactors have also been piloted. Synthesis gas conversion is about 15% per pass, but the methanol concentration is only 4-7 % because of accumulation of inerts and excess reagents in the recycle loop. After cooling, the methanol is condensed from the reactor effluent; the gases are recompressed and recycled. A purge stream is taken from the recycle loop which is rich in hydrogen if steam reforming is the source of synthesis gas. Methanol can be obtained in up to 98-99% selectivity. Ethers, aldehydes, ketones, esters, water, higher alcohols, methane and hydrocarbons are the by-products. The energy requirements for the various natural-gas based methanol processes are estimated at 32.4-35.3 GJ/ton methanol, corresponding to 78-85% carbon based efficiency.

Recent research and development efforts on methanol appear to have two different directions: 1./ Finding improved catalysts (35, 38-39). 2./ Increasing conversions to methanol by shifting the equilibrium (40-44).

HYDROCARBONS VIA FISCHER-TROPSCH (FT) SYNTHESES.

The FT synthesis dates back to 1923 with the discovery of a catalyst to convert synthesis gas to hydrocarbon mixtures. Based on this discovery, an industry was developed in Germany for the conversion of coal-based synthesis gas to synthetic fuels (45). The economic justification for this industry collapsed with the

end of World War II, when inexpensive oil became available. In the early fifties, a natural gas-based FT plant was built in Brownsville, Texas. Unfortunately, economic factors forced the shut down of the plant before sustained continuous operations could be achieved (18). At about the same time, new markets opened up for industrial and household use of natural gas by the construction of long distance pipelines, which eliminated the economic need for a FT conversion plant. However, the German and the American technological advances were utilized and further developed by South Africa where a giant coal-based synthetic fuels and chemicals industry was established (46-49). The rest of the world had very little interest in FT chemistry in the post war era until the energy crises of the seventies. These events rekindled research and development interests. Now the technology is approaching the status when natural gas conversion to liquid fuels and chemicals can be accomplished in commercially viable operations under specific circumstances. In 1993, Shell Intl. Gas Ltd has started up a large conversion plant in Malaysia, using their proprietary new technology (19). Also, since 1993, Mossgas in South Africa has been converting offshore gases to fuels using Sasol's fixed fluid bed technology (50).

The FT chemistry and technology has numerous ramifications. Only some very basic concepts will be reviewed here. E14 illustrates the basic chemistry. The reaction can be considered as a polymerization reaction of C1 intermediates. A broad range of

E14 $nCO + 2nH_2 \rightarrow (CH_2)_n + nH_2O \quad \Delta H=-40$ kcal/mole CO

E15 $C_n = (1n^2 \alpha)\, n\, \alpha^n$

where C_n is the carbon selectivity of the product having n carbon number and α is the probability of growth.

products is obtained which are defined by a single parameter, the chain-growth probability or alpha according to the Anderson-Schulz-Flory (ASF) kinetic scheme (see E15). To-day a good qualitative understanding exists about the factors which can cause deviations from the ASF kinetics (51). In E14, the products are formulated as olefins. While the primary products are, indeed, predominantly olefins, the olefins may hydrogenate to paraffins in secondary reactions. A variety of oxygenated products also forms to some extent. Furthermore, the water gas shift reaction (E4) is also a side reaction. E14 is not limited by equilibrium. Ru, Ni, Fe, and Co catalyze the reaction; the latter two are the commercial choices. The Fe catalyst are usually unsupported, but they need alkali metal and other promoters and also require operations under pressure. They can be used in a wide temperature range (200-350°C). Co is more active than Fe. It also shows greater hydrogenation tendency for paraffin formation. The exothermic heat of the FT reaction is very high, requiring well controlled heat removal. With Fe catalyst, there is a wide choice for reactor and process design: fixed bed, circulating fluid bed, fixed fluid bed and slurry bed. For Co catalysts, to date only fixed bed operations were found satisfactory. Kinetic studies have amply demonstrated that the catalytic activity is limited by diffusion (51-53).

GASOLINE VIA METHANOL. THE METHANOL TO GASOLINE (MTG) PROCESS.

As an offshoot of the pioneering work on synthetic zeolites, it was discovered in Mobil Oil's laboratories, that methanol can be converted to a variety of hydrocarbon products over ZSM-5 zeolite (54,55). E16 illustrates the types of reactions occurring.

E16 $2CH_3OH \rightleftharpoons CH_3OCH_3 + H_2O \rightarrow [CH_2{=}CH_2] + 2H_2O$

oligomerizations
isomerizations
C-C bond fissions
alkylations
aromatizations

products

Ethylene is indicated as an intermediate, though this mechanistic assumption is debated. The products are mixtures of olefins, isoolefins, isoparaffins and aromatics with less than 11 carbon per molecule. The product slate can be varied within certain

limits because the relative rates of the indicated reactions vary, aromatization being the slowest. Subsequently processes have been developed for high octane gasoline production from methanol. A fixed bed process version was commercialized in 1986 in New Zealand for the conversion of natural gas to premium grade gasoline (28,29).

COMPARATIVE ECONOMICS. OPPORTUNITIES FOR R&D.

Previous economic studies have clearly established that the large capital requirement is the major obstruction to the evolution of a natural gas-based synthetic fuel industry (19,56). Other important factors are the cost (i.e. the local value) of the natural gas, the quantities of fuel produced by the conversion (i.e. the process efficiency) and the market value of the fuel or chemicals produced. Table 1 compares salient economic features of the natural gas conversion technologies, assuming 100 MMscft/day natural gas usage. For the ammonia, methanol and syncrude technologies, it can be assumed that the capital cost requirements are approximately the same, hence the production volumes and the product heating values are directly related to the economics of these processes. The gasoline via methanol conversion has higher capital requirements because of the extra MTG process step.

Table 1. Comparison of Conversion Technologies, 100 MMscft/d Gas.

Technology	% Process efficiency	Daily production quantities Weight (tons)	Heating Gkcals
Ammonia (old)	69	3357	-
Ammonia (new)	82	3985	-
Methanol	78	3154	16.8
via combined reforming	85	3437	18.4
Syncrude (Shell MDS)	80	1414	16.2
Syncrude (possible)	88	1557	17.8
Gasoline (via methanol)	76	1317	14-15

For syncrude synthesis, 80% methane-based process efficiency is estimated from the data reported by Shell. While this is a high value, with advances much higher efficiency is possible for the following reasons: All the gaseous products from the FT reactor can be recycled into synthesis gas generation and hence 100% liquid selectivity is possible. Furthermore, energy requirements (for compressors, etc.) in the FT process are less than in methanol synthesis while more energy is produced in the reaction. Hence higher process efficiencies and lower capital requirements may be possible in the FT process. Comparing methanol and syncrude, it is apparent that methanol is a much preferred product over syncrude because of its quantity. However, this statement is valid only if methanol can be marketed for chemical use. For the fuel market, methanol and syncrude product values are nearly equal on the basis of their heating values.

To make the syncrude process viable, the simplest possible process must be assembled, requiring the lowest amount of capital. Furthermore, search must go on to enhance the value of the syncrude fractions. It is already known, that syncrude commands a premium price, because it is practically free of S and N; its Diesel fraction has high cetane value and its wax fractions have high chemical values. In Figure 3 a process scheme is shown for staged coproduction of methanol and syncrude. This seems feasible because there is an overlap around 450-500 psi where syngas generation, methanol synthesis and syncrude synthesis all could be accomplished. With coproduction of methanol, the quantity and the value of the products are increased. Substantial reduction of the capital requirements of the syncrude process may be possible by making synthesis gas by an energy efficient combined reforming technology similar to that used in the ammonia industry, with air as the oxidant. In this case, the research challenge is the efficient and selective conversion of the nitrogen-diluted synthesis gas. It may be possible to control the probability of growth in the FT synthesis around 0.82, resulting in high selectivity to liquids (see Figure 4). This would eliminate the need for hydrocracking of the heavy paraffins which is the current practice. Yet another opportunity for capital reduction and improving the process efficiency could be the introduction of efficient plate exchangers for heat

exchange duties, including in the design of the reactors. Of course, FT catalyst selection and design need to pay special attention to minimize the diffusional limitations.

Figure 3. MeOH-Syncrude Process.

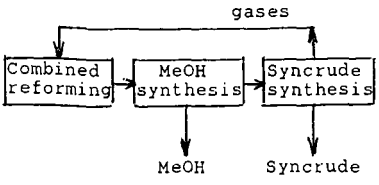

Figure 4. MWD at 0.82 Alpha.[a]

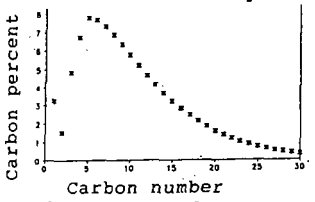

[a]Co catalyst. See reference 57.

In conclusion, the natural gas conversion technology to synthetic fuels offers the best opportunities for advances. Some approaches to reduce the capital requirements and simultaneously improve the process efficiency and product values have been outlined. Development and demonstration of these opportunities may lead to commercially attractive natural gas conversion even at the current oil price environment, if natural gas is available at low cost.

REFERENCES.

1 J.R. Rostrup-Nielsen, Catalysis Today, 21, 257 (1994).
2 J.M. Fox, Cat.Rev.-Sci.Eng., 35, 169 (1993).
3 G.A. Mills Paper C43, 13th North American Meeting of the Catalysis Society, May 2-7, 1993, Pittsburgh, PA. See also Idem, DOE, Nat. Renewable Energy Lab, HZ 1-11208-1 (1992).
4 J.L.G. Fierro, Catal. Lett, 22, 67 (1993).
5 J.H. Lunsford, Catalysis Today, 6, 235 (1993).
6 J.C.W. Kuo, C.T. Kresge and R.C. Palermo, Catalysis Today, 4, 463 (1989).
7 T.A. Czuppon, S.A. Knez and J.M. Rovner in Encyclopedia of Chemical Technology, Fourth Ed. Vol.2, p.638. Wiley 1992.
8 J.R. Rostrup-Nielsen in Catalysis Science and Technology, J.R. Anderson and M. Boudart, Eds., Vol.5, p.1, Springer 1984.
9 J.P. Van Hook, Catal.Rev.-Sci.Eng. 21, 1 (1980).
10 F.E. Biasca, R.L. Dickenson, A.J. Moll, E.D. Oliver, D.R. Simbeck, Synthesis Gas for Chemicals and Fuels. Technology, Economics and Market Outlook. SFA,Inc. Final Report, October 1983.
11 J.D. Fleshman, Chem.Eng.Progr., October 1993, p.20.
12 J.R. LeBlanc, Energy Progress 5 (1), 4 (1985).
13 J.R. Rostrup-Nielsen in Catalyst Deactivation, C.H. Bartholomew and J.B. Butt, Eds,, Elsevier, 1991. See also Idem, J.Catal., 85, 31 (1984).
14 N.R. Undergaard, J-H.B. Hansen, D.C. Hanson and J.A. Stal, Oil&Gas J., March 9, 1992, p.62.
15 S. Teuner, Hydr.Proc,, May 1985, p. 106 and July 1987, p.52.
16 H-J. Toepfer, GWF-Gas/Erdgas, 117, 412 (1976).
17 Prettre, Ch. Eichner and M. Perrin, Trans.Far.Soc., 42, 335 (1946).
18 Anonymous, Chem.Eng.Progr., 53 (10), 1957, p.50.
19 P.J.A. Tijm, Preprint, Fuel Division, ACS, 39, 1146 (1994).
20 S.S. Bharadwaj and L.D. Schmidt, J.Catal., 146, 11 (1994) and references cited therein.
21 J.B. Huttl, Eng.& Mining J., 162 (7), 82 (1961).
22 H. Sachsse, Chem.-Ing.-Technik, 21 (1/2), 1 (1949).
23 Anonymous, Chem.Eng. July 9, 1962, p.38.
24 E. Supp, Hydr.Proc., July 1984, p.43-C.
25 D. Kitchen and A. Pinto, Ammonia Plant Safety, 31, 219 (1991).
26 H-D. Marsch and N. Thiagarajan, Ammonia Plant Safety, 33, 103, (1993).
27 P. Orphanides, Ammonia Plant Safety, 34, 292 (1994).
28 J. Haggin, C&EN, June 22, 1987, p.22.
29 C.J. Maiden, Chemtech, January 1988, p.38.
30 N. Shannahan, Hydr.Proc., January 1989, p.60.
31 S.A. Knez, D.O. Moore and R.V. Schneider, Kellogg Ammonia Club Meeting, San Diego, CA, August 1990.

32 M.D. Jackson and Carl B. Moyer in Encyclopedia of Chemical Technology, Fourth Ed., Vol.1, p.826, Wiley, 1991.
33 E. Supp, How to Produce Methanol from Coal. Springer, 1990.
34 K.C. Waugh, Catalysis Today, 15, 51 (1992).
35 G.C. Chinchen, J.P. Denny, J.R. Jennings, M.S. Spencer and K.C. Waugh, Appl.Catal., 36, 1 (1988).
36 J.C.J. Bart and R.P.A. Sneeden, Catalysis Today, 2, 1 (1987).
37 K. Klier in Advances in Catalysis, Eds. D.D. Eley, H. Pines and P.B. Weisz, Vol.31, p.243, Academic Press, 1982.
38 D.L. Trimm and M.S. Wainwright, Catalysis Today, 6, 261 (1990)
39 R.A. Koeppel, A. Baiker and A. Wokaun, Appl.Catal.A:General, 84, 77 (1992).
40 D.M Brown, B.L. Bhatt, T.H. Hsiung, J.J. Lewnard and F.J. Waller. Catalysis Today, 8, 279 (1991).
41 J.M. Berty, C. Krishnan and J.R. Elliott, Chemtech, October 1990, p.624.
42 K.R. Westerterp, M. Kuczynski and C.M.M. Kamphuis, Ind.Eng. Chem.Res., 28, 763 (1989).
43 J.B. Hansen and F. Joensen in Proc. Nat. Gas Conversion Symposium, Oslo, Aug.1990, p.457, Elsevier, 1991.
44 S.G. Neophytides and G.F. Froment, Ind.Eng.Chem.Res. 31, 1583 (1992).
45 H.H. Storch, N. Golumbic and R.B. Anderson, The Fischer-Tropsch and Related Syntheses, Wiley, 1951.
46 M.E. Dry and H.B.deW. Erasmus, Ann.Rev.Energy, 12, 1 (1987).
47 M.E. Dry in Catalysis Science and Technology. Eds. J.R. Anderson and M. Boudart, Vol.1, p.159. Springer, 1981.
48 M.E. Dry, Catalysis Today, 6, 183 (1990).
49 B. Jager, M.E. Dry, T. Shingles and A.P. Steynberg, Catal. Lett. 7, 293 (1990)
50 Anonymous, Oil&Gas J., Jan.20, 1992, p.53.
51 R.S. Hurlbut, I. Puskas and D.J. Schumacher, This Symposium.
52 M.F.M. Post, A.C. van't Hoog, J.K. Minderhoud and S.T. Sie, AIChE Journal, 35, 1107 (1989).
53 R.B.Anderson, J.F. Shultz, L.J.E. Hofer and H.H. Storch, Bulletin 580, Bureau of Mines, US Govmnt. Printing Office, 1959.
54 S.L. Meisel, J.P. Mc Collough, C.H. Lechthaler and P.B. Weisz, Chemtech, February 1976, p.86.
55 C.D. Chang and A.J. Silvestri, J.Catal., 47, 249 (1977).
56 D. Gray and G. Tomlinson, Coal Liquefaction and Gas Conversion Contractor's Review Conference, Sept, 7-8, 1994, Pittsburgh.
57 I. Puskas, R.S. Hurlbut, R.E. Pauls, J.Catal., 139, 591 (1993)

NEW PROCESS DEVELOPMENT OF NATURAL GAS CONVERSION TECHNOLOGY TO LIQUID FUELS VIA OCM REACTION.

Tomoyoshi Sasaki, Shinichi Suzuki, Takashi Kojima
Japan National Oil Corporation
1-2-2 Hamada, Mihama-ku, Chiba-shi, 261 JAPAN

Masami Yamamura
Japan Petroleum Exploration Co.,Ltd
1-2-1 Hamada, Mihama-ku, Chiba-shi, 261 JAPAN

Tomohiro Yoshinari
Cosmo Research Institute Co.,Ltd
1134-2 Gongendo, Satte-shi, Saitama-ken, 340-01 JAPAN

Keywords: Natural gas conversion, Oxidative coupling of methane, Circulating fluidized bed

Abstract

The conversion of methane via an OCM (Oxidative Coupling of Methane) to transportable liquid fuel has been investigated in order to utilize remote natural gas effectively. A conceptual view of this new process was developed for gasoline production based on reviews of other conventional processes and sensitivity analyses. The process developed, "ORIGINAL", is characterized by simplification of the total process and application of an advanced fluidized bed reactor to the OCM reaction. Full economic comparisons between the "ORIGINAL" and conventional OCM technologies were carried out. The results showed that the "ORIGINAL" process is substantially more economical when compared with existing technologies under the same conditions.

Introduction

Many natural gas fields have been discovered recently in Southeast Asia, which has become one of the main areas for oil and gas exploration. In many cases, however, the developments of the discovered gas fields have been obstructed by the demand for large investments in the transportation facilities (e.g., gas pipeline) and other related infrastructure.

Some liquefaction methods of natural gas, which include liquefying natural gas at an extremely low temperature (LNG), and converting natural gas into liquid fuel through the synthetic gas, have already been put into industrial use. These methods, however, also require large investments in the facilities and are expensive to operate. Consequently, even the existing methods remain a significant obstacle in the development of natural gas fields, in particular marginal fields.

Thus, to exploit natural gas resources more widely, a new method is required which converts natural gas into liquid fuel more efficiently and economically than the existing methods. With this in mind, the purpose of this study is to research and to develop a new process which converts methane, the main component of natural gas, into liquid fuel (e.g., gasoline), rather directly than through synthetic gas.

Scope of work

First of all, we devoted our time largely to reviewing the current development trends overseas, and conducted a feasibility study. Among the various direct reaction processes in which methane is converted into a highly reactive intermediate product, the oxidative coupling of methane (OCM) reaction process, in which ethylene is the intermediate product, was chosen from the standpoint of economic efficiency and feasibility in practical use. Furthermore we conducted a sensitivity analysis on the existing OCM processes which we thought promising, to evaluate the impact of various process parameters on the economy of the process itself. A "conceptual view" of the newly integrated "ORIGINAL" process was developed on the basis of these findings and the process was evaluated from the standpoint of economy.

Description of the conventional technology

A sensitivity analysis was carried out on the conventional methane conversion technology[2] [3]. This liquid fuel synthesizing process is based on the OCM. Conceptual block flow diagrams of this process, which have been modified under our consideration to simplify the process, is shown in Figure 1.

This process called Co-feed mode is characterized by point that methane and oxygen are co-fed to the oxidative coupling reactor, therefore air separation unit is required. Pyrolysis of C2 + hydrocarbon is undergone at the upper side of the reactor which oxygen is relatively free. The pyrolysis approach leads to the removal of heat from the OCM reaction and the production of more olefins. Coupling products after separation of unconverted methane and byproducts are fed with oligomelization reactor. Higher hydrocarbon produced are refined to gasoline in a distillation unit. Unconverted methane,carbon oxide and hydrogen mixed with natural gas are fed to a decarbonator to remove carbondioxide. In the following methanation reactor, carbonoxides are converted to methane by the hydrogen produced in the pyrolysis reactor in order to utilize natural gas effectively.

Sensitivity analysis of existing processes

In discovering factors relative to product costs, we conducted sensitivity tests on the parameters listed below regarding conventional technology. When each factor was analyzed to study the causative effect on economics, other parameters took respective basic values underlined to ignore an effect of themselves.

(1) Plant scale (natural gas volume) : 10,50,100 (* 10 thousand Nm3/D)
(2) Methane conversion ratio : 10,15,20 (%),
(3) C2+ selectivity : 70,80,90 (%),
(4) Reaction pressure : 1,4,10 (Kg/cm2G)
(5) GHSV : 5000,10000,20000 (hr-1)
(6) C5+ yield rate : 60,70,80 (%)
(7) Natural gas price : 0.5,1.0,2.0 ($/MMBTU)

The impact of variable factors on the gasoline production cost is shown in Figure 2. Within the scope of the present evaluation, the reaction results of the oxidative coupling process had a much more significant impact than those of the polymerization process. In general, several sensitivity studies indicated that C2+ selectivity was more important economically to the OCM reaction than methane conversion ratio. This sensitivity analysis showed that the reaction results for the methane conversion ratio were found to have been subject to a much more significant impact within the various factors involved in the oxidative coupling reaction under these conditions. Among the factors other than the reaction result, plant size was the significant factor which had the most impact on gasoline production cost.

We also carried out the sensitivity analysis with respect to conventional Redox-mode process [1] and got the same tendency with Co-feed mode.

ORIGINAL process implication

A conceptual view of the basic original overall process "ORIGINAL" was developed for gasoline production on the basis of reviews of the conventional processes, sensitivity analysis and reaction results likely to be obtained in the oxidative coupling reaction and polymerization reaction. A general outline of the designed process can be seen on flowsheet (Figure 3).

This process incorporated the OCM and pyrolysis reaction is similar to the Co-feed mode OCM process. It also includes facilities for oligomerization, product separation and methanation. The following two points characterize the new process. In general, with conventional technology wholly recycled gas including unconverted methane is fed to the decarbonation unit to remove CO2 and treated recycled gas enters the methanator with new additional CO2 which corresponds with H2 and CO in order to enhance the carbon utilization efficiency.

Firstly, the flowsheet shows recycled unconverted methane gas, hydrogen, CO2 and CO are split in two and are fed to a decarbonator and a methanator respectively. Regarding reduction of scale of the decarbonation unit, it is effective to feed directly part of the recycled gas, including

CO2 corresponding to methanation with the methanator, not through the decarbonator. The integrated process with the conceptual view is economically competitive compared with existing methods because of the reduced plant cost.

Secondly, the question which we must consider is what types of reactor to apply to the OCM reaction. The OCM reaction is very exothermic and operated in a relatively narrow temperature range, placing high demands on heat removal and temperature control. In general, application of the fixed bed for OCM reactions has several disadvantages, difficulty selecting cooling agents and a complicated reactor structure. As for the bubbling fluidized bed reactor, which has a high heat transfer coefficient, scaling-up is known to be an important problem.

This research activity has also led to the identification of new natural gas conversion concepts using a circulating fluidized bed design with a riser reactor. This reactor is used to combine the methane oxidative coupling step with the pyrolysis of ethane and higher alkane components present in natural gas, to provide an efficient method for total conversion of natural gas to liquid fuel. The circulating fluidized bed is schematically illustrated in Fig. 4. The OCM is carried out in the riser reactor as FCC technology and an important feature of the process is pyrolytic conversion within a bubbling fluidized bed, which is the disengaging section located at the top of the riser zone, using heat generated by the OCM reaction via catalyst particles. For the circulating fluidized bed, it is possible to recycle the catalyst continuously, and to replace it if deactivation occurs. The temperature inside both reaction phases can be easily controlled and scaling-up to a commercial size is relatively simple.

Economic evaluations

The concept of the ORIGINAL process was then evaluated from the standpoint of process efficiency. From the sensitivity analysis, we understood that the methane conversion ratio is more important than C2+ selectivity under our condition. Therefore we investigated process efficiency and plant costs in a high methane conversion region. A correlation between methane conversion and C2+ selectivity, which is derived from extrapolation of catalytic performances of the best catalysts known in literatures at present[4], used in our evaluations is shown in Table 1.

Under these conditions we calculated the investment cost on plant construction regarding ORIGINAL as shown in Figure 5 and found CASE-2 to be the more economical condition. Furthermore the economic evaluations of ORIGINAL and conventional technologies in the region of high methane conversion (25～30%) are summarized in Table 2. The results showed that ORIGINAL is more economically feasible compared with existing technologies.

Conclusion

We have analyzed the relationship and causative effects of several factors on plant and product costs to existing methods. It was noted that the rate of methane conversion was economically significant compared to C2+ selectivity under 30% methane conversion. On the basis of these results we have designed a new process with conceptualized the circulating fluidized bed reactor to OCM reaction and carried out the economical evaluations. The result showed that the correlation between about 30% of methane conversion and 77% of C2+ selectivity was the optimum condition for reducing plant costs for our process. Furthermore, this ORIGINAL process has shown to be more efficient and economically feasible than conventional technologies under the same conditions.

References

1) J.A.Sofranko et al., PACIFIC ' 89 Paper No.165

2) A.Robine et al., "NOVEL PRODUCTION METHODS FOR ETHYLENE, LIGHT HYDROCARBONS, AND AROMATICS" ,DEKKER, p.141 (1992)

3) J.H.Edwards et al FUEL., 71, 325, (1992)

4) J.W.M.H.Geerts et al, "NOVEL PRODUCTION METHODS FOR ETHYLENE, LIGHT HYDROCARBONS, AND AROMATICS" ,DEKKER p.207 (1992)

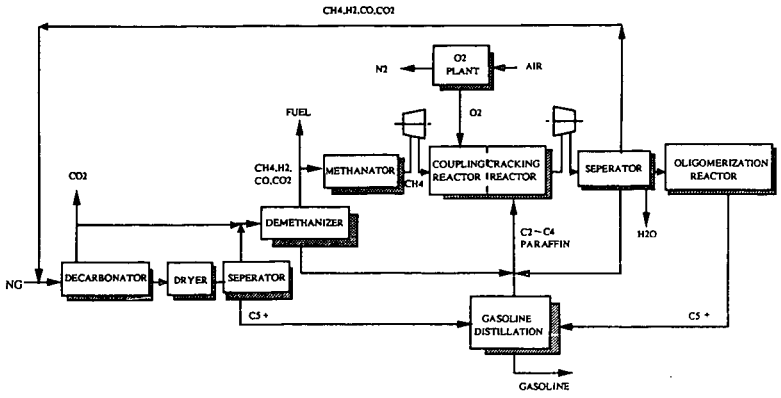

Figure 1. Block Flow Diagram of Conventional OCM Process

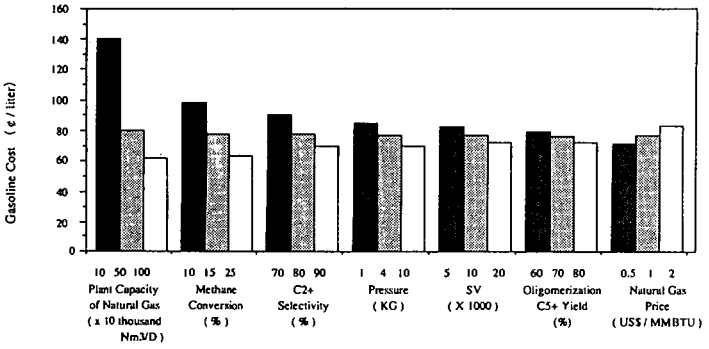

Figure 2. Effects of Various Factors on Gasoline Cost

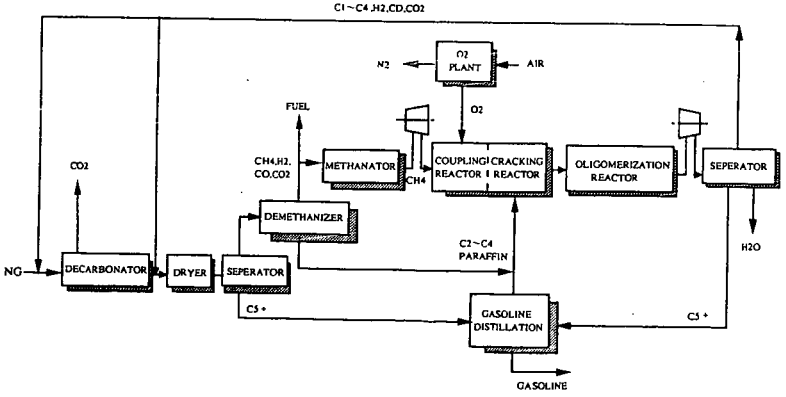

Figure 3. Block Flow Diagram of ORIGINAL Process

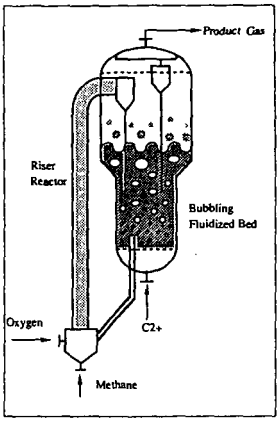

Figure 4. Circlulating Fluidized Bed Reactor

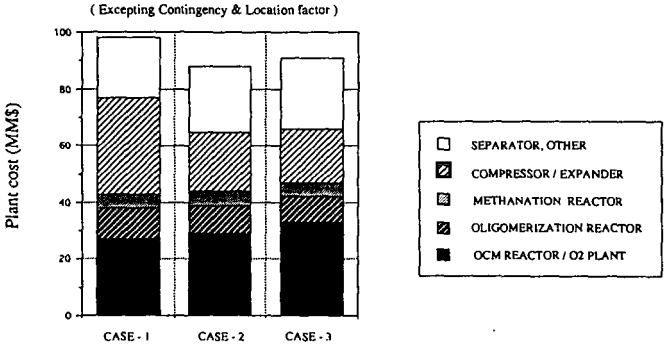

Figure 5. Constituent Proportion of Plant Costs regarding ORIGINAL processes (Plant Capacity : 2,100 BPSD)

Table 1. Estimated Correlation Between Methane Conversion and C2+ Selectivity

	CASE-1	CASE-2	CASE-3
METHANE CONVERSION (%)	20	30	40
C2+ SELECTIVITY (%)	84	77	69

Table 2. Comparison of Process Efficiencies and Plant costs
(Plant Capacity : 2,100 BPSD)

	ORIGINAL	OCM (REDOX MODE)		OCM (COFEED MODE)	
OCM REACTION CONDITION					
METHANE CONVERSION (%)	30	25	30	25	30
C2+ SELECTIVITY (%)	77	80	77	80	77
PLANT COST (MM$)	88	103	91	123	111
THERMAL EFFICIENCY (%)	57.8	57.1	55.0	60.8	58.5

PARTIAL OXIDATION OF METHANE TO SYNGAS IN DIFFERENT REACTOR TYPES.

Jacek A. Łapszewicz, Ian Campbell, Brian G. Charlton, Gary A. Foulds
CSIRO Division of Coal and Energy Technology, Lucas Heights, PMB 7, Menai 2234, Australia.
Ph. +61 2 710 6869, Fax. +61 2 710 6800

KEYWORDS: Methane, Partial Oxidation, Pressure

INTRODUCTION

Most of the reported work on catalytic partial oxidation (CPO) of methane to syngas has concentrated on catalyst development and testing in fixed bed reactors at atmospheric pressure (1). Very few workers have investigated CPO in fluidised bed reactors (2-4) or at elevated pressures (5,6). All results reported for high pressure experiments were obtained either with diluted (with excess steam or inert gas) or non-stoichiometric (low oxygen) feeds and are therefore not indicative of the performance under conditions required for a commercial plant. In this paper we report the results obtained in fixed and fluidised bed reactors at atmospheric and elevated pressures with a methane to oxygen ratio of 2. These results are discussed in the context of further development of the CPO process.

EXPERIMENTAL

The catalyst tested in this work was 0.25%Rh/5%ZnO/γ-Al_2O_3. The experiments were carried out using three reactors made of silica : fixed bed and fluidised bed, the latter type configured either in the conventional way with porous distribution plate or as a spouted reactor (Fig 1). The design of the spouted reactor was such that methane and oxygen were mixed immediately before entering the catalyst bed. The spouted reactor was designed specifically for experiments at high pressures where short mixing times were important to limit the contribution of non-catalytic gas phase reactions between methane and oxygen.

Typical experimental procedure was as follows. Prior to each experiment the catalyst was reduced in flowing hydrogen (CIG, >99%, 500 mL/min) at 500°C for 3 hrs and cooled to ambient temperature. Flows of methane (Matheson, >99%) and oxygen (CIG, 99.99%) into the reactor were adjusted to the desired level using mass flow controllers (Brooks 5850TR), keeping CH_4/O_2 ratio = 2. The reactor temperature was raised slowly until the reaction was initiated (300 - 500°C) and then stabilised at constant level. After the reaction reached steady state, the products were analysed several times under each set of conditions.

RESULTS AND DISCUSSION

The performance of the rhodium catalyst at different space velocities in the fixed bed reactor is shown in Figure 1. At temperature of 900°C methane conversion and syngas selectivity are close to equilibrium and do not vary with contact time. At 800°C the departure from this pattern becomes noticeable and both the conversion and the selectivity increases with decreasing contact time. This trend becomes even more pronounced at 700°C. At gas flows above 300 L/H/g it was impossible to maintain the reaction temperature at 700°C even after removal of the external heater. In some cases temperature differences across the catalyst bed exceeded 150°C.

This example is a good illustration of the autothermal character of the partial oxidation reaction. It also points to the major disadvantage of the fixed bed reactor, namely the heat transfer limitation leading to the formation of the " hot spot" in the upper zone of the catalyst bed. Even at lowest gas flows used overheating of the top layers of catalyst was noticeable.

Entirely different behavior was observed in fluidised bed reactor. Even though the range of space velocities feasible in this type of reactor was restricted by the terminal velocity, some valid conclusions can be drawn from the comparison.

First, methane conversions are generally lower compared with fixed bed reactor. This is most likely the result of much better heat dissipation within the catalyst bed. The highest observed temperature differences between the top an the bottom of the reactor were 40°C and in most cases fell below 20°C despite the fact that the diameter of the fluidised bed reactor was almost three times larger than the fixed bed reactor.

Second, both methane conversions and carbon monoxide selectivities tend to decrease with increasing gas flows indicating the lack of autothermal effect. Similar pattern was observed for hydrogen selectivities, except that they tend to increase at space velocities below 30 L/h/g before declining at higher gas flows. This effect is probably caused by secondary reactions (*i.e.* combustion of hydrogen) at longer contact times.

The greater thermal stability of a fluidised bed reactor makes it more suitable for carrying out the partial oxidation reaction on a larger scale. It also seems that the activity of the catalyst is not an important factor within the temperature range >900°C needed to achieve high methane conversions required by commercial application, since equilibrium is reached easily under wide range of conditions. This is well illustrated by the results shown in Figure 4. They show that variation in catalyst loading from 12g to 3g has no significant effect on performance.

It appears that apart from efficient handling of heat transfer the greatest challenge in practical implementation of partial oxidation as an alternative technology for syngas production will be successful

and safe operation of the reactor at elevated pressures. The requirement for the use of high pressure is driven mostly by economic factors. Operation at high pressure allows the use of a smaller reactor and reduces demand for syngas compression for downstream processes.

There are two major problems that arise when the reactor pressure increases. First, as pressure exceeds about 0.2 MPa, the mixture of CH_4/O_2 at ratio of 2 becomes explosive. Second, the rates of non-catalytic homogeneous gas phase reactions between methane and oxygen leading to the formation of a wide range of products (methanol, formaldehyde, light hydrocarbons, carbon monoxide) increase quickly making it difficult to preheat the reactor feed.

One possible solution to these problems is to preheat methane and oxygen separately and to mix them immediately before introduction into the catalyst bed. To achieve this, a spouted reactor equipped with low residence time mixer (approx. 0.1 ms) was built (C, Figure 1). Ambient pressure tests have shown that its performance was identical to the conventional fluidised bed reactor. The results of high pressure operation of this reactor are presented in Figure 5. They show very minor drop in performance up to 0.6 MPa pressure. Several attempts to increase the pressure beyond 0.6 MPa were unsuccessful. They led to thermal instability indicated by temperature oscillations and resulted in damage to the reactor vessel in the region where methane and oxygen were mixed.

These results clearly indicate that further research aimed at development of a commercially viable partial oxidation process will have to concentrate on the reactor design to overcome problems associated with spontaneous ignition of the feed. Possible solutions may include multi-point oxygen injection, addition of steam to control the reaction exothermicity or the use of severel reactors with heat recovery between stages.

CONCLUSIONS

The above results lead to the following conclusions :

1. Superior heat dissipation characteristics of fluidised bed reactors renders them most suitable for the partial oxidation reaction.

2. Further research should be aimed at overcoming problems associated with efficient heat removal from the reaction zone and elimination of autoignition of methane - oxygen mixtures.

ACKNOWLEDGMENT

Financial support for this project by the Energy Research and Development Corporation is gratefully acknowledged.

LITERATURE CITED

1. Foulds, G.A., Lapszewicz, J.A., (review)

2. Olsbye, U., Tangstad, E., Dahl, I.V., Stud. Surf. Sci. Catal., 81, 303 (1994)

3. Bharadwaj, S.S., Schmidt, L.D., J. Catal., 146, 11 (1994)

4. Goetsch, D.A., Say, G.R., US Patent 4,877,550 (1989)

5. Vernon, P.D.F., Green, M.L.H., Cheetham, A.K., Ashcroft, A.T., Catal. Lett., 6, 181 (1990)

6. Hochmuth, J.K., Appl. Catal. B, 1, 89 (1992)

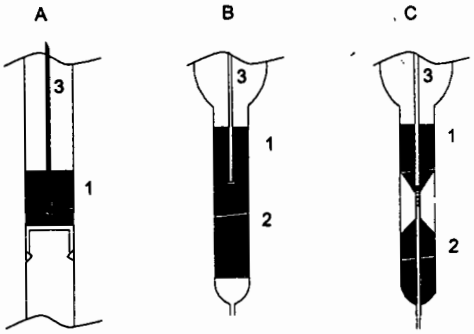

Figure 1. Design of the fixed bed (A, i.d. 10 mm), fluidised bed (B, i.d. 30 mm) and spouted (C, i.d. 30 mm) reactors. Catalyst (1), preheater (2), thermocouple well (3). All reactors made of silica.

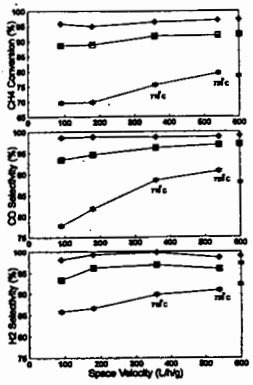

Figure 2. Space velocity vs. temperature profiles for the fixed bed reactor. (◆) 700°C, (■) 800°C, (✱) 900°C. Catalyst loading 0.25g, particle size +125-250 μm. Symbols on right axis indicate thermodynamic equilibrium.

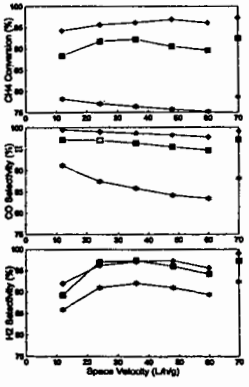

Figure 3. Space velocity vs. temperature profiles for the fluidised bed reactor. (◆) 700°C, (■) 800°C, (✱) 900°C. Catalyst loading 3.0g, particle size +180-250 μm. Symbols on right axis indicate thermodynamic equilibrium.

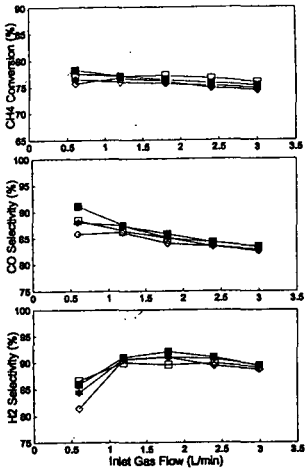

Figure 4. Effect of catalyst loading on performance in fluidised bed reactor at 700°C. (( ) 1.5g, (■) 3.0g, (∗) 6.0g, (□) 12.0g.

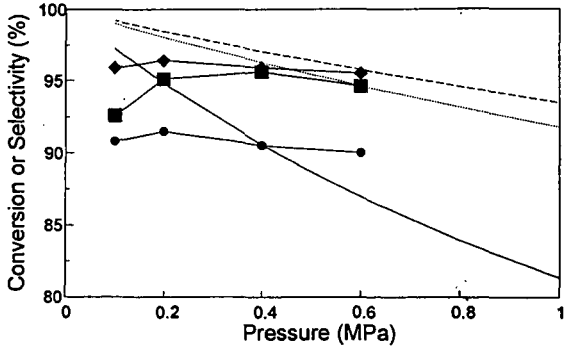

Figure 5. Performance of spouted reactor at high pressure at 900°C. Catalyst loading 3.0g, particle size +250-500 µm. (●) CH_4 conversion, (◆) CO and (■) H_2 selectivity observed.
(____) CH_4 conversion, (_ _ _) CO and (.....) H_2 selectivity predicted at equilibrium.

HEMILABILE PHOSPHONATE-PHOSPHANE-Rh-CATALYSTS FOR HOMOGENEOUS AND HETEROGENEOUS CARBONYLATION

S. Bischoff *, A. Weigt, H. Mießner, B. Lücke
Institute for Applied Chemistry Berlin, Rudower Chaussee 5,
1248 9 Berlin-Adlershof, F.R.Germany

Keywords: methanol carbonylation, rhodium catalysts, hemilabile catalysts

Introduction

Mixed bidentate phosphane ligands such as ether-phosphanes [1-3], phosphane oxide-phosphanes [4], phosphanopyridines and amine-phosphanes [5] containing weak O- or N-donor groups and a strongly electron - donating phosphane group, are known to enhance activities or selectivities of Rh-catalyzed carbonylations. Also other transition metals form hemilabile O,P-chelated complexes, which have been extensively reviewed by Lindner [6]. A row of these complexes catalyzed not only carbonylations effectively but also hydrogenation [7], hydrosilylation [8], and ethylene polymerization [9]. The assumed function of the heterobidentate ligands in the rhodium catalyzed methanol carbonylation is illustrated in Fig. 1. It has been suggested that the oxygen-donating site of the bidentade ligand changes between a coordinated and an uncoordinated state during the catalytic cycle, thus forming chelate and open-chain metal complex structures [1,4]. The intramolecular generation and occupance of free coordination sites, stabilizing Rh-intermediates of different oxidation states and proceeding faster than according intermolecular processes, is assumed to accelerate rate-determing steps in the carbonylation route.

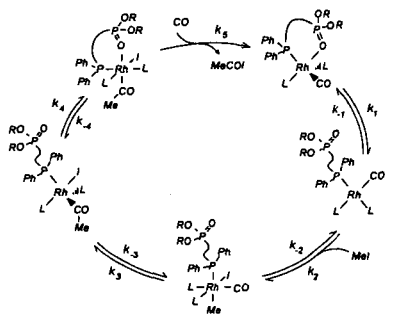

Fig. 1. Methanol carbonylation with hemilabile Rh complex catalysts

Rh-complexes with phosphonate-phosphanes [10] appeared as promising catalyst precursors because they form hemilabile complexes, which should enhance the necessary creation of free coordination sites in Rh^{I}-intermediates by ring-opening of chelate structures and ease the generation of the more oxophilic Rh^{III}-intermediates by O,P-chelate formation (Fig. 1). The concept of hemilabile catalysts with chelate structures involved in rate determining steps implies that the distance and structure between the phosphane and the phosphonate group should affect the carbonylation activity. Unlike the ether-, phosphane oxide-, amino- or pyridine- groups in previously described ligands [1-4], the phosphonate group should additionally facilitate a surface-anchoring of the transition metal complexes on oxidic materials such as silica or alumina, which is a necessary condition for stable slurry- and vapor-phase carbonylation catalysts. In this paper we wish to compare the new soluble Rh-complex catalysts **2a** - **d**, derived from ligands **1a** - **d** (Fig. 2), with known systems and report on the influence of the structure between strongly coordinated phosphane and weakly donating phosphonate moiety in homogeneous methanol carbonylation. Furthermore, we wish to report on supported hemilabile complexes and their properties in slurry- and vapor-phase methanol carbonylation.

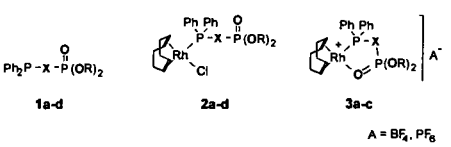

	X	R
a	$-CH_2-$	^{i}Pr
b	$-CH_2CH_2-$	Me, Et
c	$-CH_2CH_2CH_2-$	^{i}Pr
d		^{i}Pr

Fig. 2. Ligands and catalyst precursors

Experimental

The methylene bridged ligand **1a** was accessible via reaction of $LiCH_2P(O)(O^{i}Pr)_2$ with bromodiphenylphosphane. Reaction of 2-chloro-ethyl-dimethylphosphonate or 3-bromo-propyl-diisopropylphosphonate with diphenylphosphane and potassium-tert.-butylate afforded the

phosphonate-phosphanes **1b** and **1c**. Reaction of the O,P-ligands with $[ClRh(cod)]_2$ gave open-chain complexes, **2a - c** which could be easily converted with $AgBF_4$ or $AgPF_6$ into O,P-chelate structures **3a - c** (Fig.2, Fig. 4). The structures of ligands and complexes were verified by MS, NMR and IR. A detailed report on preparation details and properties of the starting complexes will be given elsewhere [11].

Catalytic activities of the soluble Rh-catalysts were tested in a stirred 100 ml-autoclave made of stainless steel. During the catalytic runs, the autoclave-pressure was kept constant at 30 bar. To exclude air contact, the autoclave was filled using Schlenk-techniques with 100 mmol methanol, 6 - 48 mmol methyl iodide, 0.05 - 0.2 mmol rhodium complex and methyl acetate was used as solvent to reach a total volume of 25 ml. After pressurizing with CO (15 bar cold), the filled autoclave was heated up to reaction temperature between 120 and 195 °C and then the pressure was adjusted to 30 bar. The CO-consumption was calculated from the pressure decrease in a closed tank with a known volume which was connected to the autoclave via a pressure regulator. Carbonylation activity was calculated from the initial CO-conversion rate (X_{CO} < 20 %). A typical plot for the CO uptake vs. time is given in Fig.3. The linearity of the plot clearly shows the zero-order of the substrate methanol and is in accord with the rate laws *Eq. (1)* and *Eq. (2)* below (p_{CO}, c_{Rh}, and c_{MeI} = constant.). Second order rate constants k_i [$l \cdot mol^{-1} \cdot s^{-1}$] were related to the concentrations of Rh and MeI.

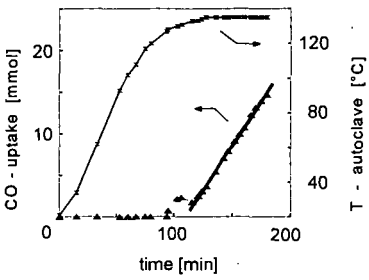

Fig. 3. Typical kinetic run

Results and discussion

The hemilabile character of phosphonate-phosphane-Rh complexes

The presumption for the catalytic concept has been preparatively confirmed for the phosphonate-phosphane-ligands. Both, cyclic and open-chain complexes were isolated after stochiometric reactions (Fig.4) at mild conditions. For instance, (cod)RhCl(pepe) is smoothly converted with $AgBF_4$ into the halogene-free chelate complex at room-temperature and the ring-opening is easily achieved with CO at room-temperature under athmospheric pressure. Reversibility of the last process under reaction-like conditions is assumed from IR investigations of supported complexes. IR shifts in the stretching band of the phosphoryl group $\nu_{(P=O)}$ to lower values in **3a - c** (KBr-wafer or solution), indicate the coordination of phosphoryl oxygen.

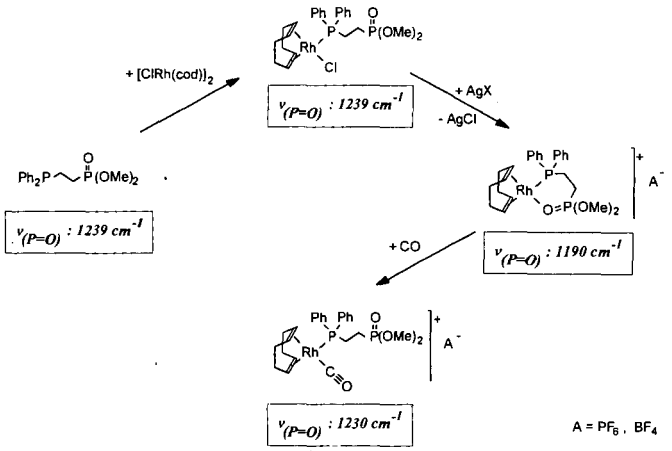

Fig. 4. Preparation and IR - data of catalyst precursors

^{31}P NMR data are depicted in Tab. 1. Not surprisingly , the shift in the ^{31}P NMR signal for the phosphane group ($\delta_{Phosphane}$) shows that this group is coordinated in the open-chain complexes. The chelate structure of **3a - c** is confirmed by low field shifts of the phosphoryl-phosphorus signal ($\delta_{P=O}$, compared to **1a - c, 2a - c)** and additionally by coupling with rhodium (J_{PORh}) . Considering the IR spectra of **3a - c**, it is concluded that the P=O - groups and not the P-O-R' - groups act as oxygen donors.

Table 1. NMR data of ligands and Rh complexes

	$\delta_{P=O}$	J_{PORh}	J_{PP}	$\delta_{Phosphane}$	J_{PRh}
			ligands		
1a	24.91 (d)	-	45.9	-25.32 (d)	-
1b	34.50 (d)	-	62.0	-12.10 (d)	-
1c	29.71 (d)	-	2.9	-17.37 (d)	-
			open-chain complexes		
2a	21.33 (d)	-	16.9	21.51 (dd)	156.8
2b	32.80 (d)	-	63.0	26.80 (dd)	150.0
2c	29.28 (d)	-	4.9	26.60 (dd)	151.6
			chelate complexes		
3a	48.85 (dd)	5.7	50.8	14.69 (dd)	149.6
3b	38.79 (dd)	2.9	13.1	21.21 (dd)	154.0
3c	40.13 (d)	8.1	-	23.74 (dd)	153.5

Catalytic properties of the hemilabile catalysts in homogeneous methanol carbonylation

The methanol carbonylation to acetic acid can roughly be formulated as a sequence of rate determining oxidative addition of the promoter MeI, methyl group migration to a CO-ligand and reductive elimination of acetyl iodide induced by CO-attack (Fig.1). The promoter is regenerated from methanol and HI, the last being liberated in the fast and irreversible proteolysis of acetyliodide. Second order rate constants in a temperature range between 120 and 195 °C were obtained for various Rh-complexes in autoclave experiments monitoring the CO-consumption. The resulting activation parameters are summarized in Tab.2.

Table 2. Ligand effects on activation parameters of the Rh-catalyzed methanol carbonylation

	active carbon	cod	PPh_3	dppe	**1a**	**1b**	**1c**	**1d**
$\Delta H^{\neq}$ [kJ/mol]	20.4	67.5	54.9	27.5	38.6	55.2	61.8	76.0
±	9.2	13.1	5.4	6.2	3.4	5.2	5.3	9.1
$\Delta S^{\neq}$ [J/mol/K]	-233	-112	-141	-211	-179	-141	-126	-90
±	22	32	13	15	8	12	12	22

cod - 1.5-cylooctadiene, PPh_3 - triphenylphosphane, PPh_3:Rh = 2:1, dppe - bis(diphenylphosphano)ethane

The activation enthalpies in Tab.2 differ significantly over a wide range, but a general superiority of the hemilabile catalysts compared to known systems can not be postulated. With the data given here, one can choose certain temperatures to show the superiority of the hemilabile catalysts and the opposite can be done at another temperature, which may illustrate the sometimes questionable comparison of activities at one more or less arbitrary choosen temperature. It is interesting that activation enthalpies of hemilabile catalysts increased with growing distances between phosphonate- and phosphane-group. The highest activation enthalpy was obtained with the p-phenylene-bridged phosphonate-phosphane **1d**, which can not form chelate complexes. This indicates that chelate structures are involved in one of the rate-limiting steps. The additionally to the oxidative MeI- addition emerging rate-limiting steps in P-ligand systems (see also Fig 5) can be the reductive elimination of acetyl iodide ($k_4 * k_5$) or methyl-group migration (k_3). With the given kinetic data, none of these alternatives can clearly be appointed to be more likely.

The hemilabile complex precursors showed generally higher activation entropies than the Rh-bisphosphane complex precursor. This is explained with the generation of open-chain structures of the phosphonate-phosphane complexes during the oxidative addition step, creating additional degrees of freedom for bond-rotation and vibrations. The apparently low activation enthalpy estimated (from only three points) for Rh supported on active carbon is probably caused by diffusion control. Observations in the vapor-phase methanol carbonylation confirmed this assumption.

It has to be stated here, that Tab. 2 shows apparent parameters, which do not merely reflect the rate determining oxidative addition of MeI as known for phosphane-free systems (e.g. cod as ligand), where a simple rate law (Eq. *(1)*) can be applied.

$$r = -\frac{dn_{CO}}{dt} = f(c_{MeI}) = k \cdot c_{MeI} \cdot c_{Rh} \qquad (1)$$

The general case, considering additional rate-determining steps to the oxidative MeI addition, is a more complex function (Eq. *(2)*). This rate law has been derived from Fig. 1 applying network techniques [12] and covers also Eq. *(1)* as a special case (when $B \gg A \cdot c_{MeI}$).

$$\frac{1}{r} = A + B \cdot \frac{1}{c_{MeI}} \qquad (2)$$

with

$$A = \frac{k_5 p_{CO} (k_3 k_4 + k_1 k_4 + k_1 k_3 + k_1 k_{-3}) + k_1 (k_{-3} k_{-4} + k_3 k_{-4} + k_3 k_4)}{k_1 k_3 k_4 k_5 c_{Rh} p_{CO}} \quad \text{and}$$

$$B = \frac{k_3 p_{CO} (k_3 k_4 k_{-1} + k_1 k_4 k_{-2} + k_1 k_3 k_4 + k_4 k_{-1} k_{-2} + k_{-1} k_{-2} k_{-3} + k_1 k_{-2} k_{-3}) + k_{-2} k_{-3} k_{-4} (k_1 + k_{-1})}{k_1 k_2 k_3 k_4 k_5 c_{Rh} p_{CO}} .$$

Indeed, Eq. *(2)* describes the influence of MeI concentration on the activity for both phosphane-containing and phosphane-free catalysts satisfactory, while the simple power law (Eq. *(1)*) failed, when phosphanes (e.g. **1a**) served as ligands (Fig.5). The changed reaction order of MeI is probably caused by the enhancement of MeI-addition due to phosphane ligands, consequently making other steps relatively slower and partly rate-limiting.

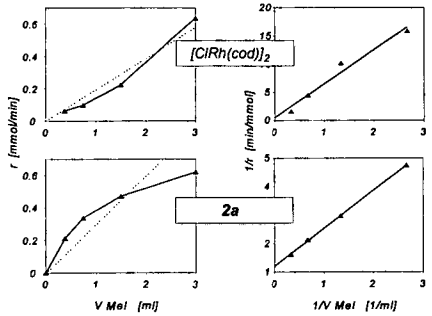

Fig. 5. Influence of MeI on the carbonylation rate; plots on the left side are derived from Eq. (1), on the right side from Eq. (2)

The new phosphonate - phosphane - complexes presented in this work were intended to be fixed on oxide surfaces via the phosphonate groups. While attempts of preparing stable complex-catalysts fixed on silica or alumina for slurry-phase reactions failed because of significant metal-leaching under carbonylation conditions, active carbon was found widely superior with respect to the leaching problem. In contrast to the results obtained for the homogeneous reaction, no significant ligand effects on the activation energies were observed, when the methanol carbonylation was conducted in the vapor-phase using active carbon supported complexes (Fig. 6). Normal diffusion of reactants begins to limit the activity of the supported Rh-complexes and leads to the observed uniform activation energies of about 30 kJ/mol.

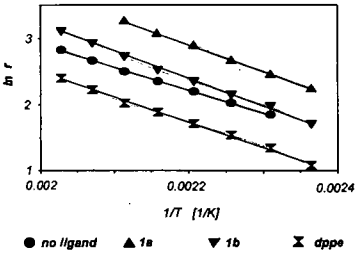

Fig. 6. Ligand effects on Arrhenius plots of active carbon-supported Rh-catalysts

IR-spectroscopic investigations of supported Rh-complex precursors revealed that the bisphosphane-ligand dppe hinders the formation of stable carbonyls (Fig. 7) and that the hemilabile ligands such as 2-(diphenyl-phosphano)ethyldimethyl phosphonate **(2b)** form very stable monocarbonyl species, which are easily converted into dicarbonyl-species with increasing CO partial pressure even at elevated temperatures (Fig.8). The catalytic results in the vapor-phase suggest that phosphonate-phosphanes can also act as hemilabile ligands on supported catalysts.

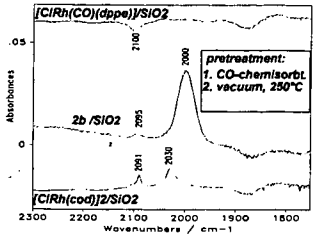

Fig. 7. FTIR spectra of supported Rh catalysts

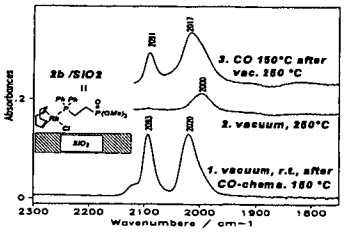

Fig. 8. Supported Rh-carbonyl species derived from **2b**

Acknowledgements
The authors thank the Deutsche Forschungsgemeinschaft for financial support and Mrs. R. Dressel for the numerous catalytic measurements.

References

[1] E. Lindner, H.A. Mayer, P. Wegner, Chem. Ber., **119** (1986) 2616
[2] E. Lindner, A. Sickinger, P. Wegener, J. Organomet. Chem., **349** (1988) 75
[3] E. Lindner, A. Bader, H. Bräunling, R. Jira, J. Mol. Catal., **57** (19990) 291
[4] R.W. Wegmann, A.G. Abatjoglou, A.M. Harrison, J. Chem. Soc., Chem. Commun., **1987** 1891; R.W. Wegmann, A.G. Abatjoglou, PCT Int. Appl. WO 8600888 (1986), C.A. **105** 174788
[5] C. Abu-Gnim, I. Amer, J. Mol. Catal., **85** (1993) L275, C. Abu Gnim, I. Amer, J. Chem. Soc., Chem. Commun., **1994** 115
[6] A. Bader. E. Lindner, Coordination Chem. Rev., **108** (1991) 27-110
[7] W.S. Knowles, Acc. Chem. Res., **16** (1983) 106
[8] Z. M. Michalska, J. Mol. Catal., **19** (1983) 345
[9] K.O. Starzewski, J.Witte, Angew. Chem. Int. Ed. Engl., **24** (1985) 599
[10] J. Freiberg, A. Weigt, H. Dilcher, J. Prakt. Chem., **335** (1993) 337
[11] A. Weigt, S. Bischoff, Phosphorus, Sulfur, and Silicone, in print
[12] H.J. Bittrich, D. Haberland, G. Just: Methoden chemisch-kinetischer Berechnungen, VEB Deutscher Verlag für Grundstoffindustrie, Leipzig, 1979

FUEL OXYGENATES: ORGANIC CARBONATE SYNTHESIS

Ajit K. Bhattacharya
Texaco Inc., Texaco R&D
Beacon, NY 12508

Keywords: C_1 Chemistry & Catalysis, Oxygenates, Organic Carbonates

INTRODUCTION

Owing to the 1990 amendments to the Clean Air Act, two major programs, namely the oxygenated fuels program and the reformulated gasoline program have been mandated. Currently, ethers (MTBE, ETBE, and TAME) and alcohols (mainly ethanol) are employed as fuel oxygenates. However, several dialkyl carbonates exhibit attractive fuel properties and might emerge as future fuel oxygenates. This paper consists of an overview of related literature and highlight of some of our work on the synthesis of organic carbonates from C_1 feedstocks.

Dialkyl carbonates such as dimethyl carbonate (DMC), diethyl carbonate (DEC), and ethyl methyl carbonate (EMC) exhibit excellent gasoline blending properties such as high blending octane numbers and low blending Reid vapor pressures (RVP). Owing to their significantly higher oxygen content compared with alcohol (e.g., ethanol) and ether (e.g., MTBE, ETBE, and TAME) oxygenates, lower volume percent of the carbonate blending components will be needed to satisfy the 2.7 and 2.0 wt% oxygen requirements of the oxygenated and reformulated gasoline programs, respectively (1).

Dimethyl carbonate, for example, may be used as a fuel oxygenate, as a nontoxic and nonpolluting solvent, or as an environmentally harmless chemical in place of toxic and corrosive phosgene in the preparation of isocyanates, polycarbonates, synthetic lubricants, and various agricultural and pharmaceutical intermediates.

Dimethyl, diethyl, and dipropyl carbonates are manufactured, for use as specialty chemical or solvent, by the reaction of the corresponding alcohols with phosgene. Major producers of dialkyl carbonates by the conventional phosgene route are Van de Mark (USA), SNPE (France), BASF and Bayer (Germany). However, tremendous amount of research and development work has been going on worldwide for over thirty years to develop environmentally compatible and economically viable nonphosgene routes for the large scale production of these dialkyl carbonates.

BACKGROUND

Among the nonphosgene routes for the preparation of dialkyl carbonates, direct oxidative carbonylation of alcohols in the presence of various metal complex catalysts has been most widely investigated. A concise description of significant patents and publications in this area during 1963 to 1983 is given below.

Mador et al(2) disclosed the preparation of aliphatic carbonates from alcohols and CO in the presence of costly platinum or palladium salts and usually large excess of an oxidizing metal salt such as copper (II) chloride. The need to use oxygen or air as an additional oxidizing agent was not mentioned. Alkyl halides, ethers, and CO_2 were obtained as undesired side products. The use of toxic mercuric salts in an organic solvent was described by D. M. Fenton (3).

The carbonylation of copper salts such as copper (II) dimethoxide or copper (II) methoxychloride was reported by Saegusa et al (4). In the presence of pyridine, the reaction proceeded even at room temperature. The reaction of copper (II) methoxychloride with CO was studied in great detail by Romano et al (5-7). Perotti et al (8,9) claimed the employment of copper complexes of pyridine and other amines, nitriles, and alkyl or aryl phosphines. However, Rivetti et al (10) showed that the reaction of methanol with CO to give dimethyl oxalate (DMO) and dimethyl carbonate (DMC) in the presence of palladium (II) acetate was inhibited almost completely by a trialkyl or an arylalkyl phosphine. Triaryl phosphines led to the formation of mostly DMO, whereas the yield of DMC was poor (1-6%). Gaenzler et al (11) patented the use of a catalyst system containing a copper salt and a phosphine oxide, phosphite, phosphate or a phosphonate.

Hallgren et al (12) described the use of catalytic amounts of a copper (II) halide, but the reaction must be carried out at elevated temperatures (above 170°C) and at elevated pressures (600-1500 psi or higher).

The role of several alkali, alkali earth, lanthanide, and actinide metal salts might be reckoned as promoters in various catalyst systems. In the presence of LiCl, $CuCl_2$ and manganese compounds afforded DMC in high yields by the oxidative carbonylation of methanol (13, 14). Itatani et al (15) disclosed the application of LiBr, NaCl, KBr, $MgCl_2$, and $CaCl_2$ in the preparation of organic carbonates in the presence of CuX (X=Cl, Br, or I), while Stammann et al (16) mentioned the optional use of group II, lanthanide and actinide metal ions. Cipris et al (17) disclosed an electrochemical process utilizing a non-fluoride halide-containing electrolyte. Gaenzler et al (18) disclosed as catalyst a complex of copper (as CuCl) with VCl_3, $CrCl_3$, $FeCl_3$, $CoCl_2$, $AlCl_3$, or $SiCl_4$. Hallgren (19) disclosed as catalyst (i) a Bronsted base such as a quaternary ammonium, phosphonium, or sulfonium compound or an alkoxide or hydroxide of alkali metal or alkaline earth metal or a salt of a strong base and a weak acid or amines etc. plus (ii) a Group VIII B element Ru, Rh, Pd, Os, Ir or Pt plus (iii) oxygen plus (iv) a redox catalyst such as a Mn or Co containing catalyst. A typical system includes (i) a pentamethylpiperidine, (ii) $PdBr_2$ and (iii) pyridine adduct of salicylaldehyde - ethylene diamine Co (II) complex. Drent (20) disclosed as catalyst a copper compound such as a halide (in the presence of an amine) plus a sulfone such as dimethyl sulfone or sulfolane.

METHODS OF PREPARATION

Various methods for the preparation of organic carbonates from alcohols fall into the following categories:

I. Direct Oxidative Carbonylation (5, 21-31)

$$2\ ROH + CO + 1/2\ O_2 \rightarrow R_2CO_3 + H_2O \qquad \text{(Eq. 1)}$$

II. Indirect Oxidative Carbonylation

(i) *Via* Phosgene

$$CO + Cl_2 \rightarrow COCl_2 \qquad \text{(Eq. 2)}$$

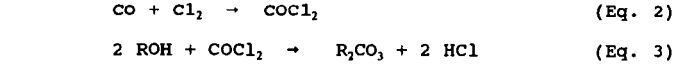

$$2\ ROH + COCl_2 \rightarrow R_2CO_3 + 2\ HCl \qquad \text{(Eq. 3)}$$

(ii) *Via* Alkyl Nitrite (32)

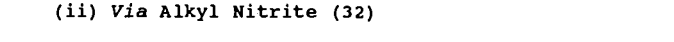

$$2\ ROH + 2\ NO + 1/2\ O_2 \rightarrow 2\ RONO + H_2O \qquad \text{(Eq. 4)}$$

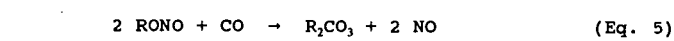

$$2\ RONO + CO \rightarrow R_2CO_3 + 2\ NO \qquad \text{(Eq. 5)}$$

III. Transesterification

(i) *Via* Ethylene Carbonate (33,34)

$$\underset{\text{Ethylene Oxide}}{C_2H_4O} + CO_2 \rightarrow \underset{\text{Ethylene Carbonate}}{C_2H_4CO_3} \qquad \text{(Eq. 6)}$$

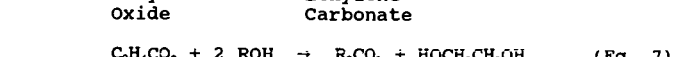

$$\underset{\text{Ethylene Carbonate}}{C_2H_4CO_3} + 2\ ROH \rightarrow R_2CO_3 + \underset{\text{Ethylene Glycol}}{HOCH_2CH_2OH} \qquad \text{(Eq. 7)}$$

(ii) *Via* Di-*tert*-butyl peroxide (DTBP) (35)

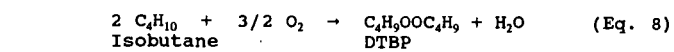

$$\underset{\text{Isobutane}}{2\ C_4H_{10}} + 3/2\ O_2 \rightarrow \underset{\text{DTBP}}{C_4H_9OOC_4H_9} + H_2O \qquad \text{(Eq. 8)}$$

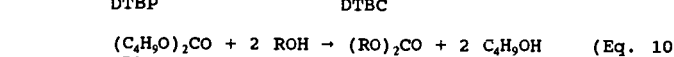

$$\underset{\text{DTBP}}{C_4H_9OOC_4H_9} + CO \rightarrow \underset{\text{DTBC}}{(C_4H_9O)_2CO} \qquad \text{(Eq. 9)}$$

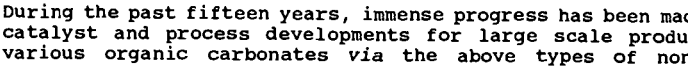

$$\underset{\text{DTBC}}{(C_4H_9O)_2CO} + 2\ ROH \rightarrow (RO)_2CO + 2\ \underset{\text{TBA}}{C_4H_9OH} \qquad \text{(Eq. 10)}$$

During the past fifteen years, immense progress has been made toward catalyst and process developments for large scale production of various organic carbonates *via* the above types of nonphosgene

routes. EniChem (Italy) has been successfully operating a stirred-tank DMC process involving the direct oxidative carbonylation method since 1983. At present, EniChem's DMC capacity at its plant in Ravenna is about 12,000 metric tons per year. EniChem has also licensed its DMC technology to GE and its joint venture partners Mitsui Sekka and Nagase & Co. for a 25,000 metric ton per year of polycarbonate plant in Japan. In 1993, Ube Industries (Japan) began operation of a semicommercial 3,000 metric ton per year DMC plant based on its proprietary vapor phase process via methyl nitrite which employes multimetallic (Pd-Cu-Mo-K) halides supported on activated carbon as a fixed bed catalyst (32). Furthermore, Ube is contemplating a 40,000 metric ton unit.

OXIDATIVE CARBONYLATION OF METHANOL

Preparation of dimethyl carbonate (DMC) by the reaction of methanol with carbon monoxide and oxygen in the presence of copper(I) chloride/copper(II) methoxychloride may be carried out in a stirred tank reactor by either a two-step batch process (Eq. 11 and 12) or a one-step catalytic process (Eq. 13), as follows.

$$2\ CuCl + 2\ MeOH + 1/2\ O_2 \rightarrow 2\ Cu(OMe)Cl + H_2O \qquad \text{(Eq. 11)}$$

$$2\ Cu(OMe)Cl + CO \rightarrow (MeO)_2CO + 2\ CuCl \qquad \text{(Eq. 12)}$$

$$2\ MeOH + CO + 1/2\ O_2 \xrightarrow[Cu(OMe)Cl]{CuCl/} (MeO)_2CO + H_2O \qquad \text{(Eq. 13)}$$

Production of DMC by the oxidative carbonylation of methanol is exothermic and occurs with the coproduction of an equimolar amount of water. The produced water should be continuously removed from the reactor for several reasons. The catalyst activity as well as selectivity to DMC may be reduced at higher water concentration. Direct oxidation of carbon monoxide to carbon dioxide is likely to increase due to formation of water soluble catalytic species. At high water concentration, the possibility of DMC decomposition due to hydrolysis is also higher.

However, continuous removal of water from the reactor, separation of the catalyst system from reactants and products, and separation of DMC from methanol and water are challenging problems. To develop an improved and continuous DMC process, one should satisfy the following conditions:

(i) the rate of DMC formation should be augmented,
(ii) the heat of reaction should be dissipated, and
(iii) the desired activity/stability of the catalyst system should be maintained while removing DMC and water from the reaction mixture.

It is noteworthy that DMC/water cannot be removed by an evaporative procedure without increasing the water concentration in the reaction mixture containing a methanolic slurry of Cu(I)Cl/Cu(II) (OMe)Cl as catalyst.

We have found that on the average, the rate of DMC formation may be enhanced by about eight times in the presence of N-methyl-2-pyrrolidone (NMP) as a high boiling point cosolvent which also helps in dissipating the heat of reaction (23). NMP can also serve as a catalyst carrier during the removal of DMC/H_2O by any flash procedure. Thus, a hot reaction mixture may be flashed to remove volatiles including DMC and water while the catalyst system, dissolved/suspended in NMP, may be recycled back to the reactor.

Low rates of DMC formation with copper(I) chloride/ copper(II) methoxychloride are partly due to low solubilities of these salts in methanol. Higher reaction rates can be attained with a solubilizing metal halide promoter such as calcium chloride (24), a phase-transfer agent such as benzyltriethylammonium chloride (25) or a polar cosolvent such as HMPA (26) or 2-pyrrolidone (23). The ability of copper to bind and activate carbon monoxide can be augmented with a nitrogenous ligand such as pyridine (27), imidazole (28), or a suitable cosolvent such as NMP or urea (29). For example, high rates of DMC formation can be achieved with copper(II) methoxychloride or imidazole-copper(II) methoxychloride in methanol-NMP.

CONCLUSIONS

A new and improved copper based homogeneous or slurry phase DMC process involving direct oxidative carbonylation of methanol can be successfully carried out in the presence of various ligands, promoters and organic cosolvents. A suitable high boiling point cosolvent (i.e., NMP) enhances the reaction-rate, helps in maintaining uniform temperature by dissipating the heat of reaction and serves as a catalyst carrier during the separation of methanol, DMC and water from the reaction mixture by a flash technique.

REFERENCES

1. A. K. Bhattacharya and E. M. Boulanger, "Organic Carbonates As Potential Components of Oxygenated Gasoline", Preprints of the Division of Environmental Chemistry, 471-473, the 208th ACS National Meeting, Washington, D.C., August 21-25, 1994.
2. I. L. Mador and A. U. Blackham, U.S. Patent 3,114,762 (1963).
3. D. M. Fenton, U.S. Patent 3,227,740 (1966).
4. T. Saegusa, T. Tsuda, and K. Isayama, J. Org. Chem., 35, 2976-2978 (1970).
5. U. Romano, R. Tesei, M. M. Mauri and P. Rebora, Ind. Eng. Chem. Prod. Res. Dev., 19, 396-403 (1980).
6. U. Romano, R. Tesei, G. Cipriani, and L. Micucci, U.S. Patent 4,218,391 (1980).
7. U. Romano, F. Rivetti, and N. Di Muzio, U.S. Patent 4,318,862 (1982).
8. E. Perrotti and G. Cipriani, U.S. Patent 3,846,468 (1974).
9. G. Cipriani and E. Perrotti, U.S. Patent 3,980,690 (1976).
10. F. Rivetti and U. Romano, J. Organomet. Chem., 174(2), 221-226 (1979); Chem. Abstr., 91, 174405e (1979).
11. W. Gaenzler, G. Schroeder, and K. Kabs, U.S. Patent 3,952,045 (1976).
12. J. E. Hallgren and G. M. Lucas, U.S. Patent 4,360,477 (1982).
13. Y.-P. Yang and A. L. Lapidus, Izv. Akad. Nauk SSSR, Ser. Khim., No. 2,363-365 (1977); Chem. Abstr., 86, 171868u (1977).
14. A. L. Lapidus and Y.-P. Yang, Izv. Akad. Nauk SSSR, Ser. Khim., No. 5,1180-1182 (1980); Chem. Abstr., 93, 72338j (1980).
15. H. Itatani and S. Danno, Jpn. Kokai Tokkyo Koho 79, 24, 827 (1979); Chem. Abstr., 91, 74204v (1979).
16. G. Stammann, R. Becker, J. Grolig, and H. Waldmann, U.S. Patent 4,370,275 (1983).
17. D. Cipris and I. L. Mador, U.S. Patent 4,131,521 (1978).
18. W. Gaenzler, K. Kabs, and G. Schroeder, U.S. Patent 4,113,762 (1978).
19. J. E. Hallgren, U.S. Patent 4,361,519 (1982).
20. E. Drent, European Patent 0,071,286 (1983).
21. F. Rivetti, U. Romano, and D. Delledonne, "Dimethyl Carbonate And Its Production Technology", Preprints of the Division of Environmental Chemistry, 332-335, the 208th ACS National Meeting, Washington, D.C., August 21-25, 1994.
22. F. Ancillotti and E. Pescarollo, European Patent 512,593 A1 (1992).
23. A. K. Bhattacharya and J. T. Nolan, U.S. Patent 4,636,576 (1987).
24. A. K. Bhattacharya, U.S. Patent 4,785,130 (1988).
25. A. K. Bhattacharya, U.S. Patent 4,879,266 (1989).
26. A. K. Bhattacharya, U.S. Patent 4,638,076 (1987).
27. A. K. Bhattacharya, U.S. Patent 4,761,467 (1988).
28. A. K. Bhattacharya and J. T. Nolan, European Patent 217,651 A2(1987).
29. A. K. Bhattacharya, U.S. Patent 5,001,252 (1991).
30. S. Yokota, H. Koyama, and H. Kojima, U.S. Patent 5,089,650 (1992).
31. European Patent 259,788 A2 (1988).
32. T. Matuzaki, T. Simamura, S. Fujitsu and Y. Toriyahara, U.S. Patent 5,214,184 (1993).
33. J. F. Knifton and R. G. Duranleau, J. Molecular Catal., 67, 389-399 (1991).
34. Y. Okada, T. Kondo, and S. Asaoka, "Dimethyl Carbonate for Fuel Additives", Fuel Chemistry Division, 359-364, the 207th ACS National Meeting, San Diego, CA, March 13-17, 1994.
35. G. E. Morris, International Patent WO84/02339 (June 21, 1984).

A NEW CATALYST FOR HIGHER ALCOHOL SYNTHESIS. J. Skrzypek, K. Krupa, M. Lachowska and H. Moroz, Institute of Chemical Engineering, Polish Academy of Sciences, Pl-44-100 Gliwice, ul. Baltycka 5, Poland.

Higher alcohols C_1-C_5 are of current interest as blending stocks for motor gasoline. Furthermore, they can be a real alternative for MTBE since they are entirely based on natural gas and are good octane boosters and combustion improves.

A catalyst containing CuO (50-60 wt.%), ZnO (25-30 wt.%), ZrO_2 (7-14 wt.%), Fe_2O_3 (1-4 wt.%), MoO_3 (7-15 wt.%), ThO_2 (1-3 wt.%), and Cs_2O (0.5-1.5 wt.%) has been developed. The catalyst was prepared by an original method of decomposition of organic complexes containing metallic components of catalyst, e.g., thermal decomposition of citrates. This catalyst yielded up to 150 $g/kg_{cat}h$ liquid product containing 30-40 wt.% of the most valuable alcohols C_{2+}.

The effect of temperature, pressure, contact time and synthesis gas composition were determined. The best results were obtained for temperature T = 630-650 K, pressure P = 10 MPa, GHSV = 6000-8000 hr^{-1} and H_2/CO = 1.0-1.3 [mol/mol].

COMMERCIAL-SCALE DEMONSTRATION OF A LIQUID-PHASE METHANOL PROCESS

Steven L. Cook
Eastman Chemical Company
Eastman Road
Kingsport, TN 37662

Keywords: Liquid-Phase-Methanol Process, Demonstration-Scale, Synthesis Gas

ABSTRACT

The Eastman Chemical Company operates a coal gasification complex in Kingsport, Tennessee. The primary output of this plant is carbonylation-derived acetic anhydride. The required methyl acetate is made from methanol and acetic acid. Methanol is currently produced from syngas by a gas-phase process, which must receive stoichiometric quantities of carbon monoxide and hydrogen to avoid overheating the catalyst. Control of this CO/H_2 ratio is accomplished with a shift reactor. A liquid-phase methanol process (LPMEOH™) has been developed by Air Products. Efficient heat removal permits the direct use of syngas without the need for the shift reactor. An Air Products/Eastman joint venture, with partial funding from the Department of Energy under the Clean Coal Technology Program, has been formed to build a demonstration-scale liquid-phase methanol plant. This talk will focus on the unique features of this plant and how it will be integrated into the existing facilities.

INTRODUCTION

Eastman Chemical Company has practiced the carbonylation of methyl acetate to acetic anhydride for many years.[1,2] In an array of integrated plants, coal is gasified and the resulting synthesis gas purified to a high degree. This gas, which consists chiefly of carbon monoxide and hydrogen, is used to feed the chemical plants. Methanol is produced in one plant by the Lurgi low-pressure gas-phase process. The methanol is combined with returned acetic acid to produce methyl acetate. Acetic anhydride is produced by the reaction of this methyl acetate with carbon monoxide.

The syngas needed for these plants is produced by two high-pressure gasifiers. High-sulfur coal is ground and fed to these gasifiers as a water slurry with pure oxygen. The hot gas is scrubbed with water to reduce the temperature and remove ash. A portion of the crude syngas is routed to a water-gas shift reactor to enrich the stream in hydrogen so that the stoichiometry required for methanol synthesis can be attained. Hydrogen sulfide is then scrubbed from the gas streams and converted to elemental sulfur. After final purification in a cryogenic "cold box" the syngas is pure enough to serve as feed to the methanol and acetic anhydride processes. Key changes to the gas stream as a result of these manipulations are illustrated in Figure 1.

DISCUSSION

In a methanol plant, the reaction between carbon monoxide, carbon dioxide, and hydrogen is exothermic and, because of the fixed bed reactor design, heat control and removal is of prime concern. If too much carbon dioxide or carbon monoxide is present, the reactor can overheat and damage the catalyst. Catalyst sensitivity to overheating is a chief reason that a more forgiving reaction system has been sought for syngas-based methanol production.

For a given catalyst, a liquid-phase reactor is preferable for numerous reasons. The basic characteristics of a liquid-phase reactor allow it to be cooled internally. This is a significant advantage for removing the rather large net heat of reaction encountered during methanol synthesis. By removing this heat with an internal heat exchanger, steam can be co-generated and employed for various process uses. In the liquid-phase reactor, an inert oil is used to slurry the methanol catalyst and to carry away the heat of reaction. Because of the efficient heat removal offered by the oil component, isothermal operation is possible, and per pass conversion is not as limited in comparison to a gas-phase reactor. While the latter reactor must rely upon dilution with recycle gas to control the reaction and carry away the heat, the inert oil in the liquid-phase reactor serves as a heat sink, thereby protecting the active sites of the catalyst from overheating. Added benefits resulting from this configuration are that the $H_2/CO/CO_2$ stoichiometry need not be controlled as closely (CO-rich mixtures are permissible) and carbon dioxide can be present in high concentrations. The net result of this last feature is that the expense and added complexity of a shift reactor can be eliminated because, in most cases, syngas can be used directly.

The liquid-phase methanol process (LPMEOH™)[3], developed by Air Products and Chemicals, Incorporated, offers a sound way to take advantage of the benefits of internal heat removal. As shown in Figure 2, this process allows purified but otherwise unaltered synthesis gas to be fed directly to the reactor. The copper/zinc oxide-based methanol catalyst is suspended in an inert oil, which serves as the heat transfer medium. Internal heat exchangers remove the heat generated by the highly exothermic reaction and provide process steam for appropriate uses. The gross effluent is separated from the oil in a cyclone separator and then cooled to condense traces of oil. The vapor

is then chilled to remove the methanol, and the off-gas is warmed and compressed for recycle or sent to downstream uses.

An Air Products/Eastman joint venture, with partial funding from the Department of Energy under the Clean Coal Technology Program, has been formed to build a demonstration-scale version of liquid-phase methanol plant. The gasification complex in Kingsport, Tennessee provides an ideal source of synthesis gas to test this plant. In addition to providing methanol for the carbonylation process, the demonstration unit will be tested under a large variety of operating conditions. This is possible because smooth operation of the integrated plants will not be completely dependent on the output of the liquid-phase methanol plant. It will therefore be possible to ramp the output up and down, co-produce dimethyl ether (DME), and produce fuel-grade methanol for testing in on- and off-site applications, such as power plant boilers, buses, and vans.

To illustrate how the new methanol process will affect the overall configuration of the coal gas facility, two schematic diagrams of the entire complex are provided below. The conventional, gas-phase methanol process is included in the first schematic (Figure 3), while changes resulting from incorporation of the liquid-phase process are summarized in Figure 4.

A brief description of the overall operation of this complex is offered: Coal is systematically unloaded from rail cars and continuously fed to grinding mills by a highly automated Coal Handling system. In the Coal Slurry section, coal is mixed with water during the grinding process to provide a mobile slurry that can be pumped to the gasifiers. Oxygen is provided by an Air Products separation plant. Use of pure oxygen allows the gasifiers to operate at over 1000°C, which eliminates the coproduction of environmentally undesirable byproducts. Within the Gasification Plant the coal slurry and oxygen combine in Texaco-designed gasifiers in a sustained reaction to produce a CO-rich product. The high-temperature exhaust is then quenched with water to cool the gas and remove ash particles. The crude gas is then passed through a water-gas shift reactor to increase the hydrogen content. Before exiting the gasification plant, the product gas is cooled by water-fed heat exchangers that produce low-pressure process steam for use elsewhere in the complex. Within the Gas Purification section hydrogen sulfide and carbon dioxide are removed by the Linde AG-developed Rectisol process. This is accomplished by selectively absorbing the gases in cold methanol. The hydrogen sulfide/carbon dioxide stream is sent to the Sulfur Recovery plant where a Claus unit, coupled with a Shell off-gas treating unit, converts it to elemental sulfur. This sulfur is clean enough to be sold as a pure byproduct. The final off-gas consists mainly of carbon dioxide, which is converted to the solid form for various commercial uses. As the syngas exits the purification section, a portion of it is passed to CO-Hydrogen Separation, essentially a cryogenic "cold box" (also developed by Linde) which permits separation of carbon monoxide and hydrogen by low-temperature distillation. The hydrogen from this unit is combined with CO/H_2 from the Gas Purification section to serve as feed for the Methanol Plant. The methanol product is fed to an Eastman-developed Methyl Acetate Plant, which uses a novel reactor-distillation column[4] to continuously convert methanol and acetic acid to methyl acetate in essential one piece of equipment. Carbon monoxide from the cryrogenic unit, along with methyl acetate, is sent to the Acetic Anhydride Plant, also developed by Eastman, where carbonylation produces acetic anhydride. If methanol is also fed to this plant, a portion of the acetic anhydride is converted to acetic acid and methyl acetate.

Although the changes appear minor from the level of detail provided in this diagram, many process details are simplified when the $CO/CO_2/H_2$ mix is not critical:

* Need for shift reactor eliminated

* Low sensitivity to flow variations

* Higher per-pass conversion requires less off-gas recycle

* Less waste CO_2 because more can be utilized in methanol production

* Less complex and expensive catalyst replacement requirements

A shift reactor is normally needed to increase the hydrogen/CO ratio of raw synthesis gas so that enough hydrogen is available to satisfy the required stoichiometry for conversion to methanol. If the methanol reactor could operate properly with syngas that is lean in hydrogen, this processing equipment could be eliminated. Moreover, processes downstream of the methanol plant that need CO containing little or no hydrogen, such as that required by the methyl acetate carbonylation process, would also benefit because the methanol plant serves to reduce the hydrogen content from the off-gas so that further processing is either not needed or requires smaller separation equipment. Because of the large heat sink provided by the internal heat exchanger of the LPMEOH™ process, excess CO/CO_2 does not damage the catalyst by inadvertent overheating.

Another way to damage the catalyst in a gas-phase reactor is by transient variations in the syngas flow rate. Here, excess reactant feed rates rather than stoichiometry are the concern. The result of

this condition is similar, however, in that the increased evolution of heat without an accompanying way to remove it can overheat the pellets.

Having an effective way to remove heat also permits the reactors to be operated at higher conversion rates. This benefits the space-time yield of the reactor and significantly reduces the off-gas recycle rate. It also serves to deplete the off-gas of hydrogen, which, as described above, is beneficial to downstream processes needing CO that is low in hydrogen content.

It is well known that the presence of CO_2 is essential to optimal operation of copper/zinc oxide-based methanol reactors. It is critical for conditioning and preventing damage to the catalyst.[5] Isotopic labeling studies have shown[6] that essentially all methanol is produced from the reaction of CO_2 with hydrogen. An internal water-gas shift reaction between the resulting water with CO generates more CO_2 for methanol production. The proposed mechanism is provided below for convenience:

$$CO_2 \rightleftharpoons CO_{2,ads}$$
$$H_2 \rightleftharpoons 2\,H_{ads}$$
$$CO_{2\,ads} + H_{ads} \rightleftharpoons HCOO_{ads}$$
$$HCOO_{ads} + 3\,H_{ads} \rightleftharpoons CH_3OH + O_{ads}$$
$$CO + O_{ads} \rightleftharpoons CO_2$$
$$H_2 + O_{ads} \rightleftharpoons H_2O$$

Again, because of the heat management capabilities of the LPMEOH™ process, the amount of carbon dioxide normally present in raw syngas can be used without concern for overheating the catalyst. This results in a much more efficient use of carbon in the syngas. Indeed, a substantial amount of waste carbon dioxide is generated by the water-gas shift reactor needed for gas balance in the gas-phase methanol process.

One final benefit of the LPMEOH™ process is that catalyst replacement is less complex and can be done on an on-going basis. Even though the catalyst in a gas-phase methanol reactor can typically operate for about two years before replacement is needed, the actual mechanics of replacement are a challenge. The catalyst itself is difficult to handle in the large quantities involved, and the reactor must be shut down, isolated and opened up to carry out the task. This can result in significant downtime resulting in inconvenience at the least to lost product sales as a major negative consequence. In the case of the liquid-phase process, the catalyst can be intermittently replaced as needed in substantially smaller amounts. Some of the benefits described above have also been discussed in a recent review.[7]

CONCLUSION

The construction and successful operation of the LPMEOH™ plant will be a landmark in development of synthesis gas technology. Given the importance of methanol not only as a chemical feedstock but as a fuel, demonstration of this technology on a commercial scale could have far-reaching importance. We at Eastman are pleased to be a part of this effort.

ACKNOWLEDGMENTS

Eastman Chemical Company gratefully acknowledges Air Products and Chemicals, Incorporated and the Department of Energy for their technological and financial support.

REFERENCES CITED

(1) V. H. Agreda, *Chemtech*, 18, 250 (1988).

(2) S. L. Cook, *Acetic Acid and Its Derivatives* (V. H. Agreda and J. R. Zoeller, ed.), Marcel Dekker, Inc. New York, 1993, Chapter 9.

(3) W. R. Brown, "Flexible Electric Power Generation, The Integrated Gasification/Liquid Phase Methanol (LPMEOH™) Demonstration Project", Third Annual Clean Coal Technology Converence, Chicago, IL, September 6-8, 1994.

(4) V. H. Agreda and R. L. Partin, U.S. Patent 4,435,595, 1984.

(5) S. Lee, B. G. Lee, and V. R. Perameswaran, Fundamentals of Methanol Synthesis, Electric Power Research Institute, Proceedings, Thirteenth Annual EPRI Contractor's Conference on Clean Liquid and Solid Fuels, Palo Alto, January 1989.

(6) G. C. Chinchen, K, Mansfield, and M. S. Spencer, *Chemtech*, 20, 692 (1990).

(7) A. Cybulski, *Catal. Rev.- Sci. Eng.*, 36, 557 (1994).

Figure 1.

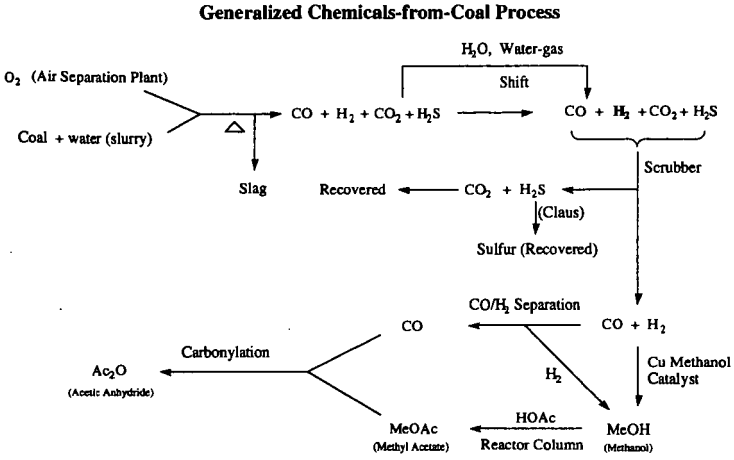

Figure 2. Air Products LPMEOH™ Process.

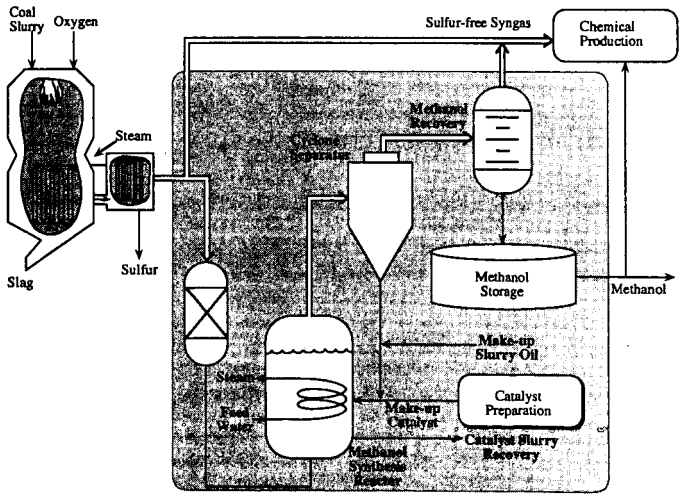

Figure 3: Configuration of Coal-Gasification/Acetic Anhydride Plant with Gas-Phase Methanol

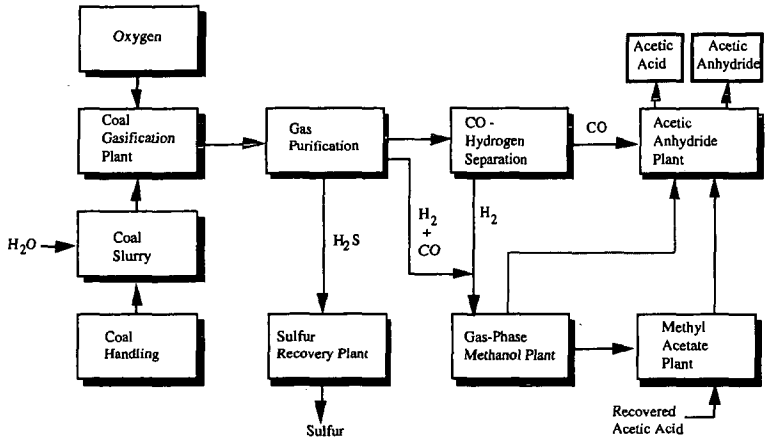

Figure 4: Configuration of Coal-Gasification/Acetic Anhydride Plant with Liquid-Phase Methanol

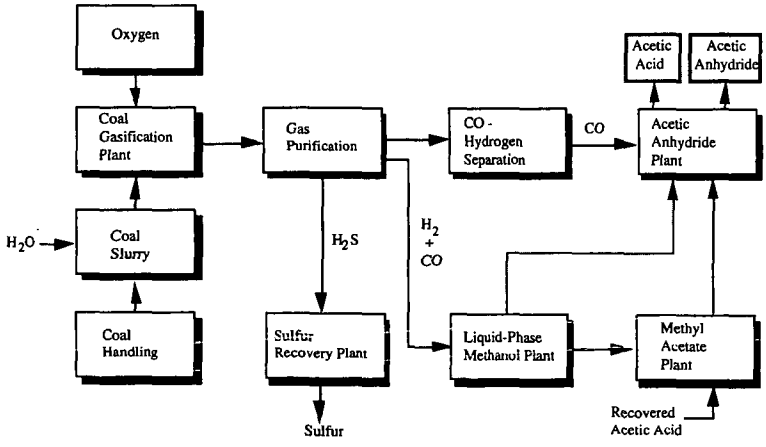

Kinetics and Dynamics of Heterogeneous Hydroformylation Rh Catalyst

Mark A. Brundage, Steven S. C. Chuang , and Michael W. Balakos
Department of Chemical Engineering,
The University of Akron,
Akron, OH 44325-3906, U.S.A.

Keywords: CO insertion, Oxygenates, Reaction pathway, Langmuir-Hinshelwood Kinetics.

Heterogeneous $CO/H_2/C_2H_4$ reaction of 4 wt% Rh/SiO_2 catalyst was studied using steady-state pulse transient method coupled with *in situ* infrared spectroscopy. The dynamic responses measured at various partial pressures of reactants show that the $CO/H_2/C_2H_4$ reaction can accurately be described by a Langmuir-Hinshelwood-Hougen-Watson (LHHW) model with the hydrogenation of adsorbed C_2H_5CO as the rate-determining step for propionaldehyde formation and the hydrogenation of adsorbed C_2H_5 as the rate-determining step for ethane formation. The kinetic model also accurately describes the adsorption isotherm of acyl intermediates measured by the pulse isotopic transient and adsorption isotherm of CO measured by IR spectroscopy. This study also demonstrates that the measurement of coverage of adsorbates by isotopic tracer pulsing and *in situ* infrared spectroscopy provides direct experimental evidence to confirm a postulated mechanism and rate law.

INTRODUCTION

The determination of reliable rate expressions is paramount in the design and modeling of heterogeneously catalyzed processes. Langmuir-Hinshelwood-Hougen-Watson (LHHW) kinetics of heterogeneous catalytic reactions has been studied for many years (1-7). However, the formalism has been the subject of much discussion and criticism. Most of the criticisms in the LHHW formalism are results of the inability to measure the coverage of adsorbates and reaction intermediates as a function of partial pressure of reactants and to identify the rate-determining step during the reaction (8,9). The objectives of this paper are to combine isotopic transient and *in situ* IR methods to study heterogeneous $CO/H_2/C_2H_4$ reaction and to test a LHHW model that can describe the overall kinetics for its ability to describe the adsorption isotherms of surface intermediates. Kinetic equations were derived from LHHW formalism with the postulation of a rate-determining step for both propionaldehyde and ethane formation. *In situ* IR coupled with transient isotopic tracing was used to observe the coverage of adsorbed species during the reaction and compared to the coverage predicted by the LHHW model.

EXPERIMENTAL

A 4 wt% Rh/SiO_2 catalyst was prepared from $RhCl_3 \cdot 3H_2O$ solution by the incipient wetness impregnation method. After impregnation, the catalyst was dried overnight in air at 300 K and then reduced in flowing hydrogen at 673 K for 16 hr. The exposed metal atoms was determined to be 122 μmol/g by H_2 pulse chemisorption at 303 K assuming an adsorption stoichiometry of $H_{ads}/Rh = 1$.

The apparatus used in this study is similar to that previously reported (10). Four independent quantities, including the rates of propionaldehyde and ethane formation and the surface converges of adsorbed CO and adsorbed acyl species, were measured as a function of partial pressure of reactants during steady-state condition. The coverage of intermediates during ethylene hydroformylation was determined from the dynamic response of $C_2H_5{}^{13}CHO$ to a ^{13}CO pulse input. The coverage of adsorbed CO was measured by *in situ* IR spectroscopy.

RESULTS

Steady-State Measurements

The steady-state rate of formation of ethane and propionaldehyde during heterogeneous hydroformylation ($CO/H_2/C_2H_4$ reaction) on 4 wt% Rh/SiO_2 was measured by a gas chromatograph at 0.1 MPa. The main products in the reaction are ethane and propionaldehyde. Other minor hydrocarbon products include methane, propylene, butene, and butane. To determine the dependence of the reaction rates on the partial pressures of reactants, the rates were measured as the partial pressures of reactant at a total pressure of 0.1 MPa and 513 K. The flow rate of He was varied to maintain a constant total flowrate of 120 cm^3/min. Both ethane and propionaldehyde formation rates are negative order in CO partial pressure while positive order in both hydrogen and ethylene.

The *in situ* IR spectra during the experiments of varying partial pressures are shown in Figure 1. The top spectra in Figure 1 show the variation of the spectra with CO partial pressure. The spectra at partial pressure of 0.083 MPa exhibit a linear CO band at 2037 cm^{-1}; a small bridged CO band at 1885 cm^{-1}; propionaldehyde band at 1740 cm^{-1}; and gaseous ethylene and ethane bands between 1900 and 3300 cm^{-1} (11,12). The intensity and the wavenumber of adsorbed CO show stronger dependence on P_{CO} then P_{H_2} and $P_{C_2H_4}$.

Dynamic Measurements

The transient response of $C_2H_5{}^{13}CHO$ and the IR spectra to 10 cm^3 pulse of ^{13}CO into the ^{12}CO feed to the reactor was recorded during the steady-state experimental runs. Figure 2 is the transient response of Ar, ^{13}CO, and C_2H_5CHO measured by mass spectrometry under the conditions of 0.1 MPa, 513 K and $CO/H_2/C_2H_4/He = 1/1/1/1$.

Infrared spectra taken during the pulse of ^{13}CO in the CO feed show that the gas phase CO and adsorbed CO exchange with their isotopic counterparts at a rate much faster than the scanning rate of the IR. No other feature in the IR spectra changed during the course of the experiment, including those attributed to gaseous ethylene.

From the transient response, the average residence time of ^{13}CO adsorbed on the catalyst surface can be obtained by (10,13)

$$\tau_{^{13}CO} = \int_0^\infty tE_{^{13}CO}(t)dt \qquad (1)$$

Since the gaseous CO and adsorbed CO exchange rapidly, the gaseous ^{13}CO response measured by mass spectrometry can be used as the response for the adsorbed ^{13}CO. The average residence time of all intermediate species leading to the formation of ^{13}C propionaldehyde from adsorbed ^{13}CO can be expressed as

$$\tau_{C_2H_5{}^{13}CHO} = \int_0^\infty tE_{C_2H_5{}^{13}CHO}(t)dt - \tau_{^{13}CO} \qquad (2)$$

Figure 3 shows the deuterated propionaldehydes response to a 10 cm^3 pulse of D_2 into the H_2 flow during steady-state ethylene hydroformylation (14). The lag of the deuterated propionaldehydes response with respect to that of D_2 indicates that the hydrogenation of acyl intermediates is a rate-determining step.

DISCUSSION

The mechanism for the formation of propionaldehyde from $CO/H_2/C_2H_4$ reaction has been postulated from analogy with the homogeneous hydroformylation reaction (12,15). The general accepted mechanism of the reaction is shown in Table 1 (12). The approach for kinetic analysis of a heterogeneous catalytic reaction involves the postulation of a rate-determining step and express the rate in terms of the concentrations of the reaction intermediates in that step. The concentrations of the intermediates must then be related to the gas phase concentration of the reactants and products (adsorption isotherms). The simplest theoretical expression for an adsorption isotherm is the Langmuir isotherm, on which the LHHW formalism is based.

Different rate-determining steps, RDS, yield different forms of the rate equations so that they can be distinguished from each other. The best fit of the data is when step 6 in Table 1 is considered as the RDS for propionaldehyde formation. Step 6 as the RDS is supported by D_2 pulse studies as shown in Figure 3. The relation between $TOF_{C_2H_5CHO}$, $TOF_{C_2H_6}$, $\theta_{*C_2H_5CO}$, and θ_{*CO}, and partial pressure of the reactants can be derived from LHHW formalism with step 6 as RDS, as shown below.

$$\theta_{*C_2H_5CO} = \frac{\sqrt{K_1}K_2K_3K_4K_5P_{CO}\sqrt{P_{H_2}}P_{C_2H_4}}{1 + K_2P_{CO} + \sqrt{K_1P_{H_2}} + K_3P_{C_2H_4}} \qquad (3)$$

$$\theta_{*CO} = \frac{K_2P_{CO}}{1 + K_2P_{CO} + \sqrt{K_1P_{H_2}} + K_3P_{C_2H_4}} \qquad (4)$$

$$TOF_{C_2H_5CHO} = \frac{k_6K_1K_2K_3K_4K_5P_{CO}P_{H_2}P_{C_2H_4}}{(1 + K_2P_{CO} + \sqrt{K_1P_{H_2}} + K_3P_{C_2H_4})^2} \qquad (5)$$

$$TOF_{C_2H_6} = \frac{k_7K_1K_3K_4P_{H_2}P_{C_2H_4}}{(1 + K_2P_{CO} + \sqrt{K_1P_{H_2}} + K_3P_{C_2H_4})^2} \qquad (6)$$

The above rate law and isotherm equations derived from LHHW were found to accurately describe the rate and isotherm data.

CONCLUSION

Four independent quantities, $TOF_{C_2H_5CHO}$, $TOF_{C_2H_6}$, $\theta_{*C_2H_5CO}$, and θ_{*CO} were measure as a function of partial pressure of reactants during steady-state ethylene hydroformylation over Rh/SiO_2. The results of this study demonstrate that the coverage of acyl intermediate determined from the dynamic response of an isotopic tracer is quantitatively consistent with that calculated from LHHW formalism; the coverage of *CO measured from IR spectroscopy is qualitatively consistent with that obtained from LHHW formalism. This study also shows that the measurement of coverage of adsorbates by both transient and IR techniques provides essential information to verify a proposed mechanism and kinetic model.

REFERENCES

1. Hougen, O., and Watson, K., *Ind. Eng. Chem.*, **35**, 529 (1943).
2. Tempkin, M., *Adv. Catal.*, **28**, 173 (1979).
3. Smith, J., *Ind. Eng. Chem. Fundam.*, **21**, 327 (1982).
4. Bourdart, M., and Djeda-Mariadassou, G., *Kinetics of Heterogeneous Catalytic Reactions*, Princeton University Press, Princeton, N.J., 1984.
5. Weller, S., *Catal. Rev. Sci. Eng.*, **34**(3), 227 (1992).
6. Hougen, O., and Watson, K., *Chemical Process Principles Part III-Kinetics and Catalysis*, John Wiley & Sons, New York, 1947.
7. Hill, C., Jr., *An Introduction to Chemical Engineering Kinetics and Reactor Design*, John Wiley & Sons, New York, 1977.
8. Kiperman, S., *Chem. Eng. Comm.*, **100**, 3 (1991).

9. Weller, S., *Adv. Chem Ser.*, **148**, 26 (1975).
10. Srinivas, G., Chuang, S., and Balakos, M., *AIChE J.* 39 530 (1993).
11. Balakos, M., Chunag S., in press *J. Catal.* (1995).
12. Chuang, S., and Pien, S., *J. Catal.* **135**, 618 (1992).
13. Fogler, H., *Elements of Chemical Reaction Engineering, 2 ed.*, Prentice Hall, Englewood Cliffs, 1992.
14. Brundage, M., M.S. Thesis, The University of Akron (1994).
15. Chuang, S., Tian, Y., Goodwin, J., and Wender, I., *J. Catal.* **96**, 449 (1985).

Table 1. The Proposed Mechanism for Heterogeneous Hydroformylation of Rh/SiO_2.

(Step 1)	$H_{2(g)} + 2^*$	$\overset{K_1}{\rightleftharpoons}$ 2^*H
(Step 2)	$CO_{(g)} + ^*$	$\overset{K_2}{\rightleftharpoons}$ $^*CO$
(Step 3)	$C_2H_{4(g)} + ^*$	$\overset{K_3}{\rightleftharpoons}$ $^*C_2H_4$
(Step 4)	$^*C_2H_4 + ^*H$	$\overset{K_4}{\rightleftharpoons}$ $^*C_2H_5 + ^*$
(Step 5)	$^*C_2H_5 + ^*CO$	$\overset{K_5}{\rightleftharpoons}$ $^*C_2H_5CO + ^*$
(Step 6)	$^*C_2H_5CO + ^*H$	$\xrightarrow{k_6}$ $^*C_2H_5CHO + ^*$
(Step 7)	$^*C_2H_5 + ^*H$	$\xrightarrow{k_7}$ $C_2H_{6(g)} + 2^*$
(Step 8)	$^*C_2H_5CHO$	$\xrightarrow{k_8}$ $C_2H_5CHO_{(g)} + ^*$

K_i is the equilibrium adsorption parameter, i=1,2, . . .
k_{+i} is the forward rate constant; k_{-i} is the backward rate constant.

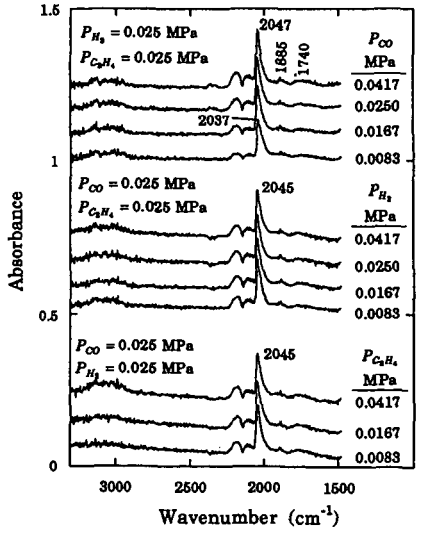

Figure 1. *In Situ* IR spectra of heterogeneous ethylene hydroformylation on 4 wt% Rh/SiO_2 at 513 K and 0.1 MPa at varying partial pressures of reactants.

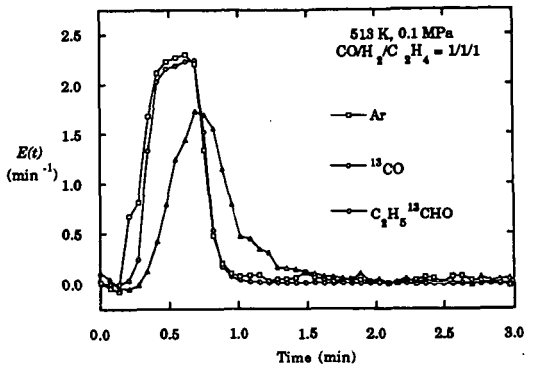

Figure 2. The Transient response of Ar, ^{13}CO, and $C_2H_5{}^{13}CHO$ to a 1 cm^3 pulse of ^{13}CO in a ^{12}CO flow during ethylene hydroformylation on 4 wt% Rh/SiO_2 at 513 K and 0.1 MPa.

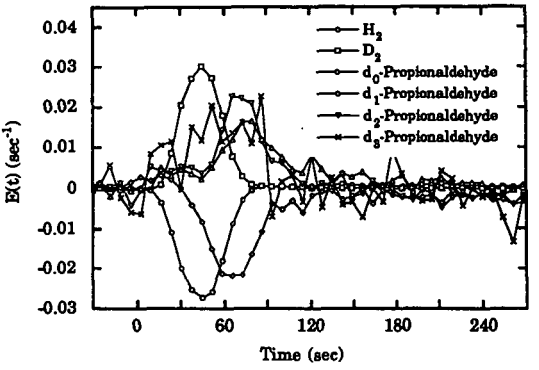

Figure 3. Transient Response of Deuterated Propionaldehydes to a 10 cm^3 pulse of D_2 into a H_2 flow during ethylene hydroformylation on 4 wt% Rh/SiO_2 at 513 K and 0.1 MPa.

DETAILED MECHANISTIC OF THE SYNTHESIS OF OXYGENATES FROM CO/H_2

Alessandra Beretta, Enrico Tronconi, Luca Lietti, Pio Forzatti, Italo Pasquon
Dipartimento "G. Natta", Politecnico, 20133 Milano-Italy

KEYWORDS: HAS, Reaction Network, Mechanistic Model

INTRODUCTION

The traditional interest for the synthesis of higher oxygenates from CO and H_2 mixtures has been recently focused on the accomplishment of high selectivities towards α-branched alcohols, such as 2-methyl-propanol and 2-methyl-butanol, which can be exploited as precursors for the synthesis of ethers (MTBE, TAME) with high octane properties [1]. Indeed isobutanol is the most abundant product of Higher Alcohol Synthesis (HAS); however, more than 100 other compounds are formed by hydrogenation of CO [2], among which commercially undesired oxygenates are also included. HAS product distribution is strongly affected by the operating conditions under which the reaction is carried out: contact time, temperature, feed composition control, infact, the yield and selectivity of the different classes of species produced. The development of an industrial process for the synthesis of branched alcohols calls for a rational optimization of the operating conditions, which may be accomplished only by means of a reliable kinetic treatment of the reacting system. Detailed kinetic models of HAS have been proposed for both the low-temperature [3] and the high-temperature [4] modified methanol catalysts; however, so far no kinetic analysis has been published which can predict the whole distribution of HAS products as a function of all the operating variables.

In the following we present the development of a mechanistic kinetic model of HAS over Cs-promoted Zn/Cr/O catalysts aimed to design purposes; the model translates the bulk of indipendent observations concerning the mechanism and the thermodynamic constraints involved in the chain-groth process.

HAS REACTION NETWORK

An extensive study was performed in the past on the evolution and reactivity of the surface intermediates involved in HAS, consisting in steady-state microreactor experiments, Temperature Programmed Desorption (TPD) and Surface Reaction (TPSR) of a wide variety of oxigenated C_1-C_5 probe molecules [5, 6]; three major chemical routes were thus identified as responsible of the chain growth process:

1) the ***aldol-type condensation*** beween carbonylic species, giving rise to the formation of branched higher aldehydes or ketones according to a "normal" or "oxygen-retention reversal" (ORR) evolution of the surface intermediate [7];

2) the so-called ***α-addition*** of a C_1 nucleophilic specie to higher aldehydes;

3) the ***ketonization reaction***, responsible of the formation of ketones *via* decarboxylative condensation of two aldehydes.

Toghether with a first C_1->C_2 step, such reactions can explain the whole variety of observed under synthesis conditions.

While the chain growth proceeds in a kinetic regime, other reactions also involved in HAS have been proved to be governed by chemical equilibrium. They include: the methanol synthesis, the hydrogenation of aldehydes and ketones to primary and secondary alcohols respectively, the ketonization reactions, the water gas shift reaction and the synthesis of methyl-esters [8].

DEVELOPMENT OF A MECHANISTIC KINETIC MODEL OF HAS

The reaction network above presented has been validated on a quantitative basis by the formulation of a kinetic analysis [4] able to reproduce HAS product distribution for specified values of the operating conditions. Such original treatment has been recently modified and adapted to optimization purposes, that is to obtain a comphehensive and predictive desciption of the reacting system as function of the major operating variables. The development of the final

kinetic model can schematized as follows in three subsequent steps:

1) ***Identification of the reacting species***. Based on the experimental evidences, classes of reactants have been defined for each reaction included in the kinetic scheme. Namely, for the case of aldol condensations a nucleophilic behavior has been attributed to all the carbonylic species with no α-branching, while an electophilic behavior has been attributed to the C_1-C_6 aldehydes, both linear and branched. The nature of formaldehyde has been assumed for the C_1 intermediate involved in α-additions, which have been considered to interest the whole class of aldehydes as possible electrophilic reactants. Finally, for each ketone a contribute of formation via ketonization has been included.

2) ***Chemical lumping***. Reaction rates and specie reactivities have been diversified along the line of the experimental observations. In the case of aldol condensations an intrinsic kinetic constant (function of reaction temperature, only) has been defined, but a set of further relative rate constants has been introduced in order to characterize the possible chain growth pathway (Normal or ORR), the nature of the nucleophilic reactant (aldehyde or ketone), the structure of the electrophilic agent (linear or branched). Similar diversification has been applied to the cases of α-additions and ketonizations.

3) ***Formulation of model equations***. Mass balances have been written for all the reacting species; the rate expressions were based on a Langmuir-Hinshelwood mechanism taking into account the competitive adsorption of water on the catalyst active sites. Assumed an isothermal PRF model for the synthesis reactor, the model resulted in 42 differential mass balances for carbonyl species, 42 algebraic equations accounting for the hydrogenation equilibria between carbonyl species and corresponding alcohols, the balances for CO, H_2, H_2O, CO_2.

RESULTS

The model parameters were estimated from multiresponse non linear regression on 11 kinetic runs performed over a Cs-doped Zn/Cr/O catalysts. The comparison between experimental and calculated effects of H_2/CO feed ratio, CO_2 feed content and reaction pressure are reported in Fig. 1-3 (symbols = experimental data, lines = model calculations).

* ***Effect of H_2/CO feed ratio.*** As shown in Fig. 1a methanol concentration is maximum when a stoichiometric mixture of H_2 and CO is fed. The model reproduces correctly the experimental data, due to the assumption of chemical equilibrium for methanol synthesis. Higher alcohol concentrations present smooth maximum-wise trends with growing values of H_2/CO feed ratio in the range 0.5-1.5; the model predicts with accuracy that the highest productivities can be obtained for H_2/CO values close to 1. and 0.5, in the cases of primary alcohols (Fig. 1a-b) and ketones (Fig. 1c) respectively. Both experimental data and model calculations indicate that at high values of hydrogen partial pressures, a significant drop in the formation of the C_{2+} oxygenates occur.

* ***Effect of CO2 feed content.*** The presence of CO_2 in the feed stream causes an overall decreasing of higher alcohols production (Fig. 2a-c). Such effect is however mostly emphazized in the case of the oxygenates with terminal behavior (isobutanol), while modest in the case of the intermediates species (ethanol): thus, the product distribution changes, with increasing fraction of CO_2, in the direction of a growing molar ratio between low and high molecular weight components. These features are well reproduced by the kinetic treatment that can explain the inhibiting effect of CO_2 on HAS by accounting for the competitive adsorption of water on the catalyst active sites; notably, water concentration increases significantly with growing CO_2 partial pressure due the thermodynamic equilibrium which governs the water gas shift reaction.

* ***Effect of reaction pressure.*** A slight promotion of HAS is obtained by increasing the reaction pressure in the range 85-100 atm (Fig. 3a-c). Experimental and calculated results show, however, that such promotion is accompanied by a significant loss in the relative selectivity higher alcohol/methanol; methanol formation is, infact, strongly enhanced at high pressures. The model fitting apprears satisfactory. We note that the adoption of of a first order depence with respect to CO partial pressure for the kinetics of the C_1->C_2 reaction has been decisive for a proper simulation of the pressure effect; this results on the contrary overestimated when the formation of the first C-C bond is described by second order kinetics, in analogy with the chain-growth reactions (e. g. aldol condensations).

The match between experimental data and model previsions is extremely satisfactory and suggests an overall adequacy of the kinetic model (reaction mechanism, kinetic expressions, diversification of the reactivities). However, we have verified to a more stringent level the chemical costistency of our treatment by adopting of a perturbative approach: we have infact applied the model to the simulation of chemical enrichment experiments. The comparison between calculated and experimental effect of adding an oxigenate (ethanol, propanol, 2-butanone) to the feed stream turned out to be highly informative on the accuracy with which reaction mechanism and the relative reactivities of the intermediates are decribed.

* ***Addition of ethanol.*** In this case a global promotion of HAS is experimentally observed. If compared to reference conditions where only syngas if fed to the reactor, the products mixture obtained with an ethanol-containing feed stream presents higher amounts of linear and branched primary alcohols, as well as of ketones (Fig. 4-a). This is in line with the well known high reactivity of the C_2 intermediate. Simulating the addition of ethanol, also the calculated product mixture distribution changes towards an increased amount of all the major classes of products (Fig. 4-b); such result proves that the model is able to reproduce correctly the key role of the intermediate specie and the network of chemical patterns which spread from it involving the whole reacting system. It is on the other hand evident that the model tends to overestimate the promotion of ketones formation, which has been related to an overestimation of the role of ketonization reactions in the kinetic scheme. We note, however, that ketones are only secondary products of HAS, their outlet concentration being usually one order of magnitude lower than the concentration of primary alcohols.

CONCLUSIONS

A mechanistic kinetic model of HAS over Cs-promoted Zn/Cr/O catalysts has been developed, the final aim being its application to process design purposes. The model adequacy has been tested by comparison with a set of kinetic data obtained under typical synthesis conditions and with the results of chemical enrichment experiments; the former are specifically demanding for a quantitative adequacy of the kinetic scheme, the latter are instead more informative on the accuracy with which the details of the reaction mechanism are taken into account. A satisfactory description of the reacting system has been obtained over a wide operational field; in line with the experimental results, the model calculations suggest that an equimolar H_2/CO feed ratio and absence of CO_2 in the feed stream are optimal conditions for the synthesis of branched oxygenates. Increments of the total pressure are then estimated to lead to a lowering of the relative higher alcohol/methanol selectivity.

ACKNOWLEDGEMENT

This research was supported by SNAMPROGETTI SpA.

REFERENCES

1. Zou, P., Summary of the HAS workshop, U.S. Dept. of Energy, Febr. 1994.
2. Forzatti, P., Tronconi, E., and Pasquon, I., *Catal. Rev. - Sci. Eng.* **33**, 109-168 (1991).
3. Smith, K. J., Young, C. W., Hermann, R. G., and Klier, K., *Ind. Eng. Chem. Res.*, **29**, 61 (1991)
4. Tronconi, E., Lietti, L., Gropi, G., Forzatti, P., and Pasquon, I., ***J. Catal.*** **135**, 99-114 (1992).
5. Lietti, L., Forzatti, P., Tronconi, E., and Pasquon, I., *J. Catal.* **126**, 401-420 (1990).
6. Lietti, L., Tronconi, E., and Forzatti, P., *J. Catal.* **135**, 400-419 (1992).
7. Nunan, J., Bogdan, C. E., Klier, K., Smith, K. J., Young, C. W., and Hermann, R. G., *J. Catal.* **116**, 195-221 (1989).

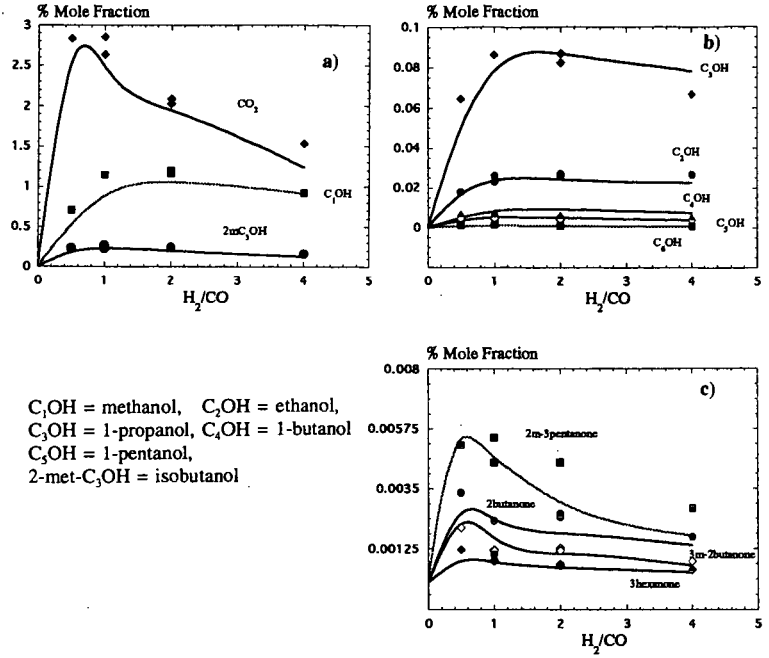

C_1OH = methanol, C_2OH = ethanol,
C_3OH = 1-propanol, C_4OH = 1-butanol
C_5OH = 1-pentanol,
2-met-C_3OH = isobutanol

Fig 1. Calculated (lines) and experimental (symbols) effect of H_2/CO feed ratio on HAS product distribution. T = 405°C, P = 85 atm, CO_2 = 0 %, GHSV = 8000 h^{-1}.

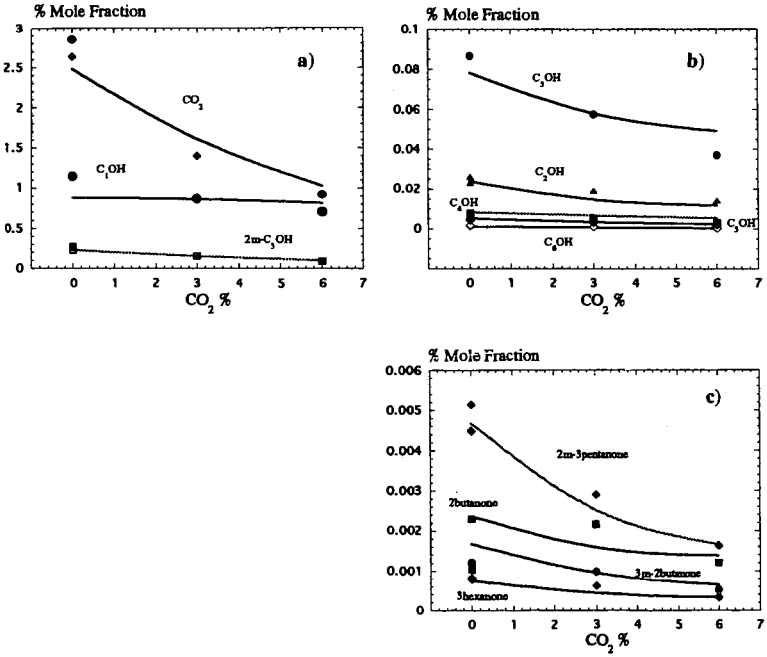

Fig. 2. Experimental and calculated effect of CO_2 feed content. T = 405°C, P = 85 atm, H_2/CO = 1, GHSV = 8000 h^{-1}.

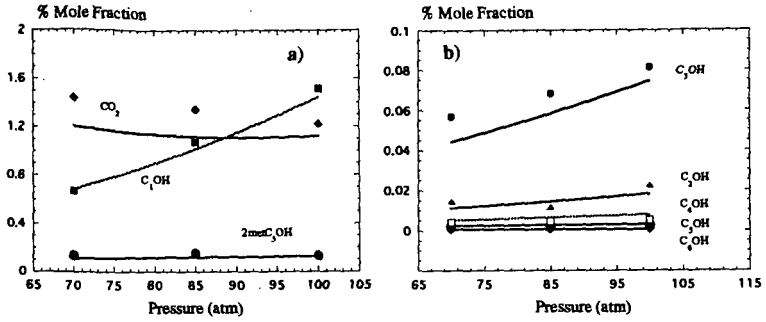

Fig. 3. Comparison between experimental and calculated effect of reaction pressure. T=405°C, $H_2/CO=1$, $CO_2=0\%$, GHSV = 8000 * P/85 h^{-1}

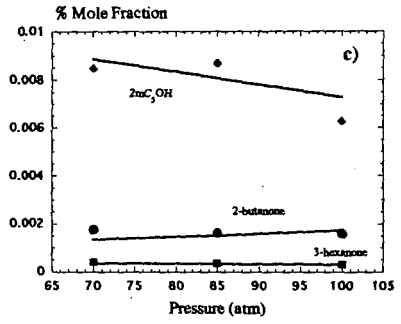

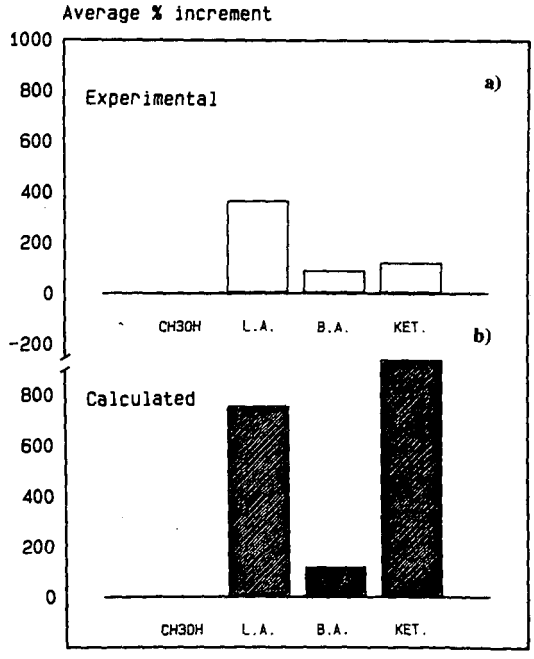

Fig. 4. Experimental versus calculated effect of ethanol addition on grouped HAS product distribution. T = 405°C, P = 85 atm, H_2/CO = 1, ethanol = 2 %, CO_2 = 0 %, GHSV = 8000 h^{-1}. The effect is expressed as average percentage increment of the molar fraction with respect to absence of ethanol in the feed stream for L.A.=linear alcohols (ethanol excluded), B.A.=branched alcohols, KET.=ketones.

MECHANISTIC STUDIES OF THE PATHWAYS LEADING TO ETHERS *via* COUPLING OF ALCOHOLS

Qun Sun, Luca Lietti, Richard G. Herman, and Kamil Klier
Zettlemoyer Center for Surface Studies and Department of Chemistry
7 Asa Drive, Lehigh University, Bethlehem, PA 18015, U.S.A.

Keywords: Alcohols, Ethers, Resin and HZSM-5 Catalysts, S_N2 reactions

ABSTRACT

The reaction mechanisms for the solid acid-catalyzed dehydrative coupling of methanol and ethanol with isobutanol and 2-pentanol to form ethers were examined by using isotope labelling and chiral inversion experiments. When the reactions were carried out at 110°C and 1 MPa with ^{18}O-ethanol and ^{16}O-isobutanol over the Amberlyst-35 resin catalyst, 95% of the major product ethyl isobutyl ether (EIBE) contained ^{16}O, while 96% of the minor product ethyl tertiarybutyl ether (ETBE) contained ^{18}O. Similar results were obtained with methanol and isobutanol over Nafion-H and Amberlyst-35 catalysts, with methyl isobutyl ether (MIBE) and methyl tertiarybutyl ether (MTBE) as the products. These results indicate that EIBE (MIBE) was produced by a surface-catalyzed S_N2 reaction, while the ETBE (MTBE) product arose *via* a carbenium intermediate. The analogous reaction carried out over Nafion-H and HZSM-5 catalysts with chiral 2-pentanol verified the surface-mediated S_N2 reaction, wherein chiral inversion of the product ether was observed relative to the S- and R-2-pentanol reactants. In addition, a remarkable shape selectivity with chiral inversion was observed over the HZSM-5 zeolite to selectively form 2-ethoxypentane but not 3-ethoxypentane.

INTRODUCTION

The dehydrative coupling of alcohols to form ethers is practiced on an industrial scale for symmetric ethers with small alkyl groups. In solution phase with an acid catalyst such as H_2SO_4, it is generally believed that the synthesis of ethers from secondary and tertiary alcohols follow the S_N1 pattern, while synthesis from primary alcohols follow the S_N2 pathway [1]. Mechanistic studies of alcohol dehydration ove solid oxide acid catalysts to form olefins and ethers *via* a consecutive-parallel pathway was reported by Knozinger et al. [2]. A series of studies on butanol dehydration over the HZSM-5 catalyst was performed by Makarova et al. [3,4], and ether formation was proposed to proceed *via* a surface-O-C_4H_9 intermediate.

Recently, we have explored some possible new routes for synthesizing high value oxygenates, e.g. fuel-grade C_5 to C_6 ethers such as MIBE, MTBE, EIBE, ETBE, ethyl isopropylether (EIPE) and diisopropylether (DIPE), from non-petroleum feed stocks [5-7] owing to the potential use of these ethers as effective anti-knock replacements for leaded gasoline. The $CH_3{}^{18}OH$/isobutanol coupling reaction over the Nafion-H catalyst was studied, and a S_N2 reaction mechanism was suggested for the production of MIBE [6]. The present work extends the mechanistic study to other alcohol reactants, e.g. ethanol, isopropanol, and chiral 2-pentanol, as well as other solid acid catalysts, i.e. Amberlyst-35 and HZSM-5, and provided additional more generalized mechanistic features of the solid acid-catalyzed ether formation from the corresponding alcohols, ROH + R'OH –> ROR' + H_2O. Experiments were carried out using reactant mixtures in which one of the alcohols (i) was isotopically labelled with ^{18}O or (ii) contained a chiral center.

EXPERIMENTAL

The solid acid catalysts employed in the present study were the commercial Nafion-H with 0.9 meq H^+/g, Amberlyst-35 from Rohm and Haas with 5.2 meq H^+/g, and HZSM-5 from Mobil Corporation with a Si/Al ratio of 32/1. The ^{18}O-MeOH and ^{18}O-EtOH reagents with greater than 97% ^{18}O content were purchased from MSD Isotopes. The S-2-pentanol and R-2-pentanol were purchased from Aldrich Chemicals. The experiments were carried out at 90-110°C and 1 MPa total pressure in a gas phase downflow stainless steel tubular reactor with on-line GC analysis of reactants and products to determine alcohol conversion and product selectivities. Typically, the reactant feed contained 3.6 ml/hr liquid alcohol mixture, 88 ml/min He and 12 ml/min N_2, where the reactant conversion was limited to less than 5%. The liquid products were trapped in a glass cold trap cooled with liquid nitrogen and examined for the source of the ether oxygen by GC/MS and for chirality by a Chirasil-CD column of fused silica column coated with beta-cyclodextrin. The reference compound R-2-ethoxypentane was prepared by using the Williamson synthesis method starting with R-2-pentanol and sodium metal. For comparison, the chiral experiment was also carried out in liquid phase at 100°C and ambient pressure for 1 hr with concentrated H_2SO_4 as the catalyst and the molar ratio of ethanol/2-pentanol/H_2SO_4 = 4.0/1.0/0.4.

RESULTS

Isotope Labelling Studies of Ether Formation Over Amberlyst-35 Catalyst. The reactants in four experiments where the incorporation of the labelled oxygen into the ether products was monitored were the following:

1. $CH_3{}^{18}OH + (CH_3)_2CHCH_2{}^{16}OH$
2. $CH_3CH_2{}^{18}OH + (CH_3)_2CHCH_2{}^{16}OH$
3. $CH_3{}^{18}OH + CH_3CH_2{}^{16}OH$
4. $CH_3CH_2{}^{18}OH + (CH_3)_2CH{}^{16}OH$.

The labelling results involving isobutanol as a reactant over the Amberlyst-35 catalyst, shown in Tables 1 and 2, were similar to those for the coupling of $CH_3{}^{18}OH$/isobutanol over the Nafion-H catalyst where the reactions were carried out at 90°C and ambient pressure [6]. In particular, DME (Table 1) and DEE (Table 2) contained almost only ^{18}O, indicating that no oxygen scrambling occurred with the acid catalyst, while MIBE and EIBE retained the ^{16}O of the isobutanol. MIBE and EIBE appear to be formed by the isobutanol attacking the acid-activated methanol and ethanol, respectively, while the methanol and ethanol attacking the isobutanol might be steric hindered. MTBE and ETBE contained ^{18}O, suggesting that these ethers were formed by the coupling of isobutene and the corresponding light alcohols. The isotope distributions in the products are not sensitive to the reaction conditions, e.g. temperature, pressure and relative concentration of the reactant alcohols, nor to the particular resin catalyst employed.

In contrast, the $CH_3{}^{18}OH/CH_3CH_2{}^{16}OH$ experiment showed that there was no steric (or other) preference in the coupling reaction over Amberlyst-35, and ^{16}O and ^{18}O were found with equal abundance in methyl ethylether (MEE) (Table 3). Again, the isotopic composition of DME and DEE demonstrated that no oxygen scrambling occurred.

In the experiment with ^{18}O-ethanol and ^{16}O-isopropanol (a secondary alcohol), with a 1.0/1.5 molar ratio respectively, the observed products were DIPE, propene, EIPE and DEE, given in order of decreasing selectivity. The isotopic distributions shown in Table 4 clearly showed that the mixed ether EIPE was formed *via* a mechanism wherein the ^{18}O from the ethanol was retained, while the ^{16}O of the reactant isopropanol molecule was predominantly lost, i.e.

$$C_2H_5{}^{18}OH + CH_3\underset{\displaystyle{}^{16}OH}{\underset{|}{C}}HCH_3 \rightarrow CH_3\underset{\displaystyle{}^{18}OH}{\underset{|}{C}}HCH_3 \bullet H_2{}^{16}O.$$

These mechanistic studies utilizing $CH_3{}^{18}OH$ and $CH_3CH_2{}^{18}OH$ to couple with higher alcohols over the resin catalysts, Nafion-H and Amberlyst-35, indicated that ether synthesis proceeds mainly *via* a S_N2 reaction pathway to form methyl and ethyl ethers.

Ether Formation From Ethanol and Chiral 2-Pentanols. The definitive proof of a S_N2 reaction mechanism is the observation of the configuration inversion of the product with respect to the reactant. The experiments were carried out with S- or R-2-pentanol and $CH_3CH_2{}^{18}OH$ over the Nafion-H and HZSM-5 catalysts under the reaction conditions similar to those utilized in the previously described isotope labelling experiments.

The dehydrative coupling of ^{18}O-ethanol and S-2-pentanol produced self-coupling products DEE and di-2-amylether (D2AE), cross-coupling products 2-ethoxypentane (2-EP) and 3-ethoxypentane (3-EP), and the dehydration product 2-pentene but not ethene. The ^{18}O content and chirality of the cross-coupling products are presented in Table 5. For the acid-catalyzed cross-coupling of EtOH and 2-pentanol, the product 2-ethoxypentane can, in principle, be formed either by EtOH attacking the activated 2-pentanol or vice versa. The experiment with $Et{}^{18}OH$ was designed to determine the contributions from these two distinct routes. Data in Table 5 demonstrated that the EtOH attack of the acid activated 2-pentanol was the predominant pathway where ^{18}O was retained in the product ether. The true configuration inversion for the ether formation due to EtOH attack of the activated 2-pentanol is given in the last column of Table 5.

The combined ^{18}O retention and the R-/S- chirality results demonstrate that the axial rear-attack S_N2 mechanism dominates (97% over HZSM-5 and 77% over Nafion-H) in this heterogeneous acid-catalyzed dehydrative coupling of alcohols. It is probably due to the steric hindrance that HZSM-5 produced remarkably higher configuration inversion than either the Nafion-H and the H_2SO_4. The Nafion-H resin catalyst behaved like an acid solution, possibly due to its flexible backbone of the acid groups. The OH group of 2-pentanol is the preferred leaving group, after being activated by the surface H^+ and subjected to the concerted nucleophilic attack by the light alcohol.

The minor paths (23% over Nafion-H and 3% over HZSM-5) can be accounted for by a less efficient carbenium ion (C^+) or olefin ($C^=$) intermediate mechanism. These minor paths are corroborated by observations of the 3-ethoxypentane product, which could only be formed *via* carbenium ion or olefinic intermediates, over Nafion-H. However, 3-ethoxypentane was not observed as a product with the HZSM-5 catalyst, indicating that the formation of 3-ethoxypentane could be further minimized by shape selectivity in the zeolite pore. The 3-ethoxypentane is more branched and is expected to pass through the HZSM-5 channel (0.55 nm) [8] at a slower rate than 2-ethoxypentane, even if it were formed by the carbenium ion or the olefin reactions at channel intersections.

CONCLUSIONS

The solid acid, Nafion-H, Amberlyst-35 and HZSM-5 zeolite, catalyzed direct coupling of alcohols to form ethers proceeds primarily through a surface-mediated S_N2 reaction pathway that is far more efficient than either a carbenium or olefin pathway. The surface-S_N2 reaction gives rise to high selectivity to configurationally inverted chiral ethers when chiral alcohols were used. This is especially observed in the case of the HZSM-5 catalyst, in which the minor C^+ or $C^=$ paths were further suppressed by "bottling" of 3-ethoxypentane by the narrow zeolite channels.

Acknowledgements

We thank the U.S. Department of Energy for financial support of this research, Rohm and Haas for providing the Amberlyst-35 catalyst, and Mobil Corporation for providing the ZSM-5 sample. Thanks to Professor J. Benbow for helpful suggestions on analysis of chiral products.

References

1 Morrison, R.T., and Boyd, R.N., *Organic Chemistry*; Chapter 17, Allyn and Bacon, Inc., Boston, (1972).
2 Knozinger, H., and Kohne, R., *J. Catal.*, **5**, 264 (1966).
3 Makarova, M.A., Williams, C., Thomas; J.M., and Zamaraev, K.I., *Catal. Lett.*, **4**, 261 (1990).
4 Makarova, M.A., Paukshtis, E.A., Thomas, J.M., Williams, C., and Zamaraev, K.I., *J. Catal.*, **149**, 36 (1994).
5 Nunan, J., Klier, K., and Herman, R.G., *J. Chem. Soc., Chem. Commun.*, 676 (1985).
6 Herman, R.G., Klier, K., Feeley, O.C., and Johansson, M.A., *Preprints, Div. Fuel Chem., ACS*, **39(2)**, 343 (1994).
7 Herman, R.G., Klier, K., Feeley, O.C., Johansson, M.A., Sun, Q., and Lietti, L., *Preprints, Div. Fuel Chem., ACS*, **39(4)**, 1141 (1994).
8 Olson, D.H., Kokotailo, G.T., Lawton, S.L., and Meier, W.M.,*J. Phys. Chem.*, **85** 2243 (1981).

Table 1. Percent isotopic composition (±2%) of O-containing products from the reaction of $CH_3{}^{18}OH/{}^{16}O$-isobutanol over Amberlyst-35 catalyst at 110°C and 1 MPa.

Isotope	MIBE	MTBE	DME
^{18}O	2	93	94
^{16}O	98	7	6

Table 2. Percent isotopic composition (±2%) of O-containing products from the reaction of $CH_3CH_2{}^{18}OH/{}^{16}O$-isobutanol over Amberlyst-35 catalyst at 110°C and 1 MPa.

Isotope	EIBE	ETBE	DEE
^{18}O	<5	96	>93
^{16}O	>95	4	<7

Table 3. Percent isotopic composition (±2%) of O-containing products from the reaction of $CH_3{}^{18}OH/CH_3CH_2{}^{16}OH$ over Amberlyst-35 catalyst at 110°C and 1 MPa.

Isotope	DME	DEE	MEE
^{18}O	<98	<2	50
^{16}O	>2	>98	50

Table 4. Percent isotopic composition (±2%) of O-containing products from the reaction of $CH_3CH_2{}^{18}OH/{}^{16}O$-isopropanol over Amberlyst-35 catalyst at 90°C and 1 MPa.

Isotope	EIBE	ETBE	DEE
^{18}O	89	<2	>98
^{16}O	11	>98	<2

Table 5. Product selectivities (±2%) (taking into account 2- and 3-ethoxypentane only) from the reaction of $Et^{18}OH$ and S-2-pentanol over Nafion-H and HZSM-5 catalysts at 100°C and 1 MPa, and in concentrated H_2SO_4 solution at 100°C and ambient pressure, where the true inversion = %X/(X+Y-Z).

Acid Catalyst	Product selectivity (%) S-2-EP	R-2-EP	3-EP	Ratio for R-2-EP/S-2-EP (X/Y)	$^{16}O/(^{16}O+^{18}O)$ % in 2-EP (Z)	Inversion (%)
HZSM-5	14.0	86.0	0.0	86/14	11.0	97
Nafion-H	32.9	60.9	6.2	65/35	16.0	77
H_2SO_4	33.6	64.0	2.4	66/34	18.0	80

HIGHER ALCOHOL SYNTHESIS OVER A Cs-Cu/ZnO/Cr_2O_3 CATALYST: EFFECT OF THE REACTION TEMPERATURE ON PRODUCT DISTRIBUTION AND CATALYST STABILITY

Alessandra Beretta, Qun Sun, Richard G. Herman, and Kamil Klier
Zettlemoyer Center for Surface Studies and Department of Chemistry
7 Asa Drive, LEHIGH UNIVERSITY, Bethlehem, PA 18015

Keywords: catalyst, higher alcohols, synthesis gas, stability

ABSTRACT

The influence of reaction temperature on methanol and higher alcohol syntesis has been investigated in the range of 310-340°C. Optimal conditions for selective production of 2-methyl primary alcohols was identified with T = 340°C and synthesis gas H_2/CO = 0.75. Deactivation features were observed after 300 hr on stream, but no significant growth of Cu crystals or reduction in surface area was observed for the catalyst after testing.

INTRODUCTION

The Cu/ZnO/M_2O_3 systems (M = trivalent metal) are well-known catalysts for methanol and higher alcohol synthesis (HAS) [1-4]; their performances are reported in the literature with particular attention being paid to the optimization of both the catalyst composition (amount of alkaline dopant, metal ion ratios) and the operating conditions [2-5]. The application of these catalysts is commonly limited to reaction temperatures not exceeding 310-325°C in order to avoid sintering phenomena that are recognized as the major constraint and drawback of all the copper-containing catalysts. At these temperatures, methanol formation is highly favored, and only by carrying out the reaction at low H_2/CO ratios can significant quantities of C_2^+ oxygenates be obtained. No specific studies have so far addressed the thermal stability of Cu/ZnO-based systems at high temperatures. However, the strong demand for selective production of branched higher oxygenates supports more extensive exploration of the range of allowable reaction temperatures that can be utilized with copper-based catalysts. Indeed, an increment in the temperature is expected to result in the desired promotion of higher alcohol production and a concurrent decrease in methanol formation. In the following, a study of the effect of reaction temperature on HAS over a Cs-doped Cu/ZnO/Cr_2O_3 catalyst is presented, and the principal interests are the changes in the product distribution and the catalyst thermal stability.

EXPERIMENTAL

Catalyst Preparation. The methodology has been been described by Nunan et al. [3,6], which consists of the precipitation of a hydrotalcite-like precursor $Cu_{2.4}Zn_{3.6}Cr_2(OH)_{16}CO_3 \cdot 4H_2O$ [7], followed by stepwise calcination to 350°C to give the mixture of oxides, $CuO/ZnO/Cr_2O_3$. Cesium doping was achieved by adding the catalyst to a N_2-purged aqueous solution of CsOOCH, which was then slowly evaporated to dryness under flowing N_2. The amount of dopant (3 mol%) was chosen on the basis of previous studies of the optimal catalyst composition with respect to higher alcohol synthesis [3]. The catalyst was finally reduced with a 2 mol% H_2/N_2 mixture at 250°C.

Activity Tests. The apparatus has been extensively described elsewhere [8]. It is noted that charcoal and molecular sieve traps, an internally copper-lined stainless-steel reactor, as well as a copper thermocouple-well were used during the catalytic testing to prevent the formation and deposition of iron-carbonyls, which are well-known deactivating agents [9,10]. The catalysts were tested under steady state conditions at 7.6 MPa with synthesis gas of various H_2/CO compositions flowing with a gas hourly space velocity of 5300 ℓ/kg cat/hr. The reaction temperature was varied between 310 and 340°C.

The exit product mixture was sampled every 30-60 min using an in-line, automated, heated sampling valve and analyzed in a Hewlett-Packard 5390 gas chromatograph. The products were analyzed *via* a Poraplot-Q capillary column alternatively connected to a flame

ionization detector and to a thermal-conductivity detector (TCD) and a Molsieve capillary column connected to TCD. The sensitivity factors of the instrument were determined on the basis of calibrated mixtures. The gas-phase on-line analyses were coupled with the analysis of liquid samples collected downstream from the reactor (atmospheric pressure) by liquid nitrogen cooled traps. The identification of the products (more than 50 components) was obtained by comparison of their retention times with those of known standards and from analysis of the liquid samples by a HP GC/MS instrument. All of the experimental data were obtained in a steady-state regime that was reached about 6-8 hr after setting the operating conditions.

Catalyst Characterization. BET measurements and XRD analyses were performed at each stage of the catalyst preparation and after testing to determine the catalyst surface area and crystalline phases, respectively.

RESULTS

Effect of the Reaction Temperature on the Product Distribution. In Fig. 1, the productivities of the most abundant oxygenated products are reported as a function of the reaction temperature, which was increased from 310°C up to 340°C over a period of about 160 hr. As the temperature was increased, a decrease of methanol productivity was observed, in line with the thermodynamic constraints that govern methanol synthesis. As shown in Fig. 1(a), the productivities of all the linear higher alcohols exhibited decreasing trends with increasing reaction temperature. In fact, the product mixture tends to become depleted in intermediate species (ethanol, propanol) and more enriched in the branched oxygenates that play a terminal role in the chain-growth process. At 325°C, a promotion of all the 2-methyl alcohols was observed (Fig. 1-b). It is noted that the molar ratio between methanol and the totality of α-branched alcohols passed from a value of about 16 at 310°C to the value of about 5 at 340°C. In the case of secondary alcohols (whose productivities are summed in Fig. 1-c with those of the corresponding ketones), it is observed that high temperatures favor the formation of high molecular weight species (e.g. 2-methyl-3-pentanol) at the expense of the intermediate species (e.g. 2-butanol).

The formation of methane and C_2^+ hydrocarbons was also observed to increase with increasing reaction temperature (Fig. 2). The overall production of hydrocarbons, equal to 15.7 g/kg cat/hr at 310 °C, grew to the value of 39.4 g/kg cat/hr at 340°C. It is worth noticing that, contrary to the case of oxygenates, hydrocarbons appear to keep an almost constant relative product distribution, which could support the hypothesis of a formation pattern independent from the higher alcohol chain-growth process.

Finally, it is noted that the productivities of all the methyl-esters detected in the product mixture decreased monotonically with increasing reaction temperature. This trend was especially evident in the case of methyl-formate and methyl-acetate, while it was less pronounced for the higher homologs (methyl-propionate, methyl-isobutyrate, methyl-butyrate).

High Reaction Temperature: Effect of H_2/CO Ratio. At the reaction temperature of 340°C, kinetic runs were performed to investigate the combined effects of high temperature and H_2/CO feed ratio on HAS product distribution. The results are reported in Fig. 3, and the data show that an excess of H_2 exclusively promoted methanol formation. The production of higher oxygenates appears to be significantly inhibited at high H_2/CO ratios. Specifically, all of the primary alcohols tended to show a maximum in productivity, with the highest value being associated with the H_2/CO value of 0.75 (Fig. 3 a-b).

With respect to the formation of hydrocarbons, the data reported in Fig. 4 indicate that while the synthesis of C_2+ hydrocarbons is strongly slowed down by decreasing CO partial pressure, methane productivity was approximately constant as a function of the H_2/CO ratio.

High Reaction Temperature: Catalyst Stability. The operating conditions of T = 340°C, H_2/CO = 0.45, 7.6 MPa, and GHSV = 5300 ℓ/kg cat/hr were periodically reproduced in order to check the stability of the catalyst. The results of the experiments are

reported in Fig. 5, where the averaged FID signals, in arbitrary units, for the most abundant products have been plotted *vs* the time of testing. As previously noted, a period of about 160 hr occurred before reaching the final temperature of 340°C, and at this high temperature a stable catalytic activity was observed during 125 hr. Subsequently, a slow loss of selectivity of the higher oxygenates in favor of an increment in methanol productivity was detected. Similar results were obtained in the past when studying deactivation caused by the deposition of iron-carbonyls onto Cu/ZnO catalysts [9]. Even though the cause of the origin of the behavior shown in Fig. 5 cannot be assessed, Cu sintering can be excluded as playing a major role, where the XRD pattern of the tested catalyst (300 hr on stream at 340°C) revealed the presence of metallic copper with crystallite size in the range of 100Å, which is comparable with the dimension of Cu crystallites observed in in the binary Cu/ZnO systems after the reduction stage and before testing [9]. Moreover, BET measures showed that no reduction in the catalyst surface area occurred during the kinetic runs, being 85 m^2/g and 89 m^2/g the surface area values before and after testing, respectively.

CONCLUSIONS

The presented experimental results suggest that:

(1) the productivity of α-branched species benefits significantly from an increment of the reaction temperature to 325°C. For further increments of temperature, the productivities of higher alcohols are almost constant but the methanol/higher alcohols molar ratio increases progressively.

(2) at high temperature, the H_2/CO feed ratio of 0.75 is optimal with respect to higher oxygenate formation. Under such conditions, an equal amount of methanol but *twice* the amount of branched higher alcohols can be obtained, compared to the optimal low temperature conditions (T = 310°C, H_2/CO = 0.45).

(3) no significant Cu sintering or surface area reduction occurred upon testing at the reaction temperature of 340°C; but iron-carbonyl formation and deactivation of the catalysts under high temperature conditions needs to be studied further.

ACKNOWLEDGMENT

This research was partially supported by the U.S. Department of Energy-Pittsburgh Energy Technology Center (contracts DE-AC22-90PC90044 and -90PC90018) and by a Fullbright Scholarship (A.B.).

REFERENCES

1. Natta, G., Colombo, U., and Pasquon, in "*Catalysis*," Vol. 5, Chap. 3, ed. by P. H. Emmett, Reinhold (1957).
2. Smith, K. J. and Anderson, R. B., *J. Catal.*, 85, 428 (1984).
3. Nunan, J. G., Herman, R. G., and Klier, K., *J. Catal.* 116, 222 (1989).
4. Herman, R. G., in "*New Trends in CO Activation*," ed. by L. Guczi, Elsevier, Amsterdam, 265 (1991).
5. Boz, I., Sahibzada, M., and Metcalfe, I., *Ind. Eng. Chem. Res.* 33, 2021 (1994).
6. Nunan, J. G., Himelfarb, P. B., Herman, R. G., Klier, K., Bogdan, C. E., and Simmons, G. W., Inorg. Chem., 28, 3868 (1989).
7. Busetto, C., Del Piero, G., Manara, G., Trifiro, F., and Vaccari, A., *J. Catal.*, 85, 260 (1984).
8. Nunan, J. G., Bogdan, C. E., Klier, K., Smith, K. J., Young, C.-W., and Herman, R. G., *J. Catal.* 116, 195 (1989).
9. Bogdan, C. E., Nunan, J. G., Santiesteban, J. G., Herman, R. G., and Klier, K., in "*Catalysis-1987*," ed. by J. W. Ward, Elsevier, Amsterdam, 745 (1988).
10. Hindermann, J. P., Hutchings, G. J., and Kiennemann, A., *Catal. Rev.-Sci. Eng.*, 35, 1 (1993).

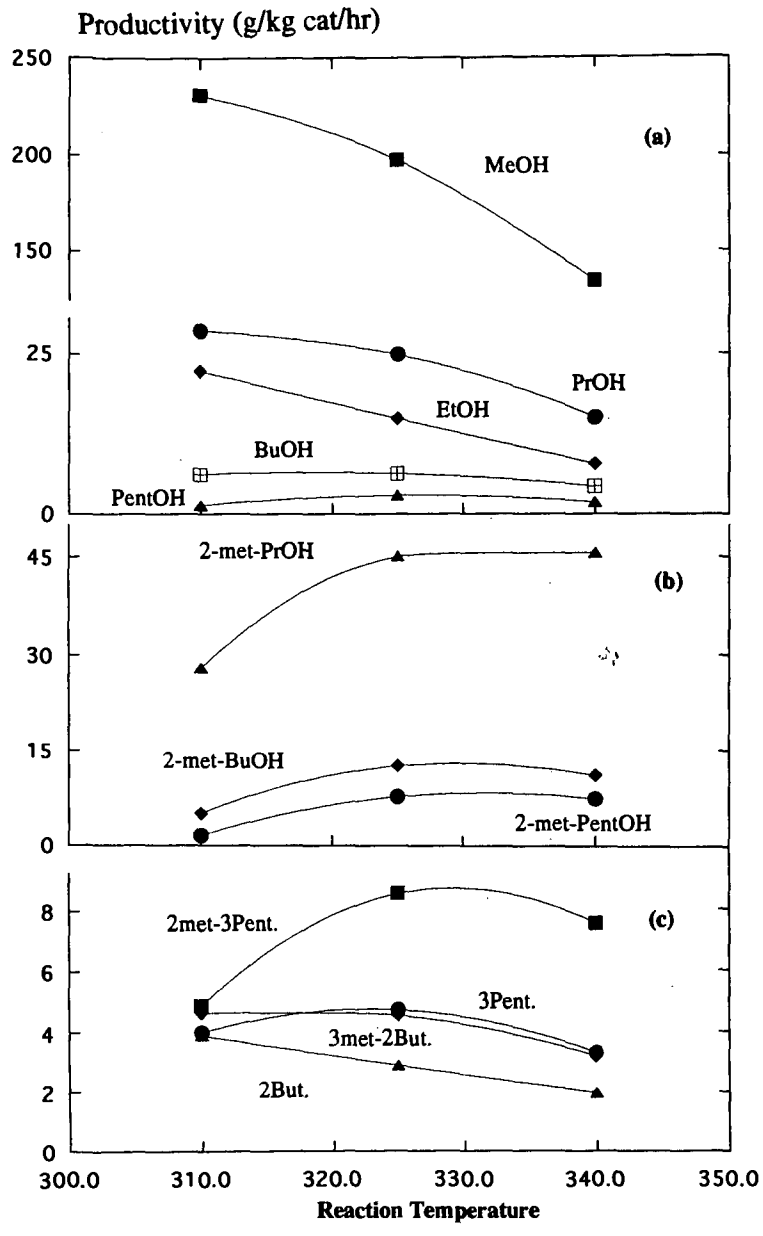

Fig. 1. Experimental effect of reaction temperature on methanol and higher oxygenates productivities. In 1-c: 2met-3Pent = 2methyl-3-pentanol + 2-methyl-3-pentanone, 3-Pent. = 3-pentanol + 3-pentanone, 3met-2But. = 3-methyl-2-butanol + 3-methyl-2-butanone, 2-But. = 2-butanol + 2-butanone.
Operating conditions: H_2/CO=0.45, P=7.6 MPa, GHSV=5300 l/kg cat/hr.

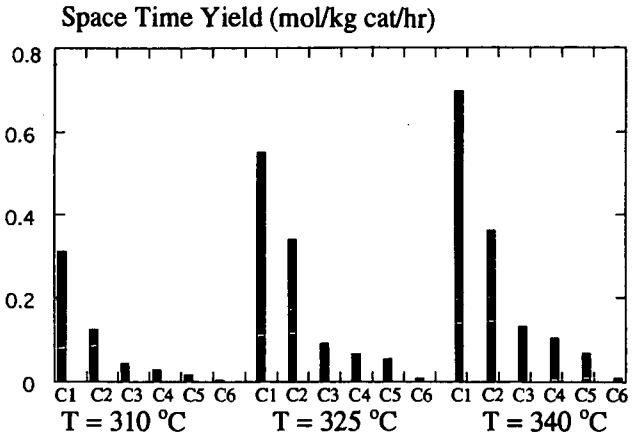

Fig. 2. Effect of temperature on C_1-C_6 hydrocarbon production and distribution.

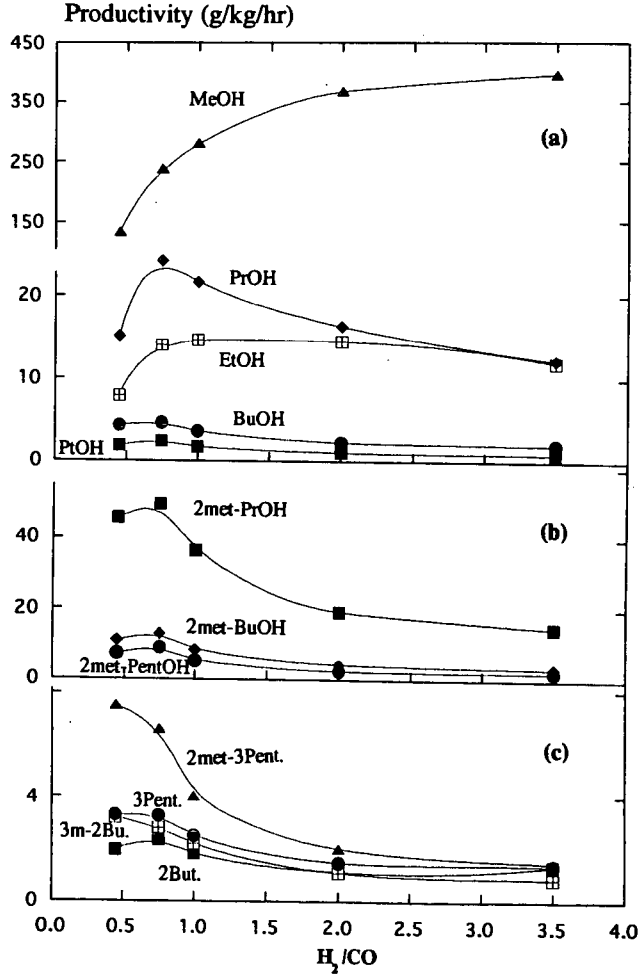

Fig. 3. Effect of H_2/CO ratio; T = 340°C, P = 7.6 MPa, GHSV = 5300 l/kg cat/hr.

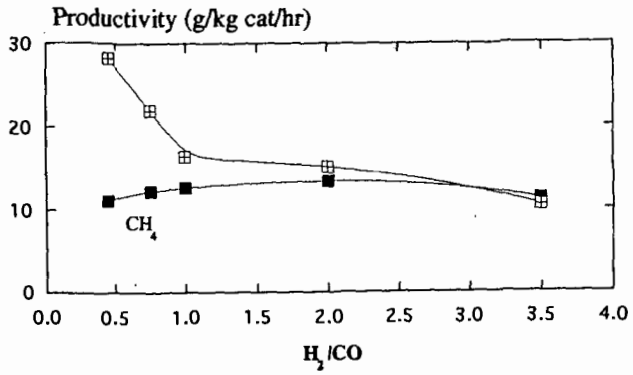

Fig. 4. Effect of H_2/CO ratio hydrocarbon formation. Conditions as in Fig. 3.

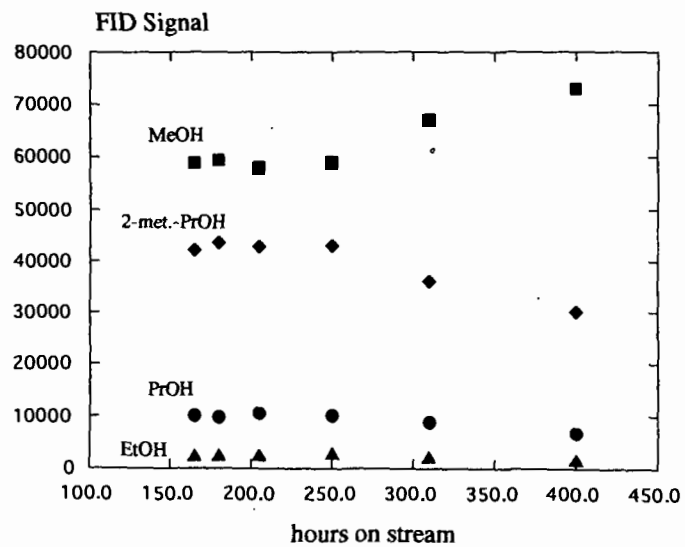

Fig. 5. Change of product distribution with time as detected by FID.

SYNTHESIS OF ALCOHOLS FROM SYNGAS AND ALCOHOL CHAIN GROWTH OVER COPPER-COBALT BASED CATALYSTS

Wei CHU*, Guoxing XIONG
State Key Laboratory of Catalysis, Dalian Institut of Chemical Physics,
Academia Sinica, P.O. Box 110, Dalian 116023, China

ABSTRACT: The alcohols synthesis were studied over copper-cobalt catalysts from syngas under pressure (6.0 MPa). The higher alcohols formation was enhanced with the cobalt content, caused probably by an increase of the number of Co-Cu bisites, and the higher hydrocarbons augmented simultaneously, explained by common reactional intermediates. The cobalt quantity on the surface influences the chain growth evolving into alcohols or hydrocarbons. It was shown that an augmentation of CO insertion and a modification of the hydrogenation property of system could be responsible of these effects, as supported by the tests of reactivities and those of probe molecules. It was illustrated that some strong interactions existed between cobalt and copper, and the influences of different pretreatments were also investigated.

1. INTRODUCTION

The syngas conversion remains one of the most interesting reactions in heterogeneous catalysis. Especially since the two energy crisis in the world, the more effective utilisations of syngas have attracted much attention [1,2]. With different catalysts and operational conditions, it could be oriented into methanolation, methanation, olefin production via Fischer-Tropsch reactions, synthesis of ethanol or acetyl aldehyde over Rhodium catalysts, or synthesis of mixed alcohols, etc. In that mixed alcohols production, the main problems were carbon chain growth, high alcohol activity and good selectivity. Several catalytic systems have been proposed [2], the copper-cobalt catalysts seem to be the most promising [1-3].

In this work, the influences of cobalt additives onto copper based catalysts were investigated, as well as the effects of pretreatments and those of supports, the temperature programmed reduction (TPR) and CO chemisorption were performed for the catalyst characterizations, the results of probe molecule tests were also discussed.

2. EXPERIMENTAL

2.1. Catalyst preparation: the supports were prepared by the coprecipitation method[4], referred as CuLaZr(i). The catalysts were prepared by impregnating the support with an aqueous solution of $Co(NO_3)_2\ 6H_2O$ to a desired content. The impregnates were dried at 70oC in a flux of argon, and calcined at 350°C in a flux of argon or in air for 5h. They are referred as x%Co/CuLaZr(i).

2.2. Syngas reactions: hydrogenation of CO was carried out in a continuous flow reactor consisting of a 6 mm ID stainless steel tube containing 0.5 g of catalyst under the reaction conditions: P = 6.0 MPa, T = 250-280°C, H_2/CO = 2, D = 4 l/h/g. The reaction products were analysed by gas chromatography.

2.3. Probe molecule tests: the samples (0.5g) were reduced in hydrogen over night, then brought into contact with synthesis gas (P = 0.1 MPa, T = 225°C). After reaching a stationary state, a small amount (2 mol%) of probe molecules (C_2H_4) were sent into the CO/H_2 stream and the generated gases were analysed by gas chromatography with flame ionization detector [5,6].

3. RESULTS AND DISCUSSION

3.1. Influence of cobalt additive

The alcohols synthesis were studied over cobalt modified copper catalysts, six samples with different cobalt content were prepared and investigated. For the monometallic copper sample CuLaZr(1), it has almost no chain growth, the higher alcohol fraction was only 0.2%. With the cobalt addition, the higher alcohols ($C_{2+}OH$) formation was enhanced, and it increases with the rise of cobalt content, as does the yield into higher hydrocarbons ($C_{2+}HC$) and that of total hydrocarbons. The simultaneous augmentation of $C_{2+}OH$ and $C_{2+}HC$ (Fig.1a) was explained as that there were common intermediates for their formation [7,8].

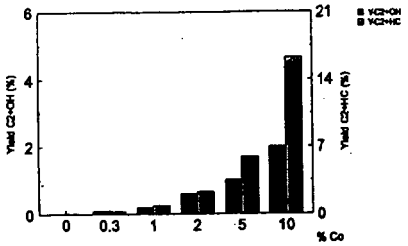

Fig.1a. Yields in C2+OH and in C2+HC
— Influence of cobalt content

As suggested, during the growth of hydrocarbonated chain, there is a competition between the CH_2* addition (formed on cobalt) which leads to the hydrocarbons formation, and the insertion of oxygenated species (formyl or CO, formed on copper) which results in alcohols. Thus the cobalt quantity on the surface influences the chain growth evolving into the alcohols or the hydrocarbons.

In the case of the production into higher alcohols $C_{2+}OH$ and their fraction in total alcohols, both increase with the rise of the cobalt content (Fig.1b).

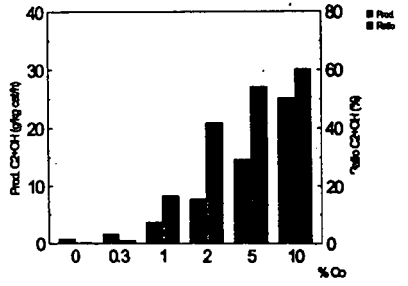

Fig. 1b. Higher alcohols productivity and ratio in total alcohols
— Influence of cobalt content

3.2. Effect of pretreatment

A pretreatment of the precursor after impregnation may be favorable to the decomposition of $Co(NO_3)_2$ and the formation of Co_3O_4, which results in a modification of the reducibility of the catalyst and eventuelly the formation of mixed oxides. We have compared the pretreatments operating at the temperatures between 350°C and 700°C, in an inert flux (argon) or in air environment (21% O_2).

As illustrated in Fig.2, the catalytic activity decreases while the calcination temperature rises, and the best results of the alcohol production and the higher alcohol ratio ($C_{2+}OH$/ROH) have been obtained by calcinating at 350°C. When calcinated in air rather than in argon, the catalytic system orient the reactions much more selectively to the alcohols, and the alcohols productivity is also better for the previous system (calcinated in air). So the pretreatment at 350°C in air has been used for the continuation of the work.

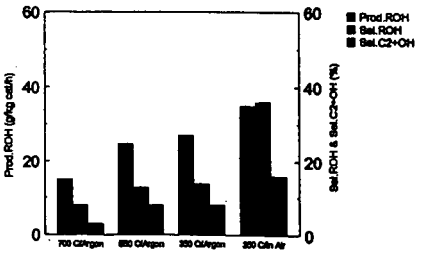

Fig.2. Effect of pretreatment on activities of the catalysts

3.3. Influence of support

In our previous work, several copper based catalysts were invesigated. It is the sample CuLaZr(2) which is the most favorable for the metthanolation, and it was then utilised as a support in the place of CuLaZr(1) for the preparation of the bimetallic catalyst. In fact, the catalyst 5%Co/CuLaZr(2) gives better results.

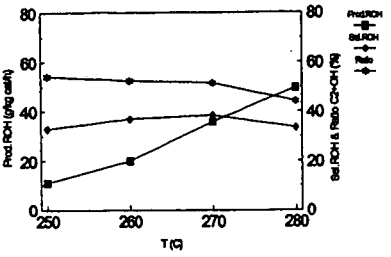

Fig.3. Influence of reaction temperature

The effects of reaction temperature were also studied. It was shown that both yields of alcohols and of hydrocarbons increased with the reaction temperature, and that the selectivity to alcohols pass a maximum of 38.4% at 270°C (Fig.3), and the alcohols productivity was 35.8 g/kg cat/h with ahigher alcohols ratio of 51.6%.

3.4. CO chemisorption and TPR

The chemisorption of reactants like CO or H_2 was the slow step in CO/H_2 reactions. The quantity and the form of CO adsorbed are often in relation to the rate and the orientation of the reaction. And the study on CO chemisorption may also give some information of the accessible metallic area ater the reduction[9].

The tests of CO chemisorption were made on three types of catalysts (CuLaZr, Co/LaZr, Co/CuLaZr) and the quantities of CO chemisorbed at ambient temperature are compared. It is shown that the addition of cobalt onto CuLaZr decreases the accessible metallic area of the catalyst, as explained by a covering of copper sites by cobalt oxide (more difficultly reducible) on the surface of the catalyst.

The temperature programmed reduction (TPR) tests were performed to see the influence of cobalt additive on the catalyst reducibilities, and the TPR spectra of the above three catalysts were compared. The maximum of the reduction peak of cobalt catalysts were at 316°C and that of copper system was at 218°C. And for the bimetallic system (Co/CuLaZr), there was only a reduction peak with a maximum at 255°C. This phenomenum suggested that there was an interaction between cobalt and copper, which resulted in a simultaneous reduction and a decrease of the Co_3O_4 reduction temperature. This interaction was also reported by Mouaddib [10].

3.5. Probe molecule tests

The effect of ethylene addition is illustrated in Fig.4. It is shown that C_2H_4 addition leads to a great augmentation of propanol, with a diminution of methanol. Propanal (propionic aldehyde) increases simultaneously. This result suggested that there is an insertion of the methanol precursor (like formyl species or CO) tto the chemisorbed olefins. The other formed products (like CH_4, C_3H_{6-8} and C_4H_{8-10}, not represented in the figure) change only a little.

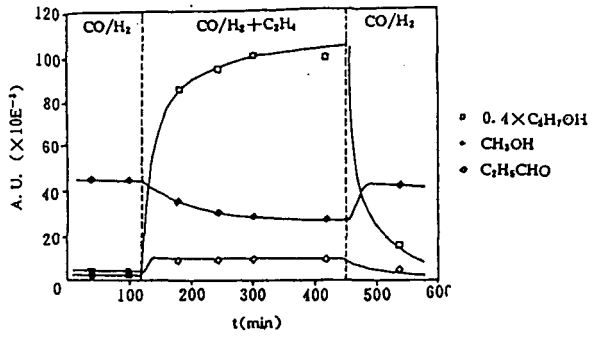

Fig.4. Effect of C_2H_4 addition to syngas stream as a probe molecule

As discussed by Chuang et al.[5], the insertion of C_1 oxygenated species (CO or formyl) into hydrocarbonated entities has particular importances as an indication of the growth of the oxygenated products. The comparison with the results of monometallic system is represented in Fig.5. It is observed that only over bimetallic catalyst a great augmentation of the C_3H_7OH formation has been achieved. It means that the simultaneous presence of copper and cobalt is important for a good chain growth formation into the alcohols.

The ratios $C_2H_6/(C_2H_4+C_2H_6)$ and C_3H_7OH/C_2H_5CHO may be good indications for the hydrogenating properties of the systems. It is observed that ethane represents 99.7% of total C_2 hydrocarbon over the catalyst CuLaZr, which indicates a great hydrogenating property of the system. However, the chain growth on this system is very low. For the catalyst Co/LaZr, the ratio of $C_2H_6/(C_2H_4+C_2H_6)$ is 2.1%, which indicates a weak hydrogenating property of the system, which may be in relation to its weak activity. In the case of Co/CuLaZr, the ratio of $C_2H_6/(C_2H_4+C_2H_6)$ is 20.5%, and C_3H_7OH/C_2H_5CHO is 30, which indicated a good hydrogenating property of the system.

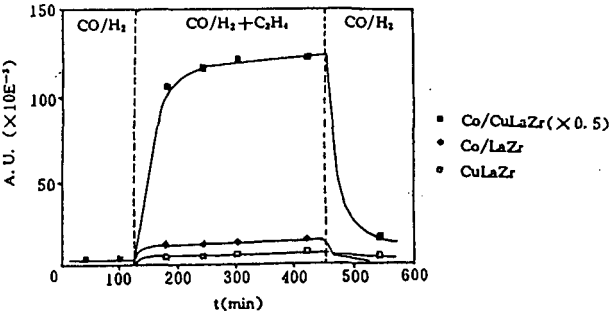

Fig.5. Effect of C_2H_4 addition to syngas on C_3H_7OH formation

4. CONCLUSION

It was shown that there were some strong interactions between cobalt and copper, and their simultaneous presence was important for a good orientation for the alcohol formation. And the addition of cobalt onto CuLaZr system may have three important effects on the higher alcohol production: an increase of the formation of hydrocarnonated species, an augmentation of the CO insertion property of the system, and a modification of the hydrogenating property of the catalyst, as supported by the tests of reactivities and those of probe molecules. With different pretreatment, the results show that the calcination at 350°C in air was most favorable.

REFERENCES

1. P.Courty, A.Forestiere, N.Kawata, T.Ohno, C. Raimbault, M.Yoshimoto, 191st ACS National Meeting, New York, 328, 42-60, 1986
2. Xu Xiaoding, E.B.Doesburg, J.J.F. Scholten, Catal. Today, 2, 125, 1987
3. P.Courty, D.Durand, J.C.Guibett, N.Kawata, T.Yasuda, M.Yoshimoto, Revue IFP, 42, 243,1987
4. W.Chu, R.Kieffer, A. Kiennemann, React. Kinet. Catal. Lett., 48, 627, 1992
5. S.C.Chuang, Y.H.Tian, J.G. Goodwin, I.Wender, J.Catal., 96, 396, 1985
6. A.Kiennemann, C.Diagne, J.P.Hindermann, P.Chaumette, P.Courty, Appl. Catal., 53, 197, 1989
7. M. Ichikawa, J.Chem. Soc. Chem. Commun., 566, 1978
8. A.Takeuchi, J.R.Katzer, G.C.A.Schuit, J.Catal., 82, 447, 1983
9. T.Fortin, PhD thesis, Poitiers University, France, 1986
10. N.Mouaddib, V.Perrichon, Proc. 9th ICC, Calgary, II-521,1988

MÖSSBAUER STUDY OF IRON-CARBIDE GROWTH AND FISCHER-TROPSCH ACTIVITY

K.R.P.M. Rao, F.E. Huggins, G.P. Huffman, R.J. O'Brien[#], R.J. Gormley[1], and B.H. Davis[#],

341, Bowman Hall, University of Kentucky, Lexington, KY 40506-0059
[#]Center for Applied Energy Research, University of Kentucky, Lexington, KY 40511,
[1]Pittsburgh Energy Technology Center, Department of Energy, Pittsburgh, PA 15236

Key words: Mössbauer spectroscopy, χ-carbide, Fischer-Tropsch synthesis

ABSTRACT: There is a need to establish a correlation between the Fischer-Tropsch (FT) activity of an iron-based catalyst and the catalyst phase during FT synthesis. The nature of iron phases formed during activation and FT synthesis is influenced by the gas used for activation. Mössbauer investigations of iron-based catalysts subjected to pretreatment in gas atmospheres containing mixtures of CO, H_2, and He have been carried out. Studies on UCI 1185-57 catalyst indicate that activation of the catalyst in CO leads to the formation of 100% magnetite and the magnetite formed gets rapidly converted to at least 90% of χ-Fe_5C_2 during activation. The χ-Fe_5C_2 formed during activation gets partly (≈ 25%) converted back to Fe_3O_4 during FT synthesis and both χ-Fe_5C_2 and Fe_3O_4 reach constant values. On the other hand, activation of the catalyst in synthesis gas leads to formation of Fe_3O_4 and which is slowly converted to χ-Fe_5C_2 and é-$Fe_{22}C$ during activation, and both carbide phases increase slowly during FT synthesis. FT synthesis activity is found to give rise to ≈ 70% (H2+CO) conversion in the case of CO activated catalyst as compared to ≈ 20% (H2+CO) conversion in the case of synthesis gas-activated catalyst.

INTRODUCTION: Pretreatment is an important step in the development of an efficient catalyst. It affects the distribution of iron phases that are formed during the pretreatment and changes that take place during synthesis. It is controlled by the type of gas, temperature (T), pressure (P) and gas space velocity (S.V.) used. The FT activity and possibly selectivity may be related to the iron phases present in the catalyst; however the role of any specific phase on the FT synthesis is not yet clearly understood.

Mössbauer characterization of two iron based catalysts,viz., UCI 1185-57 and UCI 1185-149 has been carried out with a view to identify and quantify the iron phases that are present in the activated and spent catalysts and define their influence on Fischer-Tropsch (FT) synthesis. The catalysts were activated in (i) CO or (ii) H_2/CO (syngas) and then subjected to FT synthesis.

EXPERIMENTAL:

CO-ACTIVATED UCI 1185-57 CATALYST: The UCI 1185-57 catalyst (64%Fe_2O_3/5%CuO/1%K_2O/30% Kaolin) was pretreated under CO at 270°C and then subjected to FT run conditions with a syngas of H_2/CO=0.7. Catalyst samples were withdrawn at various times during the pretreatment and FT synthesis. The phase distributions are given in Table I. The χ-Fe_5C_2 is formed rapidly during activation in CO.

SYNGAS-ACTIVATED UCI-1185-57 CATALYST: The UCI 1185-57 catalyst was preheated in He up to 200°C, then heated in H_2+CO at 280°C during the remainer of a 24 hour period and then subjected to a FT run with a syngas of H_2/CO=0.7. The catalyst samples were withdrawn at various times during pretreatment and FT synthesis. The phase distribution determined is given in Table II. As compared to the CO pretreatment, activation in synthesis gas leads to the formation and a slow increase of χ-carbide and é-carbide at the expense of Fe_3O_4. The carbides are formed in proportion to the pretreatment and synthesis duration; in addition to magnetite, some substituted magnetite and a small fraction of superparamagnetic iron oxide.

RESULTS AND DISCUSSION: As can be seen from the data in Table I, the hematite is converted into magnetite (Fe_3O_4) during heating the catalyst in CO up to 270°C in 2 hrs 43 min. The magnetite is converted into χ-Fe_5C_2 during further pretreatment under CO at 270°C; this phase represents is 90% at the end of 24hrs of pretreatment. The remaining 10% of magnetite is converted into superparamagnetic (spm) phase. Low temperature (12°C) measurement on RJO-139J has revealed that the spm phase is magnetite. During FT synthesis part of the χ-Fe_5C_2 (~25%) converted again to Fe_3O_4 and spm phase. However, after about 20 hrs of FT synthesis, the amounts of χ-Fe_5C_2 , Fe_3O_4 and the spm phases do not change further. The FT activity remains essentially constant at ≈70% H_2+CO during these changes.

The activity of the catalyst is higher when activated in CO than in synthesis gas. As compared to the CO pretreatment, the synthesis gas pretreatment leads to a slow increase in the χ-Fe_5C_2 and

é-$Fe_{2.2}C$ phases at the expense of Fe_3O_4 and the conversion ≈ 30% (H_2+CO) at the end of 24 hrs of activation. The χ-Fe_5C_2 and é-$Fe_{2.2}C$ continue to grow during FT synthesis while Fe_3O_4 continues to decrease indicating that magnetite converts into carbides, a trend which is opposite to that seen in the case of CO-activated catalyst (Fig.1a). It may be noted that there is no é-$Fe_{2.2}C$ detected in samples withdrawn during either pretreatment or FT synthesis in the case of the CO pretreated catalyst.

The ($CO+H_2$) conversion for the two types of pretreatment is shown in Fig. 1b. The ($CO+H_2$) conversion is maintained at ≈70% in the case of CO pretreated catalyst. On the other hand, in the case of synthesis gas pretreated catalyst, the conversion reaches ≈ 60% during activation but drops to ≈ 30% at the start of FT run when process conditions are changed. Some carbides were formed during activation and they continue to increase during the FT run.

We have also carried out Mössbauer investigations on the low α catalyst, UCI 1185-149 (2nd preparation) (57.2Fe/9.3Cu/0.05K) that had been subjected to pretreatment in (i) CO and (ii) H_2/CO. The pretreatment and FT synthesis conditions are given below and the results of are given in Tables III and IV.

CO-ACTIVATED UCI 1185-149 (2ND): This catalyst was pretreated in CO at 270°C, 175 psig, for 22hrs in 1.4 nL CO/g-Fe hr. FT synthesis was carried out with 10% catalyst loading in distilled Allied-Signal heavy wax at 270°C, 175psig, 2.4 nL syngas/g-Fe hr, at 1000rpm.

The activation is not complete during pretreatment. As can be observed from the Table III, the amount of χ-carbide continues to increase during FT synthesis and the FT activity decreases with increasing time on stream.

SYNGAS-ACTIVATED UCI 1185-149 (2ND): This catalyst was pretreated in H_2/CO at 280°C, 175 psig, for 14hrs in 1.4 nL CO/g-Fe hr. FT synthesis was carried out in C28 wax with 10% catalyst loading at 270°C, 175psig, 2.4 nL syngas/g-Fe hr, at 1000rpm. For this catalyst also the carbiding is not complete during pretreatment. As can be observed from the data in Table IV, the χ-carbide continues to increase during FT synthesis and the FT activity decreases with increasing time on stream, similar to the other catalyst used in this study. It may be noted that the FT activity is low even when the χ-Fe_5C_2 present in the spent catalyst is as much as 91%. This indicates that the absolute amount of χ-Fe_5C_2 present in the catalyst is not significant for FT activity.

Zarochak and McDonald [1] have carried out studies on the effects of pretreatment on the slurry phase FT synthesis activity and selectivity of a potassium-promoted precipitated iron catalyst and characterized the catalyst by Mössbauer spectroscopy measurements. They carried out two kinds of activation for the potassium promoted catalyst ((i) in CO and (ii) in syngas) were used and then the materials were subjected to FT synthesis. The catalyst activated in CO for 24 hrs gets completely converted into χ-Fe_5C_2 while the catalyst activated in syngas was converted partly to é-$Fe_{2.2}C$ during 24hrs of activation, and was completely converted to this phase only after 503 hrs of synthesis. The FT activity of the catalyst subjected to CO pretreatment was found to be higher than that found for the catalyst activated in syngas and the decrease in the FT activity with time on stream was slower for the CO pretreated sample.

References: [1] M.F.Zarochak and M.A. McDonald
Slurry-Phase Fischer-Tropsch Synthesis
6th DOE Indirect Liquefaction Contractor's Meeting
Dec 1-9, 1987, Pittsburgh Energy Technology Center, Pittsburgh

Table I†

CO-activated UCI 1185-57 catalyst: Sample		%Fe_3O_4	%χ-carbide	Spm Phase
Preheat conditions:				
RJO139A	Heating up to 270°C under CO in 2hr 43min	100	---	--
RJO139B	2.5hr under CO@270°C	95	---	5
RJO139C	6.5hr under CO@270°C	62	26	12
RJO139D	10.5hr under CO@270°C	33	56	11
RJO139E	18.5hr under CO@270°C	12	78	10
RJO139F	24hr under CO@270°C	--	90	10

Synthesis conditions

RJO139G	6hr of synthesis	--	87	13
RJO139H	19.75hr synthesis	8	69	23
RJO139I	27.75hr synthesis	10	67	23
RJO139J	48.75hr synthesis	13	62	25
RJO139K	140 hr synthesis	16	66	18

Spm= Superparamagnetic

Pretreatment conditions: Ramped up to 270°C @ 1.5°C/min. under CO @ 175 psig. Maintained at 270°C and 175psig with CO flow for 24 hr.

Synthesis conditions: H_2/CO=0.7, space velocity=3.4nL/hr/g(Fe) T=270°C and pressure 175psig.

Table II†

(H_2+CO) activated UCI 1185-57 catalyst:

Sample	α-Fe_2O_3	Fe_3O_4	S-Fe_3O_4	χ-Carbide	é-carbide	Spm
RJO-140A taken after heating to 200°C in He in 2hr 43 min	94	--	--	2	--	4
RJO-140C 7hr in (CO+H2) Taken at 250C during heat upto 280 C 150psig, TOS*=7hr, S.V.=2.	--	93	7	--	--	--
RJO-140E Taken after reaching 280°C, TOS=11.2hr	--	85	5	--	5	5
RJO-140F taken 3.75h after reaching 280°C, TOS=15hr	--	69	5	6	13	7
RJO-140G Taken 12.5hr after reaching 280°C TOS=23.75hr	--	44	5	12	23	17
FT synthesis conditions:						
RJO-140H Taken 3.25hr after switching to synthesis conditions, S.V=2.5, 200psig, TOS=27hr	--	25	4	27	33	11
RJO-140I Taken after 26.5hr under synthesis conditions, TOS=50.25hr	--	17	--	35	42	6

TOS= time on stream

S-Fe_3O_4 = substituted magnetite

† Catalyst preparation and FT synthesis runs were carried out CAER

Table III

UCI 1185-149 2nd catalyst activated in CO:

SAMPLE	χ-Fe_5C_2	Fe_3O_4	Spm	(H 2+CO) Conv%*
CW-S3-11-D TOS=84HRS	40	37	23	84.0
CW-S3-11-J TOS=235HRS	60	30	10	67.7
CW-S3-11-M TOS=305	68	27	5	51.2

* Catalyst preparation and FT synthesis runs were carried out at PETC, Pittsburgh

Table IV

UCI 1185-149 2nd catalyst activated in syngas:

Sample	χ-Fe_5C_2	Fe_3O_4	Spm phase	(H2+CO)* conversion
CW-S3-10-ACT Activated for 14hrs	36	48	16	--
CW-S3-10-A FT run for 26hrs	84	14	2	16
CW-S3-10-B FT run for 49hrs	91	7	2	6

* Catalyst preparation and FT runs were carried out at PETC, Pittsburgh

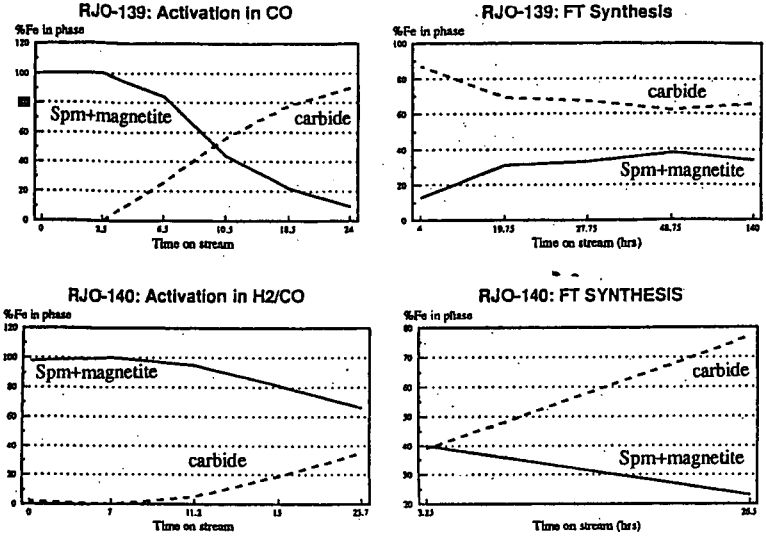

Fig.1a Variation of iron phases with time on stream

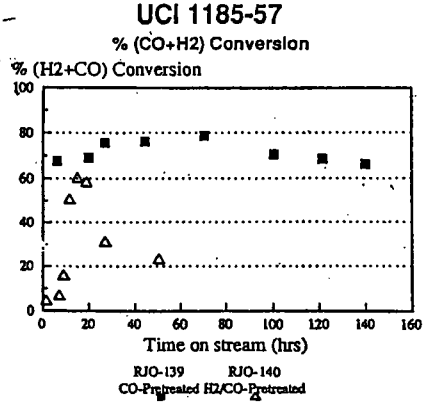

Fig.1b (H2+CO) conversion dependence on pretreatment

FINE DETAILS ON THE SELECTIVITY AND KINETICS OF THE FISCHER-TROPSCH SYNTHESIS OVER PRECIPITATED COBALT CATALYSTS BY COMBINATION OF QUANTITATIVE GAS CHROMATOGRAPHY AND MODELLING.

Ronald S. Hurlbut, Imre Puskas and Daniel J. Schumacher
Amoco Corporation, Naperville, Illinois 60566, (708) 653-4897

Keywords: Fischer-Tropsch, chain growth, kinetics, diffusion.

INTRODUCTION.

This report summarizes a part of our work carried out on the conversion of natural gas-derived synthesis gas to liquid fuels. Particularly, we were interested to find a catalyst which can convert dilute synthesis gas -such as obtainable from natural gas by partial oxidation with air- to predominantly liquid products at low pressures. For this purpose we needed to generate fundamental kinetic information on the controllability of the molecular weight distribution, which is defined by the chain growth probability of the reaction, because relatively little information is available on the subject (1-5). A wealth of information suggests, that with some exceptions in the low molecular weight regimes (1,6), the product distributions can be described by Anderson-Schulz-Flory (ASF) kinetics, using either a single chain growth probability, or separate chain growth probabilities for the light and heavy products (7). The causes of the "dual" chain growth probabilities still have not been defined. Three causes have been suggested which could account for the dual chain growth probabilities: 1./ Differences in the catalytic sites (8,9); 2./ transport-enhanced 1-olefin readsorption and incorporation into the heavy product fractions (10); 3./ operating characteristics of the reactor (3).

To aid with our objectives, we have developed an approach for product analyses which is based on a combination of quantitative gas chromatography and modelling. This resulted in instantaneous determinations of the complex product mixtures, providing an opportunity to generate instantaneous information on the selectivity and the kinetics of the reaction. The influence of experimental parameters (feed, pressure, space velocity and temperature) on the chain growth probability and on the rate was studied by this analytical approach. The results shed new information on the causes of the deviations from the ASF kinetics. Furthermore, the kinetic data also provide evidence for diffusional limitations of the reaction rates. Finally, the instantaneous analyses may aid in future research to link the kinetics and the selectivity of the reaction which seem to be interdependent and hence should require simultaneous treatment.

EXPERIMENTAL SECTION.

The methods of catalyst preparation, characterizations, evaluations and product analyses have been outlined in previous publications (6, 11-13). Full details are given in the unabbreviated version of this paper.

RESULTS AND DISCUSSIONS.

1./ Feed composition studies.

The addition of extra hydrogen to the feed was evaluated on Catalyst 1 in an experiment conducted at 197 °C, 156 kPa. Table 1 gives the detailed results. Table 1 also serves to illustrate the type of information generated by the GC-modelling combination. The data show that an increase of the H_2 to CO feed ratio from 2.0 to 3.1 resulted in substantial increase of the reaction rate as indicated by the catalyst productivities, and a modest decrease in the growth factor. The data also illustrate how the C_1 to C_4 product selectivities, expressed in percentage of the theoretical ASF predictions, change with the H_2 to CO feed ratio. The C_1 selectivity is very dependent on the feed ratio. However, the C_2 to C_4 selectivities are only little influenced by the feed ratio. This is in line with our earlier findings (6), that over Co catalysts, the fraction of C_3 to C_4 olefin incorporation by telomerization is nearly constant and little influenced by the experimental variables. The data of Table 1 suggest, that high H_2 to CO feed ratio promotes the hydrogenation of the C_2-C_4 olefins slightly more than their telomerization.

We considered the possibility that physisorbing inert components of the feed may also impact on the value of the growth factor by

creating "steric impediment" to propagation on the surface of the catalyst. This possibility was studied by nitrogen dilution of the feed on Catalyst 2, at 202 °C, 168 kPa. The highlights of the results are shown in Figure 1. Indeed, nitrogen dilution of the feed resulted in decreased growth and decreased rate (productivity). Since nitrogen dilution also resulted in increased space velocity, specifically from 131 to 177 VHSV, the possibility need to be considered that the observed changes may have been caused by space velocity changes rather than by nitrogen dilution. It will be demonstrated later, that increased feed space velocity results in increased rate, without affecting the growth factor. Hence we can conclude that nitrogen dilution was the cause of the lower reaction rate and lower growth factor.

If nitrogen dilution affects the chain growth, it is expected, that the hydrocarbon products of the synthesis may also have a similar effect. The effect of hydrocarbon dilution was studied by comparing the reaction products from one-pass operations and from recycle mode operations. In this latter mode, the reaction products were passed through an air-cooled condenser to condense out the liquids. Part of the uncondensed gases were pumped back into the reactor after mixing with fresh feed. Catalyst 3 was used in the experiments, at 200.5 °C, 103 kPa, with identical fresh feed flows. In the once-through operations. we obtained 60.4% CO conversion, 11.8% methane selectivity, 0.732 growth factor and 0.0235 g/g/hr catalyst productivities. During recycle operations, with 1.9 to 1 volumetric recycle to fresh feed ratio, we obtained 58.2% CO conversion, 13.2% methane selectivity and 0.0223 g/g/hr catalyst productivity. Unfortunately, the gas chromatographic effluent analysis was not adoptable for the determination of the growth factor on the basis of the C_6 to C_{10} products, because these were partially removed by the recycle operations. We estimate 0.725 growth factor for the recycle operations on the basis that it yields the same selectivity balance as obtained in the once-through operations. We believe that these results qualitatively demonstrate that hydrocarbon dilution of the feed results in decreased growth and decreased rate, because the inert diluents successfully compete with the chemisorbing reagents for the catalytic sites.

2./ Pressure effects.
Table 2 illustrates the effect of small pressure changes at constant temperatures and constant feed flow rates on three different catalysts. In all cases, significant increases in the growth factor and also in the rates (catalyst productivities) were caused by small pressure increases. The C_1 to C_4 carbon selectivities (not shown in the Table) followed the trends defined by the growth factors. However, the C_1 to C_4 selectivities expressed in percent of their theoretical values did not appear to change. The small scatter of data is attributable to analytical error; no trend can be recognized with the pressure changes.

3./ Space velocity effects.
The effect of space velocity changes was studied on Catalyst 6 in atmospheric experiments at 195 °C. The results are summarized in Figures 2 to 8. As Figure 2 shows, in this series of experiments we obtained essentially 100% selectivity balances, indicating that the ASF model extrapolation adequately accounted for the heavy products. Figure 2 also shows that the space velocity had little, if any effect on the growth factor. The data of Figure 3 illustrate another interesting point. While the CO conversion increased with increasing contact time (i.e. decreasing space velocity), the catalyst productivity decreased. Since the reaction occurs on the catalyst surface, and the feed composition, temperature and pressure were identical in this series of experiments, the change in catalyst productivity (rate) must have been caused by changes in the diffusion rates of the reagents to reach the catalyst surface. Faster space velocity provided faster diffusion rates. From these results, diffusional limitations of the reaction rates can be inferred.

Figures 4 to 8 show the C_1 to C_4 product selectivity dependencies on the contact time. These appear to be independent of the contact time. However, as expected, the distribution of the C_3 and C_4 products changes. The propylene and 1-butene contents decrease with increasing contact time due to hydrogenations to

propane and butane, respectively, and, in case of 1-butene, also to isomerizations to cis- and trans-2 butenes (Figures 6 to 8).

4./ Temperature effects.
The effect of temperature changes was studied at constant pressure (156 kPa) and constant space velocity (120 VHSV) on Catalyst 1. As Figure 9 illustrates, in the 190-205 °C region, the growth factor steeply increased with decreasing temperature. However, below about 180 °C, the measured growth factors did not seem to change with decreasing temperature. The carbon selectivity balances, also shown in Figure 9, may shed some information about the causes of these observations. Above about 190 °C, the carbon balances were in the 91-95 percent range, suggesting that extrapolation by the ASF model underestimated the heavy product formation. Below about 185 °C, the heavy product formation was substantially underestimated as revealed by the balance data. Hence we infer, that at decreasing temperature, heavier products with very high value of growth factor may have continued to form, but these had little impact on the relative amounts of C_i to C_{10} products which provided the basis for the determination of the growth factor. The data seem to support the theories, that the measured growth factor is a composite of a wide range of actual growth factors.

Figures 10 to 12 illustrate, that the methane selectivities, expressed in percent of the theoretical, increase with increasing temperature, but the C_2, C_3 and C_4 selectivities are unaffected. However, temperature affects the C_3 and C_4 distributions. At higher temperatures less propene (Figure 11) and less 1-butene (Figure 12) were found.

Figure 13 shows the temperature dependance of the CO conversions and the catalyst productivities. Surprisingly, the results suggest a linear correlation between temperature (T) and rate (-r), except for the high temperature (high conversion) regions:

$$-r = k\ K\ (T-T_i) \qquad (1)$$

where k is the rate constant, K is another constant characteristic for the conditions and T_i is the temperature of the start of the reaction. This means that the Arrhenius equation is not valid in this surface reaction. Nevertheless, in Figure 14, we present a pro-forma Arrhenius plot which is curved. (For the plot, we used CO conversion data in lieu of rate constants from the linear region of Figure 13). The results may not be surprising, because theoretical considerations have demonstrated that non-linear Arrhenius plots can be obtained in transport-limited catalytic reactions (14, 15). From the data, we estimate pro forma activation energies ranging from 16 to 31 kcal/mole, which cover the bulk of the previously reported values.

CHAIN GROWTH PROBABILITY AND PRODUCT SELECTIVITY.
We propose that the chain growth probability (α) is defined by the nature of the catalyst surface (C), the surface concentrations of the adsorbed species (S_1 to S_I) -which include chemisorbing reagents and non-reactive adsorbed species- and the temperature of the surface:

$$\alpha = f\ (C,\ S_1, \ldots S_I,\ T) \qquad (2)$$

It may be expected, that the nature of the catalytic metal, the size of the metal crystallites, metal-support interactions may influence the chain growth probability. Indeed, different catalytic sites were postulated in the past to give different chain growth (8,9). However, providing evidence for this was elusive, but scientific interest continues in the subject. Our results demonstrated, that not only the chemisorbing reagents, but also the physisorbing inerts can affect the chain growth probability. The surface concentrations of the adsorbed species will depend on their respective concentrations in the gas phase, on the pressure, on their rate of chemisorption, and on the diffusional conditions.

Even though it may be a long way to define an explicit form for Equation 2, the Equation my be useful for some qualitative predictions. Even if a specific catalyst were to possess only one type of catalytic site, a common plug-flow type reactor will produce a multiplicity of growth factors due to changes in the relative surface concentrations of the adsorbing species along the reactor axis arising from gas-phase compositional changes.

and due to minor temperature gradients on the surfaces. We have modelled these possibilities and some results with relevant assumptions are shown. Figure 15 gives the calculated ASF plot of a product mixture with growth factor evenly changing from 0.70 to 0.80. For all practical purpose, the product mixture can be described by a single growth factor. However, a careful examination reveals a slight break in the ASF plot at C_9-C_{10}. Figure 16 gives the ASF plots of two assumed mixtures. In one of the mixtures, the growth factor continuously changes from 0.60 to 0.85, in the other one from 0.60 to 0.95. In both examples, there is a break in the ASF plot around C_{10}. However, the C_6 to C_{10} data from the two plots are nearly parallel, yielding nearly identical growth factor values by the conventional measurements. With this example, we have simulated an explanation for the finding that the measured growth factor did not increase with decreasing temperature below about 185 °C.

The above discussion makes it clear that the operating characteristics of the reactor can result in molecular weight distributions with non-linear ASF plots. However, our results do not provide any indication that "transport enhanced olefin readsorption" can lead to increased growth probability and to non-linear ASF plots, as postulated recently (10). In our work, we have found evidence only for C_2-C_4 olefin incorporation, and possibly very little C_1 incorporation, but the degree of these incorporations was fairly constant and independent of the residence time.

REFERENCES.

1. Henrici-Olive, G., and Olive, S., Angew. Chem. Intl. Ed. Engl. 15, 136 (1976).
2. Dry, M. E., in "Catalysis Science and Technology" (J. R. Anderson and M. Boudart, Eds.), Springer Verlag, Berlin, 1981, p. 159. See also Idem, Catal. Today, 6, 183 (1990).
3. Matsumoto, D. K., and Satterfield, C. N., Energy & Fuels 3, 249 (1989).
4. Dictor, R. A., and Bell, A. T., J. Catal. 97, 121 (1986).
5. Krishna, K. R., and Bell, A. T., J. Catal. 139, 104 (1993).
6. Puskas, I., Hurlbut, R. S., and Pauls, R. E., J. Catal. 139, 139 (1993).
7. For a review, see Davis, B. H., Preprints, ACS, Fuel Division, 37, 172 (1992).
8. Huff, G. A., and Satterfield, C. N., J. Catal. 85, 370 (1984).
9. Stenger, H. G., J. Catal. 92, 426 (1985).
10. Iglesia, E., Reyes, S. C., Madon, R. J. and Soled, S. L., in "Advances in Catalysis" (D. D. Eley, H. Pines and P. B. Weisz, Eds.), Academic Press, Inc., Vol. 39, 1993, p. 221.
11. Puskas, I., Fleisch, T. H., Hall, J. B., Meyers, B. L., and Roginski, R. T., J. Catal. 134, 615 (1992).
12. Puskas, I., Catal. Lett. 22, 283 (1993).
13. Puskas, I., Meyers, B. L., and Hall, J. B., Catalysis Today, 21, 243 (1994).
14. Weisz, P. B., and Prater, C. D., in "Advances in Catalysis" (W. G. Frankenburg, V. I. Komarewsky and E. D. Rideal, Eds.), Academic Press, Inc., Vol. 6, 1954, p. 143.
15. Rajadhyaksha, R. A., and Doraiswamy, L. K., Catal. Rev.- Sci. Eng, 13, (20), 209, (1976).

FIGURE 1

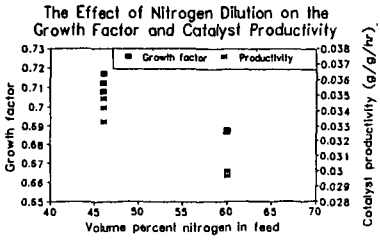

FIGURE 2

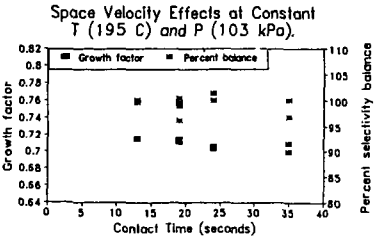

TABLE 1. Changes in Catalyst Performance and Product Selectivities with Changes in the H_2 to CO Feed Ratio.[a]

H_2/CO ratio	2.0	2.0	2.5	2.5	3.1	3.1
VHSV	120	120	131	131	141	141
% CO conv.	60.3	59.4	77.3	77.5	91.5	93.5
Productivity	0.0285	0.0281	0.0367	0.0367	0.0436	0.0443
Growth factor	0.752	0.756	0.733	0.732	0.720	0.712
% Balance	96.2	95.8	93.1	93.9	96.6	97.7
% Selectivities						
CO_2	2.9	2.8	2.6	2.7	2.2	2.7
C_1	8.9	8.8	11.5	11.8	16.2	18.7
C_2-s	2.1	2.1	2.5	2.7	3.4	3.7
C_3-s	7.1	7.0	7.0	7.3	7.7	8.0
C_4-s	9.0	8.7	9.0	9.2	9.7	9.8
% of theoretical						
C_1	151	153	167	171	213	233
C_2-s	24.4	24.6	26.4	28.0	34.1	32.4
C_3-s	69.7	70.0	66.1	68.5	71.4	73.4
Propene	38.8	39.8	23.2	23.1	9.0	6.5
Propane	30.8	30.2	42.9	45.4	62.4	66.9
C_4-s	87.2	85.8	87.1	89.1	93.3	95.7
1-Butene	23.7	23.5	14.7	14.8	9.8	9.9
n-Butane	33.6	33.1	42.6	43.8	58.9	62.8
t-2-Butene	14.3	13.7	16.2	16.6	14.9	14.5
c-2-Butene	15.6	15.5	13.7	13.9	9.7	8.5

[a]Catalyst 1 at 197+1°C, 156 kPa. The volumetric feed compositions were 18-38-46, 16-41-43 and 15-47-38 CO-H_2-N_2, repectively.

TABLE 2. The Effect of Small Pressure Changes on Catalyst Performance and Product Selectivities.

Catalyst ID NO	2		4		5	
Temperature, °C	203		193		202	
Pressure, kPa	169	241	104	170	170	202
VHSV	131	131	286	286	220	220
Contact time (sec.)	46	65	13	21	27	32
% CO conversion	79.7	90.0	32.7	39.9	68.9	78.8
Productivity (g/g/hr)	0.034	0.039	0.014	0.016	0.043	0.050
Growth factor	0.703	0.736	0.739	0.789	0.648	0.696
% Balance	99.4	98.1	96.1	102.6	96.3	93.5
% CO_2 selectivity	4.0	4.9	3.1	2.3	2.9	3.2
Selectivities, % of theoretical						
C_1	144	142	191	215	135	122
C_2	24.4	23.4	23.8	25.6	26.0	22.3
C_3	68.1	65.6	69.6	76.5	70.4	62.8
Propene	22.8	21.4	40.0	44.7	25.8	21.2
Propane	45.2	44.2	29.5	31.7	44.5	41.6
C_4	93.6	90.2	88.6	93.9	95.4	86.4
1-Butene	13.4	11.6	21.0	23.9	14.2	11.4
n-Butane	43.7	43.0	33.2	38.0	40.4	38.4
t-2-Butene	21.0	19.9	19.3	17.0	23.8	21.4
c-2-Butene	15.6	15.6	15.1	15.0	17.0	15.2

FIGURE 3

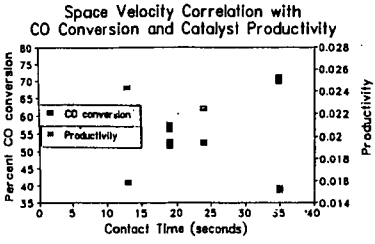

FIGURE 4

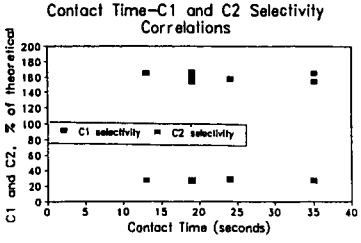

FIGURE 5
Contact Time–C3 Selectivity Correlations

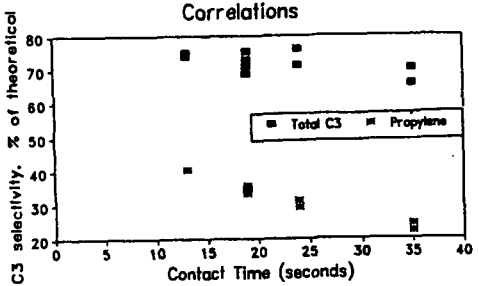

FIGURE 6
Contact Time–C4 Selectivity Correlations

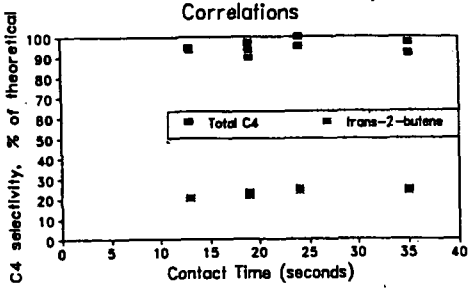

FIGURE 7
Contact Time–1–Butene Selectivity Correlation

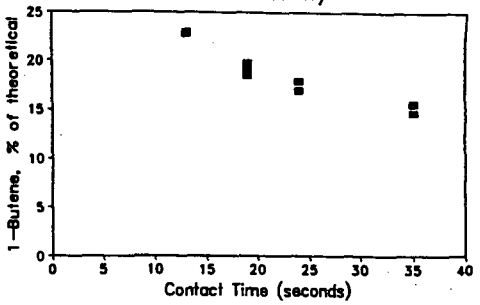

FIGURE 8
Contact Time–C4 Selectivity Correlations

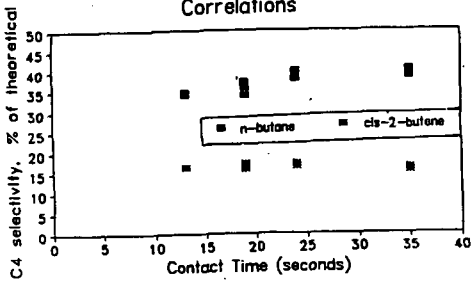

FIGURE 9
Growth Factors and Carbon Balances versus T at Constant P and SV.

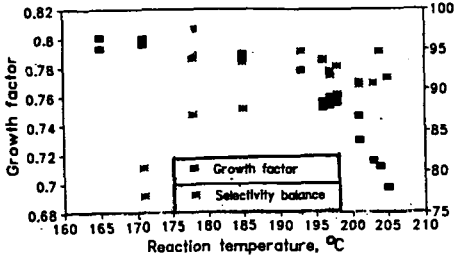

FIGURE 10
Correlation Between Temperature and the C1 and C2 Selectivities.

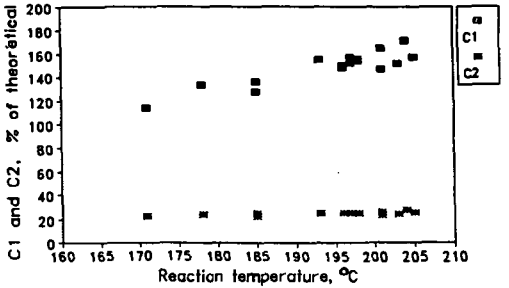

FIGURE 5
Contact Time–C3 Selectivity Correlations

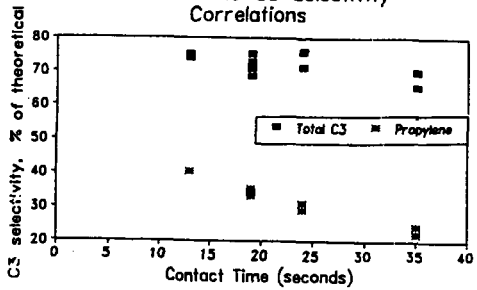

FIGURE 6
Contact Time–C4 Selectivity Correlations

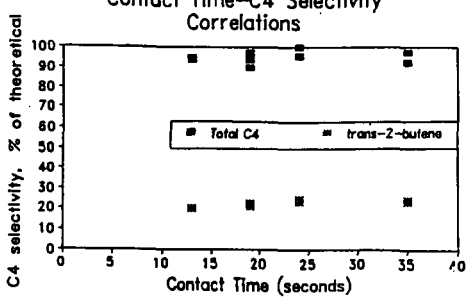

FIGURE 7
Contact Time–1–Butene Selectivity Correlation

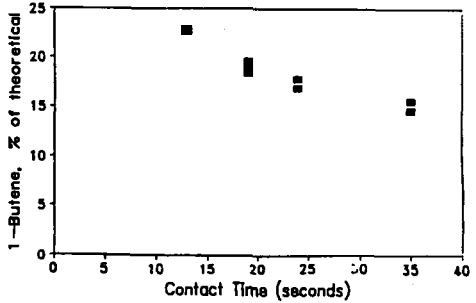

FIGURE 8
Contact Time–C4 Selectivity Correlations

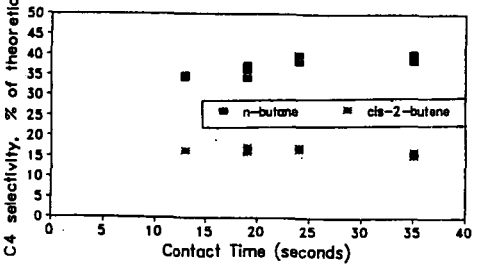

FIGURE 9
Growth Factors and Carbon Balances versus T at Constant P and SV.

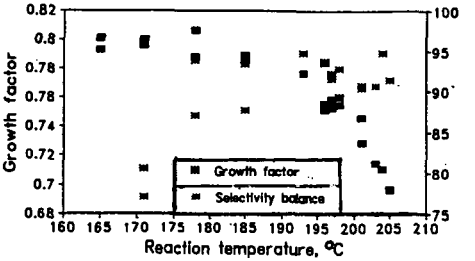

FIGURE 10
Correlation Between Temperature and the C1 and C2 Selectivities.

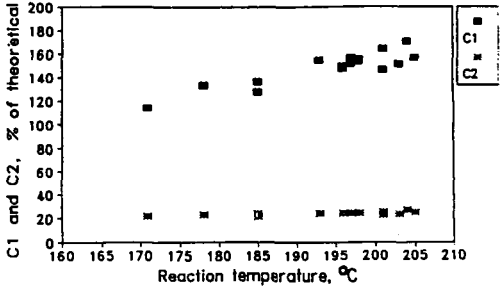

FIGURE 11

Correlation Between Temperature and the C3 Selectivities.

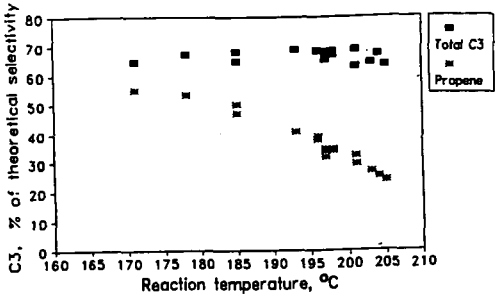

FIGURE 12

Correlation Between Temperature and the C4 Selectivities.

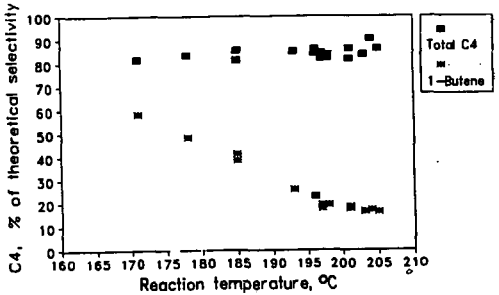

FIGURE 13

CO Conversions and Productivities vs. T at Constant Pressure and Space Velocity

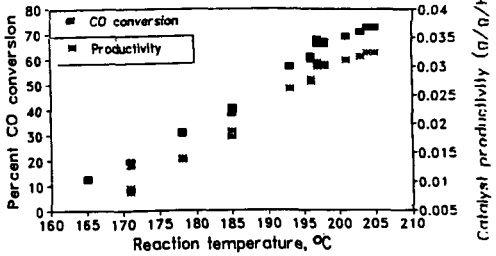

FIGURE 14. Arrhenius Plot.

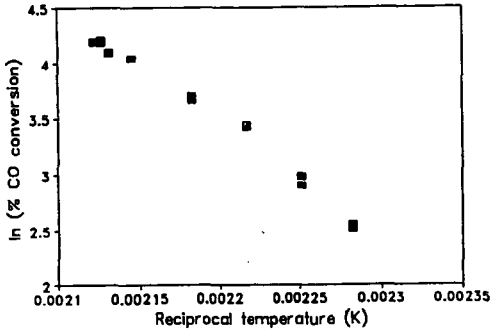

FIGURE 15. Calculated ASF Plot of a Product Distribution Continuously Changing in Alpha from 0.7 to 0.8

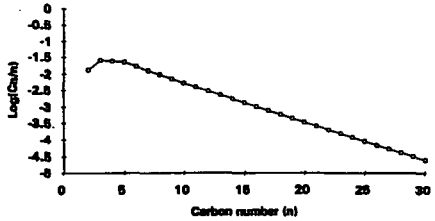

FIGURE 16. Calculated ASF Plots with Alphas Ranging from 0.60 to 0.85 and from 0.60 to 0.95

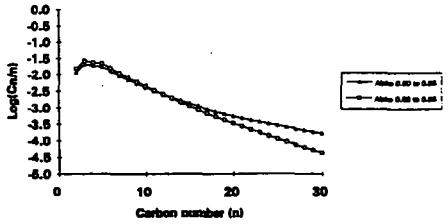

FIGURE 11

Correlation Between Temperature and the C3 Selectivities.

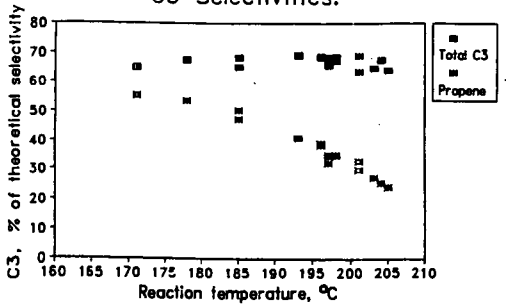

FIGURE 12

Correlation Between Temperature and the C4 Selectivities.

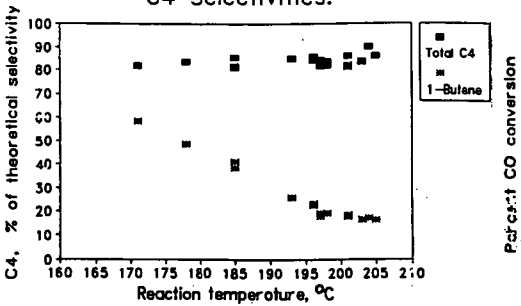

FIGURE 13

CO Conversions and Productivities vs. T at Constant Pressure and Space Velocity

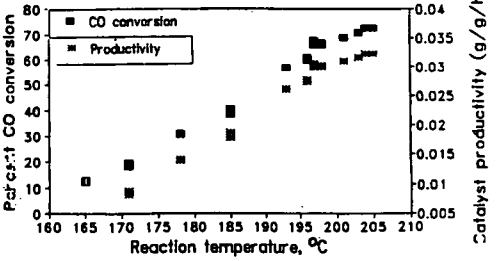

FIGURE 14. Arrhenius Plot.

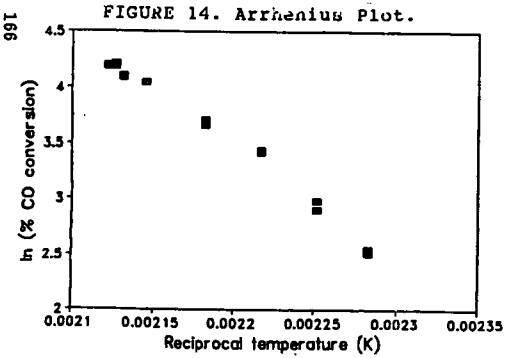

FIGURE 15. Calculated ASF Plot of a Product Distribution Continuously Changing in Alpha from 0.7 to 0.8

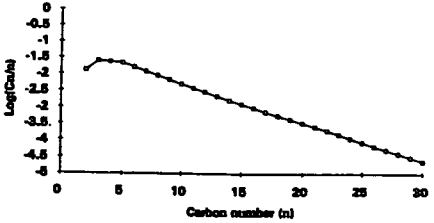

FIGURE 16. Calculated ASF Plots with Alphas Ranging from 0.60 to 0.85 and from 0.60 to 0.95

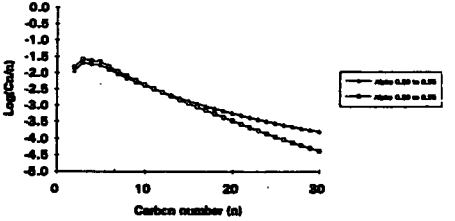

REOXIDATION AND DEACTIVATION OF SUPPORTED COBALT FISCHER-TROPSCH CATALYSTS

D. Schanke[2], A.M. Hilmen[1], E. Bergene[2], K. Kinnari[3], E. Rytter[3], E. Ådnanes[2] and A. Holmen[1]

[1]Department of Industrial Chemistry, Norwegian Institute of Technology, University of Trondheim, N-7034 Trondheim, Norway

[2]SINTEF Applied Chemistry, N-7034 Trondheim, Norway

[3]Statoil Research Centre, N-7005 Trondheim, Norway

Keywords: Fischer-Tropsch synthesis, cobalt catalysts, deactivation

INTRODUCTION

As a result of the highly exothermic nature of the Fischer-Tropsch reaction, heat transfer considerations limit the maximum conversion per pass in fixed-bed processes, whereas slurry reactors can operate at higher conversions (1). During Fischer-Tropsch synthesis on cobalt catalysts, high conversions will generate high partial pressures of water at the reactor exit, due to the low water gas shift activity of cobalt. In addition, the extensive back-mixing in slurry reactors will give a relatively uniform concentration profile in the reactor, characterized by a high concentration of water and low reactant concentrations. From the commercial iron-catalyzed Fischer-Tropsch synthesis in fixed-bed (Arge) reactors it is known that the catalyst deactivates by oxidation of iron by CO_2 and H_2O near the exit of the reactor (2). Although bulk oxidation of cobalt during Fischer-Tropsch synthesis is not thermodynamically favored, it was early speculated that surface oxidation of cobalt could occur during Fischer-Tropsch synthesis (3).

The purpose of the present work is to describe the influence of water on the deactivation behavior of Al_2O_3 supported cobalt catalysts. The possibility of cobalt oxidation during Fischer-Tropsch synthesis was investigated by model studies.

2. EXPERIMENTAL

2.1 Catalysts

Cobalt catalysts containing (by weight) ≈20% Co, 1% Re and optionally 1% rare earth oxides (designated RE) on γ-Al_2O_3, were prepared by incipient wetness coimpregnation of the support with aqueous solutions of $Co(NO_3)_2 \cdot 6H_2O$, $HReO_4$ and (optionally) the RE-oxide precursor. The rare earth oxide precursor was supplied as nitrates (Molycorp 5247) and contained 66% La_2O_3 after calcination, the remainder being other rare earth oxides. The catalysts were dried in air overnight at 393 K before calcination in air at 573 K for 2 hours. The alumina supports had a specific surface area of 174 - 182 m^2/g and 0.7-0.9 cm^3/g pore volume. The extent of cobalt reduction was ≈80% after reduction at 623 K for 14-16 hours (measured by O_2 titration at 673 K), and the cobalt dispersion (H_{ads}:Co) was estimated to 7-8% by temperature programmed desorption of H_2.

2.2 Kinetic experiments

Deactivation studies were carried out in a 0.9 cm I.D. stainless steel fixed-bed reactor heated by a fluidized sand bath. 3 g of catalyst (38-53 μm) was diluted with an inert material (non porous SiC) in a 1:3 weight ratio to minimize temperature gradients. The catalyst was reduced in flowing hydrogen (5000 cm^3 (STP)/($g_{cat} \cdot h$)) at atmospheric pressure at 623 K for 16 hours (heating rate from ambient temperature: 1 K/min). After reduction, the catalyst was cooled to 443 K in flowing H_2 and purged with He before increasing the pressure to 20 bar and switching to a feed mixture containing 97 mol% synthesis gas with H_2/CO = 2.1 and 3 mol% N_2. The reaction temperature was then slowly increased to the desired initial reaction temperature. On-line GC samples were taken at regular intervals and analyzed for N_2, CO, CO_2 and C_1+ hydrocarbons on a HP 5890 gas chromatograph. Space velocity was varied to give 20-70% CO conversion. High water partial pressures were obtained by addition of steam to the reactor inlet.

2.3 Gravimetric experiments

Reoxidation experiments were performed in a Sartorius 4436 high pressure microbalance (4). Before reduction, the catalyst was dried for 24 hours at a temperature 50 K higher than the reduction temperature to ensure minimal weight losses due to removal of water from the catalyst during reduction. After cooling to ambient temperature, the catalyst was reduced in flowing H_2 (1 K/min. to 623 K, 16 hours hold time). After reduction, the temperature was adjusted to 523 K and a feed consisting of H_2, He and H_2O (as steam) was added to the reactor for a period of 16-17 hours.

2.4 X-ray Photoelectron Spectroscopy (XPS)

XPS studies were conducted in a VG ESCALAB MkII instrument equipped with a non-monochromatic Al Kα source (1486.6 eV). The catalyst samples were treated in an integrated high pressure pretreatment cell before being transferred to the analysis chamber without exposure to air. The catalysts were analyzed in the unreduced state, after reduction and after treatment with a H_2O/H_2 mixture.

3. RESULTS AND DISCUSSION

3.1 CO hydrogenation experiments

Fig. 1. shows a typical example of the deactivation behavior of an alumina supported, Re-promoted cobalt catalyst. The results are obtained after a 50 h period of stable operation at 463 and 473 K and the CO conversion was adjusted to 31-33% before and after the period where water was added to the feed, in order to allow direct comparison of the catalyst activities. The sharp decrease in reaction rate when water is introduced into the feed is a result of a reversible kinetic effect caused by the change in feed composition and is recovered when water is removed from the feed. The drop in reaction rate is apparently greater than predicted by 1. order kinetics, meaning that the change in reaction rate can only partly be explained by the decreased partial pressure of H_2 when the feed is diluted with H_2O. The reversible part of the decrease in reaction rate must therefore also contain an inhibition term associated with the concentration of water which is not accounted for in the simple 1. order (in H_2) kinetics. Similar behavior has been reported for iron catalysts (5). The contribution of the water inhibition term is likely to be larger than indicated in Fig. 1, since the pressure order for Fischer-Tropsch synthesis on cobalt has been shown to be less than 1.0 (6).

In addition to the inhibition effect, the presence of high water partial pressures also results in relatively rapid deactivation of the catalyst. It is shown that the rate of deactivation is further increased when the inlet partial pressure of water is raised from 5 to 7.5 bar. Virtually no further deactivation was observed after the water had been removed from the feed. From comparison of rates or rate constants before and after the period where water was added to the feed, the catalyst has lost approximately 30% of its initial activity. There is a tendency for decreased rate of deactivation towards the end of the period where water was added to the feed, indicating that the rate of deactivation depends not only on the partial pressure of water, but also on the remaining activity. This is the expected behavior in the case of a parallel poisoning reaction.

The influence of water on the deactivation can also be shown indirectly by monitoring the change in reaction rate at different conversions for a fresh catalyst. Fig. 2. shows that a stable activity is obtained at ~34 and ~52% CO conversion, whereas deactivation is evident when the conversion is raised to an initial value of ~70%. These conversions correspond to H_2O partial pressures of approximately 3, 5 and 7 bar respectively at the reactor outlet. However, these partial pressures are not directly comparable to the situation where water is added to the feed. In the latter case, a uniform concentration profile of water in the reactor is obtained. In the case where all of the water is produced by the Fischer-Tropsch reaction, the concentration of water will be high only near the reactor exit.

3.2 Model studies

Model experiments at non-reacting conditions with various H_2O/H_2 feeds were carried out in order to test the hypothesis of cobalt oxidation as being responsible for the observed deactivation.

Results from the gravimetric studies are shown in Fig. 3. In the series of experiments shown here, catalysts without rare earth oxides (RE) have been used. Although this precludes direct comparison with the deactivation studies, we have generally experienced that this low level of RE loading does not influence the deactivation behavior significantly.

A common feature of all of the curves shown in Fig. 3 is the initial rapid weight increase of ~20 mg/g. Blank experiments using unreduced catalyst (curve 1 in Fig. 3) and the pure support (not shown) also showed the same initial weight increase. It is therefore concluded that the initial behavior is caused by adsorption of water on the porous support. The water adsorption equilibrium is rapidly established and the blank experiments therefore serve as a baseline for measuring weight gains associated with the possible oxidation of cobalt.

Exposure of the reduced $CoRe/Al_2O_3$ catalyst to a H_2O/He mixture (without H_2) resulted in a large weight increase, corresponding to almost complete bulk reoxidation of cobalt (curve 4 in Fig. 3). The situation is markedly different when the feed contains even small amounts of H_2, as shown for the case with H_2O/H_2 = 10 where the weight curve indicates only a limited extent of reoxidation (curve 3 in Fig. 3). This H_2O/H_2 ratio would represent a very high conversion and a stronger deactivation potential than in the kinetic experiments. At the same partial pressure of water but at a higher H_2 partial pressure (H_2O/H_2 = 1.5), which could be considered a more realistic case, an even lower weight increase suggests almost negligible bulk reoxidation (curve 2 in Fig. 3).

Significant bulk oxidation of metallic cobalt was therefore considered to be unlikely under Fischer-Tropsch reaction conditions. In view of the strong deactivating effect of water shown in Fig. 1, the possibility of surface oxidation was therefore considered.

XPS spectra of a 20%Co-1%Re-1%RE/γ-Al_2O_3 catalyst are shown in Fig. 4. The peak at 781.5 eV, which is the dominant peak in the XPS spectrum of the calcined catalyst (curve a in Fig. 4), is assigned to cobalt oxides, and is accompanied by a shake-up satelite at 787-788 eV, probably representing Co^{2+}. In the reduced catalyst (curve b in Fig. 4), the XPS peak representing cobalt metal (778 eV) is visible, but the XPS-spectrum is still dominated by the oxide peak at 781.5 eV. In general, the extent of reduction measured by XPS (given as the intensity ratio $Co^0/(Co^{2+/3+}+Co^0)$) is significantly lower than estimated by bulk methods. This is most likely caused by the presence of multiple cobalt oxide phases with widely different dispersion and reducibility, ranging from large Co_3O_4 crystallites to an atomically dispersed surface cobalt aluminate (7,8). The latter is unreducible at the temperatures used in this study but will dominate the XPS-spectrum due to the high dispersion.

Treatment of the reduced catalyst with a 1:4 H_2O/H_2 mixture, gave clear indications of reoxidation of cobalt metal to Co^{2+} or Co^{3+}, as shown by the decreased $Co^0/Co^{2+/3+}$ intensity ratio (curve c in Fig. 4). The intensity of the satelite peak appears to increase slightly, indicating some formation of Co^{2+}.

Thermodynamic calculations show that bulk cobalt metal will not reoxidize in H_2O/H_2 mixtures (3). However, highly dispersed phases or surface layers can be expected to show deviations from bulk behavior. The gravimetric studies indicated a relatively small extent of bulk reoxidation of $CoRe/Al_2O_3$ even at H_2O/H_2 = 10, and an even more modest effect at H_2O/H_2 = 1.5. The latter conditions are probably more representative of the conditions used in the fixed-bed deactivation studies. In contrast, XPS indicated significant reoxidation already at H_2O/H_2 = 0.25. From the comparison of results from surface and bulk techniques it is reasonable to suggest that surface oxidation or preferential oxidation of highly dispersed phases occurs in H_2O/H_2 or $H_2O/H_2/CO$ mixtures.

4. CONCLUSIONS

The presence of high water partial pressures during Fischer-Tropsch synthesis increases the rate of deactivation of a Co-Re-RE/γ-Al_2O_3 catalyst. In simulated high conversion conditions using H_2O/H_2 feeds, bulk reoxidation of cobalt occurs only to a very limited extent, even at high H_2O/H_2 ratios. However, XPS studies indicated that surface oxidation or oxidation of highly dispersed cobalt phases are responsible for the observed deactivation.

ACKNOWLEDGEMENT

The authors gratefully acknowledge Statoil for financial support and for the permission to publish these results.

REFERENCES

(1) Fox, J.M., Catal.Rev.-Sci.Eng., 35(2), 169 (1993).
(2) Dry, M.E., Catal. Lett., 7, 241 (1990).
(3) Anderson, R.B., in P.H. Emmett (ed.) "Catalysis" Vol.IV, Rheinhold Publ. Comp., New York (1956)
(4) Holmen, A., Schanke, D. and Sundmark, D., Appl. Catal., 50, 211 (1989)
(5) Satterfield, C.N., Hanlon, R.T., Tung, S.E., Zou, Z.-M. and Papaefthymiou, G.C., Ind. Eng. Chem. Prod. Res. Dev., 25, 407 (1986).
(6) Iglesia, E., Reyes, S., Madon, R.J. and Soled, S.L., Adv. Catal., 39, 221 (1993).
(7) Stranick, M.A., Houalla, M. and Hercules, D.M., J. Catal., 103, 151 (1987).
(8) Arnoldy, P. and Moulijn, J.A., J. Catal. 93, 38 (1985).

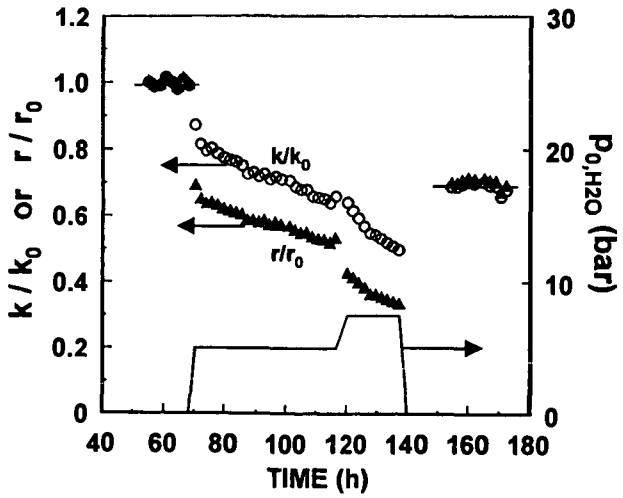

Fig. 1. Activity change during simulated high conversion conditions using a 20%Co-1%Re-1%RE/γ-Al_2O_3 catalyst.
T = 483 K, P = 20 bar, H_2/CO = 2.1.

k/k_0= (Observed rate constant)/(Initial rate constant at 483 K)
r/r_0= (Observed rate)/(Initial rate at 483 K)

k = pseudo 1. order rate constant for H_2 conversion in a plug-flow reactor (contraction factor = -0.5). r = hydrocarbon formation rate (reactor average). $p_{0,H2O}$ = partial pressure of water at the reactor inlet.

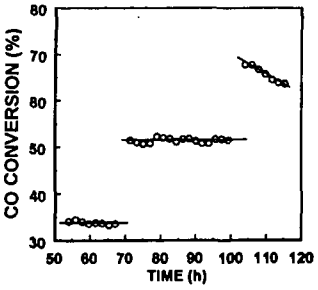

Fig. 2. Conversion vs. time using a 20%Co-1%Re-1%RE/γ-Al_2O_3 catalyst. Step changes in conversion have been obtained by changing the space velocity. T = 483 K, P = 20 bar, H_2/CO = 2.1.

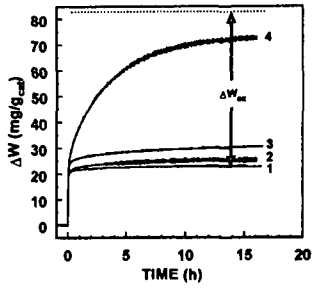

Fig. 3. Weight changes recorded by the microbalance during exposure of 21%Co-1%Re/γ-Al_2O_3 to $H_2O/H_2/He$ or H_2O/He at 523 K and 10 bar. W_{ox} = weight increase corresponding to total reoxidation of cobalt to Co_3O_4, assuming 80% initial extent of reduction.
1. Unreduced catalyst ($p_{H2O}:p_{H2}:p_{He}$ = 5.5:0:4.5 (bar))
2. Reduced catalyst ($p_{H2O}:p_{H2}:p_{He}$ = 5.5:3.7:0.8 (bar))
3. Reduced catalyst ($p_{H2O}:p_{H2}:p_{He}$ = 5.5:0.55:4.0 (bar))
4. Reduced catalyst ($p_{H2O}:p_{H2}:p_{He}$ = 5.5:0:4.5 (bar))

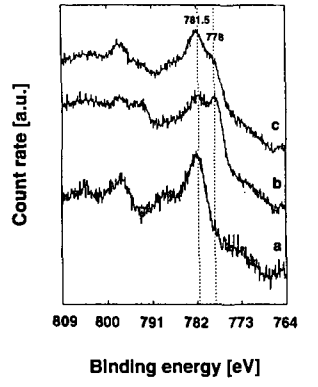

Fig. 4. Co 2p XPS spectra of 20%Co-1%Re-1%RE/γ-Al_2O_3.
a. Calcined catalyst.
b. Catalyst reduced at 723 K for 13 h
c. Reduced catalyst exposed to ~20 vol% H_2O in H_2 for 18 h
(P = 20 bar, T = 513 K)

A PRELIMINARY UNIFIED APPROACH TO THE STUDY OF FISCHER-TROPSCH KINETICS

Rafael L Espinoza
Sastech (Pty) Ltd
P.O. Box 1, Sasolburg 9570
South Africa

Keywords: Fischer-Tropsch, kinetics, modelling

INTRODUCTION

The standard approach to the study of Fischer-Tropsch (FT) kinetics is mainly based on statistical techniques. The rate expression is chosen on the grounds of the "best data fitting" as measured by the correlation factor in parity plots.

For each FT metal (like Co or Fe), there are different - and sometimes conflicting - rate expressions proposed in the literature. The development of a rate expression based on well designed experimental data is a relatively simple task. Therefore we are inclined to believe that - at least most - of the proposed rate expressions are basically correct for the catalyst used to generate the experimental data.

The objective of this study was to ascertain what role the specific characteristics of the FT catalyst plays in its kinetic behaviour. Once the main parameter(s) that affect this behaviour are identified, it should be possible to propose a general rate expression. The results of such a study are presented in this paper, in which a "unified" kinetic approach was taken and a single kinetic expression is proposed for all the different FT metals.

METHODOLOGY

The necessary data were obtained in two ways:

- Simulation of the data from well known kinetic expressions, and
- Using experimental data from the literature.

Use is made of a new kinetic technique, the "Singular kinetic path"[1] (SKP), to study kinetic data available in the literature for different FT metals. In short, the SKP technique discriminates between kinetic expressions based on the relative conversion path. This technique needs little experimental data, in the form of pairs of data points obtained at different space velocities. The two space velocities are selected to be in a ratio of 1 to 4 and this ratio is kept constant through the study. Because the data are relative and normalized, the reconstruction of the conversion path can be performed using pairs of data points obtained at different temperatures, pressures, pairs of space velocities (at a constant ratio) and feed compositions.

Use is also made of a simplified general kinetic model for the generation of the conversion path, based on the pairs of datum points mentioned above. This model is a simple stochastic model in which the feed composition generates large numbers of input molecules. These molecules go through many iterations in which they are converted into products according to the path dictated by the particular rate expression used. The new numbers and species of molecules are updated between iterations. The retention time is simulated by the number of iterations, while the space velocity is simulated by the initial numbers of molecules. Other inputs are the pressure and temperature. Factors like transport phenomena, temperature profiles, etc. do not have an effect on this study due to the relative and normalized handling of the data by the SKP technique[1].

KINETIC ANALYSIS

The following kinetic expressions were used to generate the data for the construction of the SKP plot:

Case 1. "Standard" precipitated Fe catalyst, Anderson[2]:

$$- r_{CO + H_2} = a\, P_{H_2} P_{CO} / (P_{CO} + b\, P_{H_2O}) \quad (1)$$

Case 2. "Standard" cobalt catalyst, Satterfield[3]:

$$- r_{CO + H_2} = c\, P_{CO} P_{H_2} / (1 + d\, P_{CO})^2 \quad (2)$$

Case 3. High Water-Gas-Shift (WGS) Fe catalyst, Ledakowicz[4]:

$$- r_{CO + H_2} = e\, P_{H_2} P_{CO} / (P_{CO} + f\, P_{CO_2}) \quad (3)$$

Case 4. Ruthenium catalyst, Everson[5]:

$$- r_{CO + H_2} = g\, P_{H_2} P_{CO}^{0.38} \quad (4)$$

Case 5. In addition, we used experimental data[6] for a Co-Mn catalyst that exhibited a similar degree of WGS as a typical potassium promoted precipitated iron catalyst.

The SKP plot for these 5 cases is shown in Figure 1. In this figure, the ratio of the space velocities is an arbitrary 4 to 1. Notice that the two iron catalysts (cases 1 and 3) follow a different path. The same comment applies to the two cobalt catalysts (cases 2 and 5). The most noticeable difference between these catalysts is their WGS activity.

In the case of iron catalysts, the well known Anderson equation has a water partial pressure term in the denominator. That is, the accumulation of water has a negative effect on the rate of reaction. The Anderson equation is not able to reproduce Ledakowicz's data, since almost all the reaction water disappears due to the very high WGS activity of his catalyst. To solve this problem, Ledakowicz used a CO_2 term in the denominator of his kinetic expression. Notice that both the Anderson and Ledakowicz kinetic expressions can be considered particular cases of the more general rate expression:

$$- r_{CO + H_2} = h\, P_{H_2} P_{CO} / (P_{CO} + i\, P_{H_2O} + j\, P_{CO_2}) \quad (5)$$

Where for the "standard" iron, j = 0, and for the very high WGS iron, i = 0.

The FT and WGS equations can be represented by:

$$\text{FT:} \quad CO + (1 + x/2)\, H_2 \rightarrow CH_x + H_2O \quad (6)$$

$$\text{WGS:} \quad CO + H_2O \leftrightharpoons CO_2 + H_2 \quad (7)$$

From equations (6) and (7), it is evident that the extent of the ($CO + H_2$) conversion is proportional to the generation of $CO_2 + H_2O$. Therefore, it should be possible to use the ($H_2 + CO$) conversion (CONV) in the denominator of the rate expression, instead of the CO_2 and H_2O terms.

Such an approach was used to reproduce the SKP paths shown in Figure 1. We found that it was necessary to use the square root of the CO term in the numerator. The expression to reproduce the SKP paths is:

$$- r_{CO + H_2} = m\, P_{H_2} P_{CO}^{0.5} / (P_{CO} + k\, CONV) \quad (8)$$

In this expression, the conversion can be represented in terms of the partial pressures of the H_2, CO and the generation of H_2O and CO_2.

The k constants for the different catalysts are:

Ruthenium catalyst:	about	0.01 - 0.02
"Standard" cobalt catalyst:	about	0.01 - 0.02
"Standard" precipitated iron catalyst:		0.3 - 0.5
"High" WGS cobalt catalyst:		0.4 - 0.5
High WGS iron catalyst:		3.5

The WGS activity of typical ruthenium and cobalt catalysts is very low compared to typical precipitated iron catalysts[7]. The WGS activity of the high WGS cobalt catalyst is very similar to that of precipitated iron catalysts[6], while the WGS activity of the high WGS iron catalyst[4] was so high that practically all the water reacted to CO_2. It seems therefore that the k constant in equation (8) is a function of the WGS activity of the catalyst.

This observation is reinforced by the fact that two different FT catalysts that have similar WGS activity (the cobalt catalyst of case 5 and the "standard" iron catalyst of case 1) follow the same specific kinetic equation of Anderson[2].

Equation (8) shows that it is possible to express the interaction of the reactants or SKP path for different FT catalysts using a single equation. The next step is to consider the activation energy.

The activation energies proposed in the literature are not so different from each other, even for different FT metals. Most of the published activation energies for cobalt are between 93 - 103 kJ/mol[3]. For iron, the range for the published activation energies is somewhat larger[8], mainly from 70 - 100 kJ/mol; while for ruthenium, Everson[5] proposes 80 kJ/mol.

Since these activation energies overlap, as a first approximation a figure of 93 kJ/mol will be assumed for use in equation (8). The general equation would then be:

$$- r_{CO + H_2} = n\, e^{(-93/RT)}\, P_{H_2} P_{CO}^{0.5} / (P_{CO} + k\, CONV) \qquad (9)$$

The accuracy of the proposed general equation (9) was tested by comparing it with experimental data or kinetic rate expressions and SKP path for the 5 different catalysts described previously. The range of operating conditions used in the comparison is shown in Table 1.

The results are plotted in Figure 2 in the form of a parity plot. This figure shows that the general FT equation reproduces the experimental data or the predicted conversions using specific equations in an acceptable manner. There are some deviations which could be due to the fact that the proposed equation (9) is still not the optimal one. In addition, some deviations from proposed kinetic expressions are usually present due to experimental error.

CONCLUSIONS

It seems to be possible to model the conversion shown by different FT catalysts using a single kinetic rate expression. This expression applies to different metals and for catalysts that, despite having the same FT metal, exhibit different kinetic behaviour. This general kinetic expression is a first approximation, and it should be possible to improve it. Its objective was to ascertain the feasibility of a unified kinetic approach to FT kinetics.

The only variable in this expression is a term that is a function of the WGS activity of the specific catalyst being modelled. We can only speculate about this relationship at present. There may be an overlap for the sites responsible for the FT and the WGS reactions, which could explain the intimate relationship between the FT and WGS activities (besides the one due to the effect of FT and WGS on partial pressures) and its impact on the FT kinetic rate expression.

Should this be the case, then the path followed by the FT reaction is more dependent upon the reduced/oxidized state of the surface than on the chemical composition of the FT catalyst under consideration.

The applicability of the general kinetic rate expression means that there is still much to be done in FT catalysis, particularly in the surface field, in the understanding of the nature of the active sites for the FT and the WGS reactions, and in their interaction.

The results from this study also point out that perhaps different FT metals should not be studied in isolation and that more insight could be gain from an unified research approach.

REFERENCES

1. Espinoza, R.L., *Preprints, Int. Conf. on Catalysis & Catalytic Processing*; pp 391 -402, 1993, Cape Town, South Africa.
2. Anderson, R.B., *Catalysis, Emmet, P.H., (Ed) Vol 4, Reinhold*, 1956, New York.
3. Satterfield, C.N., Yates, I.C., *Energy & Fuels*, 1991, 5, 168 - 173.
4. Ledakowicz, S.; Nettelhoff, H.; Kokuun, R.; Deckwer, W.-D., *Ind. Eng. Chem. Process Des. Dev.*, 1985, 24, 1043 -1049.
5. Everson, R.C.; Mulder, H.; Keyser, M.J. *Proceedings of 7th Nat. Meeting of the South African Institution of Chem. Engineers*; pp 840 - 848, 1994, Esselen Park, South Africa.
6. Keyser, M., Ph.D. Thesis, Potchefstroomse University, Thesis submitted.
7. Dry, M.E., *The Fischer-Tropsch Synthesis, Catal. Science and Technology*, Anderson, J.R. and Boudart, M. (Eds), Vol 1, Springer-Verslag, 1981.
8. Huff, G.A.; Satterfield, C.N., *Ind. Eng. Chem. Process Des. Dev.*, 1984, 23, 696 -705.

TABLE 1: Range of operating conditions for the comparison of the proposed General Kinetic expression versus experimental data or specific kinetic equations for the 5 cases under study.

Catalyst	Pres. (bar)	Temp. (°C)	H_2/CO (in)	Mode of comparison
Case 1	20 - 35	220 - 260	1 - 3	Anderson eq.
Case 2	20 - 35	210 - 240	0.5 - 3	Satterfield eq.
Case 3	10	220 - 260	0.7 - 0.8	Exp. data
Case 4	20 - 35	210 - 240	0.5 - 2	Everson eq.
Case 5	5 - 20	220	1 - 5	Exp. data

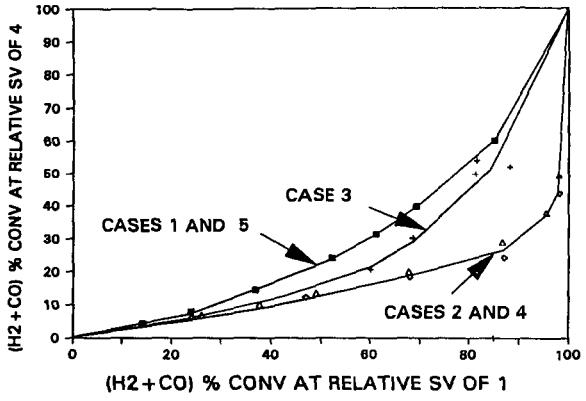

Figure 1. SKP Plot for the 5 different catalysts

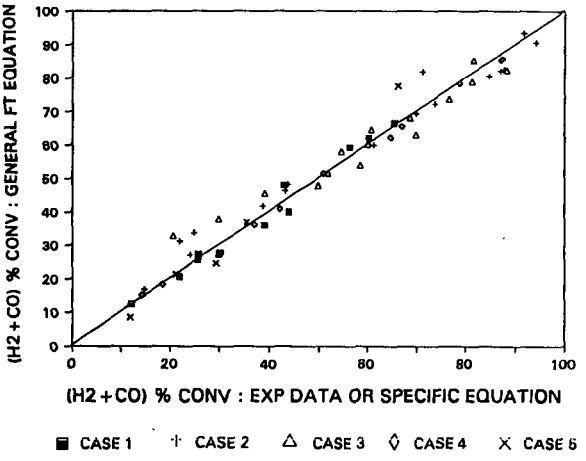

Figure 2. Parity plot between the general FT equation and specific FT equations or experimental data for the 5 cases under study

ROLE OF CO_2 IN THE INITIATION OF CHAIN GROWTH DURING THE FISCHER-TROPSCH SYNTHESIS

Burtron H. Davis, Liguang Xu, Shiqi Bao, Li-Min Tau,
Birbal Chawla and Hossein Dabbagh

Center for Applied Energy Research, University of Kentucky, 3572 Iron Works Pike, Lexington, KY 40511

Keywords: Fischer-Tropsch Synthesis, Isotopic Tracer, Iron Catalyst

ABSTRACT

Data are presented to show that alcohols produce hydrocarbons during the Fischer-Tropsch Synthesis (FTS) that are not consistent with a simple initiation mechanism. CO_2 is produced directly from the alcohol, and not by the reverse of the carbonylation reaction. CO_2 also initiates chain growth in the FTS, and the initiation intermediate is presumed to be the same intermediate as in the water-gas-shift reaction.

INTRODUCTION

The Fischer-Tropsch Synthesis involves the production of many hydrocarbon and oxygenate products from CO and H_2. This makes the analysis of the products very difficult and adds much complexity to the interpretation of the data to develop a consistent mechanism for the reaction. In an effort to obtain data to aid in understanding this complex system, isotopic tracer studies have been utilized. One approach has employed ^{14}C-labeled intermediates (1-6). The early results from the use of ^{14}C-labeled intermediates led to the proposal of an oxygen containing structure that is considered to be responsible for the initiation of the growing chain on the surface of iron catalysts (1-3). With the advent of surface analytical instrumentation, the presence of carbon, but not a significant amount of oxygen on the catalyst surface led workers to question the role of the oxygenated intermediate, and revived the carbide mechanism. However, this latter carbide mechanism differed from that of the one advanced by Fischer and Tropsch (7), where the synthesis was postulated to occur by utilizing the bulk carbide as an intermediate, since the carbide is now believed to be restricted to a surface metal carbide structure (8).

EXPERIMENTAL

The catalyst utilized for all but one of the experiments described below was a C-73 fused iron catalyst manufactured by the United Catalyst, Inc. Prior to use the catalyst was reduced at 400°C in flowing hydrogen and passivated after decreasing the temperature of the catalyst to room temperature. The passivated catalyst was slurried in octacosane in a one liter continuously stirred tank reactor (CSTR) and again reduced at 262°C for three days. The reaction was conducted using a CO/H_2 ratio of 1, 262°C, 8 atm. total pressure and a flow rate of synthesis gas to provide 60% conversion of CO. The ^{14}C-tracer compound was added, using a piston pump or as a CO_2/CO gas mixture, so that the carbon added in the tracer was 3 or less atomic % of the total carbon added to the CSTR. Liquid products were collected and analyzed for radioactivity as detailed in an earlier report (9).

Experiments with the $^{14}CO_2$ were conducted by adding the labeled-gas to the synthesis gas prior to entering a 1-liter mixing vessel. The catalyst utilized in this synthesis was a proto-type catalyst containing 0.03% K, 12% CuO and the remainder Fe_2O_3. The experimental conditions were otherwise similar to those reported for the C-73 catalyst.

RESULTS

The results for the radioactivity in liquid alkane fractions show that the normal primary alcohol is incorporated to a much greater extent that the corresponding alpha olefin (Figure 1). This result, as did earlier data, suggests that the oxygen-containing compound is a potential chain initiator.

One of the puzzling aspects of the tracer studies was the observation that the radioactivity/mole of alkane decreased approximately as the logarithm of the with carbon number. It was postulated that this was a result of the FTS involving two surface chains.

Furthermore, one chain produced alkanes, alkenes and oxygenates and was initiated by the added alcohol or alkene while the other chain was not initiated by the alcohol and produced only alkanes. These two chains could not have a common intermediate and would therefore occur on different catalytic sites (10).

Another puzzling aspect of the results obtained during the addition of the ^{14}C-labeled alcohol is the production of CO_2 that contains more ^{14}C/mole than the CO. It is generally believed that the CO_2 that is formed during the FTS with an iron catalyst is formed by the water-gas-shift reaction:

$$CO + H_2O \rightleftarrows CO_2 + H_2 .$$

If the primary alcohol formed CO through the reverse carbonylation reaction,

$$RCH{=}CH_2 + CO + H_2 \rightleftarrows RCH_2CH_2OH,$$

and this CO then underwent the water-gas-shift reaction, the CO_2 would have the same radioactivity/mole as the CO. However, when 1-^{14}C-1-pentanol was added to the synthesis gas the radioactivity/mole of the CO_2 was much greater than that of the CO (Figure 2). This means that the CO_2 could not have been formed by decarbonylation followed by the water-gas-shift reaction. In order to ensure that the results with 1-^{14}C-1-pentanol were reliable, 2-^{14}C-1-hexanol was synthesized and added to the synthesis gas under reaction conditions that were identical to those utilized with 1-^{14}C-1-pentanol. As can be seen from the data in Figure 2, the radioactivity of both CO and CO_2 are below the detection limit while that of pentane is high compared to that of 1-pentene. The radioactivities/mole of the C_3 and C_4 hydrocarbons are below the detection limit. The results in Figure 2 clearly show that the added alcohol has undergone conversion to produce CO_2 that is derived from the carbonyl carbon and that the alkyl group remaining has been converted directly to the alkane rather than to the 1-alkene which is then hydrogenated to the alkane.

The data in Figure 2 are consistent with a mechanism in which the adsorbed alcohol reacts with a surface oxygen; thus, it appears that the reaction can be adequately described by the following mechanism:

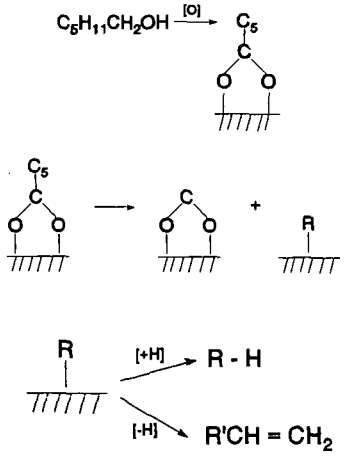

Additional data to support the above mechanism has now been obtained by adding $^{14}CO_2$ to the synthesis gas. If the FTS chains are initiated by species derived only from CO then the hydrocarbon products produced from the experiment with $^{14}CO_2$ could not have a radioactivity/mole that was greater than that of CO. The $^{14}CO_2$ was added so that it contained only 0.3% of the carbon that was added; thus, the composition of the gases in the CSTR was not altered significantly by the added $^{14}CO_2$. The radioactivity/mole of the CO, CO_2, CH_4, and C_2H_6 are given in Table 1.

If the methane had been formed only from CO then the radioactivity/mole of methane and ethane could not have exceeded that of the CO since the experiment was conducted in a CSTR where all of the catalyst particles are exposed to the same gas composition. The

methane has an activity that approaches that of the added CO_2, rather than that of the CO. This requires the formation of methane to be initiated from CO_2. The activity of ethane is also close to that of the CO_2 showing that it is the FTS that is initiated to a large extent by an intermediate derived from CO_2, and not just the formation of methane.

Data for the C_1-C_9 hydrocarbons formed during the addition of $^{14}CO_2$ are presented in figure 3. The CPM/mole for the CO and CO_2 in the exit gas are shown by the solid triangles labeled by CO and CO_2, respectively. It is apparent that the CO_2 has a much higher radioactivty than does the CO. The broken line passing through the radioactivity for the CO represents the increase in radioactivity with carbon number of the hydrocarbon products if they were formed only from CO. In this case each hydrocarbon, C_n, would contain the radioactivity of n carbons derived from the CO. It is clear that the radioactivity of each of the products is much higher than could result from synthesis using CO only. The radioactivity of the hydrocarbon products are shown in open circles, resulting from analysis using the gas analyzer, and open squares, resulting from analysis using a Porpack column that permits the analysis of hydrocarbons of higher carbon numbers. For the moment, we concentrate on the radioactivities of the C_3-C_9 products. The solid line representing these data is parallel to the broken line passing through the radioactivity for CO. For the C_3-C_5 hydrocarbons, the radioactiviy measured using the different g.c. instruments show good agreement. Futhermore, the line defined by the C_3-C_9 hydrocarbons extrapolates to a radioactivity of about 0.8×10^3 CPM/mole. The slope of the solid line in figure 3 indicates that chain growth is primarily due to addition of carbon units derived from CO; the similar slopes of the solid and the broken lines are considered to require this conclusion. However, it appears that about 60% of the hydrocarbon chains that lead to C_3-C_9 hydrocarbon products are derived from CO_2. From the higher activity of the C_1 and C_2 hydrocarbons, it appears that even more than 60% of these products are derived from CO_2 initiation. It therefore seems clear that the data in figure 3 require the species that is responsible for the chain initiation be different from the species that is responsible for chain propogation. Futhermore, the species responsible for chain initiation is derived from both CO_2 and CO but the species that is responsible for chain propagation is derived from CO. Thus, it is concluded that the species that is responsible for chain initiation retains some oxygen, and in this respect is similar to the postulates of Emmett and coworkers.

CONCLUSION

It appears that the FTS mechanism with an iron based catalyst involves an oxygenate species that can be derived from both CO and CO_2. The data generated from the above studies involving the addition of CO_2 or alcohol are consistent with a reaction mechanism that involves reactions as shown above for the alcohol. Thus, the intermediate that is involved in the water-gas-shift reaction is postulated to be an initiator for chain growth for the FTS reaction.

ACKNOWLEDGMENT

This work was supported with funding from the Commonwealth of Kentucky and the U.S. Department of Energy, Pittsburgh Energy Technology Center, through Contract No. De-AC22-84PC70029 and DE-AC22-94PC94055.

REFERENCES

1. G. Blyholder and P. H. Emmett, *J. Phys. Chem.*, **63**, 962 (1959).
2. W. K. Hall, R. J. Kokes and P. H. Emmett, *J. Am. Chem. Soc.*, **82**, 1027 (1960).
3. W. K. Hall, R. J. Kokes and P. H. Emmett, *J. Am. Chem. Soc.*, **79**, 2983 (1957).
4. L-M. Tau, H. A. Dabbagh and B. H. Davis, *Catal. Lett.*, **7**, 141 (1990).
5. L.-M. Tau, H. A. Dabbagh and B. H. Davis, *Energy & Fuels*, **5**, 174 (1991).
6. L-M. Tau, H. A. Dabbagh, J. Halasz and B. H. Davis, *J. Mol. Cat.*, **71**, 37 (1992).
7. F. Fischer and H. Tropsch, *Brennst. Chem.*, **4**, 276 (1923).
8. K. Kishi and W. M. Roberts, *J. Chem. Soc. Faraday Trans. I*, **71**, 1715 (1975).
9. L. M. Tau, H. Dabbagh, B. Chawla and B. H. Davis, Final Report, E-AC22-84PC70029, January, 1988.
10. L. M. Tau, H. Dabbagh, S. Bao and B. H. Davis, *Catal. Lett.*, **7** (127 (1990).

Table 1. Radioactivity/mole of Effluent Gas Products

Compound	Radioactivity, Counts/Min./Mole
CO	0.12×10^{-3}
CO_2	1.31×10^{-3}
CH_4	1.12×10^{-3}
C_2H_6	1.28×10^{-3}

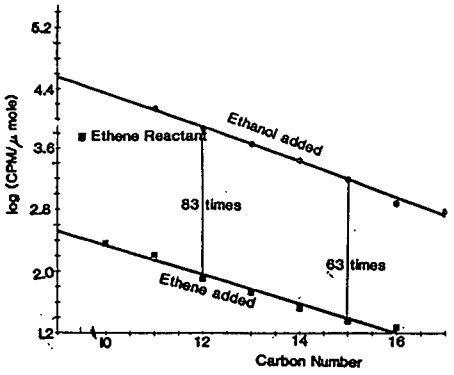

Figure 1. The ^{14}C activity in the alkane products formed when 1-pentanol (●) or 2-pentene (■) was added to the syngas feed to a C-73 catalyst (CSTR, 262°C, 8 atm).

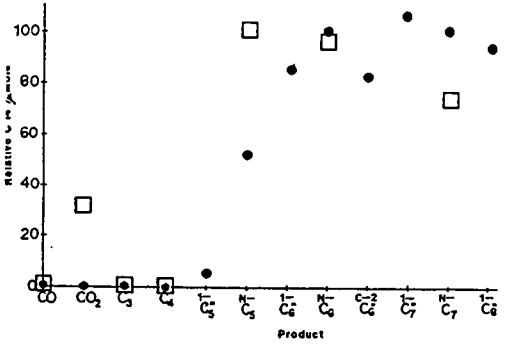

Figure 2. Products (gas phase) from the conversion of a syngas containing either 2-^{14}C-1-hexanol (◆, ●) or 1-^{14}C-1-pentanol (□) with a C-73 catalyst at 262°C and 8 atm (total) in a CSTR.

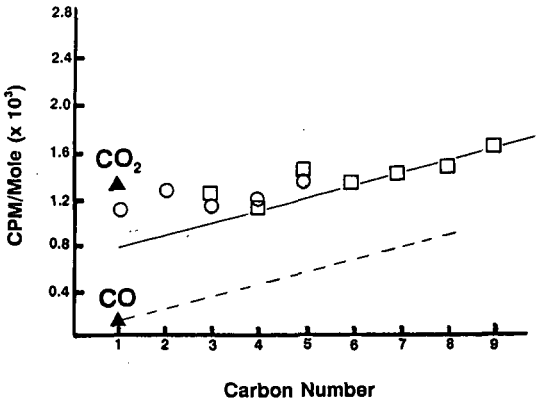

Figure 3. The ^{14}C activity in the alkane products formed when $^{14}CO_2$ is added to the synthesis gas fed to the UCI proto-type iron catalyst (CSTR, 270°C, 8 atm).

ZIRCONIA PROMOTION OF FISCHER-TROPSCH COBALT CATALYSTS: BEHAVIOR IN FIXED-BED AND SLURRY BUBBLE COLUMN REACTORS

R. Oukaci, J.G. Goodwin, Jr., G. Marcelin, and A. Singleton[1]
Chemical & Petroleum Engineering Department
University of Pittsburgh
Pittsburgh, PA 15261
[1] Energy International Corporation, 135 William Pitt Way, Pittsburgh, PA 15238.

Keywords: Fischer-Tropsch Synthesis, CO Hydrogenation, Cobalt Catalysts.

ABSTRACT
A series of cobalt-based F-T catalysts supported on alumina and silica were prepared with different loadings of Zr and different sequence of impregnation of Co and Zr. All catalysts were extensively characterized by different methods. The catalysts were evaluated in terms of their activity and selectivity both in fixed bed and slurry bubble column reactors. Addition of ZrO_2 to both Co/SiO_2 and Co/Al_2O_3 catalysts resulted in at least a twofold increase in the catalyst activity for F-T synthesis in the fixed bed reactor. In the slurry bubble column reactor, a similar promotion effect was observed for the SiO_2-supported catalysts, while the addition of Zr to a cobalt/alumina catalyst had a less significant effect.

INTRODUCTION
Cobalt has been one of the most commonly used metals for Fischer-Tropsch catalysts since the 1930's because of its high activity (1). It has received a lot of attention recently (2-8) due to its usefulness in converting CO to liquid hydrocarbons. While many promoters for Fischer-Tropsch (F-T) synthesis, such as the alkali series, have been extensively studied, others such as Zr have not. A number of studies of F-T synthesis over ZrO_2-supported Co (1,9), Ni (9), Ni/Co (9), and Pd (10) have been reported in the literature. The use of ZrO_2 as the support for these different active metals has been found to increase the higher hydrocarbon selectivity. Recently, a number of patents by Shell (11-13) have involved Zr promotion of Co/SiO_2. Addition of up to 15 wt% ZrO_2 promotor was found to increase the overall activity of the Co catalyst without affecting the selectivity for higher hydrocarbons.

A series of cobalt-based F-T catalysts supported on alumina and silica were prepared with different loadings of Zr and different sequence of impregnation of Co and Zr in order to investigate the role of ZrO_2 on affecting the F-T reaction in both fixed bed and slurry bubble column reactors.

EXPERIMENTAL
All catalysts compared in this study consisted of 20 wt% cobalt and different amounts of zirconia (up to 15 wt% Zr), the support being alumina (Vista B) or silica (Davison 952). The supports, calcined at 500°C for 10 hours prior to catalyst preparation, were loaded with Co and/or Zr by either a single or 2-step impregnation method. Aqueous solutions of cobalt nitrate and/or zirconium nitrate were used to prepare all the catalysts except in the case of $S[Co/8.5Zr(O)]/SiO_2$, where a solution of zirconium tetra-n-propoxide in a mixture of n-propanol, toluene, and acetyl acetone was used to impregnate the Zr in the initial impregnation step. In the case of single step impregnations, the SiO_2-supported catalysts were prepared by kneading (11-13) the aqueous metal precursor solution-support mixture for 3.5 hours. For the sequentially impregnated SiO_2-supported catalysts, kneading was used in the initial step for the addition of Co, followed by use of the incipient wetness method for the impregnation of Zr (11-13). For the other sequentially impregnated SiO_2-catalysts and all the alumina-supported catalysts, the incipient wetness method was used in both steps. After the first impregnation step, the catalyst was dried in an oven for 5 hours at 115°C with occasional stirring. Then, it was calcined in air by raising its temperature to 300°C with a heating rate of 1°C/min and holding for 2 hours. Also, after the second step of impregnation (if used) the catalyst was dried and calcined identically as in the first step. The catalysts are listed in Table 1 with the corresponding preparation methods.
Prior to H_2 chemisorption or reaction, the catalysts were reduced in H_2 at 250°C for the SiO_2-supported catalysts and 350°C for the Al_2O_3-supported catalysts, for 10 hours following a 1°C/min ramp. They have all been extensively characterized by different methods, including elemental analysis, BET physisorption, particle size distribution, X-ray diffraction, hydrogen chemisorption, temperature programmed reduction. Table 2 summarizes the relevant characterization data.

The catalysts were evaluated in terms of their activity and selectivity both in a fixed bed reactor and in a slurry bubble column reactor. Typically, 0.15 to 0.35 g of prereduced

catalyst were charged into the fixed bed reactor tube and rereduced overnight at 300°C. The reaction was carried out at 220°C, 1 atm, H_2/CO ratio of 2.0, and a total flow rate of 90 cm^3/min. No inert diluent was used. Sample analyses were taken after approximately 2, 5, 9, and 24 hours on-stream. In some cases the temperature was varied between 210 and 240°C in order to calculate an Arrhenius activation energy. Product analysis for C1 to C20 hydrocarbons was performed by on-line gas chromatography. CO conversion rates were calculated based on the GC analysis of the products. Anderson-Schultz-Flory (A-S-F) distributions were plotted and the chain growth probability, α, calculated using the C4 to C16 data.

For the slurry bubble column tests, the catalyst was first reduced *ex-situ* in a fluidized bed assembly and then transferred into a glove box for weighing and subsequent transfer into the slurry bubble column reactor. Approximately 15 g of catalyst and 200 g of liquid medium were used in a run. Typically, the reaction was carried out at 240°C, a total pressure of 450 psi, H_2/CO ratio of 2, and 60% N_2 diluent. Analysis of the gas products, CO, CO_2 and C1 to C5, was performed hourly. Liquid products were collected at the end of each 24 hour period, blended, and submitted for analysis. A-S-F plots of the liquid products were used to determine α. After reaching steady-state under these conditions, temperature, pressure, and H_2/CO ratio were varied in turn to study the effect of process conditions. A typical complete run lasted about 10 days. Only the base Co catalysts (non-promoted Co/SiO_2 and Co/Al_2O_3) and the most active catalysts in the fixed bed reactor were tested in the slurry bubble column reactor.

RESULTS AND DISCUSSION

From XRD measurements, it was found that the average diameter of the Co oxide crystallites for all catalysts varied within a narrow range (ca. 20-30 nm), regardless of the amount of Zr present or the support used. In addition, the XRD results suggest that Zr was highly dispersed on Co/SiO_2 since no Zr compound phases were detected.

The TPR results show little difference in the degree of reduction for all the catalysts with the exception of CI[0.7Zr+Co]/SiO_2 and S[Co/8.5Zr]/Al_2O_3 which exhibited the lowest and the highest reducibility, respectively. The Al_2O_3-supported catalysts had in general higher reducibilities than their silica-supported analogs. It was also found that all the catalysts used in this study were reduced to the maximum degree (defined as % Co reduced during TPR to 900°C) during the standard reduction procedure at 250°C.

The sequentially-impregnated Zr/Co on SiO_2 catalysts showed an increase in the amount of total hydrogen chemisorbed compared to that for [Co]/SiO_2. On the other hand, for the sequentially-impregnated Co/Zr on SiO_2 catalysts, the Zr addition did not influence significantly the amount of H_2-chemisorption. The co-impregnated catalyst (CI[8.5Zr+Co]/SiO_2 had almost twice as much H_2 uptake as either CI[0.7Zr+Co]/SiO_2 or [Co]/SiO_2. The opposite effect was observed with the Al_2O_3-supported catalysts. The sequentially-impregnated Co/Zr on Al_2O_3 catalyst and the co-impregnated catalyst with low Zr loading (CI[1.4Zr+Co]/Al_2O_3 had the highest H_2 uptakes.

Table 3 shows selected data obtained from fixed bed reaction which indicate the effect of ZrO_2 promotion on F-T activity and selectivity. While the alumina-supported Co catalysts were found to be in general more active than their silica-supported analogs, Zr promotion of both Co/SiO_2 and Co/Al_2O_3 increased significantly the overall rate of F-T synthesis, compared to the non-promoted catalysts. In addition, the promoting effect of ZrO_2 was more significant on the alumina-supported catalysts, especially the sequentially impregnated catalyst S[Co/8.5Zr]/Al_2O_3. The method of preparation and the amount of promoter used also affected the catalyst activity and selectivity. The sequentially impregnated [Co/Zr] catalysts appeared to be the most active. Addition of Zr beyond 8.5 wt% for the SiO_2-supported catalysts did not seem to have any beneficial effect. The catalysts with the highest Zr loadings (wt% Zr > 1.4) had the highest values of α compared to the non-promoted catalysts, even though the CH_4 selectivity was also slightly higher in several cases. On the other hand, small amounts of Zr promotion (wt% Zr = 0.7 or 1.4) appeared to have a slightly negative effect on the values of α.

Table 4 shows selected data obtained at 240°C, 450 psi, and H_2/CO ratio of 2, in the slurry bubble column reactor for catalysts consisting of Co supported on silica and alumina, respectively. As in the case of the fixed bed testing, the ZrO_2 promoter was found to influence the overall activity of both the silica- and alumina-supported catalysts. However, while the alumina-supported Co catalysts were also found to be in general more active than their silica-supported analogs, the promoting effect of ZrO_2 was not as significant on the

alumina-supported catalysts. Diffusion limitations in the liquid medium in the slurry bubble column reactor may be invoked to explain the discrepancies in the results obtained in the two reaction systems. The overall rate observed for the catalyst S[Co/8.5Zr]/Al_2O_3 was high, but most probably diffusion limited.

In summary, ZrO_2 appears to be an excellent rate promoter for SiO_2- and Al_2O_3-supported Co catalysts. Addition of Zr in both catalysts, probably hinders the formation of Co aluminates and Co silicates, either during the preparation and pretreatment or during the F-T synthesis reaction itself. In addition, high levels of promotion act to increase the selectivity for higher hydrocarbons.

ACKNOWLEDGMENTS
The authors gratefully acknowledge the funding of this project by DOE and the contribution of the following personnel involved in this study: S. Ali, L. Balawejder, P. Brim, B. Chen, W. Gall, and S. Renaldi.

REFERENCES
1. Withers, H. P., Jr., and Eliezer, K. F., and Mitchell, J. W., Ind. Eng. Chem. Res. **29**, 1807 (1990).
2. Brady, R. C., and Pettit, R., J. Am. Chem. Soc. **103**, 1287 (1981).
3. Reuel, R. C., and Bartholomew, C. H., J. Catal. **85**, 78 (1984).
4. Reuel, R. C., and Bartholomew, C. H., J. Catal. **85**, 63 (1984).
5. Foley, H. C., and Hong, A. J., Appl. Catal. **61**, 351 (1990).
6. Rathousky, J., Zukal, A., Lapidus A., and Krylova, A., Appl. Catal. **79**, 167 (1991).
7. Iglesia, E., Soled, S. L., and Fiato, R. A., J. Catal. **137**, 212 (1992).
8. Iglesia, E., Soled, S. L., Fiato, R. A., and Grayson, H., J. Catal. **143**, 345 (1993).
9. Bruce, L. A., Hope, G. J., and Mathews, J. F., Appl. Catal. **8**, 349 (1983).
10. Alekseev, O. S., Zaikovskii, V. I., and Ryndin, Yu. I., Appl. Catal. **63**, 37 (1990).
11. Hoek, A., Joustra, A. H., Minderhould, J. K., and Post, M. F., UK Pat. Appl. GB 2 125 062 A (1983).
12. Hoek, A., Minderhould, J. K., and Post, M. F. M., Lednor, P. W. Eur. Pat. Appl. EP 110 449 A1 (1984).
13. Post, M. F. M. B., and Sie, S. T. B., Eur. Pat. Appl. 0 167 215 A2 (1985).

Table 1: Catalyst Preparation Methods Used

Catalyst[a]	Step # 1[b]		Step # 2[b]	
	Method	Solution	Method[a]	Solution
[Co]/SiO_2	Kneading	aqueous(Co)	N/A	N/A
S[0.7Zr/Co]/SiO_2	Kneading	aqueous(Co)	Inc. Wet.	aqueous(Zr)
S[1.4Zr/Co]/SiO_2	Kneading	aqueous(Co)	Inc. Wet.	aqueous(Zr)
S[8.5Zr/Co]/SiO_2	Kneading	aqueous(Co)	Inc. Wet.	aqueous(Zr)
S[Co/4.0Zr]/SiO_2	Inc. Wet.	aqueous(Zr)	Inc. Wet.	aqueous(Co)
S[Co/8.5Zr(O)]/SiO_2	Inc. Wet.	organic(Zr)	Inc. Wet.	aqueous(Co)
S[Co/8.5Zr]/SiO_2	Inc. Wet.	aqueous(Zr)	Inc. Wet.	aqueous(Co)
S[Co/15.0Zr]/SiO_2	Inc. Wet.	aqueous(Zr)	Inc. Wet.	aqueous(Co)
CI[0.7Zr+Co]/SiO_2	Kneading	aqueous(Co+Zr)	N/A	N/A
CI[8.5Zr+Co]/SiO_2	Kneading	aqueous(Co+Zr)	N/A	N/A
[Co]/Al_2O_3	Inc. Wet.	aqueous(Co)	N/A	N/A
CI[1.4Zr+Co]/Al_2O_3	Inc. Wet.	aqueous(Co+Zr)	N/A	N/A
CI[8.5Zr+Co]/Al_2O_3	Inc. Wet.	aqueous(Co+Zr)	N/A	N/A
S[8.5Zr/Co]/Al_2O_3	Inc. Wet.	aqueous(Co)	Inc. Wet.	aqueous(Zr)
S[Co/8.5Zr]/Al_2O_3	Inc. Wet.	aqueous(Zr)	Inc. Wet.	aqueous(Co)

(a) Nomenclature: S = sequential impregnation, CI = co-impregnation; [A/xxB] = "A" impregnated after "B", [A+xxB] = co-impregnated "A" and "B"; B(O) = organic compound of B used instead nitrate (nonaqueous impregnating solution); xx = wt% Zr.
(b) Catalysts dried for 5 hrs at 115 °C and calcined for 2 hrs at 300°C after each step.

Table 2: Catalyst Characterization Results

Catalyst	H_2 Chemisorption		TPR	XRD
	Total (μmol H_2/g cat)	% Co Dispersion	% Reduct. (25-900°C)	Co_3O_4 d_p (nm)
[Co]/SiO_2	82	4.8	75	27
S[0.7Zr/Co]/SiO_2	141	8.3	80	28
S[1.4Zr/Co]/SiO_2	149	8.8	81	27
S[8.5Zr/Co]/SiO_2	122	7.2	81	29
S[Co/8.5Zr(O)]/SiO_2	87	5.1	75	31
S[Co/8.5Zr]/SiO_2	93	5.5	75	27
CI[0.7Zr+Co]/SiO_2	67	4.0	64	20
CI[8.5Zr+Co]/SiO_2	125	7.3	77	24
[Co]/Al_2O_3	48	2.8	85	20
CI[1.4Zr+Co]/Al_2O_3	71	4.2	82	19
CI[8.5Zr+Co]/Al_2O_3	55	3.2	85	26
S[8.5Zr/Co]/Al_2O_3	43	2.5	79	24
S[Co/8.5Zr]/Al_2O_3	114	6.7	96	22

Table 3: Fixed Bed Reaction Results

Catalyst	ACTIVITY		SELECTIVITY	
	% CO Conversion	Rate (g CH_2/g cat/hr)	CH_4 (wt%)	α
[Co]/SiO_2	2.9	0.094	22.4	0.61
S[0.7Zr/Co]/SiO_2	3.8	0.121	26.7	0.55
S[1.4Zr/Co]/SiO_2	3.8	0.123	28.3	0.56
S[8.5Zr/Co]/SiO_2	3.9	0.125	28.9	0.67
S[Co/4.0Zr]/SiO_2	2.6	0.161	22.2	0.73
S[Co/8.5Zr(O)]/SiO_2	5.7	0.182	28.7	0.62
S[Co/8.5Zr]/SiO_2	5.0	0.160	23.5	0.63
S[Co/15.0Zr]/SiO_2	3.1	0.179	22.7	0.73
CI[0.7Zr+Co]/SiO_2	3.6	0.114	28.0	0.56
CI[8.5Zr+Co]/SiO_2	4.6	0.147	22.0	0.69
[Co]/Al_2O_3	3.3	0.077	28.4	0.62
CI[8.5Zr+Co]/Al_2O_3	3.3	0.183	22.0	0.70
S[8.5Zr/Co]/Al_2O_3	1.3	0.73	24.1	0.67
S[Co/8.5Zr]/Al_2O_3	5.0	0.275	24.0	0.67

P = 1 atm, T = 220°C, H_2/CO = 2, Catalyst Weight = 0.15-0.35 g, Total Flow Rate = ca. 90 cm^3/min, Time-on-stream = ca. 25 hrs

Table 4: Slurry Bubble Column Reaction Results

Catalyst	ACTIVITY		SELECTIVITY	
	% CO Conversion	Rate (g CH_2/g cat/hr)	CH_4 (wt%)	α
[Co]/SiO_2	14.3	0.67	7.6	0.83
S[Co/8.5Zr(O)]/SiO_2	25.5	1.21	8.6	0.84
S[Co/8.5Zr]/SiO_2	26.6	1.24	10.7	0.82
S[Co/15.0Zr]/SiO_2	20.9	0.93	6.7	0.83
CI[0.7Zr+Co]/SiO_2	23.2	1.08	9.4	0.82
CI[8.5Zr+Co]/SiO_2	24.8	1.18	8.5	0.84
[Co]/Al_2O_3	27.1	1.34	7.9	0.82
CI[1.4Zr+Co]/Al_2O_3	30.9	1.41	12.1	0.83
S[Co/8.5Zr]/Al_2O_3	27.5	1.54	10.4	0.84

Catalyst weight: 13-17g, T = 240°C, P = 450 psi, H_2/CO ratio = 2, Total flow rate = ca.15 L/min, or 3 cm/sec linear velocity, Diluent: N_2: ca. 60%.

A NOVEL APPROACH FOR THE ASSESSMENT OF THE RATE LIMITING STEP IN THE FISCHER-TROPSCH SLURRY PROCESS

J. R. Inga and B. I. Morsi
Chemical and Petroleum Engineering, University of Pittsburgh,
1249 Benedum Engineering Hall
Pittsburgh, PA 15261, U.S.A.

Keywords: Fischer Tropsch, mass transfer, bubble column

ABSTRACT

The rate limiting step in the Fischer-Tropsch (F-T) slurry process was assessed using a simple computer model. This model, unlike others, takes into account the water gas shift (WGS) reaction in the calculation of the importance of the gas-liquid mass transfer and makes use of the "Singular Kinetic Path" concept proposed by Espinoza in 1993. The predictions from the model showed that for the available catalysts the Fischer-Tropsch synthesis could be considered a kinetically-controlled process. CO has mass transfer coefficients lower than H_2, is consumed by both F-T and WGS reactions, and is likely to be the limiting reactant in the process. The reactor performance could be improved by increasing the catalyst activity and operating in the mass-controlled regime. Also, an increase of the catalyst concentration up to a maximum of 37 - 40 wt.% could improve the reactor performance, although the reactor would be operating in a mass transfer-controlled regime due to the relatively high catalyst concentration.

INTRODUCTION

Numerous studies were dedicated to the improvement of the catalyst activity using reaction temperature for Fischer-Tropsch (F-T) synthesis and currently, a number of catalysts with high activity and better selectivity are available [5 - 7]. Several studies [12, 13] also pointed out that the kinetics of the reaction and the gas-liquid mass transfer were the only significant resistances in the slurry phase F-T process. These studies, however, failed to define whether such a process is kinetically- or mass transfer-controlled. In addition, these studies only focused on hydrogen and considered the F-T reaction expression without taking into account the Water Gas Shift (WGS) reaction. As a matter of fact, carbon monoxide is consumed by both F-T and WGS reactions and subsequently it could become a limiting reactant in the overall process.

Recently, a considerable attention has been given to the F-T synthesis in a slurry phase and several contributions covering the hydrodynamics, modeling, bubble size distribution and heat transfer have been published [1 - 4]. A detailed review on modeling of the F-T synthesis was carried out by Saxena et al. [6] and other models including complex ones such as that used in the scaleup of the Sasol I Slurry Bed Process (SSBP) [7] have been used. Most of these computer models were based on second order differential equations for both the gas and liquid phases as shown in Equation (1) for the gas phase and some include a solid mass balance to account for the catalyst concentration profiles which become an important variable when using low gas velocities.

$$D_g \epsilon_g \frac{d^2}{dz^2}(C_{g,i}) - \frac{d}{dz}(u_g C_{g,i}) - k_{L,i} a (C^*_{L,i} - C_{L,i}) = 0 \qquad (1)$$

Other models such as that by Deckwer et al. [5] includes a heat balance in order to consider the temperature difference in the slurry reactor. These complex computer models include a large number of parameters concerning the hydrodynamics, kinetics, and mass as well as heat transfer. These parameters, however, are seldom available under the operating conditions of the F-T synthesis and the only resort is to estimate them using other literature data available for air/water systems, liquid hydrocarbons [8] or wax [3]. Unfortunately, the majority of these available data were obtained under atmospheric conditions which raises a serious doubt about their applicability under actual process conditions [9]. In addition, most of these data were obtained for gas-liquid systems without the presence of catalyst particles which alter the slurry density and viscosity as well as gas bubbles coalescence tendency. A thorough review concerning the effect of solid particles on mass transfer has been recently published by Beenakers and van Swaaij [10]. Other factors such as column internals are usually overseen despite the fact that their importance on the hydrodynamic behavior of the slurry reactor was reported to be significant [11]. Thus, using these complex computer models in order to predict the reactor performance as well as the rate limiting step in the F-T slurry process could be cumbersome, expensive, and the predictions are strongly dependent on the accuracy of the literature data used in these models.

This paper presents a novel approach to assess the rate-limiting step in the slurry phase F-T process. A simple computer model which takes into account the WGS reaction and uses the "singular Kinetic Path" concept proposed by Espinoza in 1993 is presented.

Development of the simple model

The two assumptions used in this model were: (1) the gas phase is a plug flow; and (2) the liquid phase is a series of CSTRs. Several simplifications were also made in: (1) phase mixing: (2) kinetics equation; and (3) calculation of mass transfer coefficients.

(1) Phase mixing:

The mixing in the liquid phase was simulated by a number of CSTRs arranged in series based on the studies of the "La Porte Pilot Plant" [14]. This eliminated the need for the second order differential term in the mass balance equations for the liquid phase. Also, the dispersion or backmixing in the liquid phase was expressed in terms of a series of CSTRs [15] as given in Equation (2).

$$\frac{1}{n} = \frac{2}{Pe} - \frac{2}{Pe^2}*(1-e^{-Pe}) \qquad (2)$$

(2) Kinetic equation:

The use of various catalysts with different respective kinetic equations was overcame using the "Singular Kinetic Path" concept developed by Espinoza at Sasol [16]. His concept suggested that a single kinetic equation can be employed for any catalyst as long as the behavior of this catalyst resembles the shape of the F-T synthesis kinetic path when using iron catalyst. In the present model, the Anderson-Dry's equation given below (Equation (3)) was employed where the constant 3.5 was taken from Espinoza's work [16]. The Water Gas shift reaction rate was obtain by simplifying the one proposed by several authors [23,24].

$$r_{F\text{-}T} = A.e^{\frac{E}{RT}} \frac{P_{H2}P_{CO}}{P_{CO}+3.5P_{H2O}} \qquad (3)$$

$$r_{WGS} = k_{WGS}(P_{CO} - \frac{P_{H_2}P_{CO_2}}{K_{eq}P_{H_2O}}) \qquad (4)$$

(3) Mass transfer parameters:

The correlation proposed by Akita and Yoshida [17] for aqueous systems is often used for predicting mass transfer coefficients in the F-T synthesis. In the present model, the correlation by Godbole et al. [8] for predicting mass transfer coefficients for oxygen in light hydrocarbon mixtures in a bubble column operating at a superficial gas velocity up to 0.2 m/s was used. This correlation is given by Equation (5).

$$k_{L,O2}.a = 0.31\ U_g^{0.603} \qquad (5)$$

The prediction of the mass transfer coefficients for hydrogen and carbon monoxide was carried out using the ratio of the diffusivities to the power (2/3) as in the Calderbank and Moo Young's correlation [18]. The presence of solids was also accounted for using the data presented in Figure 2 in the review by Beenakers and van Swaaij [10].

Determination of the rate limiting step using sensitivity analysis

Equation (6) was used to calculate the relative importance of the gas-liquid mass transfer resistance (α). This equation is similar to that presented by Deckwer et al. [5, 12], however, since the water gas shift activity of the catalyst is significant, it was incorporated in the equation through Φ (C_i) [19].

$$\alpha = \frac{\frac{1}{k_L a}}{\frac{1}{k_L a} + \frac{1}{K.\Phi(C_i).\epsilon_L}} \qquad (6)$$

$$\phi_{H_2} = mV_T\epsilon_L(2Ae^{-\frac{E_{FT}}{RT}}\frac{m_{H_2}C_{CO}RTm_{CO}}{C_{CO}m_{CO}+3.5C_{H_2O}m_{H_2O}} - Be^{-\frac{E}{RT}}(\frac{C_{CO}}{C_{H_2}} - \frac{C_{CO_2}}{C_{H_2O}K_{eq}}) \qquad (7)$$

$$\phi_{CO} = wV_T\epsilon_L(2Ae^{-\frac{E_{FT}}{RT}}\frac{m_{H_2}C_{H_2}RTm_{CO}}{C_{CO}m_{CO}+3.5C_{H_2O}m_{H_2O}} + Be^{-\frac{E_{WG}}{RT}}(1 - \frac{C_{CO_2}C_{H_2}}{C_{H_2O}C_{CO}K_{eq}})) \qquad (8)$$

RESULTS AND DISCUSSION

Several scenarios including the Sasol I Slurry Bed Process (SSBP) were considered using the present simple model. Although the model did not considered the effect of pressure or temperature on mass transfer, the predictions from the model were comparable with those

predicted with a much more complex model used by Sasol [7]. To illustrate here the procedure, the operating conditions listed in Table 1 reported by Fox and Degen [19] were used. Different catalyst activities were also considered based on the work by Srivastava et al. [20].

The effects of the catalyst activity and concentration on the relative importance of gas-liquid mass transfer (α), relative liquid concentration ($C_{L,i}/C^*_{L,i}$), and ($CO + H_2$) conversion were studied.

Figure 1 shows the effect of the catalyst activity on (α) and as can be seen hydrogen appears to differently behave than carbon monoxide, since the resistance to hydrogen reaches only 20% of the total resistance whereas that of carbon monoxide becomes significantly large. This difference can also be observed in the corresponding liquid concentrations. The sudden drop of the CO concentration with increasing catalyst activity could be attributed to the water gas shift reaction which also increases the H_2/CO ratio in the liquid phase. Based on this behavior, one can conclude that the reactor performance can be improved by enhancing the catalyst activity although the reactor can be operating in a mass transfer-controlled regime. It should be mentioned, however, that the improvement of the reactor performance from 0.41 to 0.44 kg(HC)/kg(Fe)/hr would require an increase of about 60% in the intrinsic catalyst activity.

The effects of catalyst concentration on (α) as well as the ($CO + H_2$) conversion is illustrated in Figure 3 and as can be noticed the hydrogen and carbon monoxide resistances appear to increase with increasing catalyst concentration. Also, the increase of catalyst concentration almost produces a proportional improvement of ($CO + H_2$) conversion, particularly, at low levels. The effect of high solid loading on the mass transfer rate, however, drove the process into a mass transfer-controlled regime and subsequently, the ($CO + H_2$) conversion appeared to decrease. The maximum conversion could be achieved with a catalyst concentration between 35 and 40 wt%. Thus, the other approach to increase the reactor performance is by increasing the catalyst concentration and subsequently the catalyst becomes slightly under utilized and the mass transfer becomes the controlling rate. Nevertheless, one drawback of this approach is that at high catalyst concentrations, the separation of the catalyst from the wax becomes a critical step in the synthesis process. According to our knowledge, only two companies have successfully solved this separation step: Sasol and Exxon with their iron and cobalt catalysts, respectively.

CONCLUDING REMARKS

Based on the operating conditions and catalysts used in the simple model developed in this study, the following concluding remarks can be made:

1. The slurry phase Fischer-Tropsch synthesis with the present catalysts can be considered a kinetically-controlled process and it would require a substantial improvement of the catalyst intrinsic activity in order to change this situation.
2. The slurry reactor performance for F-T synthesis can be improved by increasing the catalyst activity and/or catalyst concentration, although, the increase of catalyst concentration up to 40 wt%, will drive the process into a mass transfer controlled-regime.
3. Since CO has a lower mass transfer coefficients than those of H_2 [22] and is consumed by Fischer-Tropsch and water gas shift reactions, it is likely to be the limiting reactant.
4. The mass transfer coefficients for H_2 and CO were predicted in this study and therefore they should be measured under the actual Fischer-Tropsch operating conditions in the presence of typical catalyst concentrations. Experimental data are also needed in the presence of high catalyst loading.

Nomenclature

A	Fischer Tropsch intrinsic catalyst activity, kmol of C to HC/kg.Fe.bar.s
B	Water Gas Shift intrinsic catalyst activity, kmol of C to HC/kg.Fe.bar.s
a	gas-liquid interfacial area relative to the expanded fluid volume, m^{-1}
C	concentration, $kmol/m^3$
C*	Concentration at saturation, $kmol/m^3$
D	Dispersion coefficient, m^2/s
E	Apparent activation energy, J/mol
K	Overall kinetic constant, s^{-1}
k_{eq}	Water gas shift equilibrium constant, $k_p = \exp(4577.8/T-4.33)$
k	mass transfer coefficient, m/s
m	solubility
n	number of CSTRs in series
Pe	Peclet number, $u_g L/\varepsilon_g D_g$
P	Partial pressure, bar
R	Gas constant, J/mol.K

u velocity, m/s
V_T Fluidized bed volume m^3
w catalyst concentration (kg/m^3)
z axial position, m

Subscript
i component i
g gas phase
L liquid phase

Greek symbols
ε holdup
α relative extent of the mass transfer resistance

References

1. Deckwer W.D., Serpermen Y, Ralek M. and Schmidt B., Modeling the Fischer-Tropschsynthesis in the Slurry Phase,Ind.Eng.Chem.Proc. Des. Dev, 21, (1982) 231-241.
2. Saxena S.C., Rosen M., Smith D. N., and Ruether J.A., Mathematical Modeling of Fischer Tropsch slurry bubble column reactors, Chem. Eng. Comm., 40, (1986) 97-151.
3. Inga J.R. and Steynberg A.P., Modelling a three phase slurry reactor, Annual Meeting of the Catalyst Society of South Africa, Cape Town, South Africa, 1990.
4. Deckwer W.D., Serpermen Y, Ralek M. and Schmidt B., On the relevance of mass transfer limitations in the Fischer Tropsch slurry process, Chem. Eng. Sci., 36, 1981.
5. Satterfield C.N. and Huff G.A., Effects of mass transfer on Fischer Tropsch synthesis in slurry reactors, Chem.Eng. Sci., 35, (1980), 195.
6. Inga J.R., Hydrodynamic studies and reactor modelling of a three phase slurry reactor in Fisher Tropsch application, M.Eng. Thesis, Potchefstroom University, Potchefstroom, 1993.
7. Inga J.R., Hydrodynamic studies for three phase fluidized Bed reactors: A critical literature review, Annual meeting of the catalyst Society of South Africa, Golden Gate, South Africa, 1991.
8. Patel S.A., Daly J.G., Bukur D.B., Bubble size distribution in Fischer Tropsch derived waxes in a bubble column, AIChE J, 36 (1), (1990) 93-105.
9. Saxena C.N., Heat transfer Investigation in a slurry bubble column, Final Report to DOE, University of Illinois, 1991.
10. Godbole S.P., Joseph S., Shah Y.T. and Carr N.L., Hydrodynamics and mass transfer in a bubble column with an organic liquid, Can.J.of Chem.Eng.,45 12),(1984) 440-445
11. Wilkinson P.M., Physical aspects and scaleup of high pressure bubble columns, Ph.D. thesis, Rijksuniversiteit, Groningen Holland, 1991.
12. Beenackers A.A.C.M., and Van Swaaij W.P.M., Mass transfer in gas-liquid slurry reactors, Chem. Eng. Sci.,48 (18),(1993) 3109-3139.
13. Bernermann K., Steiff A., Weinspach P.M., Zum Einflus von landsamgestromten Rohrbudeln auf die grosraumige flussigkeitsstromun in Blasensaulen, Chem. Ing. Tech. 63 (1), (1991) 76-77.
14. Air Products and Chemicals Inc., Liquid Phase Methanol LaPorte Process Development Unit: Modification, US. DOE DE 91-005732. Topical report Task 2.3 Tracer studies in the LaPorte LPMeOH PDU, August 31, (1990).
15. Levenspiel, Chemical Reaction Engineering , John Willey and Sons Inc., 1272.
16. Espinoza R.L., Singular Kinetic Path, Presented at the Catalyst Society of South Africa, Cape Town, South Africa, (1993), 391-402.
17. Akita K. and Yoshida F., Gas holdup and volumetric mass transfer coefficient in bubble columns, Ind. Eng. Chem. Proc. Des. Dev., 12 (1), (1973) 76-80.
18. Calderbank P.H. and Moo Young M.B., The continuous phase heat and mass transfer properties of dispersions, Chem.Eng. Sci., 16, (1961), 36-54.
19. Inga J.R. and Morsi B.I., Rate Limiting step in Fischer Tropsch Slurry Reactors, submitted for publication, Chem.Eng. Sci.
20. Fox J.M., and Degen B.D., Topical report slurry reactor design studies, DOE contract No. DE-AC22-89PC 89867, (1990)
21. Srivastava R.D., Rao V.U.S., Cinquegrane G. and Stiegel G.J., Catalyst for Fischer Tropsch, Hydroc. Process., Feb. (1990), 59-68.
22. Karandikar B. M., Morsi B.I., and Shah Y.T. , Effect of Water on solubilities and mass transfer coefficients of gases in heavy fraction of Fischer-Tropsch products, The Can. J. of Chem. Eng., 65, (1987), 973-981
23. Kuo J.C.W. "Slurry Fischer Tropsch/ Mobil Two-Stage Process of Converting Syngas to high octane gasoline", U.S. DOE Final Rep. No DOE/PC/30022-10, Dec. 1993
24. Zimmerman W.H. and Bukur D.B. "Reaction Kinetics over iron catalysts used for the Fischer Tropsch synthesis", Can. J. of Chem. Eng. 68, 292-301 (1990)

TABLE 1

Fischer Tropsch slurry bed design basis: From Fox and Degen [19]

Diameter	4.8	m
Length	12.0	m
Cross Sectional Area	15.2	m^2
Reactor Volume	211	m^3
Temperature	257	°C
Pressure	28.3	atm
Slurry Concentration	35.0	wt.%
Gas Velocity	0.14	m/s
Catalyst Performance	0.41	Kg/Kg.hr

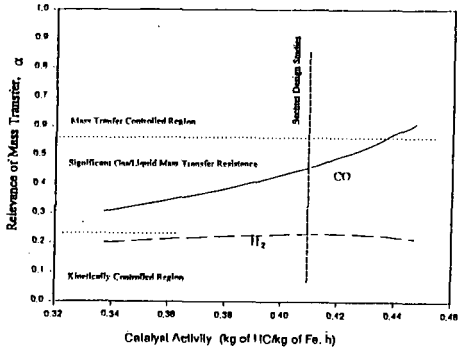

Figure 1: Effect of catalyst activity on the relative mass transfer resistance (α).

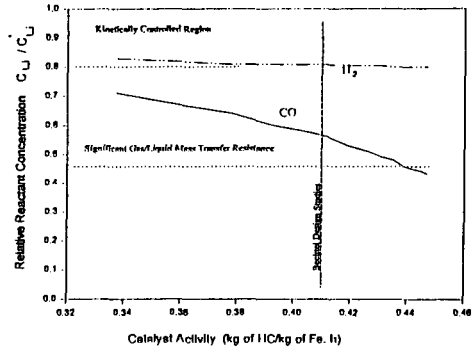

Figure 2: Effect of catalyst activity on the reactants liquid concentration.

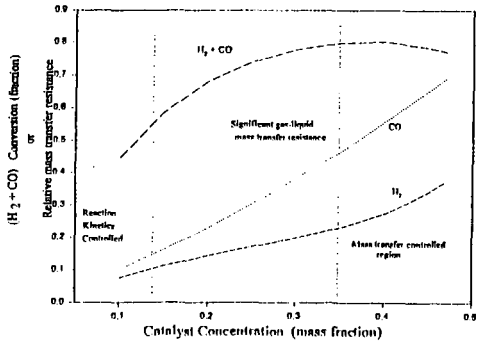

Figure 3. Effect of catalyst concentration on H2+CO conversion and on the relative mass transfer resistance (α).

SULFATED ZIRCONIA AS A CO-CATALYST IN FISCHER-TROPSCH SYNTHESIS

Xuemin Song and Abdelhamid Sayari*
Department of Chemical Engineering, Université Laval
Ste-Foy, Québec, Canada G1K 7P4

Keywords: Fischer-Tropsch synthesis, sulfated zirconia, synthesis gas, branched hydrocarbons.

INTRODUCTION

During the last decade, the average composition of gasoline underwent dramatic changes to make up for the gradual removal of lead compounds, and to meet a strong market demand for premium high octane gasoline. From 1980 to 1988, the average aromatic content in gasoline increased from 22 to 32% and consequently the average octane number increased from 83 to 88.4 [1,2]. Modest increases in olefin and light paraffin (butane) contents also took place. The same tendency was observed in Western Europe [3].

At present, most of the compounds whose concentrations have increased are considered to be directly or indirectly as a threat to the environment and/or human health [2,4]. The challenge is to bring down aromatics, olefins and light hydrocarbons in gasoline to more acceptable levels without adverse effects on the gasoline performance [4]. The most common approach to address this problem is the addition of oxygenated compounds such as MTBE, TAME or ethanol into gasoline. Another approach is to increase the concentration of branched hydrocarbons in gasoline. Indeed, such hydrocarbons have high octane numbers and no major environmental drawbacks. However, according to Unzelman [5], within the limits of existing technologies, isoparaffins cannot be made via isomerization and alkylation in sufficient amounts to replace aromatics below 30%. The objective of the present work is to synthesize branched hydrocarbons from carbon sources other than petroleum. The most obvious choice is synthesis gas (CO/H_2).

The approach we have taken is to use a hybrid catalyst comprised of a Fischer-Tropsch synthesis (FTS) catalyst and a hydroisomerization acid catalyst. The purpose is that the mainly linear hydrocarbons generated on the FTS catalyst would isomerize on the acid catalyst before leaving the reactor. Solid superacid catalysts such as sulfated zirconia (SO_4^{2-}/ZrO_2) exhibit excellent hydroisomerization properties with the formation of significant amounts of branched hydrocarbons [6]. Therefore, we chose to combine Ru loaded on Y zeolite as the FTS catalyst and SO_4^{2-}/ZrO_2 as the isomerization catalyst. In a previous paper [7], we reported data obtained using the hydrogen bracketing technique at atmospheric pressure. In the present communication, we deal with reaction studies in a continuous flow reactor at elevated pressures (mostly at 10 atm).

EXPERIMENTAL

SO_4^{2-}/ZrO_2 and $Pt/SO_4^{2-}/ZrO_2$ catalysts were prepared as described earlier [7]. Surface area and sulfur content of the two catalysts were ca. 90 m^2/g and 1.5 wt%. Pt content in $Pt/SO_4^{2-}/ZrO_2$ was 1 wt%. The FTS catalyst used in this work was 2 wt% Ru loaded on KY zeolite prepared by ion exchange using $Ru(NH_3)_6Cl_3$. Procedures for the preparation of RuKY, the decomposition of the ruthenium complex, and the prereduction of RuKY are the same as those described in [7] for RuNaY. The catalyst thus formed was exchanged again with a dilute solution of K_2CO_3 (0.006 M) to neutralize the protons formed during the decomposition of the Ru complex, and eliminate their possible contribution to the formation of branched hydrocarbons. This catalyst, designated as RuKY-K, was then reduced at 420 °C in flowing H_2 for 4 h.

FTS reaction was carried out in a CDS-804 Micro-Pilot Plant coupled with an on-line gas chromatograph (HP 5890 Series II). The reactor part was described in [7]. Product analysis was carried out using flame ionization (FID) and thermoconductivity (TCD) detectors operating in a parallel mode. A capillary column (PONA from HP, 50m x 0.2mm x 0.5μm) and a stainless-steel column (1/8 in. O.D. x 12 ft. long) packed with Porapak Q (80/100 mesh) were linked to FID and TCD respectively, and used for product separation. All valves and transfer lines between the reactor and the GC were heated to prevent the products from condensation. In a typical experiment, the same amount (0.3 g, unless specified otherwise) of prereduced

RuKY-K and SO_4^{2-}/ZrO_2 or $Pt/SO_4^{2-}/ZrO_2$ were loaded in two separate layers in the reactor, with the FTS catalyst being upstream. They were first reduced at 300 °C for 1 h under a H_2 flow of 40 ml/min and then cooled to reaction temperature (250 °C) under flowing helium. The reactor was pressurized to 10 atm with He, before switching to synthesis gas (CO/H_2 = 1:2, 20 ml/min).

RESULTS AND DISCUSSION

Under the experimental conditions used in the present work, the superacid catalyst did not contribute to CO transformation. CO conversion was due to RuKY-Y catalyst only, and was kept below 10% to minimize the effects of heat and mass transfer. The composition of the C_7 hydrocarbon fraction was used to monitor the effect of SO_4^{2-}/ZrO_2 on product selectivity. Fig. 1 shows iC_7% and $C_7^=$% vs. time-on-stream over different catalysts, where iC_7% and $C_7^=$% designate the content of branched C_7 paraffins and of C_7 olefins in the C_7 hydrocarbon fraction, respectively. Over RuKY-Y catalyst, at 10 atm and 250 °C, iC_7% was below 10 wt%, while the amount of C_7 olefins was very high ($C_7^=$% ≈ 67 wt%). When SO_4^{2-}/ZrO_2 was loaded downstream of the RuKY-K catalyst, iC_7% increased significantly, while only negligible amounts of C_7 olefins were produced in the early stages of the reaction. However, a deactivation of SO_4^{2-}/ZrO_2 catalyst was subsequently observed, as shown by the gradual decrease in iC_7% and the increase in $C_7^=$%. Addition of small amounts (1 wt%) of Pt to SO_4^{2-}/ZrO_2 significantly improved the stability of the catalyst. Under steady state, the iC_7% and $C_7^=$% reached 60 wt% and 10 wt%, respectively.

SO_4^{2-}/ZrO_2 and $Pt/SO_4^{2-}/ZrO_2$ showed different degrees of deactivation during reaction. Two possible deactivation mechanisms were proposed: (i) reduction of S^{6+} to lower oxidation states [8,9]; or (ii) coke deposition on acidic sites [8]. Our TPR results [10] showed that no reduction of surface sulfur species on both SO_4^{2-}/ZrO_2 and $Pt/SO_4^{2-}/ZrO_2$ occurs below 350 °C. The deactivation of SO_4^{2-}/ZrO_2 under our experimental conditions was attributed to coke deposition [7]. On the other hand, CO is known to chemisorb on coordinatively unsaturated surface (CUS) cations which are usually considered as strong Lewis acid sites. Pinna et al. [11] reported that CO can adsorb on CUS Zr^{4+} cations, and the adsorption of CO reversibly poisons active sites for n-butane isomerization, suggesting that the presence of Lewis sites made superacidic by the inductive effect of sulfate species is essential for the occurrence of catalytic activity. Other researchers [12-14] proposed a dual-site model to represent the nature of active sites on SO_4^{2-}/ZrO_2. They suggested that the strongly acidic Bronsted sites are responsible for the catalysis [12, 13, 15]. But the strong acidity of the Bronsted sites requires the presence of adjacent Lewis sites [12-14]. Clearfield et al. [12] and Lunsford et al. [13] argued that through an inductive effect, electrons are withdrawn from O-H bond of surface bisulfate by CUS Zr^{4+} cations, thus yielding stronger Bronsted acid sites. Therefore, whatever the nature of the active sites is, the adsorption of CO on Lewis acid sites of SO_4^{2-}/ZrO_2 will adversely influence the acid strength. As a result, isomerization of hydrocarbons, an acid catalyzed reaction, will be suppressed. To further elaborate on this point, the effect of CO on isomerization of n-butane over $Pt/SO_4^{2-}/ZrO_2$ is being investigated in our laboratory.

Hydrocarbon selectivities under steady state are shown in Fig. 2. It is seen that the presence of $Pt/SO_4^{2-}/ZrO_2$ downstream of RuKY-K has two effects: (i) it alters the normal Schulz-Flory distribution by decreasing the selectivity to C_3 hydrocarbons and by increasing that to C_4's; (ii) it shifts product distribution to lighter hydrocarbons (in particular C_1). The first effect was found to be due to an oligomerization-cracking mechanism of C_3 olefin into C_4 hydrocarbons [7]. The second effect implies the involvement of cracking or hydrogenolysis of primary FT products, which was not observed under atmospheric pressure [7]. To investigate the effect of pressure on FTS product cracking or hydrogenolysis, two reaction experiments were performed at 5 atm, with and without $Pt/SO_4^{2-}/ZrO_2$ catalyst respectively. The results are shown in Fig. 3. By comparing Fig. 2 and Fig. 3, it was found that the net increase in selectivity to C_1 due to the presence of $Pt/SO_4^{2-}/ZrO_2$ is higher at 10 atm than at 5 atm, which suggests a favorable hydrogenolysis at a higher pressure.

Table 1 depicts the effect of the amount of $Pt/SO_4^{2-}/ZrO_2$ used in the hybrid catalyst bed on the composition of C_7 hydrocarbons

under steady state. The increase in the amount of the acid component results in a decrease in olefin contents and an increase in branched C_7 paraffins. In addition, the use of a larger amount of $Pt/SO_4^{2-}/ZrO_2$ favors the formation of di-branched C_7 paraffins which have higher octane numbers than mono-branched paraffins.

REFERENCES

[1] R.A. Corbet, Oil & Gas J., June 18, 1990, p. 42.
[2] G.H. Unzelman, Oil & Gas J., April 9, 1990, p. 43.
[3] H. Hallie and P.J. Nat, Erdol Kohle, 41 (1988) 491.
[4] R.A. Corbet, Oil & Gas J., June 18, 1990, p. 33.
[5] G.H. Unzelman, Oil & Gas J., April 23, 1990, p. 91.
[6] M.Y. Wen, I. Wender and J.W. Tierney, Energy and Fuels, 4 (1990) 372.
[7] X. Song and A. Sayari, Appl. Catal. A: General, 110 (1994) 121.
[8] J.C. Yori, J.C. Luy and J.M. Parera, Appl. Catal., 46 (1989) 103.
[9] J.R. Sohn and H.W. Kim, J. Mol. Catal., 52 (1989) 361.
[10] A. Dicko, X. Song, A. Adnot and A. Sayari, J. Catal., 150 (1994), in press.
[11] F. Pinna, M. Signoretto, G. Strukul, G. Cerrato and C. Morterra, Catal. Lett., 26 (1994) 339.
[12] A. Clearfield, G.P.D. Serrette and A.H. Khazi-Syed, Catal. Today, 20 (1994) 295.
[13] J.H. Lunsford, H. Sang, S.M. Campbell, C.H. Liang and R.G. Anthony, Catal. Lett., 27 (1994) 305.
[14] P. Nascimento, C. Akratopoulou, M. Oszagyan, G. Coudurier, C. Travers, J.F. Joly and J.C. Vedrine, Stud. Surf. Sci. Catal., 75 (1993) 1185.
[15] F.R. Chen, G. Coudurier, J.F. Joly and J.C. Vedrine, J. Catal., 143 (1993) 616.

TABLE 1
Effect of the amount of $Pt/SO_4^{2-}/ZrO_2$ on the composition of C_7 hydrocarbons (RuKY-K = 0.3 g, P = 10 atm)

Amount of $Pt/SO_4^{2-}/ZrO_2$ (g)	0	0.3	0.6	0.9
$C_7^=$%	66.0	9.7	0	0
iC_7%	7.0	61.0	76.0	78.0
mono-branched C_7	100	64.0	62.2	58.0
di-branched C_7	0	36.0	37.8	42.0

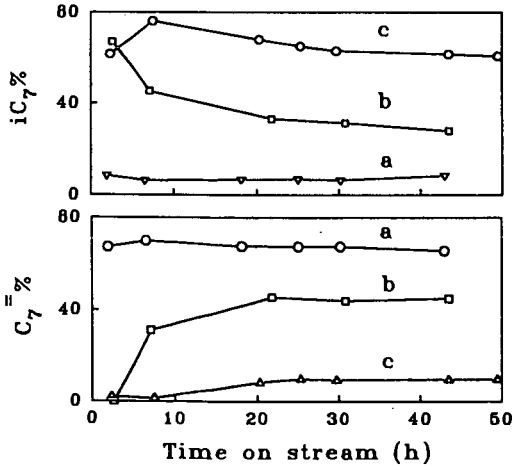

Fig. 1 The composition of C_7 hydrocarbons as a function of time on stream over (a) RuKY-K, (b) RuKY-K + SO_4^{2-}/ZrO_2, and (c) RuKY-K + $Pt/SO_4^{2-}/ZrO_2$.

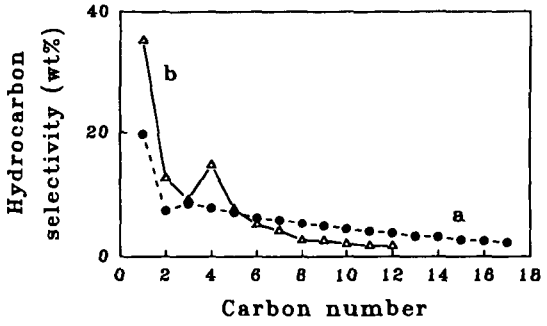

Fig. 2 Hydrocarbon selectivity under steady state at 10 atm over (a)RuKY-K, and (b) RuKY-K + $Pt/SO_4^{2-}/ZrO_2$.

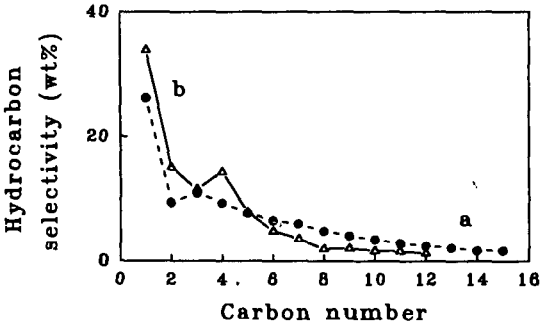

Fig. 3 Hydrocarbon selectivity under steady state at 5 atm over (a)RuKY-K, and (b) RuKY-K + $Pt/SO_4^{2-}/ZrO_2$.

PREPARATION OF FISCHER-TROPSCH CATALYSTS FROM COBALT/IRON HYDROTALCITES

B. H. Howard, J. J. Boff, M. F. Zarochak, and M. A. McDonald
U. S. Dept. of Energy-Pittsburgh Energy Technology Center
P. O. Box 10940, Pittsburgh, PA 15236

Keywords: Hydrotalcites, Fischer-Tropsch, Catalysts

ABSTRACT
Compounds with the hydrotalcite structure ("hydrotalcites") have properties that make them attractive as precursors for Fischer-Tropsch catalysts. A series of single-phase hydrotalcites with cobalt/iron ratios ranging from 3/1 to 1/3 have been synthesized. Mixed cobalt/iron oxides have been prepared from these hydrotalcites by controlled thermal decomposition. Thermal decomposition typically results in either a single mixed metal oxide with a spinel structure or a mixture of oxides with the spinel structure. The BET surface areas of the spinel samples have been found to be as high as about 150 m^2/g.

INTRODUCTION
Mixed metal oxides are important in many catalytic applications, both as catalysts and supports. The precursors used in the syntheses of mixed metal oxides are known to influence the physical and chemical characteristics of the resulting mixed metal oxides. Precursors commonly used for the preparation of these oxides include mixed metal hydroxides and carbonates coprecipitated from basic solution. Materials with a hydrotalcite-like structure, commonly referred to as hydrotalcites after one of the best known minerals of this structural group, have received much attention recently as precursors for catalytic applications. Examples include catalysts for methanol synthesis containing Cu, Zn, Cr, and Al (1,2,3) and catalysts for Fischer-Tropsch (FT) synthesis containing Co, Cu, Zn, and Cr(4).

Hydrotalcites have a layered structure similar to clays. The structure consists of stacks of brucite-like metal hydroxide sheets in which substitution of trivalent metal cations for divalent metal cations within the sheets results in a net positive charge. The positive charge is balanced in the structure by hydrated anions between the sheets. A generalized formula for hydrotalcite-like compounds can be written as:

$$[M_{1-x}^{2+}M_x^{3+}(OH)_2]^{x+}A_{x/y}^{y-}\cdot zH_2O$$

where M^{2+} and M^{3+} can be a variety of metals with appropriate ionic radii. The charge compensating anion is also variable with the ionic radius of the charge compensating anion being of only minor importance because the layer separation can adjust to accommodate size differences. Examples are:

M^{2+} = Mg, Ni, Zn, Co, Fe, Cu, etc.
M^{3+} = Al, Cr, Fe, etc.
A^{y-} = CO_3, OH, SO_4, CrO_4, $V_{10}O_{28}$, etc.

There are many naturally occurring minerals having this structure. These minerals typically have the ideal stoichiometry:

$$M_6^{2+}M_2^{3+}(OH)_{16}CO_3\cdot 4H_2O$$

Compounds with the hydrotalcite structure have several characteristics that make them valuable as precursors for Fischer-Tropsch catalysts. Among these is the ability of the structure to accommodate a variety of potentially useful transition metals in a single lattice and the ability to control the synthesis conditions to yield a high surface area material upon decomposition to a spinel phase. Furthermore, Co-containing and Fe-containing spinel phases have shown good activity and selectivity for FT synthesis and, when judiciously prepared and pretreated, have the potential for the physical stability required of a slurry FT catalyst.

The purpose of this research is to investigate the potential of hydrotalcites as precursors for the preparation of slurry Co/Fe Fischer-Tropsch catalysts. We report results from the initial phase of this work, the preparation of Co/Fe hydrotalcite samples and their thermal decomposition to spinel phases of intermediate-

to-high surface area. The emphasis of future publications will shift to modifications of the precipitation and decomposition procedures described here, the development of suitable pretreatment procedures, and catalytic tests of FT synthesis activity in a fixed bed micro-reactor and a slurry autoclave.

EXPERIMENTAL

The hydrotalcites in this study were prepared by a precipitation in base of the appropriate metal salts. The specific conditions used for the syntheses were varied to yield single-phase, well-crystallized hydrotalcites when possible. An aqueous solution of metal salts was prepared that contained the required ratio of metals for the target hydrotalcite, typically with a total metal concentration of about 0.5 M. The metal salt solution was added dropwise to an aqueous base which typically had an initial concentration of about 1 M. Concentrations were varied for some experiments. Potassium bases were used in most experiments. Potassium is typically used to promote iron F-T catalysts and additional potassium will be impregnated in many of these spinel samples before their use as catalysts. Thus, trace amounts of potassium retained in a hydrotalcite precursor are less likely to affect the behavior of the catalyst than are trace amounts of sodium from sodium bases. Additions were usually done at 25°C with magnetic stirring. The pH was monitored during the syntheses. Usually, at the end of the addition the temperature of the slurry was increased to about 60°C. The slurry was aged, typically for 18 hours, at elevated temperature to promote hydrotalcite formation. After the aging period the product was isolated by filtration, washed and dried at 50°C. Hydrotalcites were thermally decomposed in air at various temperatures between 125 and 1000°C, usually for 2.5 hours, to determine what mixed metal oxide(s) would be formed.

The phases resulting from the hydrotalcite syntheses and the thermal decompositions were determined by means of x-ray diffraction (XRD). Morphologies of these materials were studied with scanning electron microscopy (SEM). Surface areas of the mixed oxides were measured by application of the BET method to N_2 physisorption isotherms. The reduction characteristics of the mixed metal oxides were investigated by means of temperature programmed reduction (TPR) with 10% H_2 in argon, 10% CO in helium, or 5% H_2 / 5% CO in argon. The TPR studies were done using an Altamira Instruments AMI-1 unit with an Ametek mass spectrometer for gas analysis.

RESULTS AND DISCUSSION

A stepwise strategy was used to develop the hydrotalcite syntheses. First, the hydrotalcite compositional range attainable for Co (II) with Fe (III) was determined. Then a method for the addition of Cu (II) to the crystal lattice was tested. Finally, the use of Fe (II) to increase the iron content of the hydrotalcite lattice was investigated.

Cobalt (II) nitrate and iron (III) nitrate were used as starting materials for the first part of the synthesis study. Potassium bicarbonate solution at an initial concentration of 1.25 M was used as the base. Co (II) to Fe (III) atom ratios ranging from 4/1 to 1/3 were attempted in this series of experiments. The results are shown in Table 1. With this method well-crystallized, single-phase hydrotalcites could be prepared with Co (II) to Fe (III) atom ratios from 3/1 to 1/1. At lower cobalt contents some poorly-crystallized iron (III) hydroxide was produced along with hydrotalcite and, at higher cobalt contents, some cobalt carbonate was produced. The starting pH for a synthesis was about 8. During the addition of metal salt solution, the pH typically dropped below 7 and a pinkish-tan slurry formed. As the slurry was aged and heated to 60°C, the pH rose to around 9 accompanied by a change in color to a darker reddish-brown, usually indicating formation of the hydrotalcite.

Copper (II) addition to the hydrotalcite lattice was initially attempted by substituting copper (II) nitrate for part of the cobalt (II) nitrate still using the same synthesis method. (Copper is frequently added to precipitated iron catalysts to facilitate reduction.) The ratio used was 1 Cu (II) / 2 Co (II) / 2 Fe (III). The copper loading used was much higher than typical for Fischer-Tropsch promotion. This high copper concentration was used so that

any undesired phases produced during the synthesis could be detected and identified by XRD. The initial synthesis attempt resulted in primarily hydrotalcite with a trace of malachite, $Cu_2CO_3(OH)_2$. Lowering the base concentration to 1.0 M avoided the malachite contamination resulting in single phase hydrotalcite. This result showed that Cu (II) could be introduced into the Co/Fe hydrotalcite lattice.

A number of experiments were conducted in an attempt to increase the iron content of the hydrotalcite lattice. Table 2 outlines several of the more successful experiments and the resulting compounds. In all experiments in this series metal chloride salts were used. Several of the syntheses were based on the work reported by Uzunova *et al.* (5). The M^{3+} required for a stable hydrotalcite lattice was provided by the oxidation of some of the Fe (II) to Fe (III) through contact with atmospheric oxygen during the synthesis. The result of this set of experiments was the extension of the hydrotalcite cobalt to iron ratio to 1/3. Work is continuing to increase the iron content to higher levels.

The thermal decomposition behavior of several Co/Fe hydrotalcites were examined. The most extensive studies of decomposition behavior was done for an intermediate composition hydrotalcite, an atom ratio of 2Co to 1Fe, which was decomposed in air at temperatures between 125 and 1000°C. The samples were heated quickly by placing them in a muffle furnace that was already at the desired decomposition temperature and holding them at temperature for 2.5 hours. The results are shown in Table 3. It was found that a spinel phase, referred to as spinel A, was the only crystalline compound present following decomposition at temperatures of 200 to 600°C. Decomposition at 700°C produced a second spinel, spinel B, which was the dominant phase after decomposition at 800°C. Decomposition at 900°C yielded only spinel B, and decomposition above 1000°C began to decompose spinel B to cobalt oxides in addition. The surface areas for these samples were found to drop from 153 to 18 m^2/g. This loss of surface area was probably due primarily to a loss of internal particle porosity because no evidence for sintering was apparent in SEM. Hydrotalcites with other Co to Fe ratios were found to show similar behavior. However, for some high iron hydrotalcites two spinels were always present after decomposition. It was also found that the rate of decomposition at a given temperature influenced the spinels formed.

Preliminary TPR studies were done on a 2Co/1Fe sample decomposed at 600°C. In 10% CO/He, reduction proceeded rapidly above 300°C as reflected by the large mass spectrum peaks at m/z=28 and 44. The consumption of CO continued to the end-point of the temperature scan, 450°C. Much of the CO consumption at higher temperatures is likely due to carbon deposition from the Boudouard reaction. In contrast, reduction in H_2, the typical reductant for Co-rich samples, was less favorable. A TPR in 10% H_2/Ar showed less reduction at 300°C, with reduction rates peaking at about 400°C. In both experiments, the samples were cooled to room temperature in inert gas flow after reaching the 450°C end point of the TPR. In both cases, the predominant solid phase detected by XRD was a cubic phase isostructural with α-Fe. In the case of the CO-reduced sample, a small amount of an additional unidentified phase was also present.

ACKNOWLEDGEMENTS

The authors gratefully acknowledge N. E. Johnson for helpful discussions during this project. B. H. Howard gratefully acknowledges support for this research provided under Contract # DE-AC05-760R00033 between the U. S. Department of Energy and the Oak Ridge Institute for Science and Education.

REFERENCES

1. Fornasari, G.; D' Huysser, H.; Mintchev, L.; Trifirò, F.; Vaccari, A., *J. Catal.* **1992**, *135*, 386.
2. Riva, A.; Trifirò, F.; Vaccari, A.; Mintchev, L.; Busca, G., *J. Chem. Soc., Faraday Trans. 1* **1988**, *84(5)*, 1423.
3. Busetto, C.; Del Piero, G.; Manara, G.; Trifirò, F.; Vaccari, A., *J. Catal.* **1984**, *85*, 260.
4. Fornasari, G.; Gusi, S.; Trifirò, F.; Vaccari, A., *Ind. Eng. Chem. Res.* **1987**, *26*, 1500.
5. Uzunova, E.; Klissurski, D.; Mitov, I.; Stefanov, P., *Chem. Mater.* **1993**, *5*, 576.

Table 1. Results of Co (II)/Fe (III) hydrotalcite preparations using metal nitrates.

Co (II) to Fe (III)	Resulting Phases
4/1.	HTC + trace $CoCO_3$ + trace unidentified
3/1	HTC + trace $CoCO_3$
2/1	HTC
1/1	HTC
1/2	HTC + minor $Fe(OH)_3$
1/3	HTC + $Fe(OH)_3$

HTC = hydrotalcite

Table 2. Use of Fe (II) to increase iron content of hydrotalcite prepared using metal chlorides.

Co (II	Fe (II)	Base	Start pH	Result
1	3	$KHCO_3$	8.0	HTC + trace $Fe(OH)_3$
1	3	$KHCO_3$ + K_2CO_3	8.9	Goethite + $CoCO_3$
1	2	KOH + K_2CO_3	12.8	HTC
1	3	KOH + K_2CO_3	12.8	HTC

HTC = hydrotalcite

Table 3. Thermal decomposition of 2Co/1Fe hydrotalcite.

Temperature °C	Phase	Surface area m^2/g
50	HTC	-
125	HTC + amorph.	-
200	Spinel A	-
300	Spinel A	153
400	Spinel A	95
500	Spinel A	57
600	Spinel A	29
700	Spinel A + B	18
800	Spinel A + B	-
900	Spinel B	-
1000	Spinel B + CoO + Co_3O_4	-

SEPARATION OF FISCHER-TROPSCH CATALYST/WAX MIXTURES USING DENSE GAS EXTRACTION. Marc W. Eyring, Paul C. Rohar, Richard F. Hickey, and Curt M. White, U.S. Dept. of Energy, PETC, P.O. Box 10940, Pittsburgh, PA 15236-0940 and Michael S. Quiring, Kerr-McGee Corp., Kerr-McGee Technical Center, P.O. Box 25861, Oklahoma City, OK, 73125

The separation of a Fischer-Tropsch catalyst from wax products is an important issue when the synthesis is conducted in a slurry bubble column reactor. This paper describes a new technique based on dense gas extraction of the soluble hydrocarbon components from the insoluble catalyst particles using light hydrocarbons as propane, butane, and pentane as the solvent. The extractions were conducted in a continuous unit operated near the critical point of the extraction gas on a catalyst/wax mixture containing about 4.91 wt% catalyst. The catalyst-free wax was collected in the second stage collector while the catalyst and some insoluble wax components were collected in the first stage collector. The yield of catalyst-free wax was about 60 wt% of the feed mixture. The catalyst content of the catalyst/wax mixture in the first stage was about 14.8 wt%. The catalyst content in the second stage collector was less than 1 part in 100,000.

DATA ANALYSIS PROCEDURES IN FISCHER-TROPSCH SYNTHESIS

Charles B. Benham CBB
Rentech, Inc.
1331 17th Street, Suite 720
Denver, CO 80202

Keywords: Fischer-Tropsch, Schultz-Flory, Synthesis

In performing tests on Fischer-Tropsch (F-T) catalysts, it is useful to be able to assess immediately the approximate activity and selectivity of the catalyst with a minimum of information. The procedure described in this paper requires only gas chromatographic data on the gases to and from the reactor. Further, the only gases which need be analyzed are hydrogen, carbon monoxide, methane and carbon dioxide. No flowrate data is needed.
Consider the following reactions:

F-T Reaction (Alkanes) $(2n+1)H_2 + nCO \rightarrow C_nH_{2n+2} + nH_2O$

Water Gas Shift Reaction $H_2O + CO \rightarrow H_2 + CO_2$

Assume the following:

1) The F-T product carbon number distribution can be characterized using a single chain-growth parameter; and
2) The feed gas is comprised of only hydrogen, carbon monoxide and inert gases; and
3) The hydrogen to carbon monoxide ratio in the feed gas, M_f, is known.
4) The relative amounts of hydrogen, carbon monoxide, methane, and carbon dioxide in the tail gas are known.

From assumption 1, the number of moles of hydrocarbon having n carbon atoms can be expressed in the usual manner as:

$$N_n = \alpha^{n-1} N_{CH4}$$

Where N_n and N_{CH4} denote the number of moles of hydrocarbons produced having n and 1 carbon atoms respectively.

Let superscripts f and t denote feed and tail gases. Therefore, from the stoichiometry of the above reactions, the following relationships are apparent:

$$N_{H2}^t = N_{H2}^f - \sum_{n=1}^{\infty} (2n+1) N_n + N_{CO2}^t$$

$$= N_{H2}^f - \frac{(3-\alpha)}{(1-\alpha)^2} N_{CH4} + N_{CO2}^t \quad (1)$$

$$N_{CO}^t = N_{CO}^f - \sum_{n=1}^{\infty} nN_n - N_{CO2}^t$$

$$= N_{CO}^f - \frac{1}{(1-\alpha)^2} N_{CH4} - N_{CO2}^t \quad (2)$$

Let ϵ represent the overall carbon monoxide conversion:

$$N_{2CO}^t = (1-\epsilon)N_{CO}^f \quad (3)$$

The subscript i represents any component. By dividing equations (1) and (2) by N_{CO}^t, invoking equation (3), and letting the normalized composition be denoted by R's, ($R_i = N_i^t \div N_{CO}^t$) the following equations are obtained:

$$R_{H2} = \frac{M_f}{(1-\epsilon)} - \frac{(3-\alpha)}{(1-\alpha)^2} R_{CH4} + R_{CO2} \quad (4)$$

$$1 = \frac{1}{(1-\epsilon)} - \frac{1}{(1-\alpha)^2} R_{CH4} - R_{CO2} \quad (5)$$

Let $Z = 1/(1-\alpha)$. Then equations (4) and (5) can be written as:

$$R_{H2} = \frac{M_f}{(1-\epsilon)} - (2Z^2 + Z)R_{CH4} + R_{CO2} \quad (6)$$

$$\frac{\epsilon}{(1-\epsilon)} = Z^2 R_{CH4} + R_{CO2} \quad (7)$$

Equations (6) and (7) can be solved simultaneously for ϵ and Z:

For $M_f = 2$, $Z = \frac{3R_{CO2} + 2 - R_{H2}}{R_{CH4}}$

For $M_f = 2$, $Z = \frac{1 + \sqrt{1 - \frac{4(M_f-2)}{R_{CH4}}\left[(M_f - 2)(1+R_{CO2}) + 3R_{CO2} + 2 - R_{H2}\right]}}{2(M_f - 2)}$

and $\epsilon = \frac{Z^2R_{CH4} + R_{CO2}}{(Z^2R_{CH4} + R_{CO2} + 1)}$